Distribution Agreement

In presenting this thesis or dissertation as a partial fulfillment of the requirements for an advanced degree from Emory University, I hereby grant to Emory University and its agents the non-exclusive license to archive, make accessible, and display my thesis or dissertation in whole or in part in all forms of media, now or hereafter known, including display on the world wide web. I understand that I may select some access restrictions as part of the online submission of this thesis or dissertation. I retain all ownership rights to the copyright of the thesis or dissertation. I also retain the right to use in future works (such as articles or books) all or part of this thesis or dissertation.

Signature:

_____ _____

Carol Yingkai Liu Date

SARS-CoV-2 transmission and control: from understanding social contact and mobility to formulating effective vaccine policy

By

Carol Y Liu
Doctor of Philosophy
Epidemiology

_____
Benjamin A Lopman, PhD
Advisor

_____
Kristin Nelson, PhD
Committee Member

_____
Max SY Lau, PhD
Committee Member

_____
Samuel Jenness, PhD
Committee Member

_____
Stefan Flasche, PhD
Committee Member

Accepted:

_____
Kimberly Jacob Arriola, PhD, MPH
Dean of the James T. Laney School of Graduate Studies

_____
Date

SARS-CoV-2 transmission and control: from understanding social contact and mobility to formulating effective vaccine policy

By

Carol Yingkai Liu
MSc, London School of Hygiene and Tropical Medicine, 2017
BSc, Massachusetts Institute of Technology, 2015

Advisor: Benjamin A. Lopman, PhD, MSc

An abstract of
A dissertation submitted to the Faculty of the
James T. Laney School of Graduate Studies of Emory University
in partial fulfillment of the requirements for the degree of
Doctor in Philosophy
in Epidemiology
2024

Abstract

SARS-CoV-2 transmission and control: from understanding social contact and mobility to formulating effective vaccine policy

By Carol Yingkai Liu

Background: Human behavior influences the spread of SARS-CoV-2 both individually and across communities. At both levels, vaccines emerged as an instrumental tool for prevention and control. The goal of this dissertation is to understand individual-level social contact and community-level human movement patterns in the context of SARS-CoV-2 transmission and utilize this knowledge to inform effective vaccine policy.

Aim 1: We estimate the effect of receiving a COVID-19 vaccination on change in individual-level contact rates in a longitudinal cohort sampled from U.S. households. We found that in the context of increasing contact rates over survey rounds, individuals who newly completed primary vaccine series had additional increases in contacts compared to individuals who remained unvaccinated. A mathematical framework integrating competing effects of changing vaccine coverage and contact rates showed that vaccine protection against infection was insufficient to fully offset observed patterns of increase in contact rates, but transmission remained below levels expected under pre-pandemic contact rates.

Aim 2: We infer spatial patterns of transmission across waves of COVID-19 in Georgia, USA through a novel mathematical framework with a multilayered transmission process and informed by spatiotemporally resolved data on social contact, human mobility, and vaccination. We find that in counties with smaller populations, lower contact rates and higher vaccination coverage, intercounty mobility contributes to a higher proportion of onward transmission. In addition, we present evidence that in an interconnected spatial network with a patchwork of local uptake in mitigation measures, the net infection flow is still from counties with lower mitigation to counties with higher mitigation.

Aim 3: We assess the utility of guiding the timing of future COVID-19 re-vaccination strategies with serological surveillance for SARS-CoV-2 in Mozambique over a ten-year horizon. We use a mathematical model informed by local contact rates to simulate using population-level seroprevalence thresholds to trigger the timing of re-vaccination campaigns among older adults and compared this approach to re-vaccination at fixed time intervals. We find that, in this context, serology-triggered vaccination strategies are unlikely to minimize both deaths and the number needed to treat to prevent one death (NNT) compared to fixed time interval strategies.

Potential impact: This dissertation generates valuable insights on transmission dynamics and infection control, weaving together the use of novel behaviorally related data collected during a pandemic and assessing the impact of an innovative temporally targeted vaccination strategy. These insights will guide analysis of behavior data and their incorporation into mathematical models to assess the likely impact of intervention strategies for future outbreaks of infectious diseases.

SARS-CoV-2 transmission and control: from understanding social contact and mobility to formulating effective vaccine policy

By

Carol Yingkai Liu

MSc, London School of Hygiene and Tropical Medicine, 2017

BSc, Massachusetts Institute of Technology, 2015

Advisor: Benjamin A. Lopman, PhD, MSc

A dissertation submitted to the Faculty of the

James T. Laney School of Graduate Studies of Emory University

in partial fulfillment of the requirements for the degree of

Doctor in Philosophy

in Epidemiology

2024

Acknowledgements

I would first and foremost like to thank my dissertation committee for their generous guidance and support over the past five years. They have provided me with invaluable feedback, scientific insights, resources, and technical expertise, both on my dissertation and my general development as a scientist, without which my doctoral training would not have been possible. To Ben, I am incredibly grateful for the yearslong mentorship and guidance you have provided me. Thank you for your timely and thoughtful feedback, scientific guidance, encouragement, advocacy and for your open-mindedness in allowing flexibility in my doctoral studies. To Kristin, it has been a wonderful journey working with you across a range of projects and studies. Thank you for all the ideas we have exchanged and for providing clarity and logic when I found myself stuck. To Max, thank you for lending your technical expertise and creativity on mathematical modeling. We have had to problem solve one challenge after another. Without your patience and support, I would have given up on learning how to construct, parameterize and analyze a metapopulation model. To Sam, thankful for your technical inputs on model calibration and computing and for your insightful ideas on social interactions and modeling. To Stefan, thank you for your continuous valuable insights on mathematical modeling and on vaccine policy, and for allowing me to maintain connections with my alma mater.

I would like to thank my fellow PhD students. Through grit, tears, and a touch of self-deprecating humor, we labored through our coursework and qualifying exams in the middle of a raging pandemic. Your support and friendship have made the dissertation process less lonely. I would like to thank both former and current affiliates of the Lopman Lab Group. To former lab members, your work served as examples of rigorous research in infectious diseases and your characters served as role models for being personable and collaborative while pursuing difficult scientific questions. To current lab members, thank you for your engaging conversations, knowledge and friendship.

I would like to thank my family and a number of lifelong mentors. To my parents for instilling in me a strong sense of work ethic and for your determination to immigrate to provide the best opportunities for

your child. To several generations of academics, for serving as role models of scientific curiosity and academic excellence. To my partner, Luke, you detoured your career to move across the world to support my studies and have been my number one support over the past years. Thank you for always reminding me of the importance of life and staying true to my values. To Deborah and Lance for paving the way in public health, and for providing me with invaluable advice and encouragement on career and life every step of the way. To Sarita, thank you for your continued support and career advice for my pursuit of global health.

Finally, thank you to all the collaborators and study participants that have made this dissertation possible, including collaborators at Manhiça Health Research Centre (CISM), Global Mix study team, Georgia Department of Public Health, Emory COVID-19 Response Collaborative, COVIDVu study team, COVID-19 Trends and Impact Survey study team and analysts at SafeGraph and Cuebiq.

TABLE OF CONTENTS

LIST OF FIGURES

LIST OF TABLES

CHAPTER 1 BACKGROUND

1.1 COVID-19 history and disease burden

In December 2019, a cluster of severe pneumonia cases of unknown cause was first reported in a large metropolitan city in China, Wuhan[1–3]. Subsequently on January 7, 2020, a novel strain of coronavirus was first isolated in lower respiratory tract samples collected from these cases[4,5]. Since then, the virus hitched rides through transportation and human movement networks[6,7], rapidly spreading through China[8] and across the world. By March 2020, when the World Health Organization declared the COVID-19 outbreak as a pandemic, the infection had spread to more than 114 countries, leading to at least 4,000 documented deaths[9]. As of March 10, 2024, over 775 million cases and 7 million deaths have been reported worldwide[10], with infections, cases and deaths likely substantially underestimated. The disease burden of COVID-19 varied by region and country. Even though the United States documented the highest COVID-19 disease burden, reporting 103 million cumulative cases and 1.2 million cumulative deaths, multiple other countries such as the United Kingdom, Italy and Brazil experienced similar or higher per capita cases and deaths[11]. On the African continent, despite early projections suggesting high morbidity and mortality[12–15], the number of documented cases and deaths remained substantially below that of other regions[16]. Reported diseases are known to underestimate the true number of infections[17–19], particularly in regions where testing resources were constrained[20]. Infection burden estimated from serological surveys[21–27] and mathematical models[28] appeared more comparable across regions.

1.2 Natural history of SARS-CoV-2

SARS-CoV-2 is primarily transmitted through respiratory fluids[29]. Routes of exposure include contact with infectious respiratory droplets when an infected person coughs, sneezes, talks or breathes or through exposure to finer aerosolized infectious particles suspended in the air[30,31]. Symptoms of COVID-19 typically appear after the 2–14-day incubation period[32–35] and can range in severity. The most reported symptoms include fever, chills, cough, shortness of breath, fatigue, myalgia, headache, sore throat and

new loss of taste or smell[36]. Between 20%-35% of infected individuals remain asymptomatic throughout the course of their infection[37,38]; however, onward transmission can occur regardless of the presence of symptoms[39–41]. The basic reproduction number, R_0, defined as the average number of new infections generated by an infectious person in a fully susceptible population, serves as an indication of infection transmissibility. R_0 values >1 suggest a growing outbreak and rising infection incidence[42]. Early estimates of R_0 for SARS-CoV-2 varied, but consistently ranged between 2-6[43,44].

Immunity following exposure to SARS-CoV-2 is complex. Following infection or vaccination, most individuals develop a humoral and cell-mediated immune responses, leading to protection against subsequent infection and disease[45]. However, protection is imperfect, wanes over time, and is further influenced by the emergence of new SARS-CoV-2 variants[46–49]. Protection against severe disease and deaths remains durable but protection against infection is transient. Variants with high immune escape properties, like the omicron variant, resulted in a large number of re-infections or breakthrough infection post-vaccination[50,51].

1.3 Evolving data sources on human behavior relevant to infection transmission

Human behavior effects SARS-CoV-2 transmission at the individual-level[52], where close interactions result in exposure to respiratory fluids carrying the virus[29] and at the community-level, where individual movement facilitates importation of infections from one location to another[53,54]. Over the past two decades, several key sources of data relevant to quantifying human behavior in the context of infection transmission have emerged. Relevant to this dissertation are: 1) social contact data actively collected through surveys[55] and proximity sensors[56–58] and their projections onto populations without empirical data[59,60] and 2) human mobility data actively collected through travel or commuter surveys or passively collected through either mobile phone Call Data Records (CDR)[61,62] or app-based geolocation[63–65].

Social contact studies are commonly used to measure contact rates, defined as the average number of other people a person encounters per day[55]. Participants are asked to enumerate the number of individual

contacts over a specified time frame, and report on a range of attributes for each contact such as the duration, proximity, frequency, and locations of contact. Since the first multi-country social contact study conducted across eight European countries[55], a number of localized social contact studies in various geographical settings continue to inform context-specific insights on patterns of human interactions important for transmission[55,66–70]. Social contact studies have increasingly leveraged social media and online marketing platforms[71], facilitating the rapid sampling of an unprecedented number of participants for response. Large scale online panels facilitated the real-time surveillance of contact rates that captured contemporaneous changes in social interactions during the COVID-19 pandemic, particularly in the US[72–77] and in numerous European countries[71,78–84]. In the U.S., the COVID-19 Trends and Impact Survey (CTIS), operated jointly by Meta Data for Good and Carnegie Mellon University, sampled over 50,000 Facebook users on a daily basis to measure behaviors and attitudes relevant to the pandemic, including contact rates[72,85]. The extensive scope and large sample size of the CTIS allowed the tracking of trends in behavior over short time scales and granular geographical areas.

Human movement data passively collected from mobile phone traces has become widely available and offers new possibilities for understanding infection transmission and control. Modern mobile phone devices routinely transmit location data, providing a massive and readily available source of data to study population-level human mobility patterns. Mobile phone tracts are created, timestamped and location-tagged each time a subscriber uses a specific mobile phone application, recording a trace of movement. Multiple commercial companies (ex. Safegraph[86], Cuebiq[87], Google mobility[88] and Unacast[89] among others) recently developed tractable pipelines for mobile phone app-based Global Positioning System (GPS) location data that readily summarize cumbersome mobility traces into sensible and usable formats. Partnerships between mobile data aggregators and academic institutions have enabled their use in research. Cell phone-based geolocation is unique in its ability to capture real-time population-level mobility changes at fine spatiotemporal scales[90]. Accurate quantification of such changes is critical for transmission models during epidemics when human behavior and mobility are rapidly changing. During

early phases of the pandemic, mobile phone geolocation data captured spatial heterogeneities in adherence to social distancing measures and served as an early proxy for changes in human interactions predicting transmission risk[64,91–97] and further characterized spatial networks as input into spatially-explicit mathematical models[6,64,98–102].

1.4 Individual-level human behavior and infection transmission

1.4.1 Social contact patterns relevant for infection transmission

Contact patterns are a key determinant for the size, speed of spread and peak timing of an epidemic, as well as the intensity of interventions needed to prevent and contain it[103]. Specifically, R_0 is the product of the contact rate, probability of transmission per contact, and duration of infectious period. Contact patterns consistently show age-based assortativity across geographical settings[66,104], highlighting the general tendency for individuals to interact preferentially with peers of the same age group more frequently than individuals of other age groups. Nuances in contact patterns are further shaped by demographic structure, social and cultural norms and daily behavior patterns of individuals[105]. For example, in European countries, older individuals display strong assortative mixing. In contrast, in countries like Zimbabwe[105] and Kenya[106,107] with younger population-level age distributions and where extended-family households are more common, older individuals are more likely to contact younger individuals. Contact patterns are commonly quantified by the contact rate, which serves as a direct input into mathematical models linking individual behavior and population-level transmission. Prior to the COVID-19 pandemic, contact rates were shown to differ by age group, household size, occupation, income status day of week and sometimes by gender[55,60,66,104,108]. Heterogeneity in contact rates further influences the impact of non-pharmaceutical interventions (NPI) such as shelter-in-place orders, school and workplace closures and restrictions on large gatherings[109].

Population-level contact rates evolved throughout the COVID-19 pandemic, characterized by historical lows during universal lockdowns[110], slow rebounds during relaxation of the most stringent measures followed by continued fluctuations[78,80] in response to new COVID waves and changing policies. In the

U.S., after the most stringent shelter-in-place orders in March 2020, contact rates broadly increased as risk mitigation policies relaxed. During this gradual return-to-normal, contact rates were highest among young adults 18-35 years of age, individuals in lower income households and individuals in occupations such as retail, hospitality and food service, and transportation[73] and lower among individuals with comorbidities[111]. Contact rates further varied by race and ethnicity although the subgroup with the highest contact differed between studies. Spatiotemporal trends in contact patterns were also observed. Contact rates were consistently highest in the southern U.S., followed by the Midwest and noticeably lower in the Northeast and West[72].

1.4.2 Behavioral adaptations during outbreaks

During infectious disease outbreaks, human behavior is responsive to various individual-level and community-level changes. For example, contact reductions in response to case surges of COVID-19 in fall 2020 often preceded policy changes[112], supporting the theory of a behavioral feedback mechanism where rising incidence in a community prompts risk avoidance and reductions in contact which subsequently curbs tranmission[113,114]. Similarly, risk compensation is the idea that individuals may offset perceived gains in safety from adopting a risk mitigation behavior by increasing risk-taking behavior due to decreased risk perception and overvaluing of protection[115–117]. Despite concerns of risk compensation for a range of public health measures such as HIV prevention[118,119], motorcycle helmet laws[120] and vaccinations against HPV[121], Lyme disease[121] and influenza[122], the evidence is mixed and inconsistent.

Following the rollout of COVID-19 vaccination, speculations emerged on whether individuals would excessively relax their behavior too soon and inadvertently offset the protective effects of vaccination[115]. Evidence on relaxations in behavior following COVID-19 vaccination is mixed and likely driven by a balance between subjective risk-value trade-offs between transmission risk and the desire to return to normal for social and economic benefits. In several studies in the United Kingdom (UK)[123–125] and a cross-sectional study across 12 countries[126], little to no differences in social distancing and mask-wearing were observed between those receiving one dose versus unvaccinated individuals. Other cross-sectional

surveys in Japan[127], Italy[128], Bangladesh[129], Israel[130], and Brazil[131] found decreased mask-wearing and social distancing among vaccinated individuals, especially among younger adults. In the US, longitudinal panel data between March-June 2021 suggested that relative to unvaccinated individuals, vaccinated individuals experienced a larger decline in risk perception and protective behaviors despite negligible differences in preventative behaviors prior to vaccination[132].

An additional feature of human behaviors during outbreaks is that risk mitigation tends to cluster within individuals. During the COVID-19 pandemic, individuals who adopted one mitigation measure were more likely to adopt multiple protective measures[133–135]. For example, individuals who wore a mask were more likely to accept vaccination against SARS-CoV-2 and conversely[134,136], individuals who reported lower social distancing behavior were more likely to be vaccine hesitant[137,138]. This feature effectively partitions populations into distinct groups: those who rigorously adhere to multiple risk mitigation behaviors that substantially limit their exposure and are highly protected, and those who adopt few or no risk mitigation measures and are highly exposed[139].

1.5 Human movement and spatial patterns of transmission

1.5.1 Human movement and spatial patterns of transmission

Human mobility plays an important role in determining spatial patterns of infectious disease transmission. Patterns of human movement contribute to importation of malaria from endemic to low-transmission areas[61,140] and predicts timing and geographical scope of importations into previously uninfected locations during epidemics of dengue[141] and cholera[142]. Prior to the availability of detailed data on human movement, “traveling waves” during periods of endemic measles were observed to follow a spatial hierarchy where infections moved from large cities to small towns[143]. However, as vaccination against measles increased, infection spread that was once predictable and structured based on the distance to large cities was disrupted[144]. Moreover, uptake of mitigation policies in one community not only affects transmission within its boundaries but can also impact the epidemic trajectory of other mobility-linked communities, giving rise to sources and sinks of infection. Traditionally, infections are hypothesized to

flow from source locations with fewer mitigation efforts and lower vaccination coverage (i.e., net exporters) to sink locations with more mitigation measures and higher vaccination coverage[145–148] (i.e., net importers).

At the onset of the pandemic, the sequence in which infections spread from Wuhan to other Chinese cities and onwards to international destinations, was readily predicted by human movement networks[53,54]. As the pandemic wore on, cases surged and peaked asynchronously across different regions and subregions of the world[149]. Localized patterns of rapidly changing immunity, pathogen transmissibility and human behavior likely increasingly underpinned traveling waves of COVID-19 cases[150].

1.5.2 Incorporating human movement into mathematical models

Spatially explicit mathematical models serve as a framework to understand infection propagation through time and geographical area. Originating from the field of ecology, this class of models divides a population into discrete localized subpopulations, often delineated based on administrative boundaries such as neighborhoods, cities, or states. Connections between subpopulations represent movement by the host[99,151–155]. Within each subpopulation, the local epidemic is described using conventional compartmental models. Human movement data are essential for more realistic parameterizations of spatially explicit mathematical models. Increasing availability of mobility data across a range of sources described in the previous section improves upon gravity- and radiation- models where contagion between two subpopulations is proportional to the population size of origin and destination and the distance between them[144,156]. Parameterizing spatially explicit models with real-world data requires summarizing empirical mobility data into origin-destination matrices that reflect either the population-level probability of travel from origin to destination or the number of trips between them[151,157,158].

1.6 Intervention strategies for SARS-CoV-2 control

Prior to the widespread availability of COVID-19 vaccinations, a number of NPIs were proposed to reduce virus spread. Specific NPI strategies and their level of enforcement differed by geographical location[159]. In the early months of the pandemic, the most disruptive NPIs included shelter-in-place

orders, closure of educational institutions, workplaces, businesses and public venues and restrictions on public gatherings, frequently complemented by test-trace-isolate strategies and mask mandates[160]. By May 2020, many states in the U.S. began to relax blanket shelter-in-place orders[160]. At this point, restrictions and risk mitigation measures became increasingly heterogeneous, with counties, cities, schools, workplaces, and businesses often adopting individualized policies.

Vaccines rapidly emerged as an instrumental tool for SARS-CoV-2 prevention and control. Vaccines showed high efficacy and effectiveness in preventing severe COVID-19 disease and deaths[161–163], thus permitting the safe relaxation of NPIs while maintaining a manageable disease burden[164,165]. A primary goal of vaccination was to reduce severe disease and deaths. While early vaccine supply was limited, vaccination strategies prioritized population groups at the highest risk for severe outcomes such as older adults and frontline healthcare workers[166].

Mathematical models were critical in estimating the likely impact of intervention strategies for COVID-19, weighing tradeoffs in costs and benefits of potential strategies to inform policies for mitigation and control. For example, mathematical models informed combinations and timing of NPIs best suited to reduce strain on hospital capacity[167,168]. Models further guided vaccine allocation to maximize their population-level health impact by determining priority population groups[169,170], assessing a strategy of a delayed second dose to reach a larger population with a single dose[171,172], and informing subsequent decisions and target populations for booster vaccination[173–178]. Models also served as an experimental platform for untested potential strategies. For COVID-19, these included proposals on shielding high risk individuals[179], individualized serology testing prior to relaxing NPIs[180] or prioritizing seronegative individuals for vaccination[181], among others.

CHAPTER 2 STUDY RATIONALE AND SPECIFIC AIMS

2.1 Overarching goal

Understanding changing human interactions and mobility in the context of transmission is key to designing suitable long-term infection prevention and control strategies for both SARS-CoV-2 and ongoing and future outbreaks of other infectious pathogens[149]. The goal of this dissertation is to understand social contact and mobility patterns in the context of SARS-CoV-2 transmission and utilize this knowledge to inform effective vaccine policy.

2.2 Aim 1 rationale and overview

Improved understanding of social contact and human mobility guides more realistic estimations of the population-level impact of interventions for COVID-19 control. Although broad trends in contact rates prior to and during the pandemic were well-documented, individuals likely have displayed different "trajectories" in contact and less is known about sociodemographic and behavioral determinants of changing contacts during the pandemic. For example, it is often assumed that receiving a vaccine, an important risk mitigation measure, impacts contact rates[182–185]; however evidence of such causality is mixed[123,186] and largely based on cross-sectional data or measurements of behavior rather than contact rates[126,187]. Longitudinal data spanning the duration of vaccine rollout can quantify the extent vaccination changed contact rates, a metric with direct implications for disease transmission.

Aim 1: Estimate the effect of receiving a COVID-19 vaccination on change in individual-level contact rates. This aim used data from COVIDVu, a geographically representative cohort from the US sampled over 18 months during the COVID-19 pandemic. A multivariate mixed linear regression was used to estimate the effect of vaccination on change in contact rate and a mathematical framework was used to jointly assess the effect of protection from vaccination amidst observed increases in contact on transmission intensity.

2.3 Aim 2 rationale and overview

Spatial patterns of transmission in a highly interconnected spatial network of communities with heterogeneous demography, dynamically changing immunity levels and within-community contact rates, remain to be characterized. The state of Georgia, USA, with its diverse demographics, varying levels of urbanization and highly heterogeneous COVID-19 containment policies presents a unique case study for examining these dynamics. In Georgia, the COVID-19 pandemic unfolded in an asynchronized mosaic of localized transmissions characterized by surges varying in timing and intensity during the first two years, increasingly shaped by fluctuations in human behaviors and population-level immunity. Identifying sources and sinks of transmission and their correlates can guide more localized interventions and assist in the mitigation of infection spread.

Aim 2: Quantify the relative contribution of local exposure versus intercounty mobility across waves of the COVID-19 pandemic in Georgia, USA. We developed a metapopulation model where the transmission process is decomposed into between county and within county components. Between county transmission was informed by cell phone-derived mobility data and within-county transmission is modeled using an SEIR-like framework informed by county-level age-specific mixing, vaccination rates and reported cases. We calibrate the model to reported case data stratified by age group and by county population group. We analyze relative contributions of intercounty mobility to onward transmission with respect to county-level attributes and infer directionality of net infection flow across pairwise counties.

2.4 Aim 3 rationale and overview

Despite high worldwide vaccination coverage[188] and substantial previously exposed individuals, pockets of susceptible individuals, waning immunity, and new immunity-escaping variants will drive future resurgences. Monitoring the level of susceptible individuals can enable targeted interventions, but estimating contemporary population immunity from routine surveillance is challenging[189]. Serological assays can measure prevalence of immunological markers that are potential markers for prior infection or vaccination. In the past, population-level immunity markers have been used to direct measles, rubella, and

polio vaccination campaigns[190] to areas and age groups with the highest immunity gaps. Monitoring changing immunity for SARS-CoV-2 to trigger subsequent rounds of booster vaccines was proposed for COVID-19 control[191], yet its potential utility is unknown.

Aim 3: Evaluate the utility of guiding the timing of COVID-19 vaccination strategies with serological surveillance for SARS-CoV-2 in Mozambique. We developed an SEIR-like model with varying immunity tiers for subgroups with prior exposure through infection or vaccination and simulated the impact of triggering re-vaccinations based on 1) fixed time intervals; 2) population seroprevalence, using Mozambique as a case study. Tradeoffs in the number of deaths averted and number-needed-to-vaccinated to avert one death were compared.

CHAPTER 3 THE EFFECT OF COVID-19 VACCINATION ON CHANGE IN CONTACT RATES

[Manuscript 1]

The effect of COVID-19 vaccination on change in contact rates during the pandemic among a US cohort

Carol Y Liu, Aaron Siegler, Patrick Sullivan, Samuel M Jenness, Stefan Flasche, Ben Lopman, Kristin Nelson

3.1 Abstract

Background

The COVID-19 pandemic drastically altered social behaviors, initially shaped by strict non-pharmaceutical interventions (NPIs), and subsequently through individual choice as restrictions eased. The development of COVID-19 vaccines, which were highly effective at reducing illness and death, was a watershed event in the pandemic. This intervention altered individual risk perception, which could have increased contact rates. Evidence for this hypothesis is mixed, and most studies do not explicitly estimate the effect of vaccination on contact rates, which are an explicit input into mathematical models that could quantify the population-level impact of such interventions on morbidity and mortality. The goal of this analysis is to estimate the effect of individual-level COVID-19 vaccination and population-level vaccination coverage on change in contact rates in a U.S. cohort and their subsequent impact on transmission.

Methods & results

We analyzed data from a longitudinal survey of individuals sampled from U.S. households that measured contact rates, risk mitigation and COVID-19 vaccination status between August 2020-April 2022. We used a multilevel generalized linear mixed effects model to assess the effect of individual-level COVID-19 vaccination status and county-level vaccination coverage on change in contact rates. We adjusted for

sociodemographic factors, self-reported concern for the pandemic and stringency of COVID-19 policies over time. Contact rates increased across survey rounds for nearly all groups. We found individuals who had newly completed a primary vaccine series had an additional increase of 1.93 (95% CI: 0.27-3.59) contacts compared to individuals who remained unvaccinated, and that fully vaccinated individuals continued to increase their contact across multiple periods after becoming vaccinated (2.72 (95%CI: 0.71-4.73) additional contacts compared to unvaccinated). County-level vaccination coverage had minimal impact on individuals' change in contacts. We inferred reproduction numbers from changes in contact rates mathematical framework and found that the reduction in transmission due to vaccination was insufficient to fully offset the observed increase in contact rates, but transmission was still maintained below what it would have been pre-distancing levels.

Conclusion

These findings reveal the complex interplay between vaccination, behavior, and transmission dynamics, emphasizing the importance of considering changing behavior in mathematical models for transmission and underscores the need for ongoing monitoring of contact patterns during pandemics.

3.2 Introduction

The COVID-19 pandemic profoundly altered social behaviors and contact patterns[192]. Early in the pandemic, efforts to reduce transmission (e,g., shelter-in-place policies; and closures of schools, workplaces and public locations) prompted dramatic reductions in person-to-person interactions in many places.[110] As initial measures were relaxed, rates of contact gradually rebounded and began to fluctuate, increasingly shaped by individual choice rather than policy mandates.[78,80] In January 2021, the widespread rollout of COVID-19 vaccinations marked a new phase in the control of COVID-19. COVID-19 vaccinations substantially reduced morbidity and mortality[149,193,194] and permitted the easing of risk mitigation policies such as school closures and restrictions on indoor gatherings.

At the individual level, the extent of behavior change following vaccination was likely driven by risk-value trade-offs. Individuals weighed the benefits of in-person activities against the perceived and real risk of infection, severe illness and onward transmission post-vaccination[115]. Community-level vaccination rates also played a role in behavior change. Increased vaccination rates among one's social network may have led to decreased risk perception regardless of one's own vaccination status[115,124]. Lower risk perception was associated with less frequent adherence and adoption of risk mitigation measures during the COVID-19 pandemic[195].

Contact rates in populations provide a quantifiable link between shifting individual behavior and population-level transmission and are an important assumption in mathematical models, tools that are critical to estimating the impact of interventions for SARS-CoV-2 control. R_0, the number of secondary infections generated by an average infectious individual in a fully susceptible population, is a function of both the number of contacts made by individuals and their level of susceptibility against infection. Although vaccines provide strong protection against severe SARS-CoV-2 infection, vaccine protection against infection and onward transmission is incomplete[196]. Therefore, if vaccinated individuals drastically increased their contact post-vaccination, they may inadvertently have a higher probability of infection and potential for onward transmission than unvaccinated individuals with lower contact. At the

population-level, incomplete vaccine protection against infection followed by increasing contact rates post-vaccination could lead to higher incidence than pre-vaccination[115]. Understanding potentially counterintuitive population-level effects of vaccination, whereby the introduction of vaccination increases disease incidence among some groups, is critical to understand the overall health impact of a COVID-19 vaccine program in the context of a protracted pandemic.

Evidence on behavior change following COVID-19 vaccination is mixed and primarily from earlier periods of vaccine rollout. Moreover, most studies compared the adoption of protective behaviors between vaccinated and unvaccinated individuals rather than estimating differences in contact rates. Only one previous study assessed differences in contact rates between vaccinated and unvaccinated individuals across multiple European countries between Dec 2020 – Sept 2021[197], observing that vaccinated individuals had higher contact rates compared to unvaccinated individuals. At present, there is a lack of evidence on the effect of COVID-19 vaccination on changes to individual-level contact rates in the U.S, where attitudes towards vaccination and other social distancing measures were different than in Europe, and the subsequent impact of such changes on population-level transmission.

Our analysis leverages longitudinal data obtained from a diverse U.S. cohort that spans the duration of vaccine rollout and multiple subsequent waves of the pandemic from August 2020 to March 2022. We separately assess the impact of changing individual-level vaccination and community-level vaccination coverage on changes to an individual's contact rate. We further estimate the impact of changing contact rates on population-level transmission using a model that estimates the relative transmissibility (ratio of R_t to R_0) from contact rates, vaccination coverage and vaccine protection.

3.3 Methods

3.3.1 Sampling

The COVIDVu study is a longitudinal survey that was conducted during the COVID-19 pandemic, consisting of a diverse and geographically representative cohort of individuals sampled from households in the United States. The address-based household sampling frame was previously described[198]. In brief,

residential addresses were chosen to be representative of the U.S. population in terms of age, gender, race/ethnicity, education level, household income, region of residence and home ownership. From each household, a single household member >18 years of age was randomly chosen to participate in the study. Surveys were conducted at four time points representing distinct periods of the COVID-19 pandemic in the U.S.: 1) August–December, 2020, during initial relaxation of the most stringent pandemic restrictions followed by a rise in cases in the winter of 2020; 2) March–April, 2021; during the start of widespread COVID-19 vaccine availability and a fall in cases 3) July–August, 2021; during continued relaxations in policies and case surges during the Delta wave and 4) March–April, 2022; shortly after the Omicron wave[199]. The COVIDVu study was approved by the Emory University Institutional Review Board (STUDY00000695).

3.3.2 Survey data

Participants completed an online survey which included a set of questions that measured vaccination status[198], risk mitigation behaviors, level of concern for new variants during the four survey periods, and included a contact survey adapted from previously published contact surveys[55,79,200,201]. Participants reported on the number of contacts they had the day before the survey by age of contact (0-4 years, 5-9 years, 10-19 years, 20-39 years, 40-59 years, 60-69 years, and 70 years and older) and by location (home, work, school, other locations). Contacts were classified as physical (physical touch, such as hug or kiss) or non-physical (being within 6 feet with an exchange of three or more words or for longer than 15 minutes)[202],[55,66,105,203–205]. Other information collected as part of the survey included sociodemographic characteristics (age, gender, race/ethnicity, household size, occupation status), presence of comorbidities and political affiliation at baseline. Age, gender and race/ethnicity were imputed when missing using hierarchical hot deck imputation[206,207].

3.3.3 Latent class model to classify risk tolerance at baseline

We conducted latent class analysis (LCA) to classify participants into unobserved groups of similar patterns of intrinsic risk tolerance. We used participant-reported level of adoption of various risk

mitigation behaviors at baseline as indicator inputs into the LCA. We used the R software package "poLCA"[208] and considered several sets of indicator variables (Table 3-5). To select for the number of classes, we considered statistical criteria of model fit (Bayesian information criteria) and model diagnostics (target mean posterior probability for classification and entropy)[209]. To decide on the set of indicator variables and number of classes, we aimed to select the best-fitting model that met diagnostic criteria that allowed for more classes for more distinguishing power. Individuals were assigned to latent classes based on the probabilities of belonging to each class based on the model of choice. LCA classes were considered as model covariates. Detailed methods can be found in 3.7.2.

3.3.4 Modeling effect of vaccination on contact rate

We fit a multivariate mixed linear regression to estimate the effect of vaccination on change in contact rate, with a random intercept for the individual to account for repeated survey responses from the same participants. The primary outcome was change in number of contacts made in one day between two consecutive periods of data collection, chosen to examine how contacts evolved over time and to isolate the effect of vaccination from broader temporal trends in contact rates. Secondary outcomes were change in location-specific contacts between two consecutive periods made at work, home and at other locations (i.e., stores and restaurants, public transit, gym). Before calculating change in contact rate, we truncated the number of location-specific contacts at the 99th percentile of responses for each round to reduce the effect of unrealistic survey responses and computed the truncated number of total contacts by summing the truncated location-specific contacts. Previous studies chose 100[197,210] or 450 contacts as cutoffs.[202] In sensitivity analysis, we considered other truncation criteria of 1) 95th percentile; 2) 97.5th percentile and 3) 100 contacts per location.

The primary exposure was change in vaccination status: 1) unvaccinated at current period (no change); 2) one SARS-CoV-2 vaccine dose between previous period and current period; 3) completed primary series between previous period and current period; 4) completed second dose between previous period and current period and 5) fully vaccinated before current period (no change) (schematic in 3.7.3). The

secondary exposure was vaccination coverage in the participant's county of residence at the time of survey completion. We decided *a priori* to adjust for age group and household size, which are known to influence both contact and COVID-19 vaccine uptake[112,211]. Since contact rates fluctuated during the pandemic in response to both policy measures and individual risk perception[197,210], we decided *a priori* to adjust for time-varying covariates of state-wide COVID-19 stringency level, using the Oxford Stringency Index (OSI)[160]) and the level of changing personal concern for new variants. The OSI is a composite index of nine mitigation interventions (stay-at-home orders, closure of schools, workplaces and public transport, restrictions on gatherings, cancellation of public events, movement restrictions and international travel controls) and is used as a comparable time-varying measure of stringency of risk mitigation policies at the state-level. We used the OSI of participant's state of residence on the date of survey completion.

We conducted stepwise backwards selection to decide on the most parsimonious set of additional covariates (gender, race/ethnicity, self-reported political affiliation, income status, employment status, comorbidity, baseline LCA) to include in the fully adjusted multivariate model. Briefly, an initial model was fit with all potential covariates. The covariate producing the lowest change in effect estimate of primary outcome was removed until removing any additional covariate produced an important change (>10%).

3.3.5 Estimating the impact of contact change on transmission potential

We incorporated both vaccine effectiveness and changing contact rates among vaccinated and unvaccinated participants into a mathematical framework to estimate their joint effects on transmission using the Next Generation Matrix (NGM) at each round *t*. The NGM quantifies the number of secondary infections generated in each population subgroup based on heterogeneous mixing patterns between and within subgroup**Error! Reference source not found.**. Here, we stratify the population into vaccinated a nd unvaccinated subgroups (Eq 1). Briefly, R_{vv} is the number of secondary infections generated between vaccinated persons interacting with other vaccinated persons. Under assumptions of proportional mixing between the two subgroups based on the vaccine coverage in the US at the time of each survey, R_{vv} is

defined by $c_{v,t}$, contact rate among vaccinated persons in data collection round t; χ_t, vaccine coverage; β, the probability of transmission between two unvaccinated individuals; VE_s, vaccine effectiveness against susceptibility (50% for main analysis) and d, the duration of infection (7 days)[212]. We estimate β through the formula $\beta = \frac{R}{d*c}$, assuming an initial reproduction number, R, of 3[43,213,214] and a daily mean contact rate of 16 in the U.S. under no social distancing[60]. R_t is estimated by solving for the dominant eigenvalue of the NGM[200,212,215] (Eq 2). We then produce NGMs exploring a range of vaccine coverage, accounting for heterogeneity in local coverage, and a range of mixing assortativity where vaccinated individuals preferentially mix with other vaccinated individuals and unvaccinated with other unvaccinated.

$$NGM_t = \begin{pmatrix} R_{vv} & R_{vu} \\ R_{uv} & R_{uu} \end{pmatrix} = \begin{pmatrix} c_{v,t}\chi_t\beta(1-VE_s)d & c_{v,t}(1-\chi_t)\beta d \\ c_{u,t}\chi_t\beta(1-VE_s)d & c_{u,t}(1-\chi_t)\beta d \end{pmatrix} \quad \text{Eq 1}$$

$$R_t = \lambda(NGM_t) \quad \text{Eq 2}$$

3.4 Results

3.4.1 Participant description

A total of 2403 adult participants aged 18 years and above completed all four survey rounds and were included in the analysis. Among the included participants, the median age was 52 years (IQR: 36-65) at baseline and 1496 (62%) were female. Most identified as non-Hispanic White (n=1657, 69%), followed by non-Hispanic Black (n=302, 13%), Hispanic (n=276, 11%), non-Hispanic Asian (n=126, 5%) and non-Hispanic Other (n=42, 2%), comparable to the distribution of race and ethnicity in the U.S[216].

Latent Class Analysis of risk mitigation measures to classify risk tolerance

We included all available variables on risk mitigation behavior into the latent class classification (distribution of responses in Figure 3-3 and radar plots in Figure 3-4). We found that BIC values were lower (indicating a better fit) among 2-, 3- and 4-class solutions and model diagnostic criteria were met for 3- and 4- class solutions (Table 3-6) and decided to use a 4-class solution for increased distinguishing

power offered by more classes. In the 4-class solution, individuals classified into the lowest risk tolerance group were substantially more likely to engage in risk mitigation behavior. For example, 90% of individuals with the lowest risk tolerance reportedly always wore a mask when going out compared to 8% of individuals with the highest risk tolerance (Table 3-7). Individuals with the lowest risk tolerance at baseline were less likely to remain unvaccinated although Spearman's rank correlation coefficient showed only a weak correlation between vaccination status and risk tolerance classification (-0.16 on a scale of -1 to 1 where 0 is no correlation) (Table 3-9).

3.4.2 Change in contact rates over time

Overall, the mean number of total daily contacts increased across survey rounds, from 8.4 (95% CI: 7.8-9.0) at baseline, 9.8 (95% CI: 9.1-10.6) at round 2, 11.7 (95% CI: 10.8-12.8) at round 3 and 14.7 (95% CI: 13.7-15.8) at round 4 (Table 3-1). At baseline, mean numbers of contacts reported by participants varied by locations: 4.0 (95% CI: 3.4-4.5), 2.4 (95% CI: 2.2-2.6), 1.9 (95% CI: 1.8-2.0) and 0.1 (95% CI: 0.1-0.1) contacts at work, other locations, home, and school, respectively, accounting for 48%, 29%, 22% and 1% of all contacts, respectively. Mean contact rates increased at both work and other locations throughout the survey rounds but remained similar at home and at school. Contact rates at work increased to 4.8 (95% CI: 4.1-5.4) in round 2, 5.3 (95% CI: 4.6-6.0) in round 3, 7.5 (95% CI: 6.7-8.4) in round 4 and contact rates at other locations increased to 2.7 (95% CI 2.4-3.0) in round 2 to 4.1 (95% CI 3.7-4.4) in round 3 to 4.4 (95% CI 4.0-4.9) in round 4 (Table 3-1).

3.4.3 Vaccination and contact rates

COVID-19 vaccinations became available for the general population during round 2, and vaccination rates among participants increased between round 2 and round 4. In round 2, 1,773 (49%) of participants were unvaccinated and by round 4, only 255 (11%) remained unvaccinated. In each round, contact rates were higher among participants remaining unvaccinated compared to those who had completed the primary series (10.8 contacts (95% CI: 9.5-12.0) versus 8.6 contacts (95% CI: 7.6-9.5 in round 2 and 15.2 contacts (95% CI: 11.7-18.6) versus11.2 contacts (95% CI: 10.4-12.1) in round 3) (Figure 3-1; Table

3-11Table 3-11. Mean contact rates over survey round and time-varying covariates). The overall primary series vaccination coverage among all age groups in the U.S. rose from 11.5% in round 2 to 65.9% by round 4[40]. Contact rates were comparable across counties with different levels of vaccination coverage in rounds 2 and 3 but participants residing in counties with higher coverage had lower contact rates compared to those residing in counties with lower coverage (Figure 3-8).

3.4.4 Variation in contact rates by key covariates

At baseline, contact rates differed by age group, employment status, risk tolerance, presence of comorbidities and household size. Younger individuals had higher contact rates, with 18-24-year-olds reporting the most contacts at 12.9 (95% CI: 9.1-16.8) and 65+ year olds reporting the fewest contacts at 3.9 (95% CI: 3.3-4.4). Employed individuals required to work outside of their homes reported the most contacts at 14.1 (95%CI: 12.8-15.5), while employed individuals permitted to work at home and unemployed individuals had similarly low contacts of 4.8 and 4.1, respectively. Individuals classified as having high risk tolerance had the highest contacts at 14 (95% CI: 11.4-16.7) and those classified as medium-low risk tolerance had the lowest contacts at 4.2 (95% CI: 3.7-4.7). Individuals without comorbidities had more contacts (9.1; 95% CI: 8.2-10.0) than those with at least one comorbidity (7.7; 95% CI: 6.9-8.5). (Table 3-1). Contact rates were more comparable by gender, household income, race/ethnicity, and political affiliation at baseline.

Contacts increased in all subgroups through survey rounds across almost all sociodemographic groups (Table 3-1; Figure 3-1. Distribution of mean contact rates and exposure over survey round). Absolute increases in contact between rounds one and four were comparable across age group, gender, those with and without comorbidities and political affiliation. For example, mean contacts among 18-24-year-olds increased by 6.2 contacts between rounds one and four, comparable to an increase of 5.0 contacts among 65+ year olds. In contrast, Hispanic individuals, individuals classified as having the highest risk tolerance and those working at home at baseline had the most absolute increase in contact compared to individuals in all other racial/ethnic, risk tolerance and employment subgroups.

Contact rates further differed by time-varying covariates of self-reported concern over new variants and stringency of state-level COVID-19 mitigation policy. Over survey round, participants reported decreased concern over new variants and were less likely to live in states with stringent COVID-19 mitigation policies such as restrictions to public gatherings and school closures. Participants who reported increased concern over new variants and participants who resided in states with more stringent mitigation policies reported fewer contacts (Figure 3-6; Figure 3-7).

3.4.5 Change in individual-level vaccination status over time

We categorized our main exposure as the change in vaccination status between rounds to isolate the effect of receiving vaccination on change in contact behavior. Between round 1 and 2, 1173 (49%) remained unvaccinated, 484 (20%) newly received the first dose and 746 (31%) newly completed the primary series. Between round 2 and 3, 254 (11%) remained unvaccinated, 149 (6%) newly received the first dose, 1,254 (53%) newly completed the primary series. Between round 3 and 4, 148 (6%) remained unvaccinated, 50 (2%) newly received the first dose, 204 (9%) newly completed the primary series and 2001 (83%) were already fully vaccinated before round 3 (Figure 3-1).

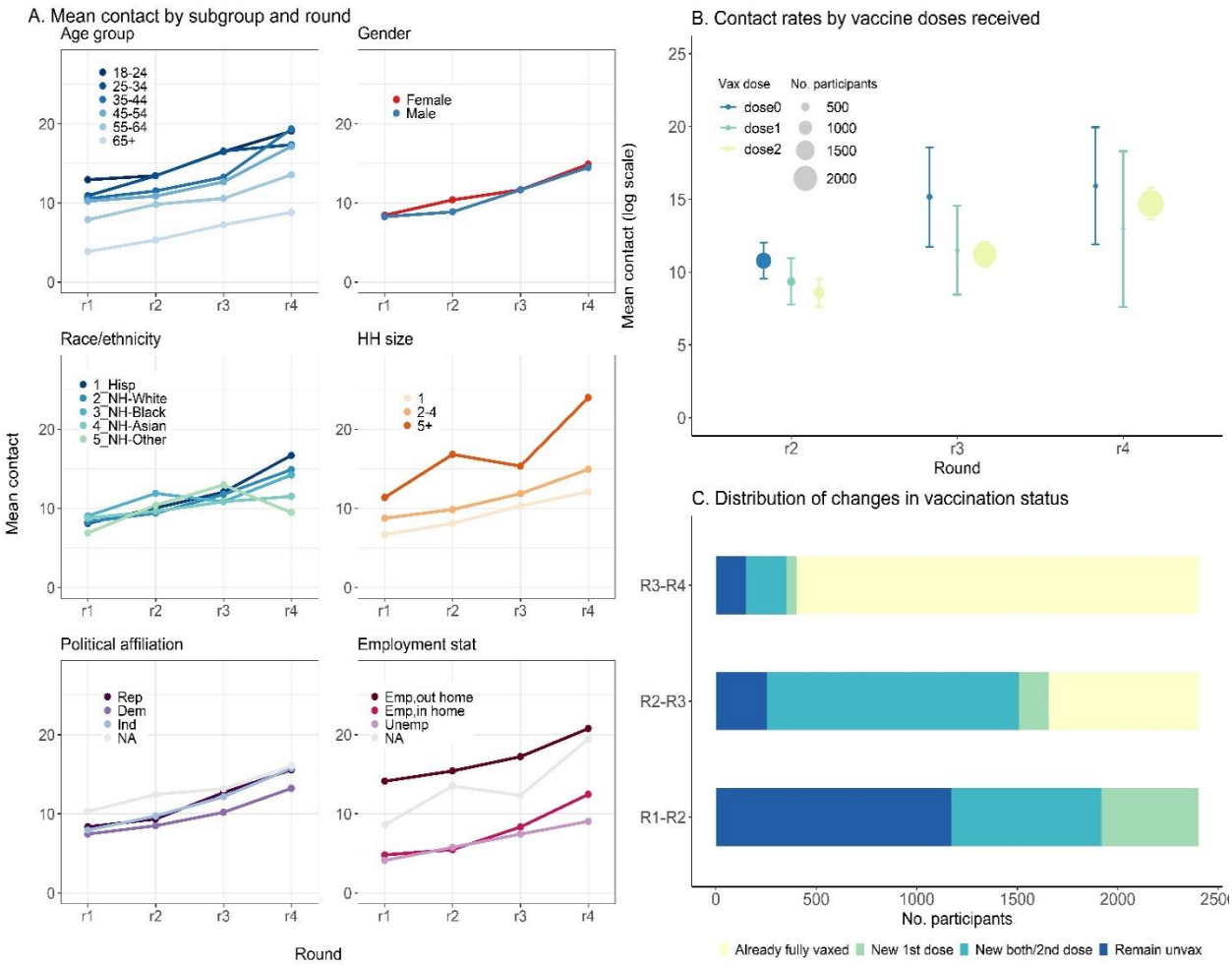

Figure 3-1. Distribution of mean contact rates and exposure over survey round

A. Distribution of mean contact over survey round stratified by age group, gender, race/ethnicity, household size, political affiliation, and employment status. B. Mean contact rates by vaccine doses (0-blue, 1-green, 2-yellow) received for each round with the size of circle representing the number of participants reporting each vaccination status in each round. C. Distribution of the main exposure, change in vaccination status, over round of survey.

Variable	Value	Total (%) (N=2403)	Mean contact rate (95% CI)			
			Round 1 (Aug-Dec, 2020)	Round 2 (Mar-Apr, 2021)	Round 3 (July-Aug, 2021)	Round 4 (Mar-April, 2022)
Location-specific contacts among all participants						
	Work		4 (3.4-4.5)	4.8 (4.1-5.4)	5.3 (4.6-6)	7.5 (6.7-8.4)
	Other	2403	2.4 (2.2-2.6)	2.7 (2.4-3)	4.1 (3.7-4.4)	4.4 (4-4.9)
	Home	(100%)	1.9 (1.8-2)	2.2 (2.1-2.4)	2.3 (2.1-2.4)	2.3 (2.2-2.4)
	School		0.1 (0.1-0.1)	0.1 (0.1-0.1)	0.1 (0.1-0.1)	0.5 (0.4-0.6)
All-location contacts stratified by population subgroup						
Overall			**8.4 (7.8-9)**	**9.8 (9.1-10.6)**	**11.7 (10.8-12.5)**	**14.7 (13.7-15.8)**
Age group	18-24	111 (5%)	12.9 (9.1-16.8)	13.4 (9.9-17)	16.5 (11-22)	19.1 (14.2-24)
	25-34	345 (14%)	10.9 (9.1-12.8)	13.4 (10.9-15.9)	16.6 (13.6-19.6)	17.4 (14.5-20.2)
	35-44	407 (17%)	10.6 (9-12.2)	11.5 (9.6-13.4)	13.3 (11.1-15.4)	19.3 (16.3-22.4)
	45-54	417 (17%)	10.2 (8.5-12)	10.9 (9-12.8)	12.7 (10.7-14.7)	17.2 (14.4-19.9)
	55-64	502 (21%)	7.9 (6.6-9.1)	9.8 (8-11.7)	10.6 (9-12.2)	13.6 (11.3-15.8)
	65+	621 (26%)	3.9 (3.3-4.4)	5.3 (4.6-6)	7.2 (6.3-8.1)	8.8 (7.7-10)

Gender	Female	1496 (62%)	8.4 (7.7-9.2)	10.4 (9.4-11.4)	11.7 (10.6-12.7)	14.9 (13.6-16.2)
	Male	907 (38%)	8.3 (7.3-9.2)	8.9 (7.8-10)	11.7 (10.4-12.9)	14.5 (12.9-16.1)
Race/ethnicity	Hispanic	276 (11%)	8.1 (6.5-9.7)	10 (7.8-12.3)	12.1 (9.6-14.5)	16.7 (13.1-20.3)
	Non-Hispanic, White	1657 (69%)	8.3 (7.6-9)	9.4 (8.6-10.2)	11.8 (10.8-12.8)	14.9 (13.7-16.1)
	Non-Hispanic, Black	302 (13%)	9 (7-11.1)	11.9 (9.1-14.7)	10.9 (8.7-13.1)	14.2 (11-17.4)
	Non-Hispanic, Asian	126 (5%)	8.8 (6.1-11.5)	9.6 (6.7-12.6)	10.8 (7.3-14.3)	11.5 (8.4-14.6)
	Non-Hispanic, Other	42 (2%)	6.9 (3.6-10.2)	10.4 (3.7-17.1)	13 (5.3-20.6)	9.5 (5.3-13.6)
Household size	1	638 (27%)	6.7 (5.6-7.8)	8.1 (6.7-9.5)	10.3 (8.8-11.8)	12.1 (10.3-13.9)
	2-4	1619 (67%)	8.8 (8-9.5)	9.9 (9-10.7)	11.9 (10.9-12.9)	14.9 (13.8-16.1)
	5+	146 (6%)	11.4 (8.7-14.1)	16.8 (12.3-21.3)	15.3 (11.3-19.4)	24 (17.3-30.7)
Self-reported political affiliation	Democratic	996 (41%)	7.4 (6.6-8.3)	8.5 (7.5-9.5)	10.2 (9.1-11.3)	13.2 (11.7-14.8)
	Republican	378 (16%)	8.4 (7-9.8)	9.3 (7.7-11)	12.7 (10.7-14.7)	15.5 (13.2-17.9)
	Independent	445 (19%)	7.9 (6.6-9.3)	9.7 (8-11.5)	12.2 (10.1-14.2)	15.7 (13.2-18.2)
	Unknown	584 (24%)	10.3 (8.9-11.7)	12.4 (10.6-14.3)	13.1 (11.2-15.1)	16.1 (13.9-18.3)
Employment status	Emp,in home	472 (20%)	4.8 (4.1-5.5)	5.5 (4.6-6.4)	8.3 (6.8-9.9)	12.5 (10.2-14.7)
	Emp,out home	950 (40%)	14.1 (12.8-15.5)	15.4 (13.9-17)	17.2 (15.6-18.9)	20.8 (18.8-22.8)
	Unemp	891 (37%)	4.1 (3.7-4.5)	5.8 (5.1-6.5)	7.4 (6.6-8.2)	9 (8.1-10)
	Unknown	90 (4%)	8.6 (6.3-10.9)	13.5 (7.7-19.3)	12.3 (7.5-17.1)	19.5 (12.8-26.2)

Household income	0-$24,999	250 (10%)	8.6 (6.6-10.7)	11 (8.3-13.7)	10.4 (8-12.8)	14.1 (10.8-17.4)
	$25,000-$74,999	756 (31%)	9 (7.8-10.2)	11.6 (9.9-13.2)	13.1 (11.3-14.8)	15.8 (13.8-17.8)
	$75,000-$149,999	695 (29%)	8.3 (7.2-9.3)	8.7 (7.5-9.9)	10.9 (9.7-12.2)	14.2 (12.5-15.9)
	Greater than $150,000	384 (16%)	8.4 (6.9-9.9)	9.3 (7.8-10.8)	12.4 (10.4-14.5)	15.5 (13-18)
	Unknown	318 (13%)	6.8 (5.4-8.2)	7.7 (6.3-9.1)	10 (7.9-12)	12.9 (10.3-15.6)
Comorbidities	No	1151 (48%)	9.1 (8.2-10)	10.3 (9.2-11.4)	12.4 (11.2-13.6)	15.7 (14.2-17.3)
	Yes	1252 (52%)	7.7 (6.9-8.5)	9.4 (8.3-10.4)	11 (9.9-12.1)	13.8 (12.5-15.2)
Risk tolerance[1] (from Latent Class Analysis)	High	208 (9%)	14 (11.4-16.7)	18.2 (14.6-21.8)	20.8 (16.5-25.2)	24 (19.5-28.4)
	Med-high	841 (35%)	9.1 (8.1-10)	9.7 (8.6-10.8)	11.2 (10-12.3)	14.9 (13.4-16.5)
	Med-low	856 (36%)	4.2 (3.7-4.7)	6.6 (5.6-7.7)	8.3 (7.2-9.3)	10.9 (9.5-12.4)
	Low	498 (21%)	12 (10.2-13.8)	12 (10.1-14)	14.5 (12.3-16.7)	17.1 (14.4-19.8)

Table 3-1. Mean contact rate stratified by participant characteristics

[1] Risk tolerance characterized by latent class analysis of responses to a set of survey questions related to risk mitigation behavior.

3.4.6 Effect of vaccination on change in contact rates

After stepwise backwards regression, we arrived at a multivariate model that was adjusted for age group, household size, political affiliation, employment status, risk tolerance at baseline estimated by a Latent Class Analysis, baseline contact rates, change in concern over pandemic and stringency of COVID-19 policy at the state-level (OSI). Our model outcome is change in contact rates between consecutive survey rounds, chosen to explore marginal differences in increases due to vaccination in the context of universally increasing contact rates. In the fully adjusted model, individuals who completed a primary series between two survey rounds increased their contacts by an additional 1.93 (95% CI: 0.27-3.59) contacts compared to individuals who remained unvaccinated. Individuals already fully vaccinated had an additional increase of 2.72 (95%CI: 0.71-4.73) contacts, and individuals who newly received the first vaccine dose had a slight increase of contacts 0.99 (95%CI: -1.12-3.1) (Figure 3-2; Table 3-2). Multivariate models using change in location-specific contacts at work, other leisure locations and home as the outcome showed that individual-level vaccination status affected contacts at work and at other locations and did not affect contacts at home. Individuals newly completing a primary series reported additional increases of 0.99 (95% CI: -0.4-2.39), 0.63 (95% CI: -0.15-1.51) and 0.94 (95% CI: 0.16-1.73) contacts at work, other locations, and home, respectively (Figure 3-2; Table 3-2). We did not find evidence that increasing vaccination coverage in participants' county of residence was associated with a change in contact (Figure 3-2; Table 3-2).

In sensitivity analysis using various thresholds for truncating survey responses of high numbers of contacts, we find similar trends in the effect of vaccination on change in contact regardless of the threshold used (Table 3-16). Truncating at 100 contacts per location provided similar effect estimates whereas more stringent truncation at 97.5^{th} and 95^{th} percentiles produced smaller effect estimates, but similar trends.

Covariate	Category	Change in number of contacts	
		Univariate associations	Multivariate associations
Intercept			6.95(1.65-12.25)
Change in vaccination status	Remain unvaxed		
	First dose new	0.59(-1.46-2.64)	0.99(-1.12-3.1)
	Newly completed series	1.11(-0.37-2.58)	1.93(0.27-3.59)
	Already fully vaxed	1.9(0.48-3.31)	2.72(0.71-4.73)
Every 20% increase in county-level vax coverage		0.41(-0.01-0.83)	-0.37(-1.02-0.29)
Age group	18-24 yrs		
	25-34 yrs	0.1(-2.71-2.92)	-0.06(-2.98-2.86)
	35-44 yrs	0.88(-1.88-3.65)	0.63(-2.24-3.51)
	45-54 yrs	0.26(-2.5-3.02)	0.42(-2.47-3.31)
	55-64 yrs	-0.15(-2.86-2.56)	-0.07(-2.89-2.75)
	65+ yrs	-0.39(-3.06-2.27)	-0.67(-3.52-2.18)
Gender	Female		
	Male	-0.08(-1.16-1.01)	
Race ethnicity	Hispanic		
	Non-hispanic, White	-0.67(-2.35-1.01)	
	Non-hispanic, Black	-1.13(-3.29-1.02)	
	Non-hispanic, Asian	-1.95(-4.72-0.83)	
	Non-hispanic, Other	-2.01(-6.28-2.27)	
Household size	1		
	2-4	0.25(-0.95-1.46)	0.16(-1.08-1.39)
	5+	2.4(0.03-4.77)	1.56(-0.96-4.08)

Political affiliation	Dem		
	Rep	0.47(-1.09-2.03)	-0.04(-1.7-1.62)
	Ind	0.67(-0.8-2.15)	0.68(-0.81-2.18)
	Unknown	0.47(-1.09-2.03)	-0.04(-1.7-1.62)
Employment status	Emp,in home		
	Emp,out home	-0.33(-1.78-1.13)	-0.39(-1.9-1.12)
	Unemp	-0.91(-2.38-0.56)	-0.67(-2.33-0.99)
	Unknown	1.07(-1.9-4.04)	0.43(-2.59-3.46)
Household income	$0-$24,999		
	$25,000-$74,999	0.44(-1.5-2.37)	
	$75,000-$149,999	0.16(-1.8-2.12)	
	More than $150,000	0.55(-1.61-2.71)	
Comorbidities	No		
	Yes	-0.18(-1.23-0.88)	
Risk tolerance (from Latent Class Analysis)	High		
	Med-high	-1.35(-3.35-0.65)	-1.28(-3.4-0.84)
	Med-low	-1.08(-3.08-0.92)	-0.94(-3.12-1.25)
	Low	-1.61(-3.74-0.53)	-1.61(-3.86-0.64)
Unit increase in baseline contact rates		-0.16(-0.2--0.13)	
Change in concern over pandemic	Decreased greatly		
	Decreased slightly	-2.3(-6.25-1.66)	-2.39(-6.37-1.58)
	No change	-4.07(-7.14--1)	-3.83(-6.93--0.74)
	Increased slightly	-5.35(-8.4--2.3)	-5.06(-8.19--1.93)
	Increased greatly	-4.46(-7.82--1.11)	-4.25(-7.7--0.81)

Unit increase in state-wide Oxford Stringency Index	-0.04(-0.08-0)	-0.01(-0.07-0.04)

Table 3-2. Univariate and multivariate effect estimates of individual-level vaccination status and county-level vaccination status on change in contact rates

[a] Main effect is the difference in change in contact rates between rounds among individuals with various vaccination status (first dose new, both dose new, second dose new and already fully vaccinated) compared to the change in contact rates among unvaccinated individuals.

[b] The multivariate model adjusted for age group, household size, political affiliation, employment status, risk tolerance at baseline estimated by a Latent Class Analysis, change in concern over pandemic and the state-wide Oxford Stringency Index approximating stringency of COVID-19 policy at the state-level.

3.4.7 Impact of differential changes in contact rates among vaccinated and unvaccinated on transmission

When we jointly modeled the effects of contact rates and reduced transmissibility from vaccine protection using the NGM, we found that assuming up to 50% vaccine effectiveness against susceptibility, vaccine protection was unable to offset increases in contact rates. Despite increases in transmission intensity, relative transmissibility (ratio of $R_t/R_{(t=0)}$) remained below one in round 2 and round 3, suggesting that R_t remained less than $R_{(t=0)}$, the pre-social distancing estimate for transmissibility of the original SARS-CoV-2 strain. In round 4, contact rates among both vaccinated and unvaccinated increased to an extent that relative transmissibility could have exceeded one (Figure 3-2). Areas with low vaccination coverage or highly assortative mixing where unvaccinated individuals mix preferentially with other unvaccinated individuals are most likely to have increased relative transmissibility.

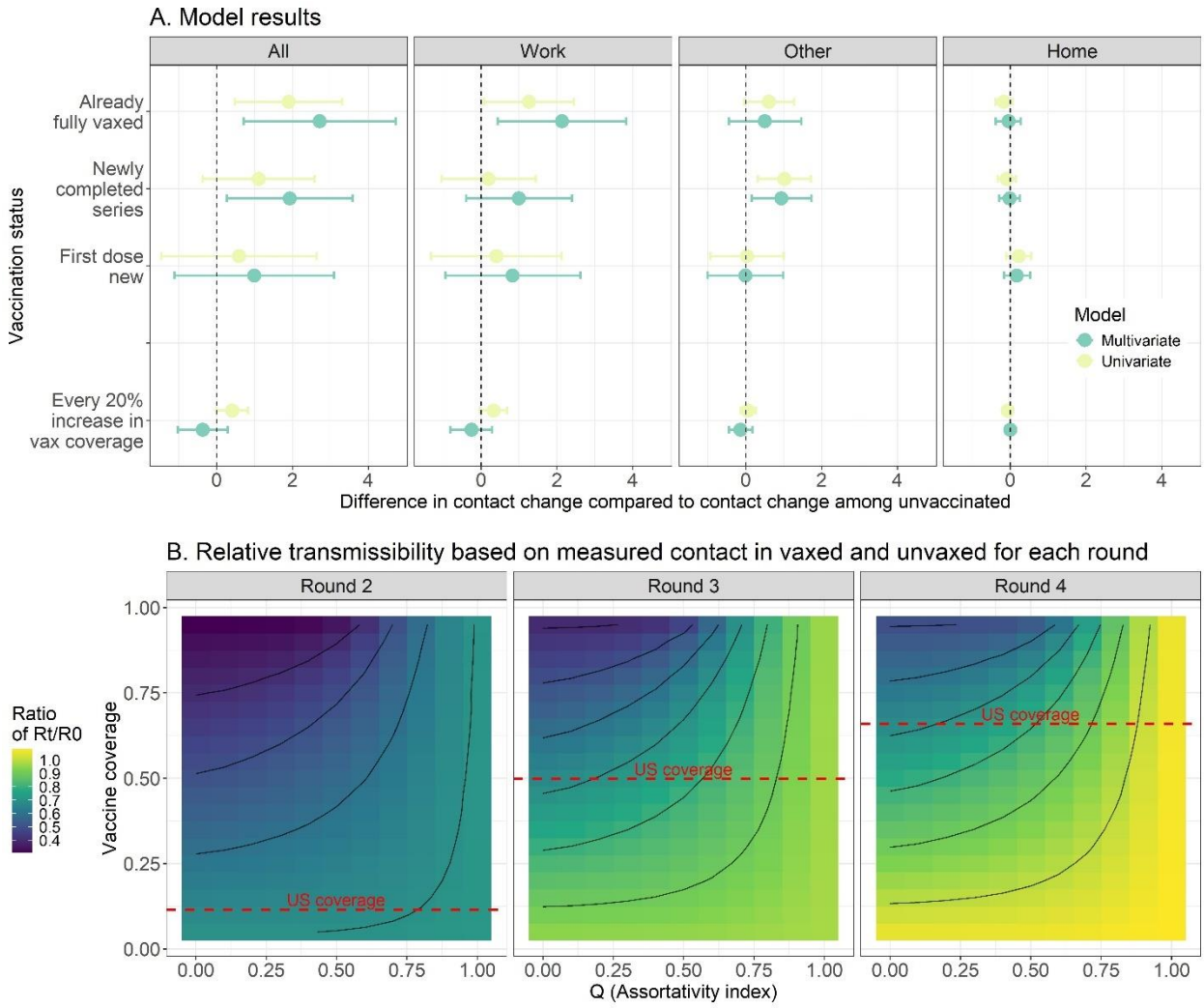

Figure 3-2. Plots of main effect estimate and change in relative transmissibility

A. Plots of difference in contact change among vaccinated groups compared to contact change among unvaccinated and the effect estimate for every 20% increase in county-level vaccination coverage for multivariate (blue) and univariate (yellow) estimates among contacts in all locations, at work, at other leisure locations and at home.

B. Relative transmissibility based on measured contact in vaccinated and unvaccinated for each round using a vaccine effectiveness against susceptibility of 50% and sweeping across vaccine coverage (0%-100%) and assortativity (0-1). Relative transmissibility is the ratio of R_t to $R_{(t=0)}$., $R_{(t=0)}$ is estimated at 3 for the transmissibility of the original SARS-CoV-2 strain pre-social distancing.

3.5 Discussion

Using longitudinal data from the U.S. spanning 18 months of the pandemic, we found that while unvaccinated individuals persistently had the highest contact rates, those newly completing their primary series had a greater increase in contact compared to unvaccinated individuals. Fully vaccinated individuals continued to increase their contact through subsequent survey rounds suggesting continued effects beyond the initial post-vaccination phase. Further, individual-level vaccination had more impact on changes in contact rates at work and at other locations than at home and we did not find evidence of an effect of county-level vaccination coverage on changes in contact rates. Lastly, transmission intensity remained below that of pre-distancing levels despite increases in transmission observed from modeling the joint effects of vaccine protection against infection and increasing contact rates following vaccination.

Our findings of increased changes in contact among those newly completing a primary vaccine series aligns with evidence from the U.S.[132], Japan[127], Italy[128], Bangladesh[129], Israel[130], and Brazil[131] that observed a decline in protective behaviors among vaccinated individuals. While these studies assessed the adoption of risk mitigation behavior post-vaccination[217], we focused on quantifying effects on contact rates which we used to estimate population-level changes in transmission due to vaccination. Our findings further isolated the effect of vaccination on individual-level changes in contact rates, extending on evidence from a multi-country European study that found increased contacts among vaccinated individuals[197]. Evidence from the UK[123–125] and a cross-sectional study across 12 countries[126] found no change in behavior post-vaccination. The restricted timing of these studies to the first months of vaccine rollout in early 2021 likely explains the difference in conclusion compared to our study that expanded over 18 months.

We further show that the extent of contact increase following vaccination is unlikely to raise transmissibility to above that of pre-social distancing levels, particularly under sufficient (>50%) vaccine coverage and moderately assortative ($Q<0.5$) to proportional mixing ($Q=0$) between vaccinated and unvaccinated individuals. The hypothesized effect of county-level vaccine coverage on contact rates

assumes that information on which people act is available to them. In reality, most are unlikely to monitor local vaccination coverage beyond their most immediate social networks, potentially explaining the lack of effect of county-level coverage on change in contact rates. Similar to previous studies conducted both during[72,75,110,200,202,210,218–220] and before the pandemic, contact rates differed by age group, employment status, risk tolerance, presence of comorbidities and household size[55,221], across all data collection periods. Despite these differences, contact rates universally increased across most sociodemographic groups across survey round.

The observed clustering of risk mitigation behaviors was consistent with previous analyses[133–135]. Individuals who adopted one mitigation measure at baseline were more likely to adopt multiple, partitioning the population into highly protected groups reporting low contact rates and highly exposed groups reporting high contact rates. Moreover, individuals who remained unvaccinated had persistently higher contact, and presumably had higher probability of infection prior to vaccine rollout. While contact rates universally increased among both vaccinated and unvaccinated individuals, additional increases in contact among vaccinated individuals, who were on average more cautious prior to vaccination and thus less likely to have infection-induced immunity, likely has implications on changing infection probabilities among vaccinated and unvaccinated individuals. Empirical data on differences in contact change can inform infectious disease models seeking to directly incorporate complex behavioral feedback loops to improve estimations of population-level vaccine impact. Our estimates on the expected increase in contact rates from changes in individual vaccination status and community vaccination coverage enables the explicit representation of the relationship between vaccination and contact rates in mathematical models.

There are several limitations to this analysis. Baseline participation rates were 10-15% which are low but typical for mailed surveys using address-based sampling frames[222]. Because attrition between survey rounds was also likely differential, the subset of participants who responded to all four surveys is not rigorously representative of the U.S. population; however, we find similar distributions of key covariates among those initially enrolled and among those completing all survey rounds (3.7.1). Our cohort had a

higher rate of completing primary series of vaccination than the general U.S. population. We find that by round 4, 91% of our cohort had completed the primary series compared to 79% of the U.S. population aged 18 years and above. This suggests that our cohort has more health awareness and results may not be generalizable to the larger U.S. population. Social desirability bias from self-report may result in underestimates of contact and overestimates to adherence of other risk mitigation measures; however, if underestimation was consistent across rounds, changes in contact rates would remain valid even if the absolute rates are underestimated. Many individuals received either their first or second dose of the vaccine between the second and third time points when a range of policies and sentiments regarding COVID-19 precautions were changing. Additional contemporaneous and unmeasured changes such as remote work policies, increasing population-level vaccine coverage could have affected changes in contact rates. Despite challenges in disentangling the effects of vaccination on changing contact rates from other contemporaneous changes is difficult, we adjusted for numerous important factors that affect contact rates such as the OSI, baseline risk tolerance and concern for new variants.

3.6 Conclusion

In conclusion, our study sheds light on the complex interplay between COVID-19 vaccination, individual behavior, and population-level transmission dynamics. We find that COVID-19 vaccination can influence individual behavior, leading to an increase in contact rates. Given the substantial vaccine protection against severe disease, vaccinations permitted the safe relaxation of the most disruptive social distancing measures, but also resulted in behavioral changes that had a net effect of increasing transmission. These findings underscore the importance of considering behavioral changes when modeling the impact of vaccination strategies and highlight the need for continued monitoring of contacts as they evolve in response to current and future pandemics.

3.7 Supplementary File

3.7.1 Comparing distribution of covariates among initially enrolled study population and those completing follow-up

Variable	Value	Total completing follow-up (%) (N=2403)[1]	Total initially enrolled (N=4654)
Age group	18-24	111 (5%)	308(7%)
	25-34	345 (14%)	705(15%)
	35-44	407 (17%)	777(17%)
	45-54	417 (17%)	765(16%)
	55-64	502 (21%)	926(20%)
	65+	621 (26%)	1173(25%)
Gender	Female	1496 (62%)	2727(59%)
	Male	907 (38%)	1927(41%)
Race/ethnicity	Hispa nic	276 (11%)	607(13%)
	Non-Hispanic, White	1657 (69%)	3063(66%)
	Non-Hispanic, Black	302 (13%)	683(15%)
	Non-Hispanic, Asian	126 (5%)	221(5%)
	Non-Hispanic, Other	42 (2%)	80(2%)
Household size	1	638 (27%)	1204(26%)
	2-4	1619 (67%)	3093(66%)
	5+	146 (6%)	357(8%)
Self-reported political affiliation	Democratic	996 (41%)	1201(26%)
	Republican	378 (16%)	464(10%)

	Independent	445 (19%)	529(11%)
	Unknown	584 (24%)	2460(53%)
Employment status	Emp,in home	472 (20%)	857(18%)
	Emp,out home	950 (40%)	1854(40%)
	Unemp	891 (37%)	1734(37%)
	Unknown	90 (4%)	209(4%)
Household income	0-$24,999	250 (10%)	608(13%)
	$25,000-$74,999	756 (31%)	1470(32%)
	$75,000-$149,999	695 (29%)	1222(26%)
	Greater than $150,000	384 (16%)	717(15%)
	Unknown	318 (13%)	637(14%)
Comorbidities	No	1151 (48%)	2237(48%)
	Yes	1252 (52%)	2417(52%)

Table 3-3. Covariate distributions among those initially enrolled versus those included in the study

[1]Participants included in the study completed all four rounds of follow-up surveys.

3.7.2 Additional details for Latent Class Analysis (LCA)

3.7.2.1 Survey questions on risk mitigation behavior at baseline

Table 1. Survey questions and values on risk mitigation behavior that were considered in as indicator variables for the Latent Class Analysis used to classify participants into different levels of inherent risk tolerance at baseline

Variable	Question	Values
Social distancing	How often are you trying to keep at least 6 feet between you and other people you don't live with to avoid spreading illness?	1 = Never 2 = Rarely 3 = Sometimes 4 = Often 5 = Always
Essential travel	In the last month, how often have you gone out to grocery stores, pharmacies, or visiting other essential service providers?	1 = Daily 2 = Several times a week 3 = Once a week 4 = Once every two-three weeks 5 = Monthly or less often 6 = Never
Nonessential travel	In the last month, how often have you gone out to bars, dining at restaurants, exercising at gyms or other non-essential venues?	1 = Daily 2 = Several times a week 3 = Once a week 4 = Once every two-three weeks 5 = Monthly or less often 6 = Never

Face mask	When you go out, do you wear a face mask?	1 = Never (0%) 2 = Rarely (1 - 30%) 3 = Sometimes (31 - 69%) 4 = Often (70 - 99%) 5 = Always (100%)
Public transport	In the last month, how often have you used public transportation (bus/train) or car service (taxi/Uber/Lyft/other rideshare)?	0 = 0 times 1 = 1 - 2 times 2 = 3 - 5 times 3 = 6 - 10 times 4 = More than 10 times
Intention to vaccinate	How likely are you to get vaccinated for coronavirus once a vaccination is available to the public?	1 = Very unlikely 2 = Somewhat unlikely 3 = Somewhat likely 4 = Very likely 5 = Unsure
Handwashing with soap	Estimate how many times you washed your hands with soap and water yesterday	Quantiles for analysis
Hand sanitizing	Estimate how many times you used hand sanitizer on your hands yesterday	Tertiles for analysis

Table 3-4. Survey questions on risk mitigation behavior at baseline and response choices

3.7.2.2 Distribution of reported risk mitigation measures at baseline

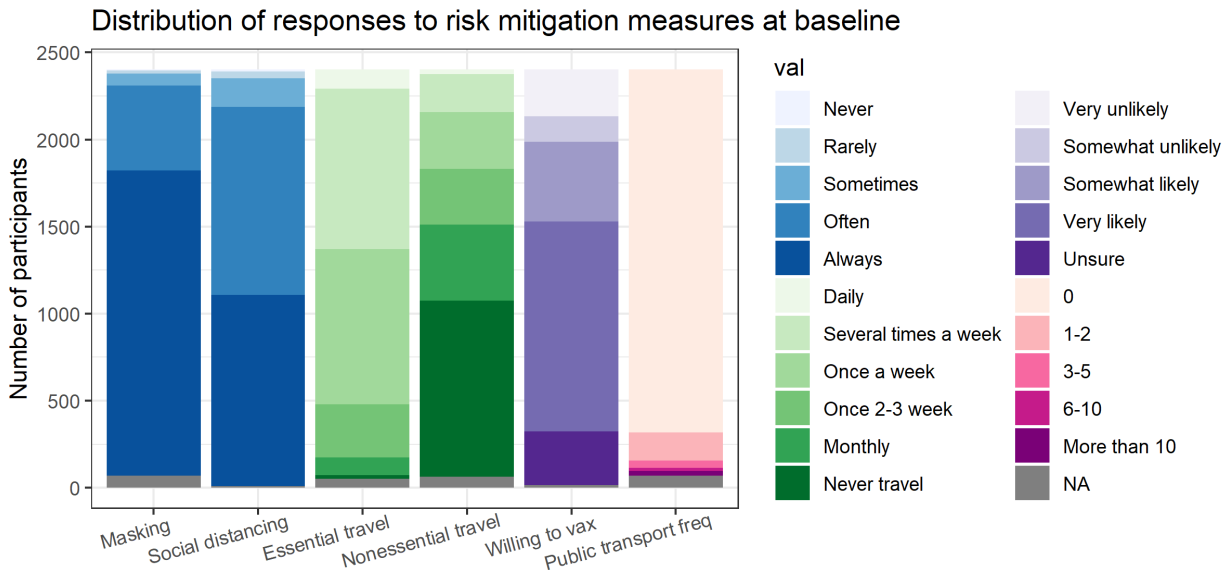

Figure 3-3. Distribution of indicator variables related to risk mitigation for COVID-19 prevention at baseline[1]

[1]Categorical responses vary based on the variable but in general, darker colors indicate more precaution.

3.7.2.3 Detailed methodologies for LCA

We conducted latent class analysis (LCA) on level of adoption of risk mitigation behaviors reported at baseline to classify participants as having different intrinsic levels of risk tolerance. Participants were further asked to report on the level of adoption of recommended COVID-related risk mitigation strategies such as frequency of mask-wearing, social distancing, essential and non-essential travel and handwashing with soap. LCA assumes the presence of an underlying, unobserved latent variable that can explain patterns among observed indicator variables and identifies latent typologies of similar response patterns within indicator variables, classifying participants into unobserved groups of similar patterns of COVID-19 risk mitigation behaviors. Here, we assume that the level of cautionary behavior during the acute phase of the pandemic is closely correlated with an inherent level of risk tolerance. Table 1 shows the survey questions related to risk mitigation available for the LCA analysis at baseline.

We use the R software package "poLCA"[208] and considered several sets of indicator variables. To select for the number of classes, we considered statistical criteria of model fit and model diagnostics. For model fit, we primarily considered the Bayesian information criteria (BIC) which penalizes the log-likelihood by a function of the number of parameters estimated. We further considered the mean posterior probability for classification (target >80%); the entropy (target >0.8 but minimum >0.6) as diagnostic criteria and ensured that no class sizes are smaller than 50[209]. To decide on the set of indicator variables and number of classes, we aimed to select the best-fitting model that met diagnostic criteria that allowed for more classes for more distinguishing power. Individuals are assigned to latent classes based on the probabilities of belonging to each class based on the model of choice.

Model	Indicator variables
Full model	All indicator variables
Model 1	Social distancing + Essential travel + Nonessential travel +Face mask + Intention to vaccinate + Handwashing with soap + Hand sanitizing
Model 2	Social distancing + Essential travel + Nonessential travel +Face mask + Intention to vaccinate
Model 3	Social distancing + Essential travel + Nonessential travel +Face

Table 3-5. Sets of indicator variables considered for the Latent Class Analysis

3.7.2.4 Radar plots for LCA solutions

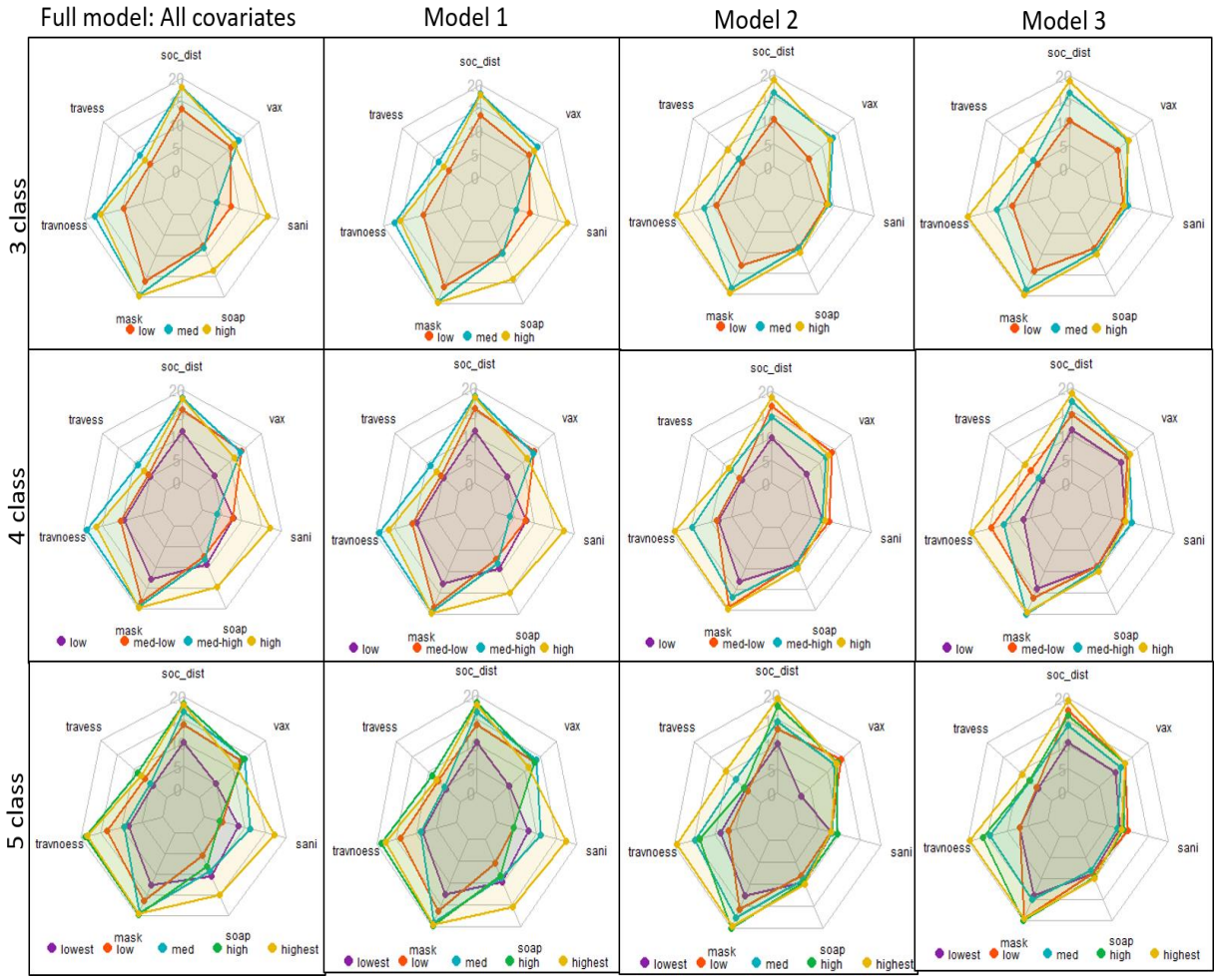

Figure 3-4. Radar plots of average profiles of each class classified under various solution sizes and variable groupings

Latent class models including frequency of handwashing with soap and hand sanitization added an additional dimension to the classification scheme (non-concentric area plots).

3.7.2.5 Model fit and diagnostics

		1 class	2 class	3 class	4 class	5 class	6 class
BIC	**Full model**	40867	40352	40352	40418	40575	40781
	Model 1	38742	38219	38197	38239	38361	38531
	Model 2	27824	27269	27266	27358	27491	27640
	Model 3	21379	20835	20876	20940	21064	21166
AIC	**Full model**	40681	39976	39785	39661	39627	39641
	Model 1	38580	37889	37700	37573	37528	37530
	Model 2	27697	27009	26873	26832	26831	26847
	Model 3	21275	20621	20552	20506	20520	20512
Smallest class (N,%)	**Full model**	2403	808(34%)	645(27%)	219(9%)	175(7%)	102(4%)
	Model 1	2403	756(31%)	567(24%)	223(9%)	187(8%)	167(7%)
	Model 2	2403	763(32%)	239(10%)	197(8%)	120(5%)	105(4%)
	Model 3	2403	879(37%)	326(14%)	291(12%)	239(10%)	50 (2%)
Mean posterior probability	**Full model**	1	0.87	0.82	0.8	0.73	0.69
	Model 1	1	0.88	0.82	0.8	0.74	0.68
	Model 2	1	0.88	0.8	0.77	0.67	0.65
	Model 3	1	0.86	0.78	0.71	0.67	0.72
Entropy	**Full model**	NA	0.55	0.6	0.6	0.56	0.53
	Model 1	NA	0.56	0.58	0.6	0.58	0.55
	Model 2	NA	0.55	0.59	0.53	0.49	0.47
	Model 3	NA	0.53	0.5	0.48	0.45	0.53

Table 3-6. Statistical criterion for model fit and model diagnostic criteria for LCA

3.7.2.6 Distribution of behavioral-related survey responses across the final LCA categories

Survey question	**Value**	**4-Low risk tolerance**	**3**	**2**	**1-High risk tolerance**
When you go out, do you wear a face mask?	Never (0%)	0.20%	0%	0%	1.70%
	Rarely (1-30%)	0.20%	0%	0.10%	7.80%
	Sometimes (31-69%)	0%	0.60%	1.60%	21.30%
	Often (70-99%)	6.90%	9.20%	29.20%	56.10%
	Always (100%)	90.10%	87.70%	66.30%	8.30%
	Unknown	2.60%	2.60%	2.70%	4.80%
How often are you trying to keep at least 6 feet between you and other people you don't live with to avoid spreading illness?	Never	0.40%	0.10%	0%	3.50%
	Rarely	0.80%	0.40%	0.10%	14.30%
	Sometimes	1.20%	0.50%	7.30%	40%
	Often	32%	30.70%	67.50%	40.90%
	Always	65.20%	68.30%	24.50%	0%
	Unknown	0.40%	0%	0.60%	1.30%
In the last month, how often have you gone out to bars, dining at restaurants, exercising at gyms	Daily	1.20%	0%	1.40%	4.30%
	Several times a week	4.20%	0%	15.50%	27.80%
	Once a week	7.90%	0.20%	27.10%	24.30%
	Once 2-3 week	10.70%	1%	25.80%	16.10%

or other non-essential venues?	Monthly	19.40%	17.10%	19.70%	14.80%
	Never	54.50%	79.20%	8%	7.80%
	Unknown	2.20%	2.40%	2.50%	4.80%
In the last month, how often have you gone out to grocery stores, pharmacies, or visiting other essential service providers?	Daily	5.50%	0%	5.80%	14.80%
	Several times a week	40.70%	22.20%	48.80%	52.20%
	Once a week	32.80%	41.90%	39.50%	20.40%
	Once 2-3 week	13.40%	23.20%	3.80%	6.10%
	Monthly	5.70%	8.70%	0%	1.30%
	Never travel	0.20%	2.20%	0.10%	0%
	Unknown	1.60%	1.70%	2.10%	5.20%
In the last month, how often have you used public transportation (bus/train) or car service (taxi/Uber/Lyft/other rideshare)?	0 times	88.70%	92.50%	82.30%	78.70%
	1-2 times	4.70%	3.20%	10%	10.90%
	3-5 times	0.80%	1.30%	2.60%	3%
	6-10 times	0.40%	0.20%	1.30%	1.30%
	More than 10	3%	0.10%	1.10%	0.90%
	Unknown	2.40%	2.60%	2.70%	5.20%
How likely are you to get vaccinated for coronavirus once a vaccination is	Very unlikely	18.60%	7%	3.50%	39.10%
	Somewhat unlikely	7.90%	4.20%	2%	23.50%
	Somewhat likely	18.80%	16%	21.80%	20.40%

available to the public?	Very likely	35.40%	59.90%	60.10%	11.70%
	Unsure	18.80%	12.30%	12%	4.30%
	Unknown	0.60%	0.60%	0.60%	0.90%
Estimate how many times you used hand sanitizer on your hands yesterday	0 times	0%	35.70%	20.50%	28.70%
	1-3 times	1%	42.70%	41.60%	24.30%
	4-5 times	36%	2.30%	8.80%	12.20%
	6 or more times	54.90%	0%	10.40%	15.70%
	Unknown	8.10%	19.30%	18.70%	19.10%
Estimate how many times you washed your hands with soap and water yesterday	0-4 times	1.80%	24.90%	30.30%	23.90%
	5-6 times	14.20%	23%	25.80%	20%
	7-10 times	39.90%	22.70%	17.70%	23%
	11 or more times	36.80%	10.90%	8.10%	15.70%
	Unknown	7.30%	18.50%	18.10%	17.40%

Table 3-7. Distribution of behavioral-related survey responses across LCA categories

3.7.3 Exposure classification

1) Unvaccinated at recent period
2) Completed first dose between previous period and recent period
3) Completed primary series between previous period and recent period
4) Fully vaccinated before previous period

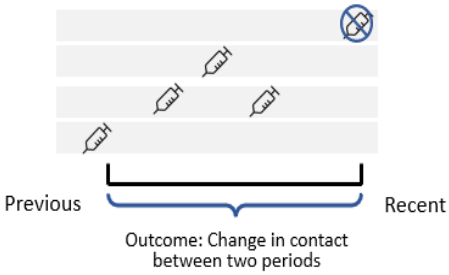

Figure 3-5. Schematic for exposure classification

3.7.4 Exploring relationship between key covariates

	Risk tolerance at baseline	**Total**	**Concern Increased greatly**	**Concern Increased slightly**	**No change in concern**	**Concern Decreased slightly**	**Concern Decreased greatly**	**Unknown**	**Spearman's Rank Correlation Coefficient**
			n (%)	**n (%)**	**n (%)**	**n (%)**	**n (%)**	**n (%)**	
Round 2	High	208	3(1%)	53(25%)	128(62%)	1(0%)	4(2%)	19(9%)	-0.1625
	Med-high	841	52(6%)	432(51%)	313(37%)	3(0%)	4(0%)	37(4%)	
	Med-low	856	96(11%)	480(56%)	240(28%)	7(1%)	1(0%)	32(4%)	
	Low	498	68(14%)	226(45%)	165(33%)	3(1%)	2(0%)	34(7%)	
Round 3	High	208	14(7%)	70(34%)	115(55%)	3(1%)	5(2%)	1(0%)	-0.157
	Med-high	841	122(15%)	493(59%)	196(23%)	15(2%)	14(2%)	1(0%)	
	Med-low	856	201(23%)	489(57%)	142(17%)	12(1%)	11(1%)	1(0%)	
	Low	498	116(23%)	245(49%)	122(24%)	7(1%)	7(1%)	1(0%)	
Round 4	High	208	1(0%)	16(8%)	138(66%)	19(9%)	34(16%)	0(0%)	-0.1691
	Med-high	841	19(2%)	204(24%)	446(53%)	100(12%)	71(8%)	1(0%)	
	Med-low	856	49(6%)	287(34%)	403(47%)	71(8%)	43(5%)	3(0%)	
	Low	498	31(6%)	147(30%)	247(50%)	41(8%)	31(6%)	1(0%)	

Table 3-8. Correlation between risk tolerance at baseline and changes in concern for new variants

	Risk tolerance at baseline	Total	Remain unvaccinated	First dose new	Newly completed series	Already fully vaccinated	Spearman's Rank Correlation Coefficient
			n (%)	n (%)	n (%)	n (%)	
Round 2	High	208	159(76%)	21(10%)	28(13%)	0(0%)	0.0865
	Med-high	841	398(47%)	173(21%)	270(32%)	0(0%)	
	Med-low	856	369(43%)	210(25%)	277(32%)	0(0%)	
	Low	498	247(50%)	80(16%)	171(34%)	0(0%)	
Round 3	High	208	79(38%)	15(7%)	86(41%)	28(13%)	0.09582
	Med-high	841	58(7%)	61(7%)	452(54%)	270(32%)	
	Med-low	856	45(5%)	41(5%)	493(58%)	277(32%)	
	Low	498	72(14%)	32(6%)	223(45%)	171(34%)	
Round 4	High	208	53(25%)	13(6%)	28(13%)	114(55%)	0.087
	Med-high	841	31(4%)	18(2%)	69(8%)	723(86%)	
	Med-low	856	26(3%)	11(1%)	49(6%)	770(90%)	
	Low	498	38(8%)	8(2%)	58(12%)	394(79%)	

Table 3-9. Correlation between risk tolerance at baseline and vaccination status over round

	Concern for pandemic	Total	Remain unvaccinated	First dose new	Newly completed series	Already fully vaccinated	Spearman's Rank Correlation Coefficient
			n (%)	n (%)	n (%)	n (%)	
Round 2	Increased greatly	219	123 (56%)	48 (22%)	48 (22%)	0 (0%)	-0.00675
	Increased slightly	1191	527 (44%)	246 (21%)	418 (35%)	0 (0%)	
	No change	846	415 (49%)	173 (20%)	258 (30%)	0 (0%)	
	Decreased slightly	14	6 (43%)	2 (14%)	6 (43%)	0 (0%)	
	Decreased greatly	11	10 (91%)	1 (9%)	0 (0%)	0 (0%)	
Round 3	Increased greatly	453	25 (6%)	24 (5%)	255 (56%)	149 (33%)	-0.1587
	Increased slightly	1297	81 (6%)	69 (5%)	705 (54%)	442 (34%)	
	No change	575	129 (22%)	54 (9%)	263 (46%)	129 (22%)	
	Decreased slightly	37	10 (27%)	1 (3%)	15 (41%)	11 (30%)	
	Decreased greatly	37	8 (22%)	1 (3%)	14 (38%)	14 (38%)	
Round 4	Increased greatly	100	5 (5%)	1 (1%)	14 (14%)	80 (80%)	-0.108
	Increased slightly	654	12 (2%)	6 (1%)	36 (6%)	600 (92%)	

	No change	1234	96 (8%)	30 (2%)	125 (10%)	983 (80%)	
	Decreased slightly	231	11 (5%)	6 (3%)	12 (5%)	202 (87%)	
	Decreased greatly	179	24 (13%)	7 (4%)	17 (9%)	131 (73%)	

Table 3-10. Correlation between concern for new variants and vaccination status over round

3.7.5 Mean contact rate by time-varying covariates

		Round 1		Round 2		Round 3		Round 4	
Variable	**Value**	**Total (%)**	**Mean contact (95% CI)**	**Total (%)**	**Mean contact (95% CI)**	**Total (%)**	**Mean contact (95% CI)**	**Total (%)**	**Mean contact (95% CI)**
Overall		2403 (100%)	8.4 (7.8-9)	2403 (100%)	9.8 (9.1-10.6)	2403 (100%)	11.7 (10.8-12.5)	2403 (100%)	14.7 (13.7-15.8)
Oxford Stringency index[1]	High	24 (1%)	10 (2-17.9)	2 (0%)	26 (20.1-31.9)	-	-	-	-
	Med-high	457 (19%)	6.4 (5.5-7.4)	718 (30%)	7.6 (6.6-8.6)	-	-	-	-
	Med-low	1647 (69%)	8.6 (7.8-9.3)	555 (23%)	10.4 (8.7-12.1)	13 (1%)	6.3 (3.2-9.4)	-	-
	Low	275 (11%)	10.4 (8.1-12.7)	1128 (47%)	10.9 (9.7-12.1)	2390 (99%)	11.7 (10.9-12.5)	2403 (100%)	14.7 (13.7-15.8)
Self-reported level of concern for new variants	Increased greatly	-	-	219 (9%)	9.1 (6.6-11.6)	453 (19%)	10.4 (8.5-12.3)	100 (4%)	15.4 (9.2-21.6)
	Increased slightly	-	-	1191 (50%)	8.4 (7.5-9.3)	1297 (54%)	10.8 (9.8-11.8)	654 (27%)	11.7 (10.1-13.4)
	No change	-	-	846 (35%)	11.1 (9.7-12.4)	575 (24%)	13.7 (11.7-15.7)	1234 (51%)	15.2 (13.8-16.6)
	Decreased slightly	-	-	14 (1%)	15.4 (-0.3-31.1)	37 (2%)	14.2 (8-20.5)	231 (10%)	16.7 (12.7-20.7)
	Decreased greatly	-	-	11 (0%)	15 (-3.3-33.3)	37 (2%)	22.8 (12-33.5)	179 (7%)	20.2 (16.2-24.3)
	Unknown	2403 (100%)	8.4 (7.8-9)	122 (5%)	15 (9.9-20.1)	4 (0%)	4 (-1.9-9.9)	5 (0%)	4 (1-7)
Self-reported	None	-	-	1173 (49%)	10.8 (9.5-12)	255 (11%)	15.2 (11.7-18.6)	153 (6%)	15.9 (11.9-20)

vaccination status	One dose	-	-	484 (20%)	9.3 (7.8-10.9)	153 (6%)	11.5 (8.5-14.5)	54 (2%)	13 (7.6-18.3)
	Series complete	-	-	746 (31%)	8.6 (7.6-9.5)	1995 (83%)	11.2 (10.4-12.1)	2196 (91%)	14.7 (13.6-15.8)
	Unknown	2403 (100%)	8.4 (7.8-9)	-	-	-	-	-	-
County-level vaccination coverage	0%-20%	-	-	2313 (96%)	9.7 (9-10.5)	304 (13%)	12.7 (10-15.3)	-	-
	21%-40%	-	-	84 (3%)	11.9 (6.4-17.3)	705 (29%)	12.4 (10.7-14)	74 (3%)	16.1 (9.9-22.3)
	41%-50%	-	-	-	-	510 (21%)	11 (9.4-12.6)	284 (12%)	18 (14.8-21.3)
	51%-60%	-	-	-	-	600 (25%)	11 (9.5-12.5)	797 (33%)	15.1 (13.2-16.9)
	61%-100%	-	-	-	-	278 (12%)	11.3 (8.8-13.8)	1239 (52%)	13.7 (12.3-15)
	Unknown	2403 (100%)	8.4 (7.8-9)	6 (0%)	13.5 (4.6-22.4)	6 (0%)	18.2 (-3.2-39.5)	9 (0%)	13.9 (-0.2-28)

Table 3-11. Mean contact rates over survey round and time-varying covariates

[1]A standardized weighted metric of level of stringency of state-level COVID-19 risk mitigation policies

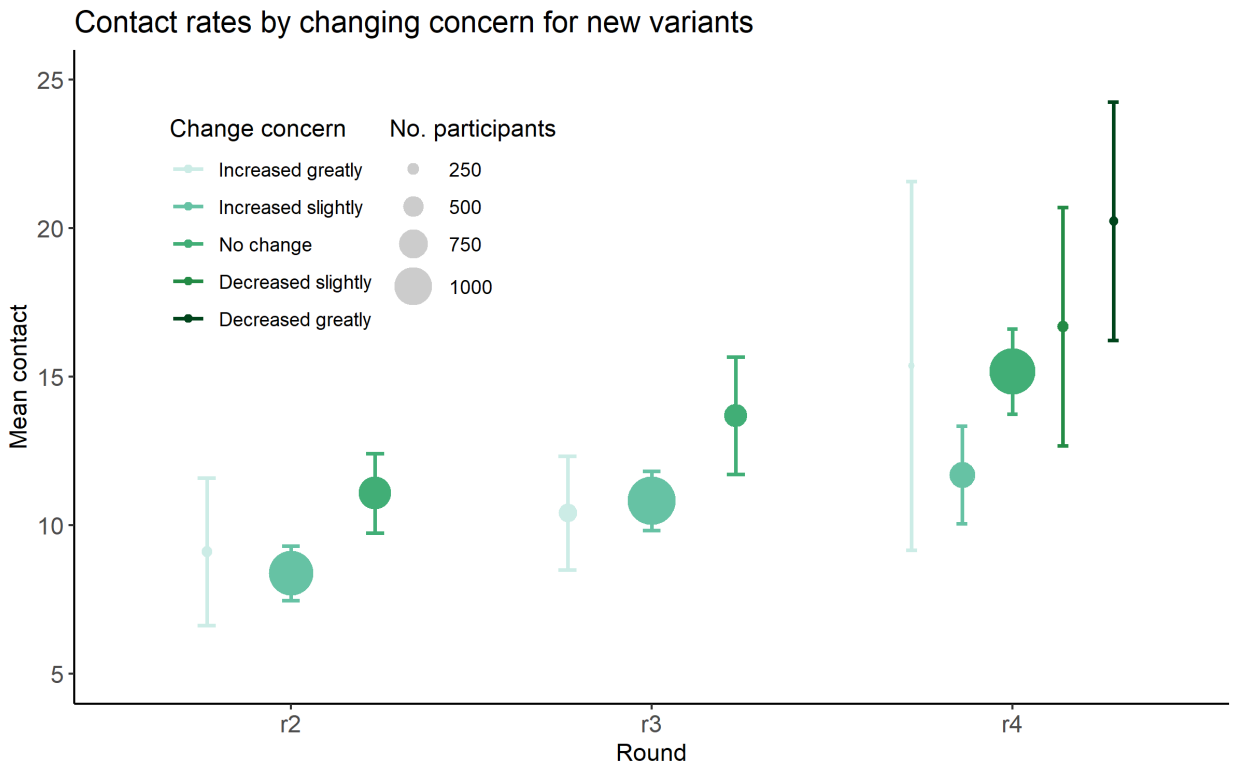

Figure 3-6. Mean contact rates over survey round by self-reported changing concern for new variants

Across survey round, participant attitude shifted from more concern to less concern (number of respondents denoted by the size of the dot). Within each survey round, individuals who had decreased concern had higher overall contacts.

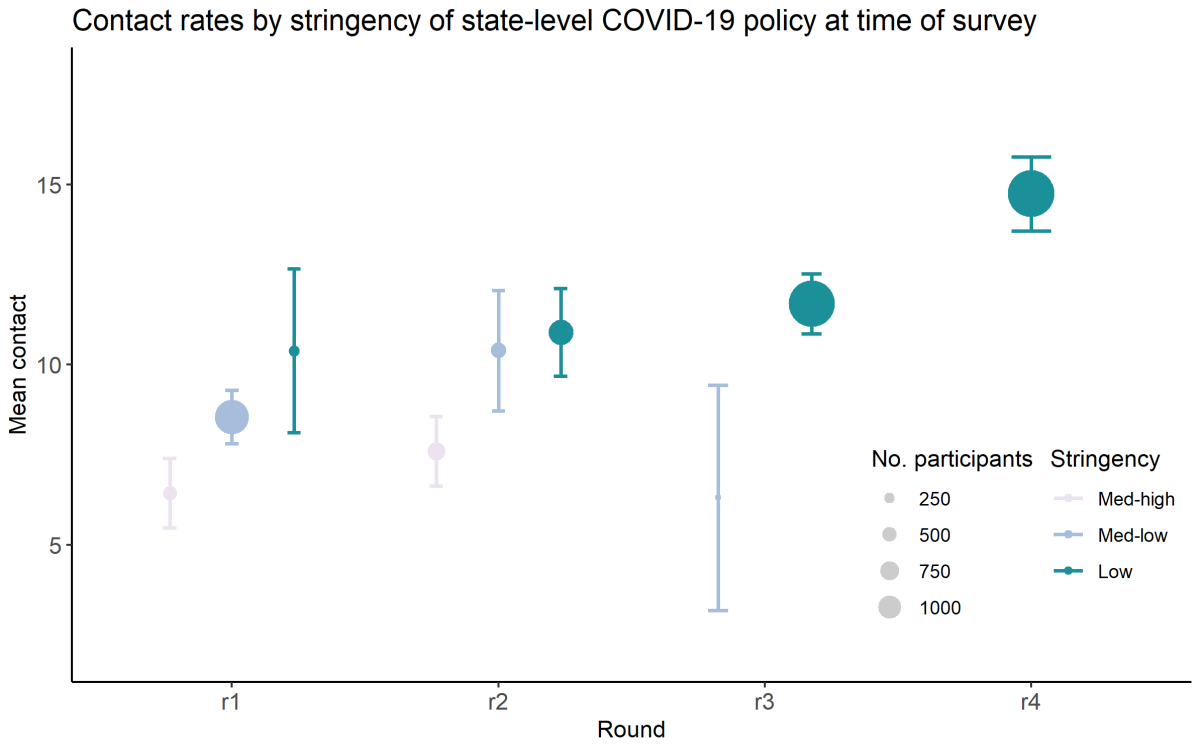

Figure 3-7. Mean contact rates over survey round by stringency of state-level COVID-19 policy[1]

[1]Stringency of state-level COVID-19 policy classified using the Oxford Stringency Index at time of survey

Across survey round, more participants resided in states with less stringent COVID-19 policy (number of respondents denoted by the size of the dot), aligning with relaxation of risk mitigation policies during the study period (August 2020 to March 2022). In earlier survey rounds (round 1 and 2), participants who lived in states with less stringent policies had higher contact compared to those who lived in states with more stringent policies. By round 3, almost all participants lived in states with low stringency COVID-19 policies.

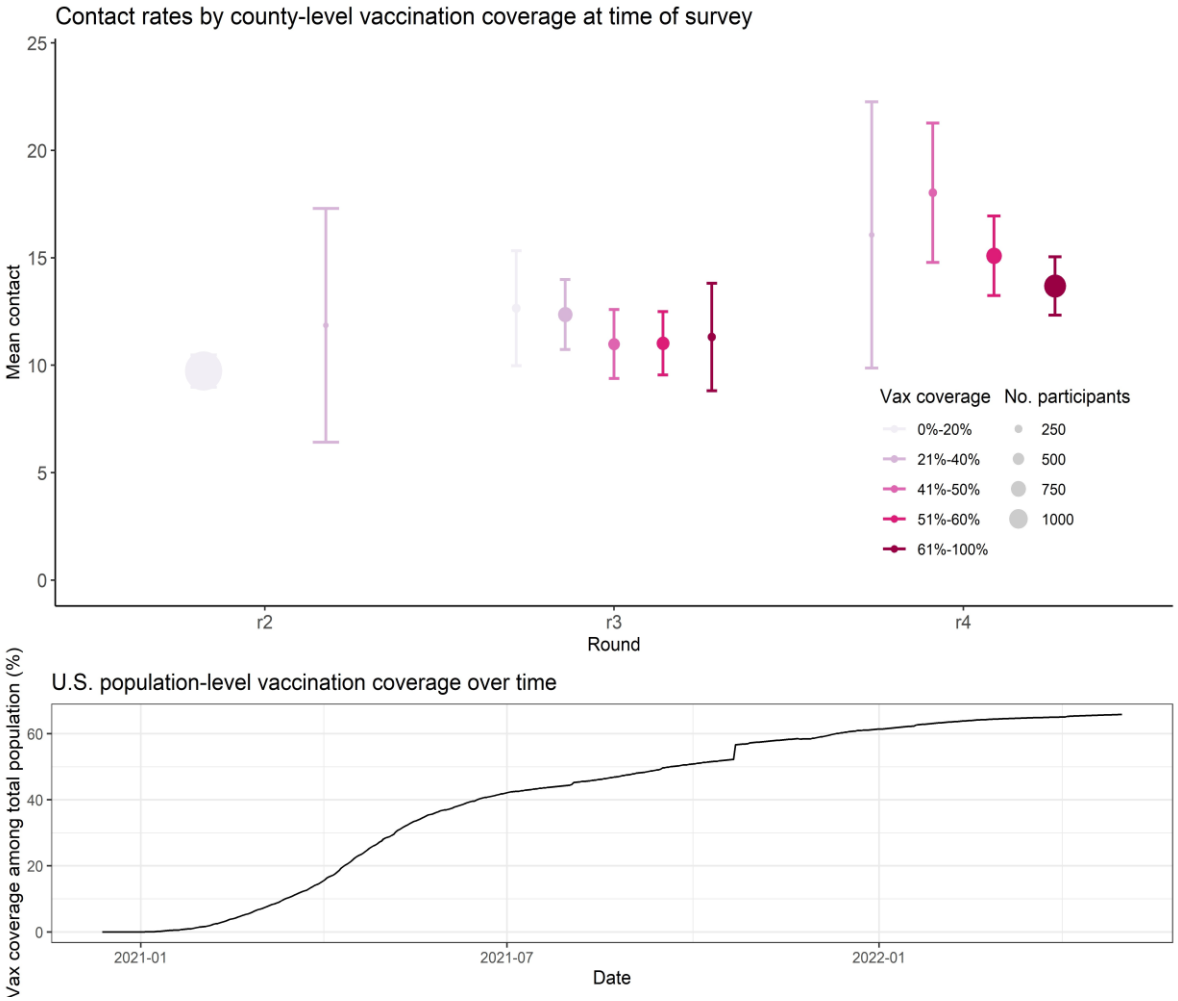

Figure 3-8. Mean contact rates over survey round by county-level vaccination coverage at time of survey

Across survey round, participants increasingly resided in counties with higher vaccination coverage, aligning with increasing vaccination from the start of vaccine rollout in January 2021 (round 2 data collection) and March 2022 (round 4 data collection). There were no clear patterns between mean contact rates and county-level vaccination coverage in rounds 2 and round 3 but by round 5, participants residing in areas with the highest vaccination coverage (>60% of total population) appeared to have the lowest mean contact.

3.7.6 Effect of vaccination on changes in location-specific contact

Covariate	Category	Change in number of contacts	
		Univariate associations	**Multivariate associations**
Intercept			5.05(0.59-9.51)
Change in vaccination status	Remain unvaxed		
	First dose new	0.4(-1.32-2.12)	0.83(-0.94-2.61)
	Newly completed series	0.19(-1.05-1.44)	0.99(-0.4-2.39)
	Already fully vaxed	1.26(0.07-2.45)	2.13(0.44-3.83)
Every 20% increase in county-level vax coverage		0.33(-0.03-0.68)	-0.26(-0.82-0.29)
Age group	18-24 yrs		
	25-34 yrs	-0.02(-2.39-2.35)	-0.26(-2.72-2.2)
	35-44 yrs	0.34(-1.99-2.67)	-0.02(-2.45-2.4)
	45-54 yrs	-0.02(-2.34-2.3)	-0.12(-2.55-2.32)
	55-64 yrs	-0.7(-2.98-1.58)	-0.92(-3.29-1.46)
	65+ yrs	-1.44(-3.68-0.8)	-1.83(-4.23-0.57)
Gender	Female		
	Male	-0.23(-1.14-0.69)	
Race ethnicity	Hispanic		
	Non-hispanic, White	-0.89(-2.3-0.52)	
	Non-hispanic, Black	-0.96(-2.77-0.85)	
	Non-hispanic, Asian	-1.5(-3.84-0.84)	
	Non-hispanic, Other	-1.97(-5.57-1.63)	
Household size	1		

	2-4	-0.02(-1.04-0.99)	-0.25(-1.29-0.79)
	5+	1.53(-0.46-3.53)	0.51(-1.62-2.63)
Political affiliation	Dem		
	Rep	-0.29(-1.6-1.02)	-0.45(-1.85-0.95)
	Ind	0.23(-1.01-1.47)	0.36(-0.91-1.62)
	Unknown	-0.59(-1.72-0.54)	-0.85(-2.05-0.34)
Employment status	Emp,in home		
	Emp,out home	-0.56(-1.79-0.66)	-0.47(-1.74-0.8)
	Unemp	-1.5(-2.73--0.26)	-0.85(-2.25-0.54)
	Unknown	0.57(-1.93-3.07)	0.16(-2.39-2.71)
Household income	$0-$24,999		
	$25,000-$74,999	0.29(-1.35-1.93)	
	$75,000-$149,999	0.06(-1.6-1.71)	
	More than $150,000	0.25(-1.58-2.07)	
Comorbidities	No		
	Yes	-0.18(-1.07-0.71)	
Risk tolerance (from Latent Class Analysis)	High		
	Med-high	-0.46(-2.14-1.23)	-0.44(-2.23-1.34)
	Med-low	-0.43(-2.11-1.25)	-0.23(-2.07-1.61)
	Low	-0.88(-2.68-0.91)	-0.98(-2.88-0.92)
Unit increase in baseline contact rates		-0.19(-0.22--0.15)	
Change in concern over pandemic	Decreased greatly		
	Decreased slightly	-0.81(-4.14-2.53)	-1.03(-4.37-2.32)
	No change	-2.32(-4.91-0.26)	-2.09(-4.7-0.51)
	Increased slightly	-3.3(-5.87--0.73)	-3.14(-5.78--0.51)

	Increased greatly	-2.87(-5.69--0.05)	-2.74(-5.64-0.16)
Unit increase in state-wide Oxford Stringency Index		-0.03(-0.06-0.01)	0(-0.05-0.05)

Table 3-12. Effect of vaccination on changes in contact at work

Covariate	**Category**	**Change in number of contacts**	
		Univariate associations	**Multivariate associations**
Intercept		0.2(0.02-0.38)	0.09(-0.77-0.95)
Change in vaccination status	Remain unvaxed		
	First dose new	0.22(-0.11-0.55)	0.17(-0.17-0.52)
	Newly completed series	-0.1(-0.33-0.14)	-0.02(-0.29-0.25)
	Already fully vaxed	-0.17(-0.39-0.06)	-0.05(-0.38-0.27)
Every 20% increase in county-level vax coverage		-0.07(-0.14-0)	0(-0.11-0.11)
Age group	18-24 yrs		
	25-34 yrs	0.18(-0.28-0.63)	0.24(-0.24-0.71)
	35-44 yrs	0.21(-0.23-0.66)	0.27(-0.2-0.74)
	45-54 yrs	0.13(-0.31-0.58)	0.19(-0.27-0.66)
	55-64 yrs	0.22(-0.21-0.66)	0.27(-0.18-0.73)
	65+ yrs	0.22(-0.21-0.65)	0.25(-0.21-0.71)
Gender	Female		
	Male	0.06(-0.11-0.24)	
Race ethnicity	Hispanic		
	Non-hispanic, White	-0.13(-0.4-0.14)	
	Non-hispanic, Black	-0.23(-0.58-0.11)	
	Non-hispanic, Asian	-0.23(-0.68-0.22)	

	Non-hispanic, Other	0.21(-0.48-0.9)	
Household size	1		
	2-4	0.01(-0.19-0.2)	0(-0.2-0.2)
	5+	0.08(-0.3-0.47)	0.09(-0.32-0.5)
Political affiliation	Dem		
	Rep	0.07(-0.18-0.32)	0(-0.27-0.27)
	Ind	0.11(-0.13-0.34)	0.08(-0.16-0.33)
	Unknown	0.12(-0.1-0.34)	0.07(-0.16-0.3)
Employment status	Emp,in home		
	Emp,out home	0.14(-0.09-0.38)	0.13(-0.11-0.38)
	Unemp	0.18(-0.06-0.41)	0.2(-0.07-0.47)
	Unknown	0.16(-0.32-0.64)	0.11(-0.38-0.6)
Household income	$0-$24,999		
	$25,000-$74,999	-0.02(-0.33-0.28)	
	$75,000-$149,999	-0.09(-0.4-0.22)	
	More than $150,000	-0.05(-0.38-0.29)	
Comorbidities	No		
	Yes	-0.01(-0.18-0.16)	
Risk tolerance (from Latent Class Analysis)	High		
	Med-high	-0.12(-0.44-0.2)	-0.08(-0.42-0.26)
	Med-low	-0.21(-0.53-0.11)	-0.17(-0.53-0.18)
	Low	-0.06(-0.41-0.28)	-0.04(-0.4-0.33)
Unit increase in baseline contact rates		-0.19(-0.23--0.16)	
Change in concern over pandemic	Decreased greatly		
	Decreased slightly	-0.36(-1-0.28)	-0.34(-0.99-0.3)

No change	-0.44(-0.93-0.06)	-0.51(-1.01-0)
Increased slightly	-0.39(-0.89-0.1)	-0.46(-0.96-0.05)
Increased greatly	-0.51(-1.05-0.03)	-0.56(-1.12--0.01)
Unit increase in state-wide Oxford Stringency Index	0.01(0-0.01)	0.01(0-0.02)

Table 3-13. Effect of vaccination on changes in contacts at other locations

Covariate	Category	Change in number of contacts	
		Univariate associations	Multivariate associations
Intercept			1.13(-1.39-3.65)
Change in vaccination status	Remain unvaxed		
	First dose new	0.03(-0.94-1)	-0.01(-1.01-0.99)
	Newly completed series	1.02(0.32-1.72)	0.94(0.16-1.73)
	Already fully vaxed	0.61(-0.05-1.28)	0.5(-0.45-1.46)
Every 20% increase in county-level vax coverage		0.06(-0.14-0.26)	-0.14(-0.45-0.17)
Age group	18-24 yrs		
	25-34 yrs	0.46(-0.87-1.79)	0.48(-0.91-1.87)
	35-44 yrs	0.85(-0.46-2.16)	0.91(-0.45-2.28)
	45-54 yrs	0.71(-0.6-2.01)	0.89(-0.48-2.26)
	55-64 yrs	0.9(-0.38-2.18)	1.13(-0.21-2.47)
	65+ yrs	1.49(0.23-2.75)	1.58(0.22-2.93)
Gender	Female		
	Male	0.08(-0.43-0.6)	
Race ethnicity	Hispanic		
	Non-hispanic, White	0.4(-0.39-1.19)	
	Non-hispanic, Black	0.13(-0.89-1.15)	
	Non-hispanic, Asian	-0.32(-1.63-1)	
	Non-hispanic, Other	-0.08(-2.1-1.95)	
Household size	1		
	2-4	0.2(-0.37-0.78)	0.37(-0.22-0.96)
	5+	0.42(-0.7-1.55)	0.74(-0.46-1.94)

Political affiliation	Dem		
	Rep	0.73(-0.01-1.47)	0.42(-0.37-1.21)
	Ind	0.31(-0.39-1)	0.22(-0.49-0.93)
	Unknown	0.39(-0.24-1.03)	0.44(-0.24-1.11)
Employment status	Emp,in home	0.46(-0.1-1.03)	
	Emp,out home	0.08(-0.61-0.77)	-0.04(-0.75-0.68)
	Unemp	0.45(-0.25-1.14)	0(-0.79-0.79)
	Unknown	0.4(-1.01-1.8)	0.23(-1.21-1.66)
Household income	$0-$24,999	0.42(-0.36-1.2)	
	$25,000-$74,999	0.24(-0.66-1.14)	
	$75,000-$149,999	0.31(-0.6-1.23)	
	More than $150,000	0.48(-0.53-1.49)	
Comorbidities	No	0.62(0.26-0.98)	
	Yes	0.1(-0.39-0.6)	
Risk tolerance (from Latent Class Analysis)	High	1.23(0.38-2.08)	
	Med-high	-0.74(-1.69-0.2)	-0.8(-1.81-0.21)
	Med-low	-0.46(-1.4-0.48)	-0.66(-1.7-0.38)
	Low	-0.63(-1.64-0.37)	-0.66(-1.73-0.41)
Unit increase in baseline contact rates		-0.21(-0.25--0.16)	
Change in concern over pandemic	Decreased greatly	1.82(0.42-3.22)	
	Decreased slightly	-1.06(-2.94-0.83)	-0.92(-2.8-0.97)
	No change	-1.11(-2.57-0.36)	-1.1(-2.57-0.37)
	Increased slightly	-1.33(-2.79-0.12)	-1.23(-2.72-0.26)
	Increased greatly	-0.7(-2.3-0.89)	-0.65(-2.28-0.99)
Unit increase in state-wide Oxford Stringency Index		-0.02(-0.03-0)	-0.02(-0.04-0.01)

Table 3-14. Effect of vaccination on changes in contacts at home

3.7.7 Sensitivity analysis

3.7.7.1 Effect of vaccination on changes in all contacts without concern for new variants

Covariate	Category	Change in number of contacts	
		Univariate associations	**Multivariate associations**
Intercept			2.44(-1.91-6.78)
Change in vaccination status	Remain unvaxed		
	First dose new	0.59(-1.46-2.64)	1.08(-1.01-3.17)
	Newly completed series	1.11(-0.37-2.58)	1.66(0.03-3.3)
	Already fully vaxed	1.9(0.48-3.31)	2.69(0.69-4.7)
Every 20% increase in county-level vax coverage		1.4(0.98-1.82)	-0.01(-0.07-0.05)
Age group	18-24 yrs		
	25-34 yrs	0.1(-2.71-2.92)	0.05(-2.81-2.92)
	35-44 yrs	0.88(-1.88-3.65)	0.64(-2.19-3.46)
	45-54 yrs	0.26(-2.5-3.02)	0.24(-2.59-3.08)
	55-64 yrs	-0.15(-2.86-2.56)	-0.09(-2.87-2.68)
	65+ yrs	-0.39(-3.06-2.27)	-0.6(-3.41-2.21)
Gender	Female		
	Male	-0.08(-1.16-1.01)	
Race ethnicity	Hispanic		
	Non-hispanic, White	-0.67(-2.35-1.01)	
	Non-hispanic, Black	-1.13(-3.29-1.02)	
	Non-hispanic, Asian	-1.95(-4.72-0.83)	

	Non-hispanic, Other	-2.01(-6.28-2.27)	
Household size	1		
	4-Feb	0.25(-0.95-1.46)	0.16(-1.08-1.39)
	5+	2.4(0.03-4.77)	2.18(-0.31-4.67)
Political affiliation	Dem		
	Rep	0.47(-1.09-2.03)	0.56(-1.09-2.21))
	Ind	0.67(-0.8-2.15)	0.82(-0.68-2.31)
	Unknown	0.47(-1.09-2.03)	0.15(-1.25-1.55)
Employment status	Emp,in home		
	Emp,out home	-0.33(-1.78-1.13)	-0.53(-2.04-0.97)
	Unemp	-0.91(-2.38-0.56)	-0.79(-2.44-0.87)
	Unknown	1.07(-1.9-4.04)	1.07(-1.94-4.08)
Household income	$0-$24,999		
	$25,000-$74,999	0.44(-1.5-2.37)	
	$75,000-$149,999	0.16(-1.8-2.12)	
	More than $150,000	0.55(-1.61-2.71)	
Comorbidities	No		
	Yes	-0.18(-1.23-0.88)	
Risk tolerance (from Latent Class Analysis)	High		
	Med-high	-1.35(-3.35-0.65)	-1.6(-3.69-0.49)
	Med-low	-1.08(-3.08-0.92)	-1.25(-3.4-0.9)
	Low	-1.61(-3.74-0.53)	-1.85(-4.06-0.37)
Unit increase in baseline contact rates		-0.16(-0.2--0.13)	
	Increased greatly		

	Increased slightly	-2.3(-6.25-1.66)	
Change in concern	No change	-4.07(-7.14--1)	
over pandemic	Decreased slightly	-5.35(-8.4--2.3)	
	Decreased greatly	-4.46(-7.82--1.11)	
Unit increase in state-wide Oxford Stringency Index		-0.04(-0.08-0)	-0.17(-0.82-0.48)

Table 3-15. Effect of vaccination on changes in contact without adjusting for concern for new variants

3.7.7.2 Sensitivity analysis on contact outlier cutoff

While we used the 99th percentile to right truncate responses on number of contacts per location and age group, previous studies chose 100[197,210] or 450 contacts as the cutoff[202]. We chose the 99th percentile for our main analysis to remove only the most extreme outliers that were least likely to be accurate and to increase the absolute truncation thresholds across the rounds as social distancing relaxed and individuals were more likely to truly have high numbers of contact. For sensitivity analysis, we considered other truncation criteria of 1) 95th percentile; 2) 97.5th percentile and 3) 100 contacts per location. The truncation thresholds used for each round and location can be found in table below). Results for the main model with sensitivity analysis on choice of right truncation and be found in Figure 7.

		Truncation value for various percentiles			**No. reporting more than 100 contacts**
Survey round	**Contact location**	**95th**	**97.5th**	**99th**	
Round 1	Home	6	10	13.98	2
Round 1	Other	11	19	35	4
Round 1	School	0	0	5	0
Round 1	Work	23	45	89.96	21
Round 2	Home	7	10	22.98	1
Round 2	Other	12	21	47.98	7
Round 2	School	0	0	6.98	2
Round 2	Work	26.9	49.9	116.92	28
Round 3	Home	7	10	19.98	1
Round 3	Other	18	29.9	66.92	12
Round 3	School	0	0	4	1
Round 3	Work	30	54.95	119.9	30
Round 4	Home	8	10	22.96	5

Round 4	Other	20	34	73.96	17
Round 4	School	0	5	23.98	6
Round 4	Work	42.9	77	142.98	43

Table 3-16. Cutoff values for various right truncation methods to remove extreme outliers in contact numbers

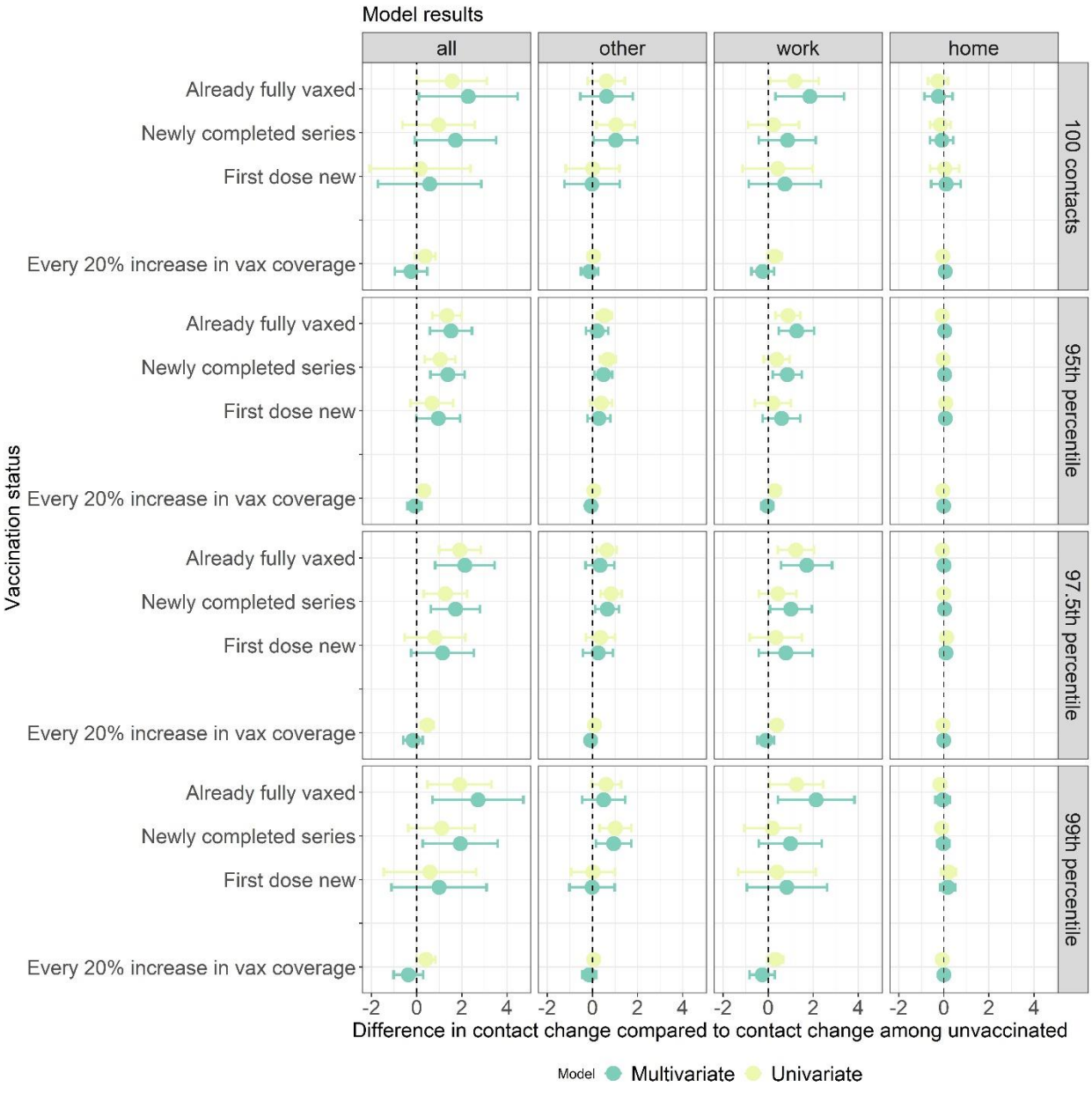

Figure 3-9. Plot of model results for main analysis comparing different right truncation choices

3.7.8 Additional Next Generation Matrix analysis on impact on transmission

For each level of vaccination coverage and for each round, we perturb the Next Generation Matrix by allowing for increasingly assortative mixing where vaccinated individuals mix more preferentially with other vaccinated individuals and unvaccinated individuals mix more preferentially with other unvaccinated individuals. We quantify the extent of assortativity with the Q index, which is calculated as Q = [Tr(P)-1]/(n-1), where P is a matrix with elements of $P_{ij} = M_{ij} / \sum_j M_{ij}$ is the matrix of average contacts between vax groups[223,224]. Tr(P) is the trace of the matrix or the sum of its diagonals and n is the number of subgroups (n=2). The Q index is 0 when mixing between subgroups is completely proportional and 1 when mixing is completely assortative (vaccinated individuals only contact other vaccinated individuals).

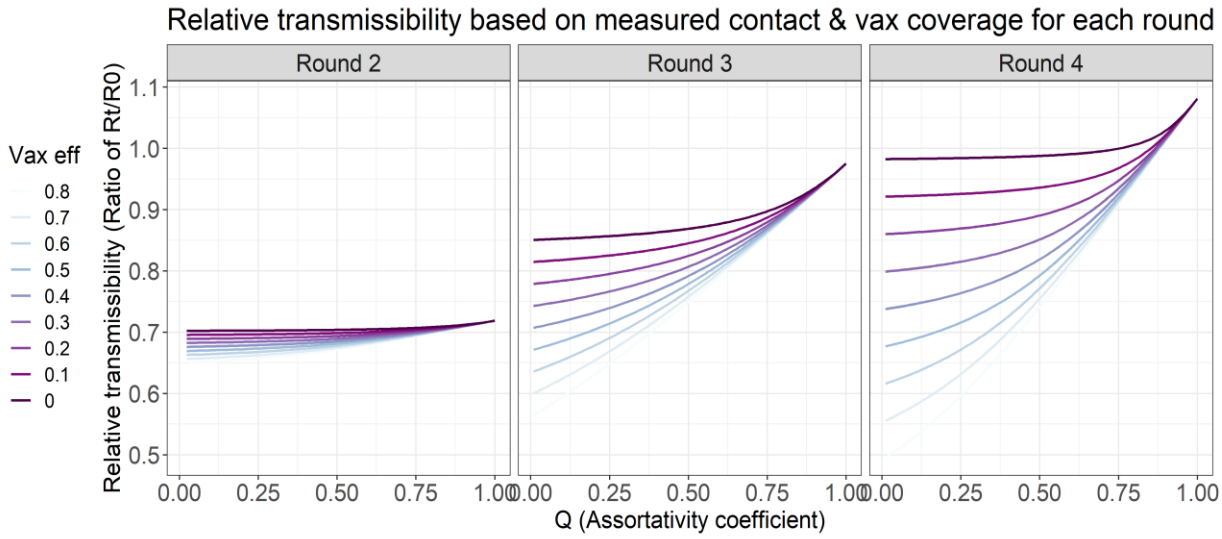

Figure 3-10. Relative transmissibility calculated using the Next Generation Matrix

Relative transmissibility (Rt/R0) calculated using the Next Generation Matrix (see methods section in main paper) based on measured contact in vaccinated and unvaccinated individuals in each round and overall vaccine coverage in the US, sweeping over a range of vaccine effectiveness against susceptibility

and assortativity coefficient (Q=0 for proportional mixing based on vaccine coverage, Q=1 for assortative mixing where vaccinated individuals only mix with other vaccinated individuals and unvaccinated individuals only mix with other unvaccinated individuals). From round 2 (March-April, 2021) to round 4 (March-April, 2022), the average daily contact rates among vaccinated individuals were 9.2, 11.6 and 14.9; average daily contact rates among unvaccinated individuals were 11.5, 15.6, 17.3 and the primary series vaccine coverage in the U.S. was 11.5%, 49.8% and 65.9%. As contact rates increased across survey rounds, relative transmissibility increased even as more individuals in the population became vaccinated. We find the relative transmissibility increases as the population mixes more assortatively (increasing Q values) and that with fully assortative mixing (Q=1), the relative transmissibility converges regardless of the vaccine effectiveness.

CHAPTER 4 METAPOPULATION MODEL TO QUANTIFY TRANSMISSION

[Manuscript 2]

Integrating multi-dimensional data streams to infer spatial patterns of transmission across waves of COVID-19 in Georgia, USA

Carol Y Liu, Kristin Nelson, Samuel M Jenness, Stefan Flasche, Benjamin A Lopman, Max SY Lau

4.1 Abstract

Spatial patterns of transmission in a highly interconnected spatial network of communities with heterogeneous demography, dynamically changing immunity levels and within-community contact rates, remain to be characterized. We infer spatial patterns of transmission across waves of COVID-19 in Georgia, USA through a novel mathematical framework with a multilayered transmission process and informed by spatiotemporally resolved data on social contact, human mobility, and vaccination. We find that in counties with smaller populations, lower contact rates and higher vaccination coverage, intercounty mobility contributes to a higher proportion of onward transmission. In addition, we present evidence that in an interconnected spatial network with a patchwork of local uptake in mitigation measures, the net infection flow is still from counties with lower mitigation to counties with higher mitigation. Identifying sources and sinks of transmission and their correlates can guide more localized interventions and assist in the mitigation of infection spread.

4.2 Introduction

Human mobility plays an important role in determining spatial patterns of infectious disease transmission. Specifically, human movement determines the frequency of contacts between susceptible and infected individuals within a community and the rate of importations from other communities[225]. Uptake of mitigation policies in one community not only affects transmission within its boundaries but can also impact the epidemic trajectory of other mobility-linked communities, giving rise to sources and sinks of

infection. Traditionally, infections are hypothesized to flow from source locations with fewer mitigation and lower vaccination coverage (i.e., net exporters) to sink locations with more mitigation measures and higher vaccination coverage[145–148] (i.e., net importers). Additionally, the mechanism of spatial hierarchical spread, which predicts travelling waves from source regions with higher population density to sink regions with lower population density, is often assumed[143]. However, in a highly interconnected spatial network of communities with heterogeneous demography, dynamically changing immunity levels and within-community contact rates, the impact of intercounty mobility on local transmission intensity and the directionality of infection flows between locations remains to be characterized.

Novel time- and space- resolved data on human behavior can be integrated with routine surveillance and vaccination data for more nuanced understanding of spatial patterns of infection transmission. During the COVID-19 pandemic, data on social contact patterns and human mobility emerged as two information sources that readily captured rapid fluctuations in human behavior and generated crucial epidemiological insights on transmission[63,65,110,226]. Information on human-to-human interactions derived from social contact surveys facilitated the estimation of the time-dependent reproductive number, R_t[200,215]. Global Positioning System (GPS) location data from smartphone devices were used to passively captured contemporaneous, granular changes in population-level mobility flows and informed spatial patterns of transmission in multiple countries[54,91,92,95,97].

Metapopulation models enable the integration of these multiple data streams across different spatiotemporal scales into a unified modeling framework to capture multiscale transmission dynamics. In this framework, individuals are partitioned into geographical units within which contact is frequent and between which contacts are less frequent. Metapopulation models with simple Susceptible-Exposed-Infectious-Recovered disease states were deployed extensively to capture early dynamics of SARS-CoV-2 transmission. Yet few such models extend into the post-vaccination period, where the need to represent dynamically changing immunity and behavior increases model complexity.

The state of Georgia, USA, with its diverse demographics, varying levels of urbanization and highly heterogeneous COVID-19 containment policies presents a unique case study for examining these dynamics. In Georgia, the COVID-19 pandemic unfolded in an asynchronized mosaic of localized transmissions characterized by surges varying in timing and intensity during the first two years, increasingly shaped by fluctuations in human behaviors and population-level immunity. To jointly capture these changes and explore their impact on spatial patterns of transmission, we designed a metapopulation modeling framework that readily integrates space and time-resolved data streams of social contact, human mobility and changing immunity. The model was formulated with a multilayered transmission process decomposed into household, local and non-local components, allowing for the explicit quantification of the relative contribution of local dynamics versus imported infections on overall incidence and for the inference of the directionality of county-level infection flow. Identifying sources and sinks of transmission and their correlates can guide more localized interventions and assist in the mitigation of infection spread.

4.3 Methods

4.3.1 Model structure

We extended a previously published stochastic Susceptible-Exposed-Infectious-Recovered (SEIR) model inference framework[227,228] into a metapopulation framework for the state of Georgia, USA. We partitioned the population of Georgia into weakly interacting counties and three age groups within each county. The transmission process of the model system was represented on a matrix of three age groups (0-17 years, 18-64 years, and 65 years and above) multiplied by 159 counties. Each age group within each county can infect all other age groups of other counties based on a two-layered infection network informed by age-specific contact rates, derived from data collected during the pandemic[72,112] and mobility patterns derived from mobile app-based GPS location data[63–65,103]. A stochastic SEIR-like model captured the relevant disease states, where, upon exposure, susceptible individuals enter a latent, non-infectious period (E), after which they become either reported (I) or unreported (U) based on the age-specific proportion of

unreported infections P_{u_i}, before recovering (R). After a period of immunity (w_r days), individuals transition into a partially susceptible class (Figure 4-1). Population-level susceptible for each county is dynamic over time. Susceptibility decreases following periods of concerted vaccination efforts or periods of intense transmission and subsequently increases as protection from immunizing events wane over time. We succinctly capture changing population-level susceptible for each county informed by triangulating data from vaccination and infection from Georgia's case and vaccination surveillance system[229–231].

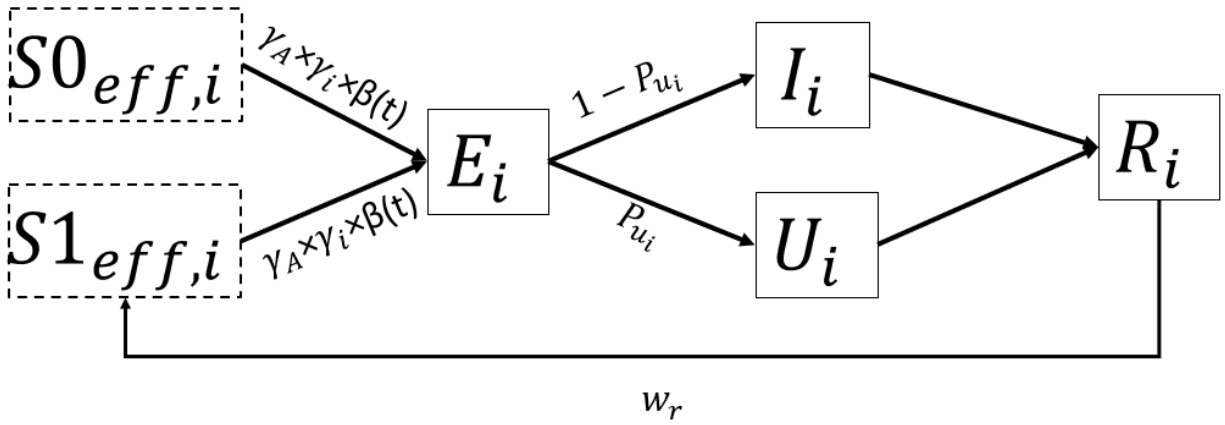

Figure 4-1. Schematic of within-county transmission process[1]

[1]Model with the following disease classes: the disease classes are as follows: S0 (susceptible individuals with no prior infection), S1 (susceptible individuals with one or more prior infection), E (latent infection, exposed but not yet infectious), U (infectious and unreported), I (infectious and reported as a case) and R (recovered and temporarily immune). $\Upsilon_A \times \Upsilon_i \times \beta(t)$ is the probability of transmission upon contact with Υ_A (fitted) being county-strata dependent susceptibility Υ_i (fitted) being age-dependent susceptibility, and $\beta(t)$ (fitted) a scaled to the pathogen transmissibility of the dominant variant for each wave (three waves in the study period). P_{u_i} is an age-dependent probability of underreporting (informed by data), w_r is waning immunity for individuals with infection-derived immunity. The time step t is in days.

4.3.2 Infection process

The infection process for susceptible individuals in age group i at time t in county A is decomposed into three components: 1) within-county household component; 2) within-county non-household component; and 3) between-county non-household component (Eq 3). All infectious individuals (either reported in class I or unreported in class U) contribute to transmission within their household based on the within household contact rate ($c^{j,i}{}_{A,HH}(t)$), parameterized by the term $\sum_{j=1}\beta \times c^{j,i}{}_{A,HH}(t) \times \{I^{j}{}_{A}(t-1) + U^{j}{}_{A}(t-1)\}$. Infected individuals who travel outside of their home contribute to either transmission within their county or in another county, parameterized by the term $\sum_{j=1}\beta \times c^{j,i}{}_{A,NH}(t) \times \sum_{B} m^{j}_{B\to A}(t-1)$. $c^{j,i}{}_{A,NH}(t)$ is the average number of non-household contacts per day made by age group j to i and $\sum_{B} m^{j}_{B\to A}(t-1)$ sums all the outflowing infections from age group j at time t based on all other counties where mobility between B→A is observed, including those who moved outside of the home but within their own county, where A=B (details in section below).

The infection process is further modified by three key fitted parameters: Υ_{A}, a county-dependent susceptibility based on eight population strata, introduced to broadly capture spatial heterogeneities in behavior such as masking and distancing beyond contact rates alone; Υ_{i}, an age-dependent susceptibility, and β(t), the per contact probability of infection, scaled to the pathogen transmissibility of the dominant variant for each wave. The following equation summarizes the number of new infections from the susceptible class with no prior exposure (S0) that transition into the exposed class (E):

$$n^{i}_{S0E_{A}}(t) \sim Poi\left(S0^{i}_{A}(t-1) \times \Upsilon_{A} \times \Upsilon_{i} \times \{\sum_{j=1}\beta(t) \times c^{j,i}{}_{A,HH}(t) \times \left(I^{j}{}_{A}(t-1) + U^{j}{}_{A}(t-1)\right) + \sum_{j=1}\beta(t) \times c^{j,i}{}_{A,NH}(t) \times \sum_{B} m^{j}_{B\to A}(t-1)\}/N^{i}_{A} \right) \quad \text{Eq 3}$$

where i denotes the age group of the susceptible class, j denotes the age group of the infectious class, A denotes the susceptible county being infected, B denotes the infecting county and t is time in days.

4.3.3 Parameterizing between-county transmission

Individuals can move between counties based on mobility networks derived from smartphone app-based GPS location. The outflow of infections from county B to county A for age group j ($m^{j}_{B\to A}$) was parameterized using the following equation:

$$m(t)^{i}_{B\to A} \sim Bin\left[I(t)^{j}_{B} + U(t)^{j}_{B}, \delta(\mathrm{t})_{c} \times \frac{n(t)_{BA}}{\sum_{B=1}^{c} n(t)_{BA}}\right] \qquad \text{Eq 4}$$

where I^{j}_{B} and U^{j}_{B} are the number of daily infectious individuals, reported and unreported respectively, from county B, age group j. $n(t)_{BA}$ is the daily number of unique visitors from county B to county A and $\sum_{B=1}^{c} n(t)_{BA}$ is the sum of all daily movements out of county B to c other counties, both derived from a commercialized aggregator of mobility data, SafeGraph[86]. δ_{c} is the county-specific probability of leaving their home, estimated from a separate mobility data aggregator, Cuebiq[87]. In this framework, infectious individuals within county B at time t is split into 1) a group that stays at home, 2) a group that leaves their home and moves to other locations within their home county 3) a group that moves to other counties, with the latter two groups informed by an origin-destination matrix generated from SafeGraph.

4.3.4 Key model inputs for transmission process

4.3.4.1 Age-specific contact rates

Contact rates likely varied at the local county-level and over time during the pandemic; however, time-resolved, county-level data on age-specific contact rates is rare. We draw on a several data sources in order to capture variations in age-specific contact rates by county and over time using the following data sources: DELPHI group's COVID-19 Trends and Impact Surveys (CTIS)[232], Berkeley Interpersonal Contact Study[77] (BICS) and projected contact rates from Prem et al[60].

The COVID-19 Trends and Impact Survey (CTIS) randomly sampled active Facebook users in the US to collect data on COVID-19 symptoms, testing and preventive behaviors on a daily basis. Between April 2020 and April 2021, the survey asked participants to estimate the number of people outside of their household with whom they had direct contact with, at 1) work; 2) shopping for groceries and other

essentials; 3) social gatherings; and 4) other. The survey defines a direct contact as "a conversation lasting more than 5 minutes with a person who is closer than 6 feet away from you, or physical contact like hand-shaking, hugging or kissing"[232]. In Georgia, the monthly sample sizes with valid responses for the questions on non-household contacts range from 5000 to 48,234. We weighed responses to account for survey design and to provide adjustments for non-response and coverage errors[233].

We considered the 97.5th percentile of contacts reported for each county, month and location as extreme outliers, comparable to previous online surveys of contact rates[71,110,234], and right truncated the contact rate at this threshold. We sum the contacts from the four locations for the total number of non-household contacts per participant and aggregate by county, month, and age group. To smooth over sampling errors from small numbers by borrowing information from neighboring counties, we fit a Bayesian generalized linear mixed model (GLMM) with a spatiotemporal autoregressive process and a piecewise constant intercept term. The model included several county-level covariates associated with contact rates: the urban-rural continuum code classified by U.S. Department of Agriculture[235], percentage of black inhabitants and percentage of trump vote share[236].

Outputs of average contact rates per person per day from the GLMM model were then projected onto a Georgia state age-specific contact matrix derived from multilevel regression with poststratification from the BICS survey on contact patterns[77,237]. For example, if the overall daily non-household contact rate made by 18–64-year-olds in a single county was estimated as 15 contacts per person per day from CTIS, we then assigned the 15 contacts to recipient age groups based on the age structure of the county and on the average age-specific mixing patterns from Georgia. Since CTIS did not sample children, we assumed symmetrical mixing patterns and took the weighted reciprocal for contacts made by 0–17-year-olds with 18–64-year-olds and 65+ year olds. For contacts made between 0–17-year-olds and other 0–17-year-olds, we applied a county-level scaling factor to the estimated Georgia average from BICS. Lastly, we modeled a recovery process where contact rates gradually recovered to pre-pandemic estimates[60] starting in January 2021 when schools were increasingly in-person for the spring semester[238].

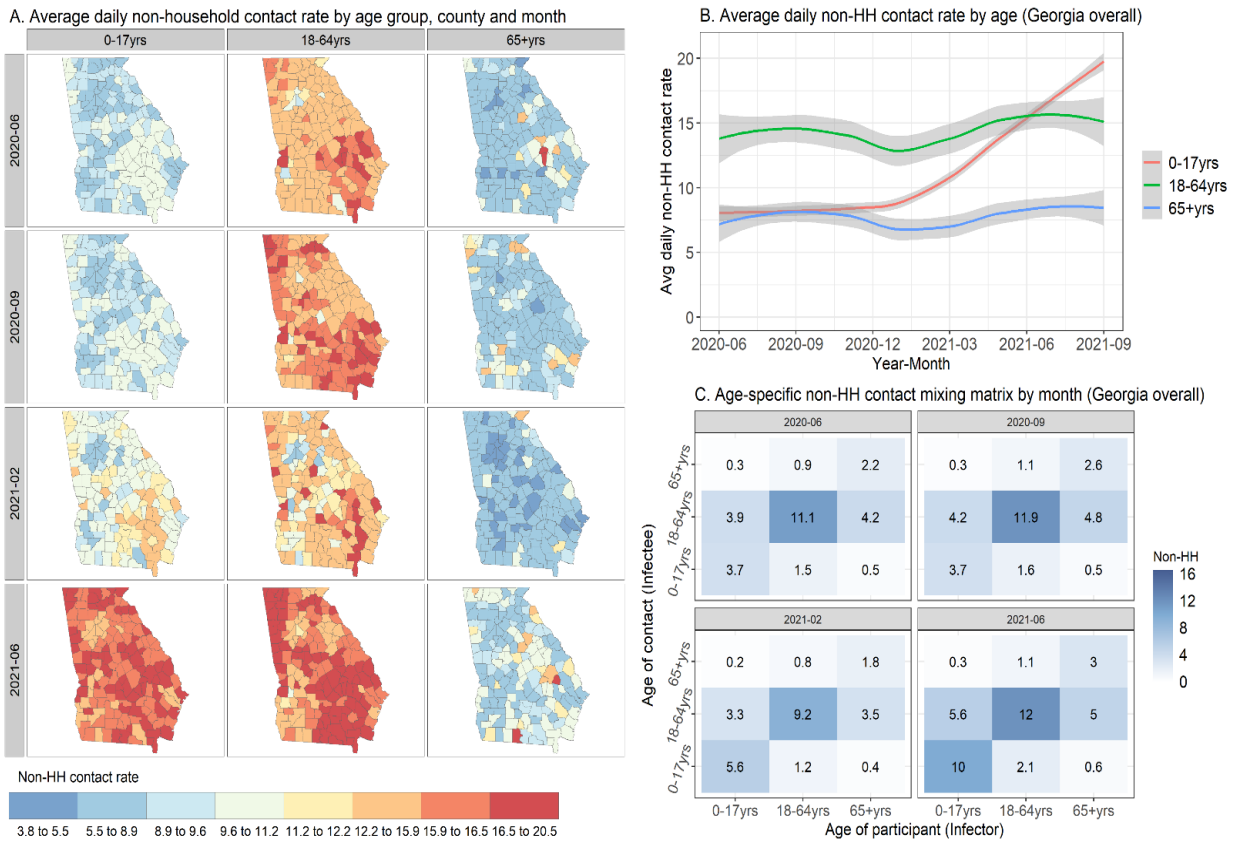

Figure 4-2. Summarizes non-household age-specific contact rates by county, age group and over time that were inputs into the metapopulation model

4.3.4.2 Origin-destination matrices

We primarily used SafeGraph to construct county-level origin-to-destination matrixes. SafeGraph provides anonymized cell phone-based geolocation data from anonymous mobile phone users in the United States[101]. The dataset includes traffic from around 47M mobile phone devices (~10% of all devices in the U.S.). Data are captured when geolocation is enabled for specific, but undisclosed, smartphone mobile applications. Devices represented in the SafeGraph data are assigned to a home census block group (CBG) based on its most common nighttime (6pm-7am local time) location during the previous six weeks[86]. To protect privacy, the data itself is pre-aggregated into a weekly visit and visitor count to points-of-interest (POI), which can be further stratified into weekly CBG-POI visitor flows. POIs are public locations designated by SafeGraph such as stores, schools, parks, health facilities, offices, hotels

etc[239], bounded by a polygon. Devices are counted as visiting a POI when a ping is captured within the polygon with a dwell time of longer than four minutes. Mobility counts were inverse-weighted based on weekly, CBG-specific sampling fraction and origin CBGs with sampling fraction.

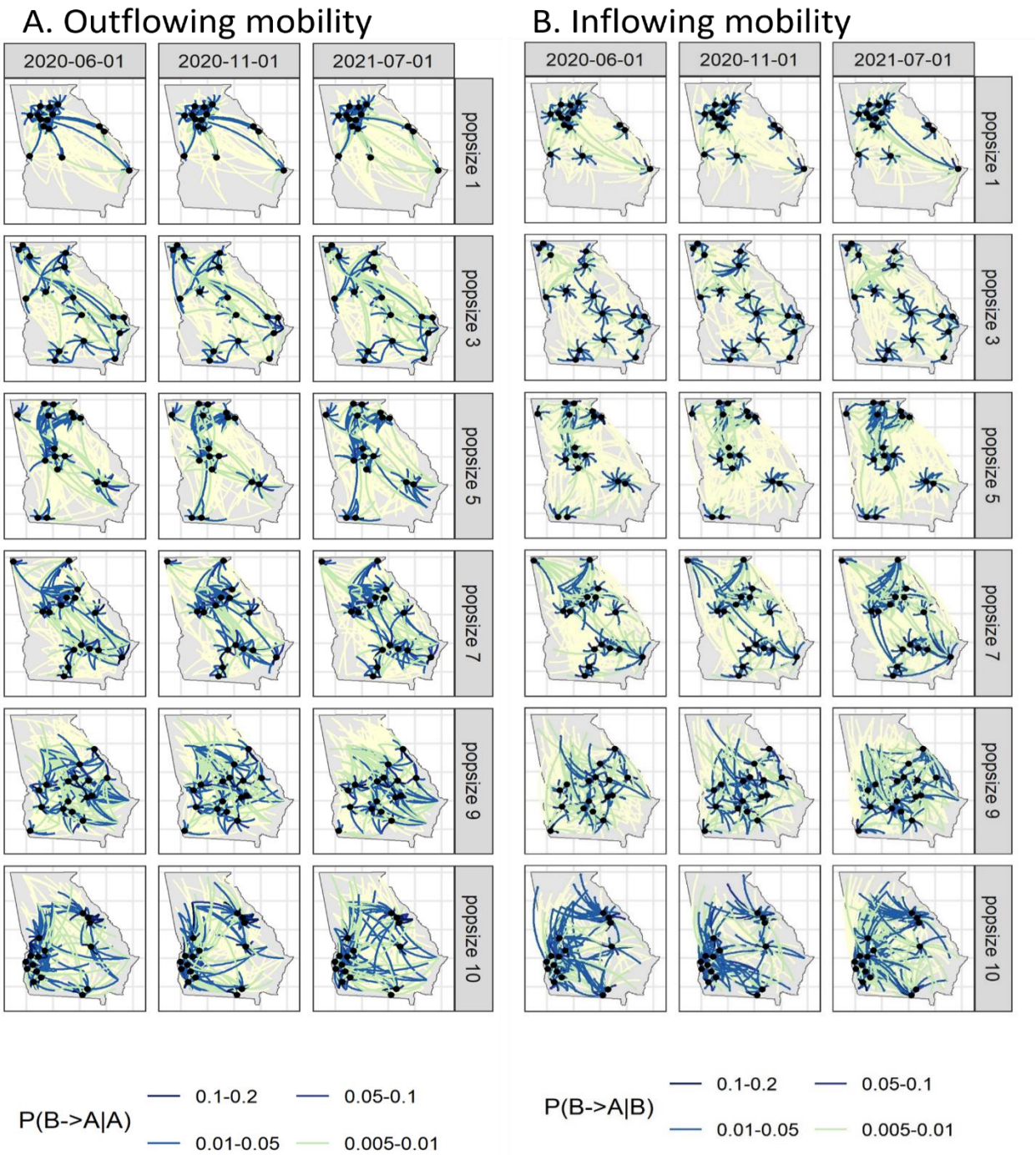

Figure 4-3. Visualization of outflowing and inflowing mobility.

A. Visualization of outflowing mobility from counties of varying population sizes (probability of trip from origin county B to destination county A out of all trips originating from county B). B. Visualization of inflowing mobility from counties of varying population sizes (probability of trip from origin county B to destination county A out of all trips into destination county A).

>100% were removed and aggregated into weekly origin-to-destination (O-D) population flows at the county level, reflecting the number of trips between a device's home county (county A) and the county of the destination POI (county B) per day. In the model equations, the O-D matrix of trip counts is then converted into a daily probability of travel from county A to county B given residence in county A (Eq 4).

The available SafeGraph data product did not account for individuals who did not leave their homes. We expect the proportion of individuals who left their home to differ by county and over time during the pandemic and integrate this probability into (Eq 4). We use a secondary mobility data product from Cuebiq to calculate a daily probability of a resident of county A leaving their home. Similar to SafeGraph, Cuebiq also aggregated anonymized cell phone-based geolocation data during the pandemic and provided a daily estimate of a county-level proportion of devices captured through their platform that remained home.

4.3.4.3 Representing changing susceptibility

We mathematically account for decreasing susceptibility following combinations of both vaccination and infection in a parsimonious way without introducing additional compartments. Individuals in the S0 (fully susceptible, no prior exposure) state are partitioned into six different mutually exclusive states based on combinations of prior infection and vaccination and time since last immunizing event: 1) V0 (unvaccinated); 2) $V1_{21+days}$ (21 days or more after first dose, but no second dose or second dose within 14 days); 3) $V2_{14\text{-}133days}$ (14-133 days after second dose, no additional doses); 4) $V2_{134\text{-}193days}$ (134-193 days after second dose, no additional doses); 5) $V2_{194+days}$ (194 days after second dose, no additional doses); 6) V3+ (more than two doses).

For each county A, age group i, at each time step t, we calculate an "effective" S0 that accounts for the distribution of vaccination states within S0 individuals (no prior infection) and their respective differences in susceptibility. The same is done for the S1 state (one or more prior infection). A multinomial random draw was used to sample the number of susceptible individuals in each vaccination state (as above). The following is the equation:

$$S0_{eff,i=} \sum_{V=v} [Multinomial(S0_i, P_{S0,V=v,i,A})] \times \sigma_{S0,V=v} \quad \text{Eq 5}$$

Where $S0_{eff,i}$ is the "effective" number of susceptible individuals with no prior infection in age group i, $N_{S0,i}$ is the total number of susceptible individuals with no prior infection in age group i and $P_{sv,i,A}$ is a vector of the probability distribution for the susceptibility states for each age group i and county A, and $\sigma_{S0,V=v}$ is reduced susceptibility for each of the states (4.7.2.2 lists the values inferred from the literature[51]). $P_{sv,i,A}$ is calculated for each age group i, county A and time t from vaccination and case data from Georgia. In the model implementation, we combine the calculation of "effective" numbers for $S0_{eff,I}$ and $S1_{eff,I}$ and the probability distribution is a joint probability distribution between the S and V states. To calculate, $P_{sv,i,A}$, we use a combination of lab-confirmed reported case data from Georgia Department of Public Health State Electronic Notifiable Disease Surveillance System (GDPH SENDSS) and from the Georgia Immunization Registry (GRITs). The linked dataset from GDPH SENDSS and GRITs allows us to estimate the proportion of individuals in each vaccination tier (unvaccinated, one dose, two dose, two dose and waned etc) and among each vaccination tier, the proportion with prior infection. We further account for underreporting through an age-specific underreporting informed by state-level seroprevalence and state-level reported cases to date and available literature (Eq 20; 4.7.6)

4.3.5 Model initialization

We initialize the age structure across three age groups (0-17 years, 18-64 years and 65 years and above)[236]. We stratify PCR lab-confirmed reported cases using the GDPH SENDSS data by county, age

group and day of positive test to estimate the infection prevalence (E, I and U compartments) and the number of immune individuals (R compartment) at start of model simulation (June 1st, 2020). Since the I compartment represents reported cases and with a 7-day infectious period and 7-day incubation period, we consider the number of reported cases between June 1st and May 26th, 2020, as infectious, reported, and symptomatic and those reported between June 2nd-June 8th as exposed and incubating. For the U compartment, we apply a similar age-specific underreporting as was done to infer immunity from reported cases and vaccinations. For the R compartment, we consider the number of reported cases between March 2nd, 2020 (date of first reported case in Georgia) and May 25th, 2020, and apply the same age-specific underreporting rate to estimate the number of recovered and immune individuals (Eq 20).

4.3.6 Model calibration

The model was run from June 2020 to Nov 2021, chosen to allow for enough variation in mobility, transmission, and vaccination while having comparable test reporting. In Georgia, testing criteria was initially restricted and tests did not become widely available until June 2020. In the fall of 2021, near ubiquitous availability of at-home testing likely drastically decreased the proportion of infections that were reported through the state surveillance system.

We proposed a set of parameters for calibration related to the probability of transmission (β), relative susceptibility among different age groups and groupings of counties by population size, and changes in probability of transmission over different waves of the pandemic. Counties were grouped into seven categories based on population size (4.7.3.2): six categories grouped by population sizes with the largest group further stratified by metro Atlanta and non-metro Atlanta. The categorization of counties allowed for additional flexibility to capture relative susceptibility due to differential policies and adherence to guidance on masking and social distancing. The population sizes of counties in the lowest category (pop size 7) ranged from 1500 to 8700 and the population sizes counties in the highest category with metro Atlanta (pop size 1) ranged from 100,000 to 1 million (metro Atlanta).

We calibrated the model using an Approximate Bayesian Computation (ABC) rejection algorithm[240]. Parameter sets Θ* were sampled from uniform prior distributions p(Θ) bounded by a minimum and maximum using Latin Hypercube Sampling[241] and then used as inputs for the model simulation (4.7.3). The parameter set Θ* is accepted if the distance between empirical data D and the model simulated data D* is less than a pre-specified threshold ϵ. The process is repeated until 1000 parameter sets were accepted. We chose several summary statistics, each with a separate threshold, to improve the model fit across age and county strata over waves. The distance measures used as criteria were square root of the sum of squared differences of 1) the number of daily, age-stratified reported cases (0-17 years, 18-64 years and 65 years and older); 2) the number weekly reported cases stratified by eight county-level population sizes; 3) the peak number of overall state-wide reported cases for the third wave. We use an intersection metric with a binary indicator where all criteria must be satisfied for the parameter set to be accepted. The tolerance levels were selected to reduce the inter-quartile range of model parameters and for a reasonable acceptance probability (4.7.3.1).

4.4 Results

4.4.1 Results from model calibration

We achieved 1000 accepted parameter sets after over 1.2 million parameter sets were sampled for an acceptance probability of 0.000821. Density plots of the posterior distributions and the ranges of accepted parameters can be found in 4.7.3.4. We find the model was able to generally reproduce epidemic patterns across three age groups and 159 counties and over multiple epidemic waves (Figure 4-4; Figure 4-9). Using the rejection algorithm, adults and older adults were more susceptible to infection than children, with medians of 1.7- and 2.3-times increased susceptibility. Counties with smaller population sizes have slightly higher susceptibility. The probability of transmission is 1.086 times higher for wave 2 compared to wave 1 and 1.9 times higher for wave 3 compared to wave 1 (Table 4-4).

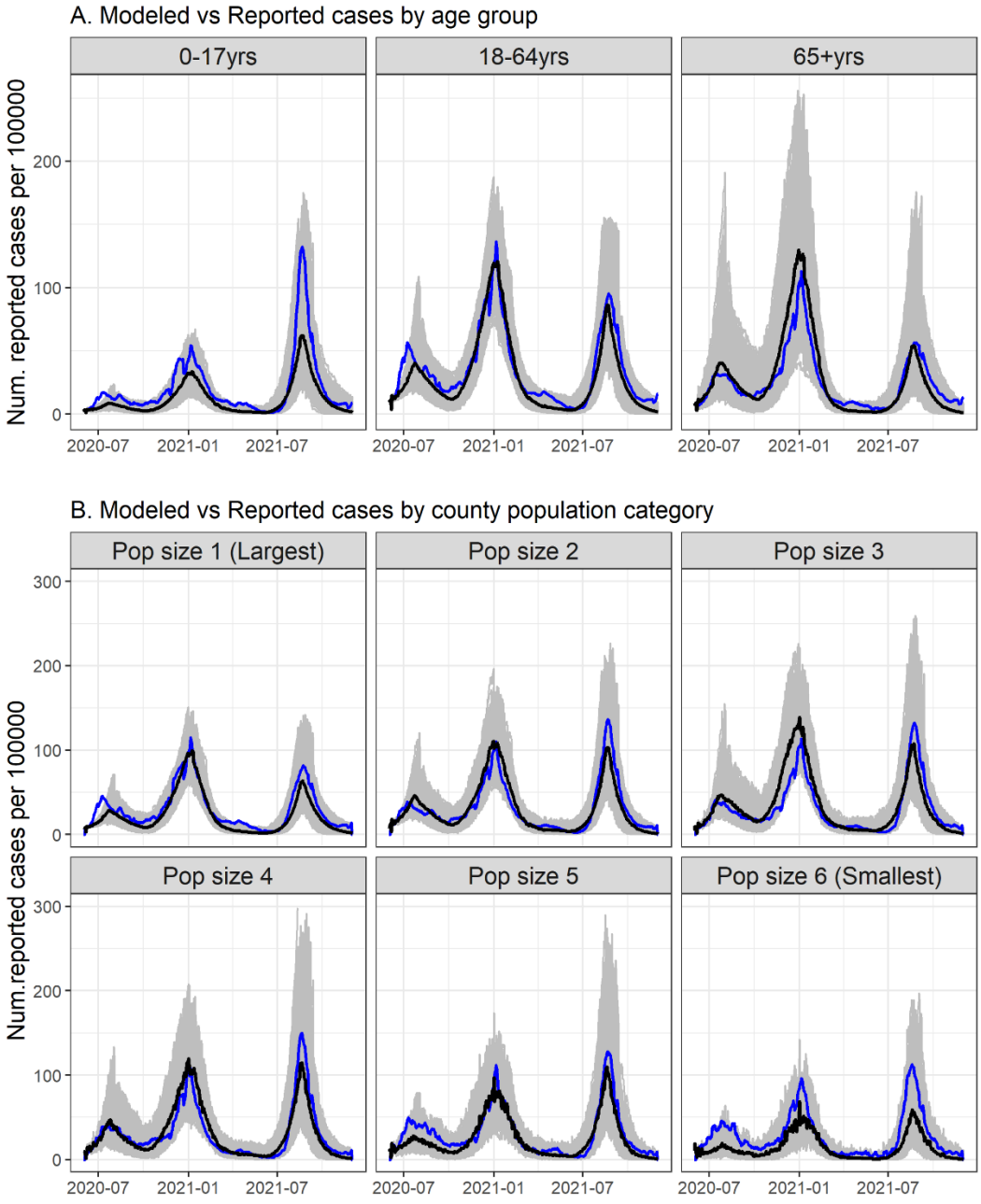

Figure 4-4. Temporal Comparison of Modeled and Reported COVID-19 Cases per 100,000

A. Number of reported and modeled cases per 100,000 among three age groups: 0-17 years, 18-64 years, and 65+ years. B. Number of reported and modeled cases per 100,000 across six categories of county population sizes, with Pop size 1 being the largest and Pop size 6 the smallest. Blue line represents the 7-

day rolling average of reported cases, black line represents the median of the 7-day rolling average of modeled cases and gray area represents the simulated range from 1000 accepted parameter sets.

4.4.2 Proportion of SARS-CoV-2 infections imported through intercounty mobility

The infection process in the model is decomposed into three components: household, non-household within county and non-household between counties, allowing for the calculation of the number of new infections generated by each component, stratified by county, age group and day. We calculate median and ranges of proportion of infections generated through intercounty mobility from the 1000 accepted parameter sets. Across the 550-day simulation period and all counties, 30.5% (2.5^{th}-97.5^{th} percentile: 30.0%-31.1%) SARS-CoV-2 infections were imported through intercounty mobility, 57.0% (2.5^{th}-97.5^{th}: 56.3%-57.8%) were generated through within county mobility.

We observe heterogeneities in proportion of imported SARS-CoV-2 infections across counties. Counties with smaller population size had higher proportions of imported infections compared to counties with larger population size. Counties in the lowest decile of population size (population size of 1,596-6,888) had a median of 51% (25^{th}-75^{th} percentile: 39%-68%) of infections imported through intercounty mobility. Counties in the highest decile (population size of 154,257 – 1,051,550) had a median of 30% (27%-36%) of infections imported through intercounty mobility (Figure 4-5).

Counties were categorized into different levels of within-county contact rates based on the contact rate of non-household contacts per person per day at the start of each wave, with the lowest quintile consisting of counties with contact rates between 7.5-12.3 and the highest quintile consisting of counties with contact rates between 15.2-18.7. Counties with lower contact rates had higher proportions of imported infections compared to counties with higher contact rates. Among counties in the top tertile of population sizes, counties with the lowest quintile of contact rates had a median of 42% (33%-46%) infections imported through intercounty mobility while counties with the highest quintile of contact rates had a median of 27% (20%-31%) infections imported through intercounty mobility. Similar trends were observed in counties with the smallest population size but less so among mid-sized counties (Figure 4-5).

Counties were categorized into quintiles of vaccination coverage of one or more doses of vaccine among adults aged 18 years and above, prior to the start of the third wave (July 1st, 2021). The lowest quintile had a single-dose vaccination coverage of between 11.1% to 22.7% and the highest quintile had a coverage between 35.5% - 55.0%. Counties with lower vaccination coverage had lower proportions of imported infections compared to counties with higher vaccination coverage. Among counties in the top tertile of population size, counties with the lowest quintile of vaccination coverage had a median of 24% (21%-31%) infections imported through intercounty mobility and those with the highest quintile of vaccination coverage had a median of 33% (29%-44%) infections imported. Similar trends were observed in mid-size and small-size counties. Small sized counties with the highest quintile of vaccination coverage had a median of 51% (42%-61%) of infections imported through intercounty mobility (Figure 4-5).

Lastly, for each county, we categorized periods of surges and declines for each wave based on the timing of minimum and maximum new infections per day for each wave. We did not observe substantial differences in proportion of infections imported through intercounty mobility across periods of surges and declines of each wave (Figure 4-5).

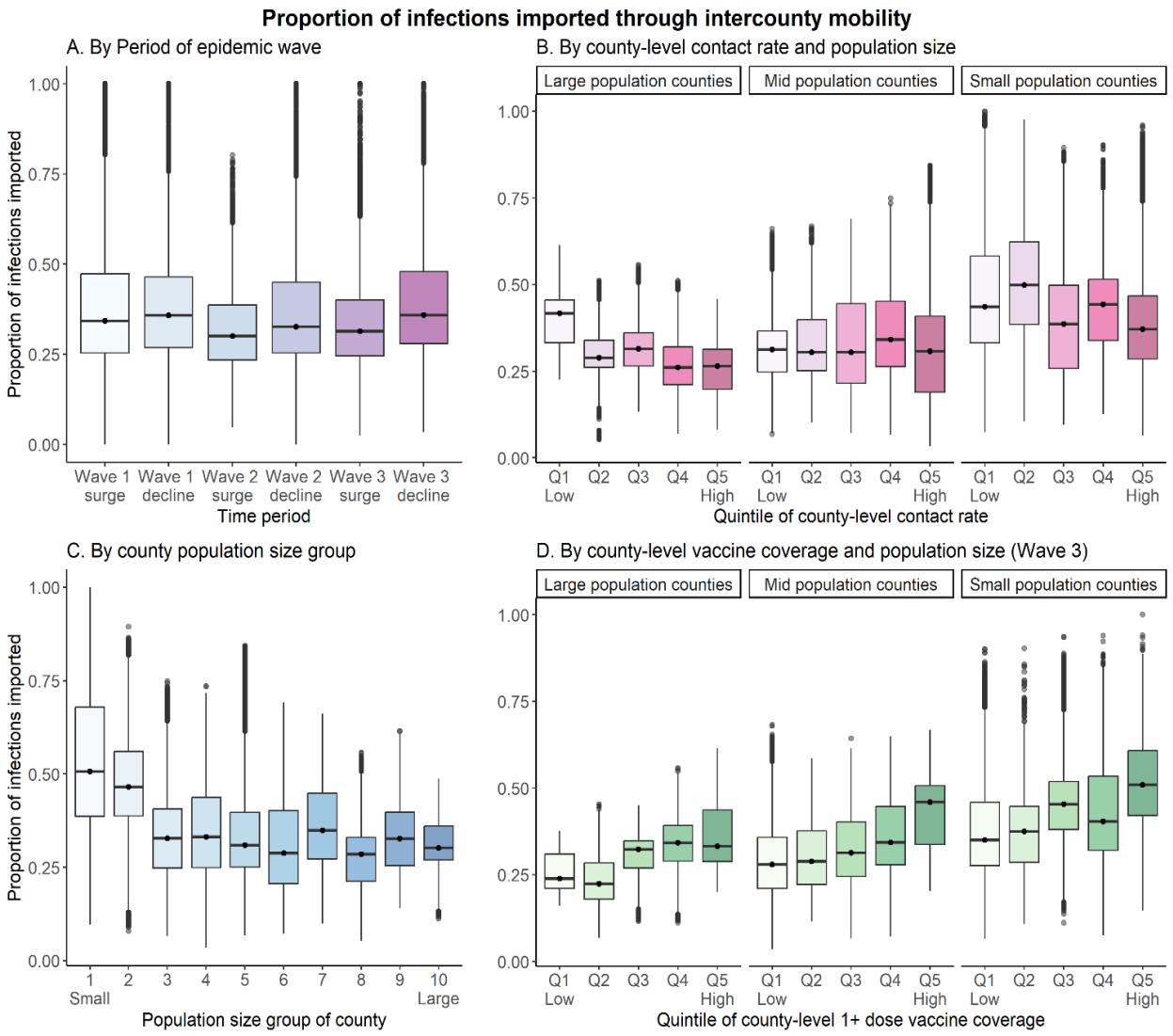

Figure 4-5. Variations in Proportion of Imported SARS-CoV-2 Infections Across County Attributes and Epidemic Phases Coverage.

Boxplots comparing the proportion of infections attributed to intercounty mobility, segmented by (A) deciles of county population size (1-smallest, 10-largest), (B) quintiles of county-level average contact rates per person per day at start of each wave (Q1-lowest, Q5 highest), and tertile of population size, (C) periods of epidemic wave (surges and declines), and (D) quintiles of county-level vaccination coverage of one or more doses among adults aged >18 years at the start of wave 3 (Q1- lowest, Q5-highest) and tertile of population size (wave 3 only) .

4.4.3 Directionality of infection flow

We further explored the directionality of infection flow between pairs of counties. Across 159 counties and 12,561 unique county pairs, 12,298 had at least one trip recorded in either direction during the 550-day simulation period. On any given day, between 7,848 and 5,877 county pairs recorded at least one trip in either direction. Among pairs with at least one trip recorded, the median number of directed trips per day was 43 (2.5^{th}-97.5^{th} percentile: 5-3,660, minimum =1, maximum=223,147. The distribution of trips between county pairs and their difference in strength of connectivity in either direction underpinned infection flows and the difference in strength of connectivity in either direction.

To understand the key drivers of importation dynamics, we analyze the correlations between differences in vaccination coverage, contact rates, and population sizes among county pairs with the difference in imported infections among county pairs across three time points, representing the beginning (June 30^{th}, 2021), peak (Aug 24^{th}, 2021) and the end (Sept 28^{th}, 2021) of the third wave. We find that when considering each county pair individually, the number of infection importations from the county with lower vaccination coverage to the county with higher coverage is higher than importations from the county with higher coverage to the county with lower coverage (Figure 4-6). The number of infection importations is higher from the county with higher contact rate to the county with lower contact rate than the reverse (Figure 4-6). The number of importations is on average higher from the county with lower population size to the county with higher population size than the reverse (Figure 4-6). This is counter to the directionality of mobility flows, where on average the number of trips from the county with lower population size to the county with higher population size is lower (Figure 4-20). The magnitude of these correlations is the highest at the beginning of the wave (R=0.54, R=-0.4 and R=0.55 for correlations with difference in vaccination coverage, contact rates, and population sizes, respectively). The same directionality of correlations was observed across other time periods (Figure 4-19).

We find that the number of infections from origin to destination is correlated with the number of trips between origin to destination (Figure 4-6) and the difference in vaccination coverage, contact rates and population size between the origin and destination further modulates this relationship.

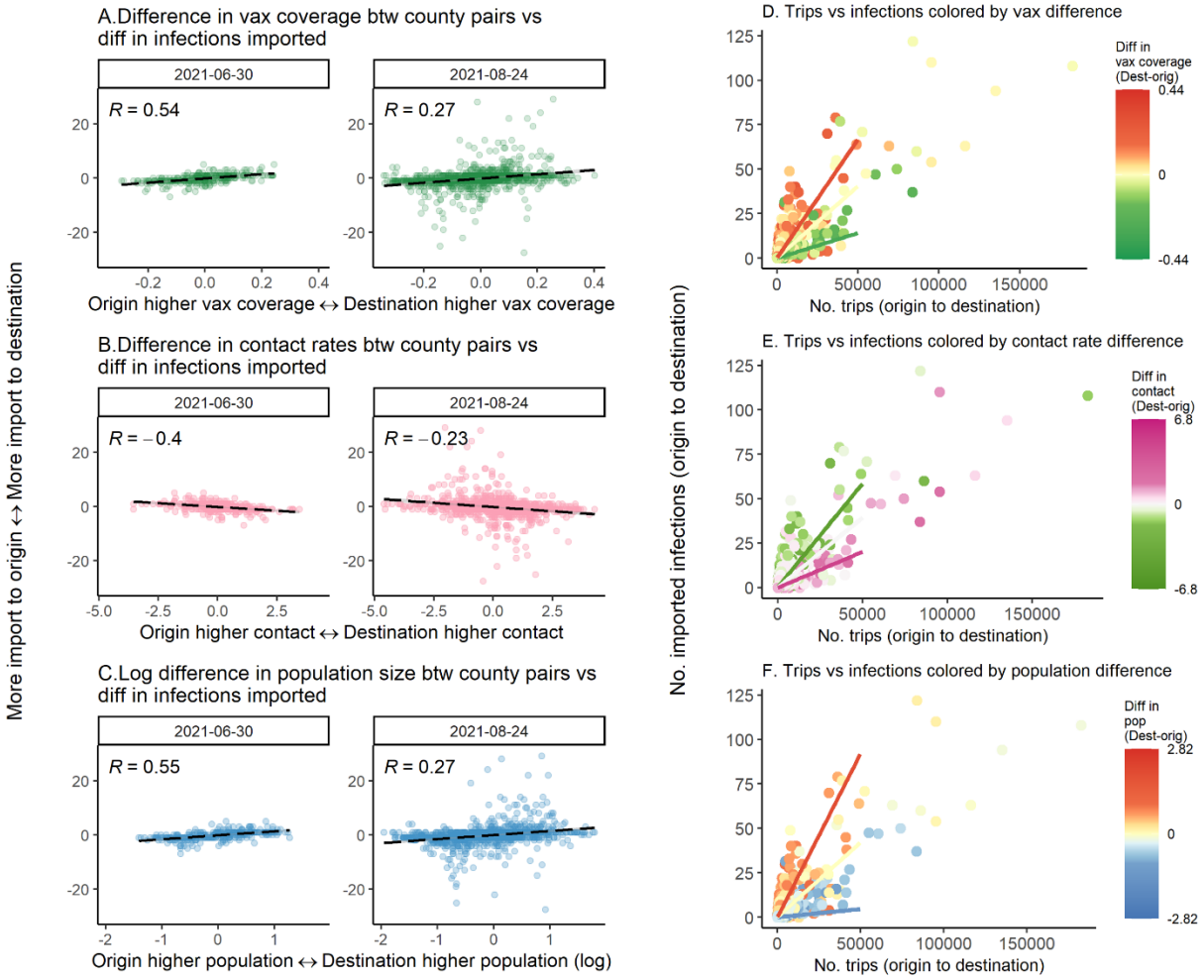

Figure 4-6. Correlations Between County Pair Attributes and Infection Importation Dynamics

Panels A-C) Scatter plots analyzing the correlations between differences in vaccination coverage, contact rates, and population sizes among county pairs with the difference in infections imported, across three select dates during the third wave. Panels (D-F) Scatter plots of the number of infections generated from origin to destination and the number of trips from origin to destination, colored by county pairwise differences in vaccination coverage, contact rates and population size.

4.5 Discussion

In this study, we examine spatial patterns of SARS-CoV-2 transmission across counties in Georgia, USA by developing and implementing a novel analytical framework that integrates multiple fine-grain spatiotemporally-resolved data streams, fitted to time series of age- and county-stratified case data. We highlight spatial heterogeneities in the importation of SARS-CoV-2 infections between the state's counties, driven by an interplay of human mobility, local contact and vaccination rates and population size.

We show that areas with lower uptake of mitigation measures such as vaccination or social distancing measures can inadvertently drive transmission in areas with higher uptake of mitigation measures. Similarly, previous work showed human movement linking locations with asynchronized local-level risk mitigation measures heightened global infection prevalence and degraded overall pandemic control[145,242]. Spatial asynchrony prompted by a lack of coordination in lifting or re-implementing containment measures facilitates re-importations of community transmission. Outbreak response plans would benefit from coordination across geographical areas to reduce the likelihood of resurgences.

We find an average net flow of infections from counties with lower population to counties with higher population, counter to the direction of net flow for mobility. Counties with larger populations also had higher uptake of risk mitigation behaviors such as vaccination and social distancing. This suggests that differential local immunity and behavior can reverse expected source-sink dynamics hypothesized from the strength of mobility flows alone. We further observe that for smaller counties, imported infections compose of a larger proportion of the counties' total infections, suggesting that even if the smaller county on average acts as the net exporter in pairwise relationships, a larger proportion of their own infections are imported. The theory of spatial hierarchical spread suggests that infections diffuse from areas with high population density to areas with low population density[143], yet in practice the directionality of transmission along the rural-urban gradient is often variable. For example, during the early stages of COVID-19 pandemic, cities were determined to have higher incidence and infections were hypothesized

to flow from urban to rural areas[243]. However, genomic studies have identified scenarios of virus importation from rural to urban areas. In Missouri, phylodynamic analysis showed frequent bi-directional diffusions between rural and urban communities[244].

Further, the extent of mobility between counties was correlated with but not synonymous with infection importation. We found that the relationship between mobility flows, and infection flows was further modified by the differential gradient of vaccination coverage, contact rates and population sizes between pair-wise counties, suggesting while mobility is important in determining local epidemic trajectories it is far from the only factor. This highlights the need to analyze mobility data in conjunction with additional data that informs other key aspects of transmission such as contact rates and vaccination rates. Therefore, the impact of monitoring and controlling movement is contextual because their dynamics effects are intertwined with the magnitude of asynchrony in local transmission across space.

Lastly, we find that the relative contribution of infection importation remains consistent across different phases of a pandemic wave at the state level, despite observable variances at the county level. We did not observe substantial differences in the relative contribution of importations during surges versus declines of each wave at an aggregated state level. This suggests that once the virus is locally introduced through initial seeding events, the ensuing transmission dynamics within the community becomes the dominant driver, superseding the role of importations.

We report several limitations. App-based GPS tracking using mobile devices track individuals who own and regularly use specific smart-phone mobile applications and may not be fully representative of population-level mobility flows. The mobility data is thus a measure of relative connectivity between counties rather than an exact quantification of movement and improves on previous methods used to parameterize metapopulation models such as mathematical assumptions or survey data on commuting patterns. We do not consider long-distance movements via air travel that could be important in seeding events but occur at lower frequencies than daily commuting. We do not account for counties outside of Georgia, underestimating the extent of intercounty mobility for counties on the state borders. Disease and

vaccination data were obtained from Georgia Department of Public Health, and we did not have access to comparable data from other states. An underlying assumption is intercounty mobility is distributed proportionally by age and infection-status. Age-stratified or infection-status stratified mobility data is rare, and homogeneity is a common assumption for metapopulation models. Our model goes beyond typical metapopulation models by introducing age-specific transmission within county. Future work can explore relaxing these assumptions.

4.6 Conclusion

In conclusion we integrate multi-dimensional data streams to infer spatial patterns of transmission across waves of COVID-19 in Georgia, USA using a metapopulation mode. We find that in counties with smaller populations, lower contact rates and higher vaccination coverage, intercounty mobility contributes to a higher proportion of onward transmission. In addition, we present evidence that in an interconnected spatial network with a patchwork of local uptake in mitigation measures, the net infection flow is still from counties with lower mitigation to counties with higher mitigation. An understanding of spatial patterns of transmission can guide public health strategies and policymaking and inform preparedness and response for future public health emergencies.

4.7 Supplementary File

4.7.1 Detailed model structure and equations

4.7.1.1 Model equations

The model equations is as follows:

$$S0^i(t) = S0^i(t-1) - n^i_{S0E}(t) \quad \text{Eq 6}$$

$$S1^i(t) = S1^i(t-1) + n^i_{RS}(t) - n^i_{S1E}(t) \quad \text{Eq 7}$$

$$EU^i(t) = EU^i(t-1) + n^i_{SEU}(t) - n^i_{EU}(t) \quad \text{Eq 8}$$

$$EI^i(t) = EI^i(t-1) + n^i_{SEI}(t) - n^i_{EI}(t) \quad \text{Eq 9}$$

$$U^i(t) = U^i(t-1) + n^i_{EU}(t) - n^i_{UR}(t) \quad \text{Eq 10}$$

$$I^i(t) = I^i(t-1) + n^i_{EI}(t) - n^i_{IR}(t) \quad \text{Eq 11}$$

$$R^i(t) = R^i(t-1) + n^i_{IR}(t) + n^i_{UR}(t) - n^i_{RS}(t) \quad \text{Eq 12}$$

Where t represents time t, i represents model age groups (i=1 is 0-17 years, i=2 is 18-64 years and i=3 is 65 years and above), $n_{XY_i}(t)$ is the number of transitions from class X to class Y for age group i at time t. The disease classes are as follows: S0 (susceptible individuals with no prior infection), S1 (susceptible individuals with one or more prior infection), E (latent infection, exposed but not yet infectious), U (infectious and unreported), I (infectious and reported as a case) and R (recovered and temporarily immune).

The rate individuals in each age group infect each other is determined by the age-specific mixing matrix and age group infection density within the county. The number of transitions from susceptible to exposed class for group i at time t in county A is modelled by the following equation that also incorporates infection flow from all other counties where i denotes the age group of the susceptible class and j denotes the age group of the infectious class:

$$n^{i}_{S0E_A}(t) \sim Poi\left(S0^{i}_{A}(t-1) \times \Upsilon_{\mathrm{A}} \times \Upsilon_i \times \{ \sum_{j=1} \beta(t) \times {c^{j,i}}_{A,HH}(t) \times \left({I^{j}}_{A}(t-1) + {U^{j}}_{A}(t-1) \right) + \sum_{j=1} \beta \times {c^{j,i}}_{A,NH}(t) \times \sum_{B} m^{j}_{B \to A}(t-1) \} / N^{i}_{A} \right) \quad \text{Eq 13}$$

$$n^{i}_{S1E_A}(t) \sim Poi\left(S1^{i}_{A}(t-1) \times \Upsilon_{\mathrm{A}} \times \Upsilon_i \times \{ \sum_{j=1} \beta(t) \times {c^{j,i}}_{A,HH}(t) \times \left({I^{j}}_{A}(t-1) + {U^{j}}_{A}(t-1) \right) + \sum_{j=1} \beta \times {c^{j,i}}_{A,NH}(t) \times \sum_{B} m^{j}_{B \to A}(t-1) \} / N^{i}_{A} \right) \quad \text{Eq 14}$$

Where $\Upsilon_i \times \beta(t)$ denotes the average probability of transmission from an infectious individual in any age group to susceptible individuals in age group i, modified by an age-specific ratio for susceptibility (Υ_i) , with the youngest age group as the reference group. All infectious individuals contribute to transmission within their household based on the within household contact rate (${c^{j,i}}_{A,HH}(t)$), parameterized by the term $\sum_{j=1} \beta \times {c^{j,i}}_{A,HH}(t) \times \left\{ {I^{j}}_{A}(t-1) + {U^{j}}_{A}(t-1) \right\}$. Infected individuals who travel outside of their home contribute to either transmission within their county or in another county, parameterized by the term $\sum_{j=1} \beta \times {c^{j,i}}_{A,NH}(t) \times \sum_{B} m^{j}_{B \to A}(t-1)\}$. ${c^{j,i}}_{A,NH}(t)$ is the average number of non-household contacts per day made by age group j to i and $\sum_{B} m^{j}_{B \to A}(t-1)$ sums all the inflowing infections from age group j at time t based on all other counties where mobility between B→A is observed, including those who moved outside of the home but within the county (details in section below).

p_{U_i}, the probability that an infection is unreported at times t for age group i, is defined through a cubic spline function with two fitted parameters α_i and b_i, which will be used to model time-varying average reporting rate in a particular age group i. Here, we assume the reporting rate increases over time due to

increasing efforts for asymptomatic screening and testing and subsequently declines at the beginning of widespread availability of self-testing around the

Transitions for $n^{i}_{S0E_A}$ and $n^{i}_{S1E_A}$ are discussed above. Transitions between other classes are modelled as:

$$n_{EU_i}(t) \sim Bin(n_{SE_i}(t - D_{EU}), p_{U_i}(t - D_{EU})) \quad \text{Eq 15}$$

$$n_{EI_i}(t) = n_{SE_i}(t - D_{EI}) - n_{EU_i}(t) \quad \text{Eq 16}$$

$$n_{IR_i}(t) = n_{EI_i}(t - D_{IR}) \quad \text{Eq 17}$$

$$n_{UR_i}(t) = n_{EU_i}(t - D_{UR}) \quad \text{Eq 18}$$

$$n_{RS_i}(t) = n_{IR_i}(t - D_{RS}) + n_{UR_i}(t - D_{RS}) \quad \text{Eq 19}$$

Where D_{EI}, D_{EU}, D_{IR}, D_{UR}, D_{RS} denote the mean time-to-transition between the indicated two classes. p_{U_i} represents probability that an infection is unreported for age group I (in years), through a piecewise function (Eq 20).

$$p_{U_i} \begin{cases} 0.2; & 0 \leq i \leq 17 \\ 0.3; & 18 \leq i \leq 64 \\ 0.4; & i > 65 \end{cases} \quad \text{Eq 20}$$

4.7.2 Additional data descriptions

4.7.2.1 Estimated proportion who stay at home in each county over the pandemic

Figure 4-7. Mean proportion of devices in each county that do not leave their house[1]

[1]Mean proportion of devices that do not leave their house estimated from Cuebiq data on the first day of each month. This measure is used as an input to inform non-household transmission including both non-household within county and non-household between county transmission processes.

4.7.2.2 Relative susceptibility values for susceptibility tiers

Vaccination state	Prior infection	
	S0	S1
V0	1	0.4
$V1_{21+days}$	0.35	0.2
$V2_{14-133days}$	0.15	0.18
$V2_{134-193days}$	0.33	0.18
$V2_{194+days}$	0.49	0.2

V3+	0.1	0.1

Table 4-1. Relative susceptibility ($\sigma_{S,V}$) for susceptibility tiers based on combinations of prior infection and prior vaccination[1]

[1]A value of 1 means fully susceptible, 0 is fully immune, increasing vaccination and more recent vaccination confers more immunity.

4.7.3 Additional model calibration details

4.7.3.1 Distance and tolerance for algorithms used in calibration

Algorithm	Distance measure	Tolerance
1	$\sqrt{\sum_{t=1}^{t=550}\sum_{i=1}^{i=3}(I_{t,i}-I_{t,i}^{*})^2}$, where i is age groups of 0-17 years, 18-59 years and 60 years and above and $I_{t,i}$ is number of reported cases at time t, age group i and $I_{t,i}^{*}$ is number of modeled cases at time t, age group i	18000
2	$\sqrt{\sum_{t=1}^{t=550}\sum_{c=1}^{c=8}(I_{t,c}-I_{t,c}^{*})^2}$, where c is county grouped by population size and $I_{c,i}$ is number of reported cases at time t, county group c and $I_{c,i}^{*}$ is number of modeled cases at time t, county group c	3000
3	$\sqrt{\sum_{i=1}^{i=3}(I_{tmax,i}-I_{tmax,i}^{*})^2}$, where i is age groups of 0-17 years, 18-59 years and 60 years and above and $I_{tmax,i}$ is number of reported cases at time of wave 3 peak, age group i and $I_{tmax,i}^{*}$ is number of modeled cases at time of wave 3 peak, age group i	4000

Table 4-2. Equations for distance calculations and the accepted tolerance for algorithms used in the calibration[1]

[1] All three criteria must be met for parameter set to be accepted.

4.7.3.2 Categorization of county population sizes

County population category	**Min population size**	**Max population size**
Pop size 1 (Metro Atlanta)	106,456	1,051,550
Pop size 1 (Non-metro Atlanta)	85,008	289,649
Pop size 3	35,745	81,294
Pop size 4	22,509	34,676
Pop size 5	15,548	22,072
Pop size 6	8,787	15,489
Pop size 7	1,596	8,701

Table 4-3. Summary of minimum and maximum population sizes for each population size category[1]

[1]Each population size category was assigned a separate value for relative susceptibility.

4.7.3.3 Model Calibration results

Parameter	**Initialized Range**	**Accepted range (Median, 25th-75th percentile)**
Beta	0.0065-0.015	0.011 (0.007-0.015)
Relative susceptibility (adults)	0.8-3	1.739 (1.245-2.879)
Relative susceptibility (older adults)	0.8-3.75	2.329 (1.542-3.606)

	Relative susceptibility (county popsize 1 metro)	0.7-1	0.771 (0.703-0.886)
	Relative susceptibility (county popsize 1 non-metro)	0.9-1.2	1.047 (0.96-1.098)
	Relative susceptibility (county popsize 2)	1-1.2	1.102 (1.006-1.195)
	Relative susceptibility (county popsize 3)	1-1.4	1.179 (1.009-1.391)
	Relative susceptibility (county popsize 4)	1-1.4	1.188 (1.013-1.387)
	Relative susceptibility (county popsize 5)	1-1.4	1.202 (1.011-1.386)
	Relative susceptibility (county popsize 6)	1-1.4	1.197 (1.012-1.391)
Wave 1	Relative decrease beta	0.5-0.9	0.607 (0.509-0.732)
	Time decrease	41-57	50 (42-57)
Wave 2	Relative increase beta	1.05-1.2	1.086 (1.052-1.161)
	Time increase	115-140	130 (117-139)
	Relative decrease beta	0.68-0.95	0.816 (0.702-0.868)
	Wave 2 length	80-110	92 (81-109)
Wave 3	Relative increase beta	1.05-2.46	1.909

		(1.564-2.375)
Time increase	360-386	373 (362-385)
		0.79
Relative decrease beta	0.4-0.95	(0.498-0.895)
Wave 3 length	60-80	71 (61-80)

Table 4-4. Initialized and accepted ranges for calibrated parameters in the model[1]

[1]We used Latin Hypercube Sampling to sample from a uniform distribution where the minimum and maximum are described in the initialized range.

4.7.3.4 Posterior density plots of calibrated parameters

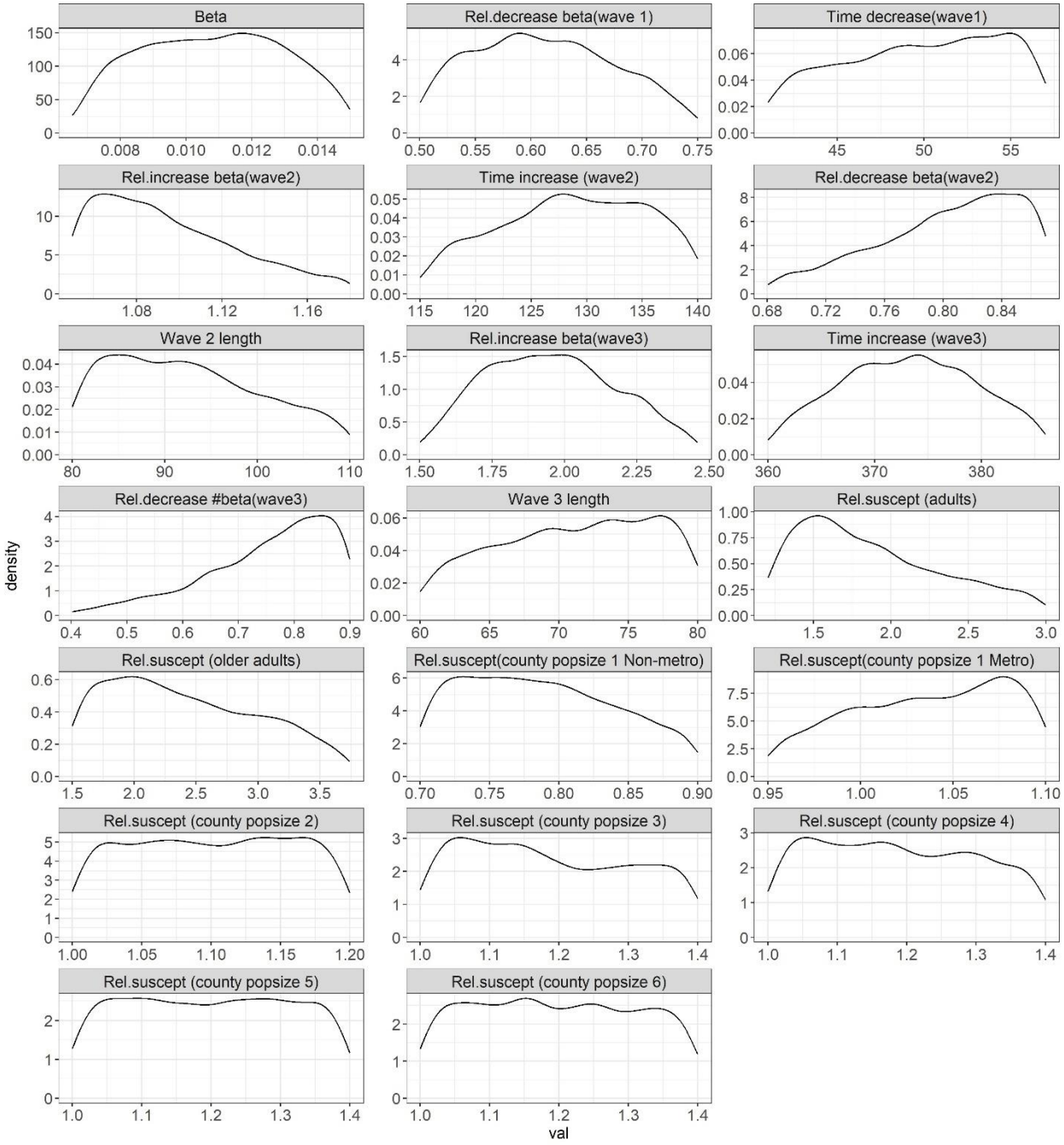

Figure 4-8. The posterior distributions obtained for calibrated parameters using the ABC rejection algorithm.

4.7.3.5 County-level reported vs modeled cases

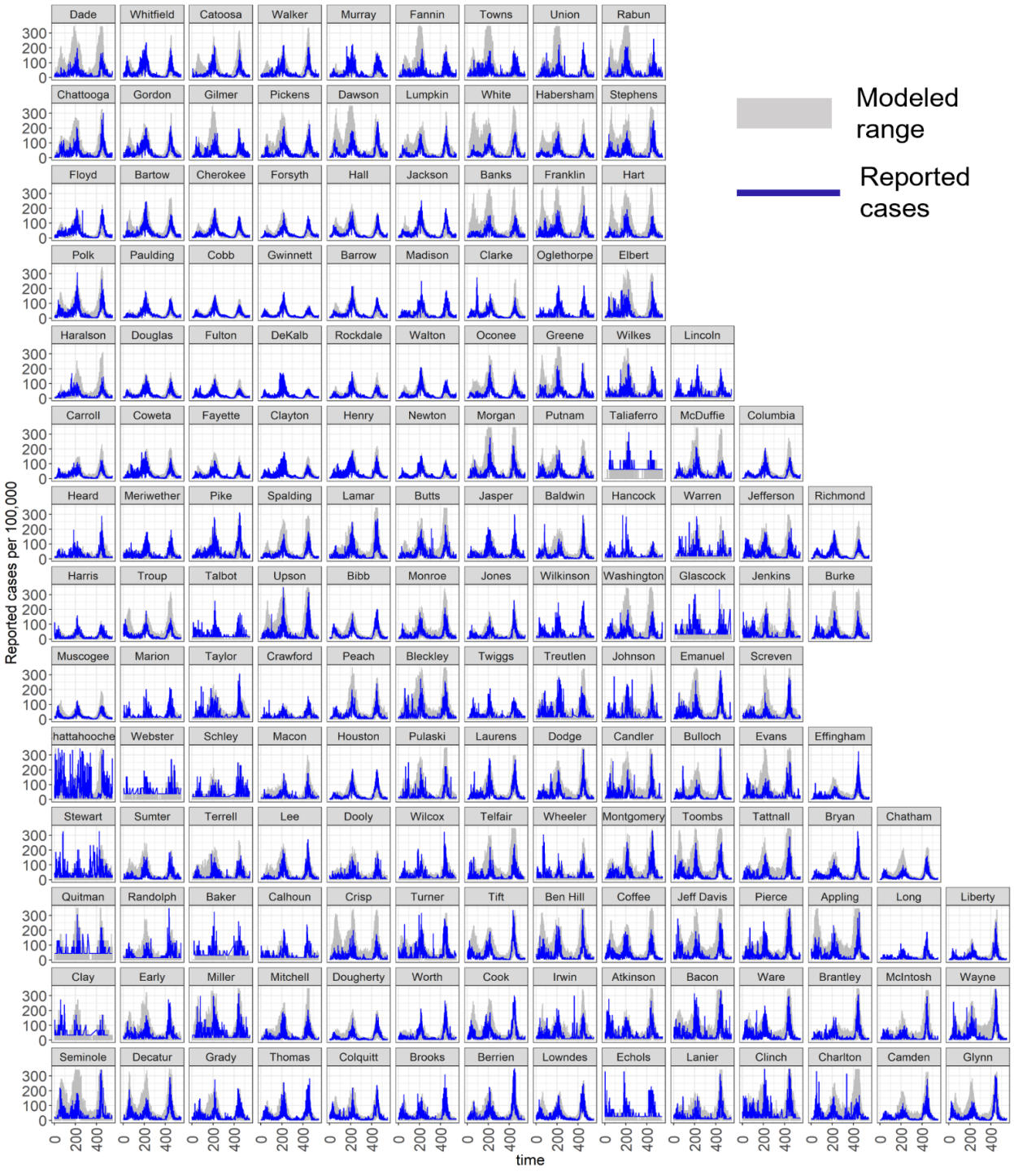

Figure 4-9. Facet grid of reported cases per 100,000 and modeled range of cases per 100,000 for each of the 159 counties in Georgia[1,2]

[1]Counties are arranged based on their spatial position in the state

[2]Time period between June 2020-December 2021

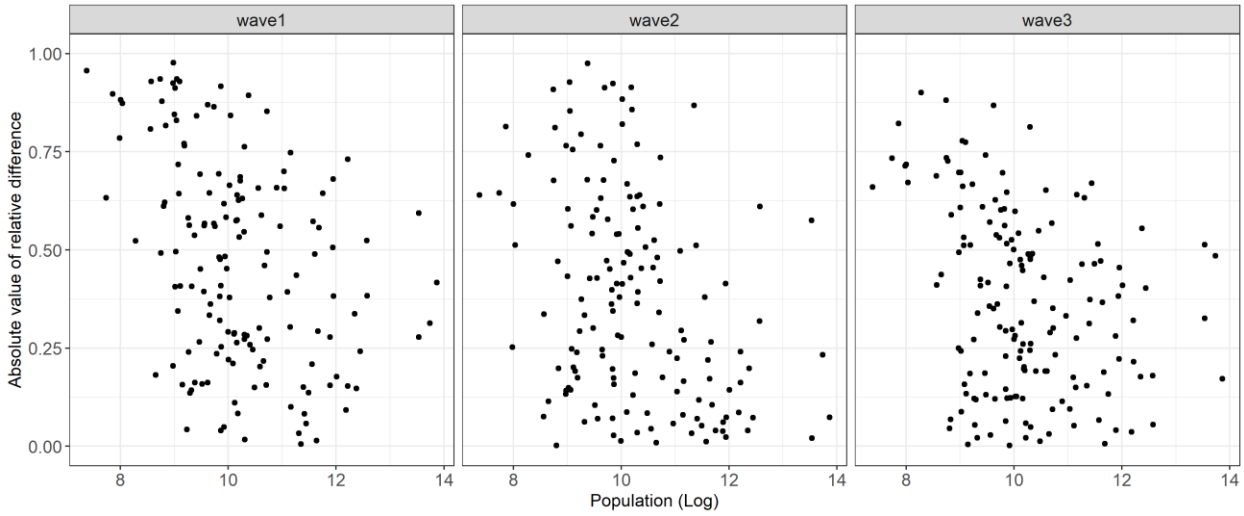

Figure 4-10. Scatterplots depicting of the relative difference between modeled and reported COVID-19 cases plotted against county population size[1,2]

[1]Population size plotted on a logarithmic scale

[2]Each panel represents one of the three waves. Generally, the magnitude of relative difference is unrelated to the population size of the county.

4.7.4 Proportion infections from intercounty mobility

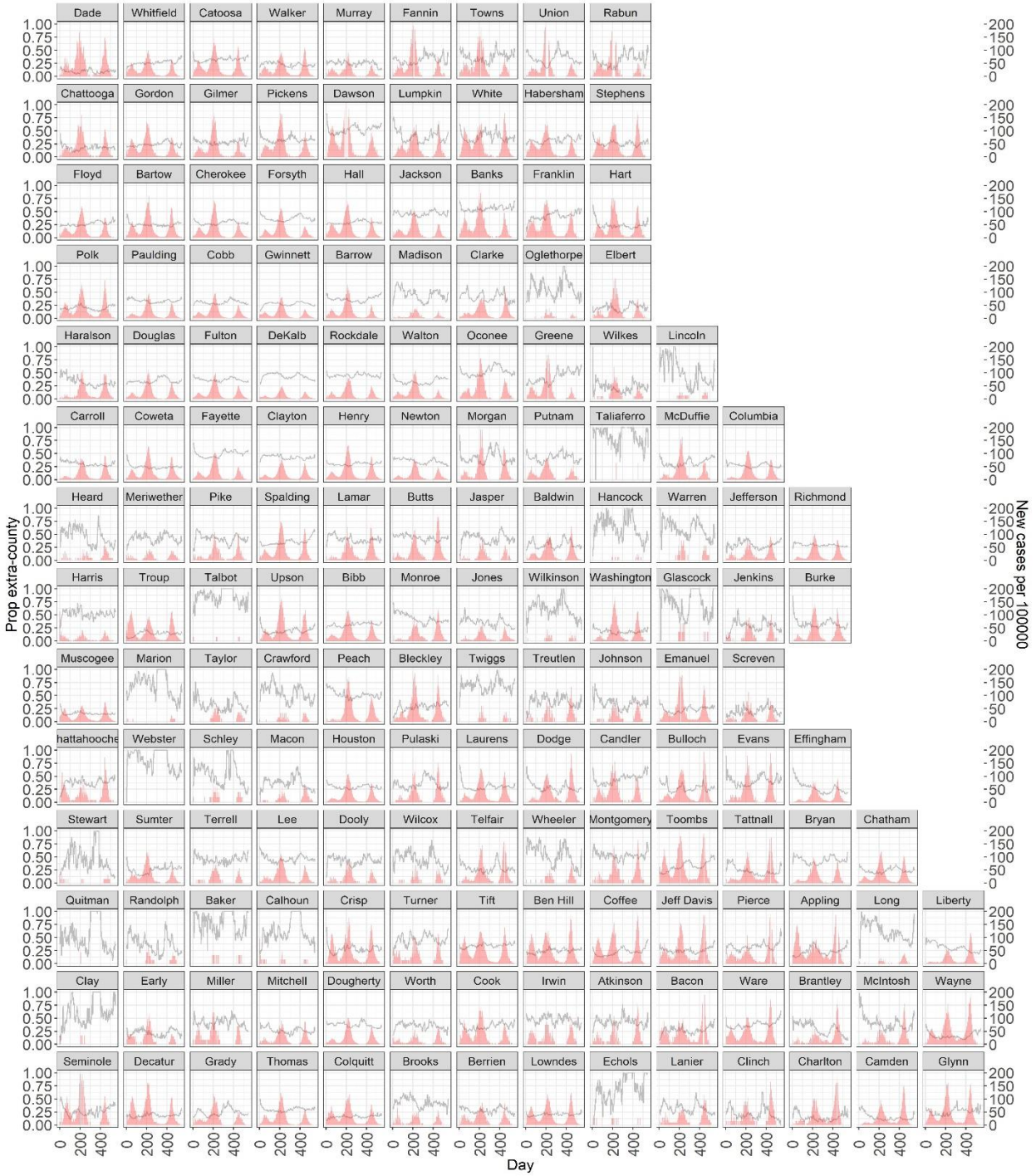

Figure 4-11. Facet grid of proportion of SARS-CoV-2 infection imported through intercounty mobility, stratified by county[1,2,3]

[1]Time period between June 1st, 2020 – Dec 3rd, 2021 (three waves)

[2]Grey line shows the median of proportion imported across 1000 accepted parameter sets over time

[3]Pink shade shows the modeled new cases per 100,000

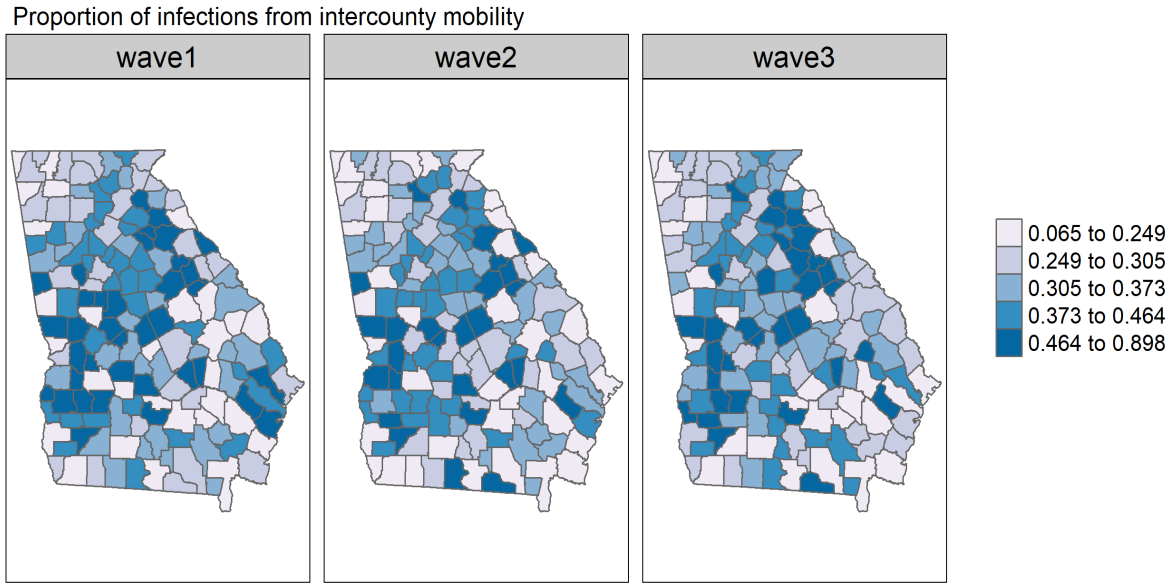

Figure 4-12. Proportion of infections imported through intercounty mobility by county summarized by epidemic wave[1]

[1]The median of proportion imported from the accepted parameter sets are displayed.

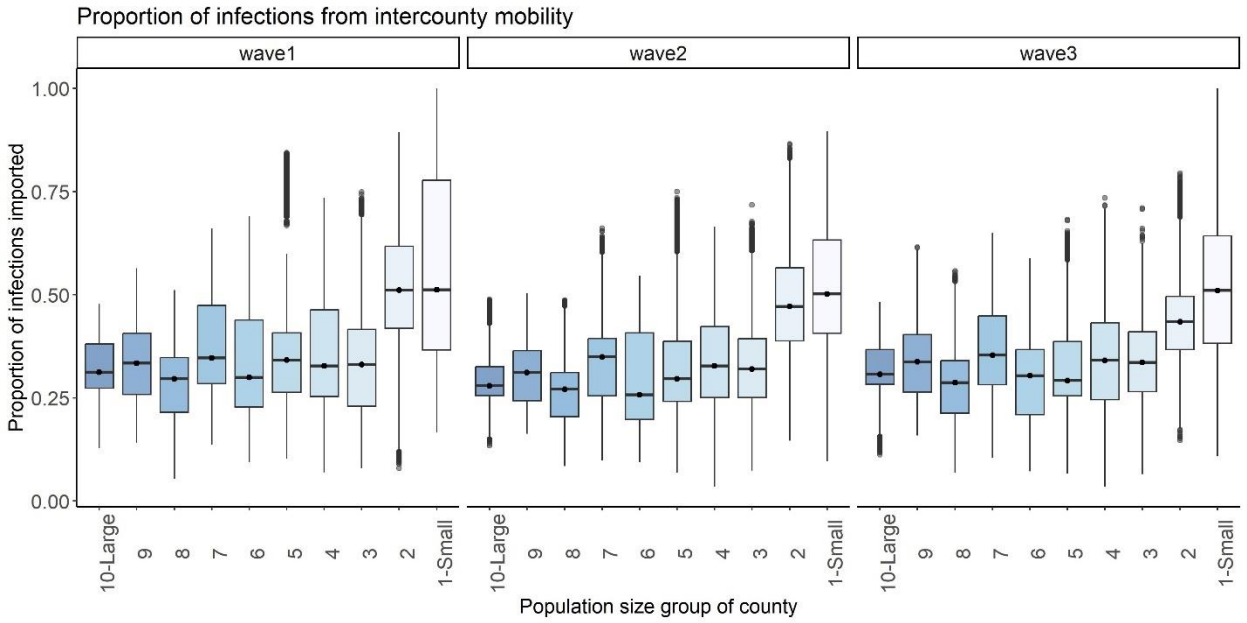

Figure 4-13. Proportion of infections imported through intercounty mobility summarized by population size group of the county and by epidemic wave[1]

[1]The median of proportion imported from the accepted parameter sets are displayed.

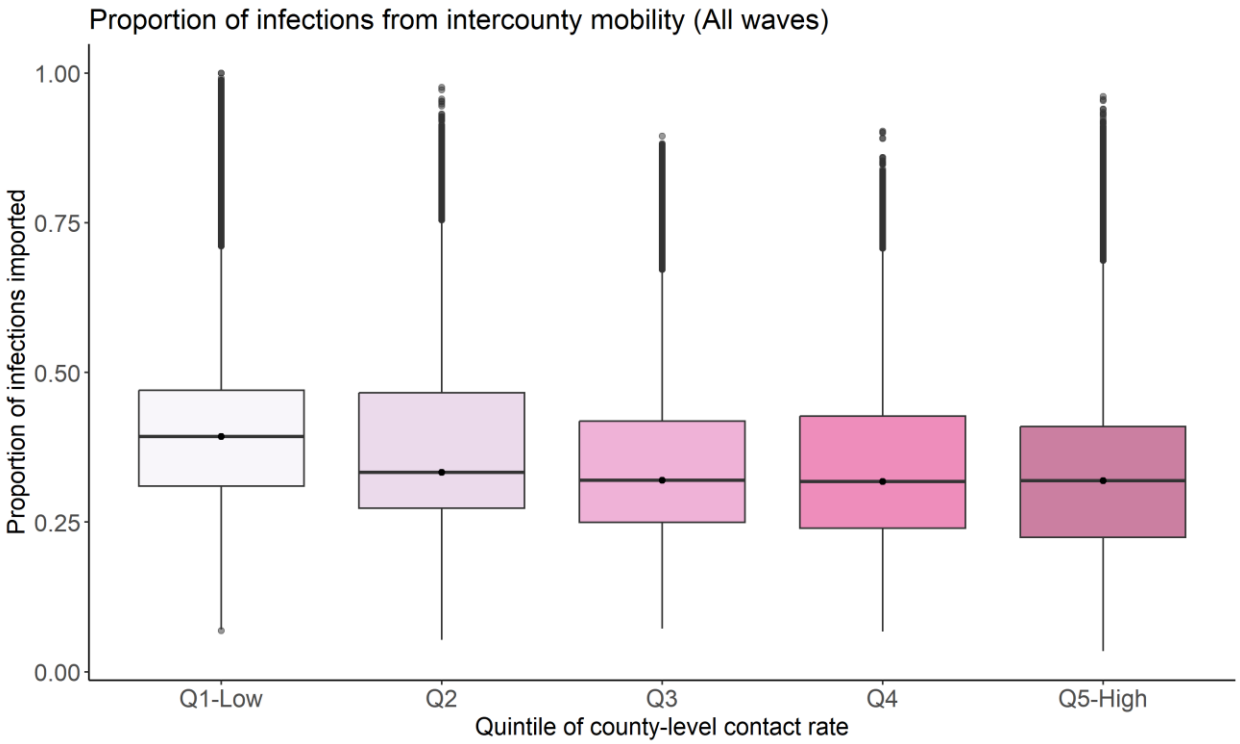

Figure 4-14. Proportion of infections imported through intercounty mobility summarized by quintile of county-level contact rate[1,2]

[1]Q1 is counties with the lowest contact rates, Q5 is counties with the highest contact rates.

[2]The median of proportion imported from the accepted parameter sets are displayed.

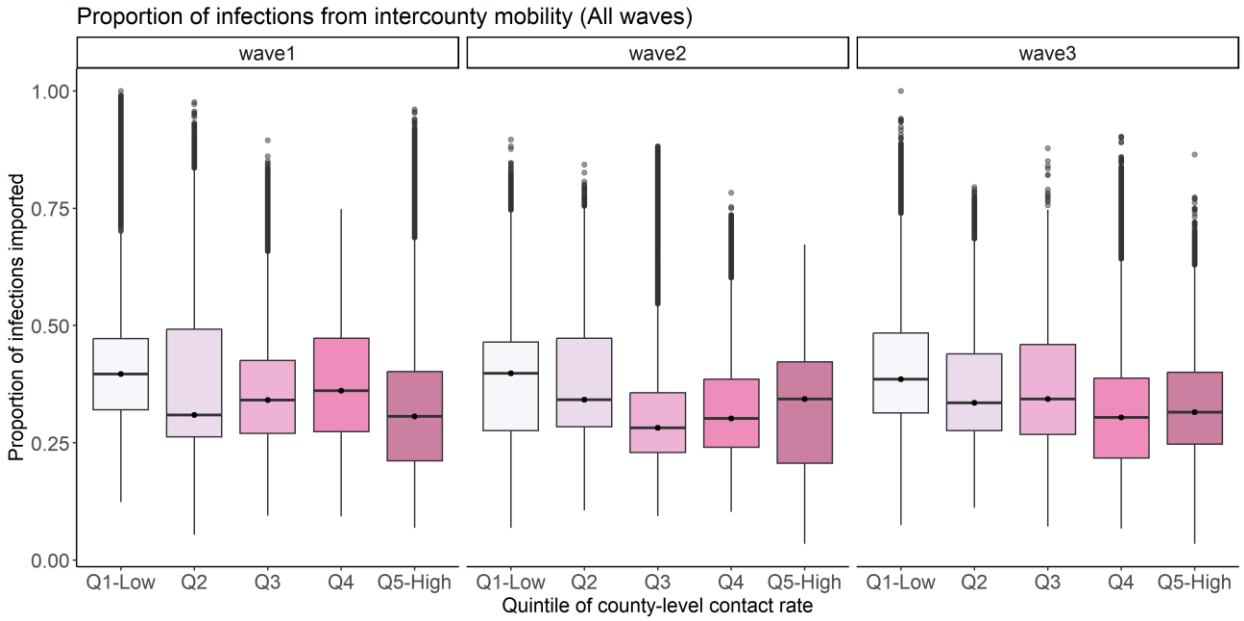

Figure 4-15. Proportion of infections imported through intercounty mobility stratified by quintile of county-level contact rate, epidemic wave, and of county population size[1,2.]

[1]Q1 is counties with the lowest contact rates, Q5 is counties with the highest contact rates.

[2]The median of proportion imported from the accepted parameter sets are displayed.

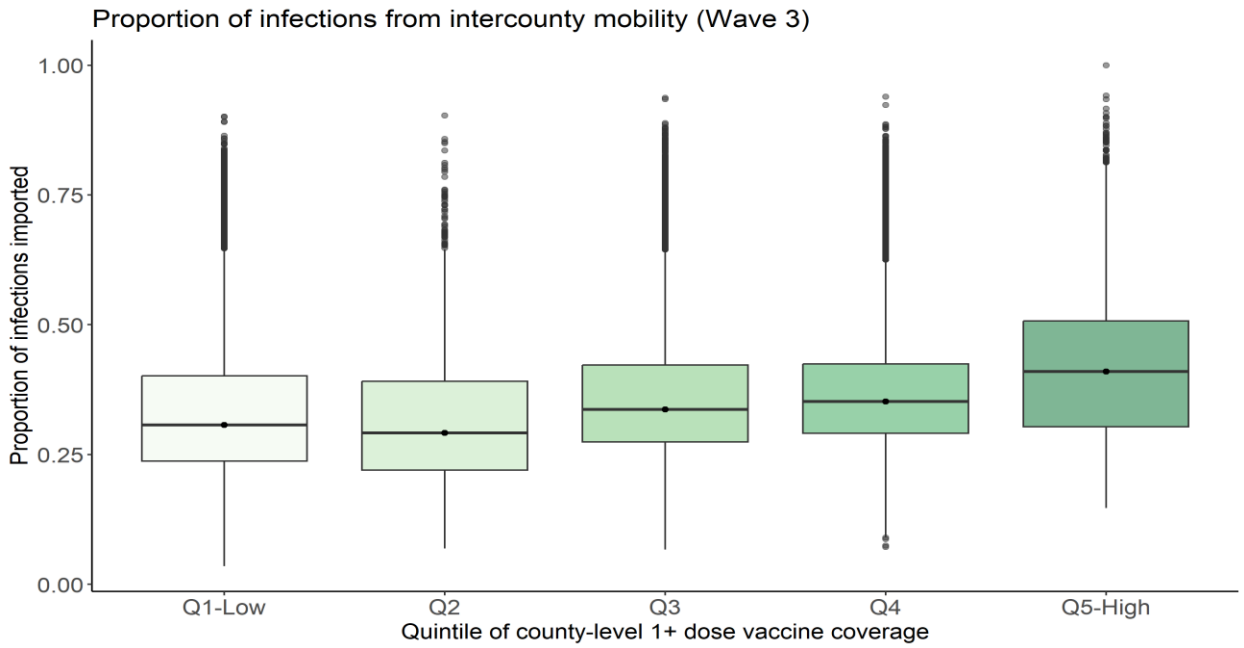

Figure 4-16. Proportion of infections imported through intercounty mobility stratified by quintiles of county-level vaccination coverage[1,2]

[1]Vaccination coverage of one or more doses among adults with Q1 as the counties with the lowest vaccination coverage and Q5 as counties with the highest vaccination coverage. Analysis for the third modeled epidemic wave only

[2]The median of proportion imported from the accepted parameter sets are displayed

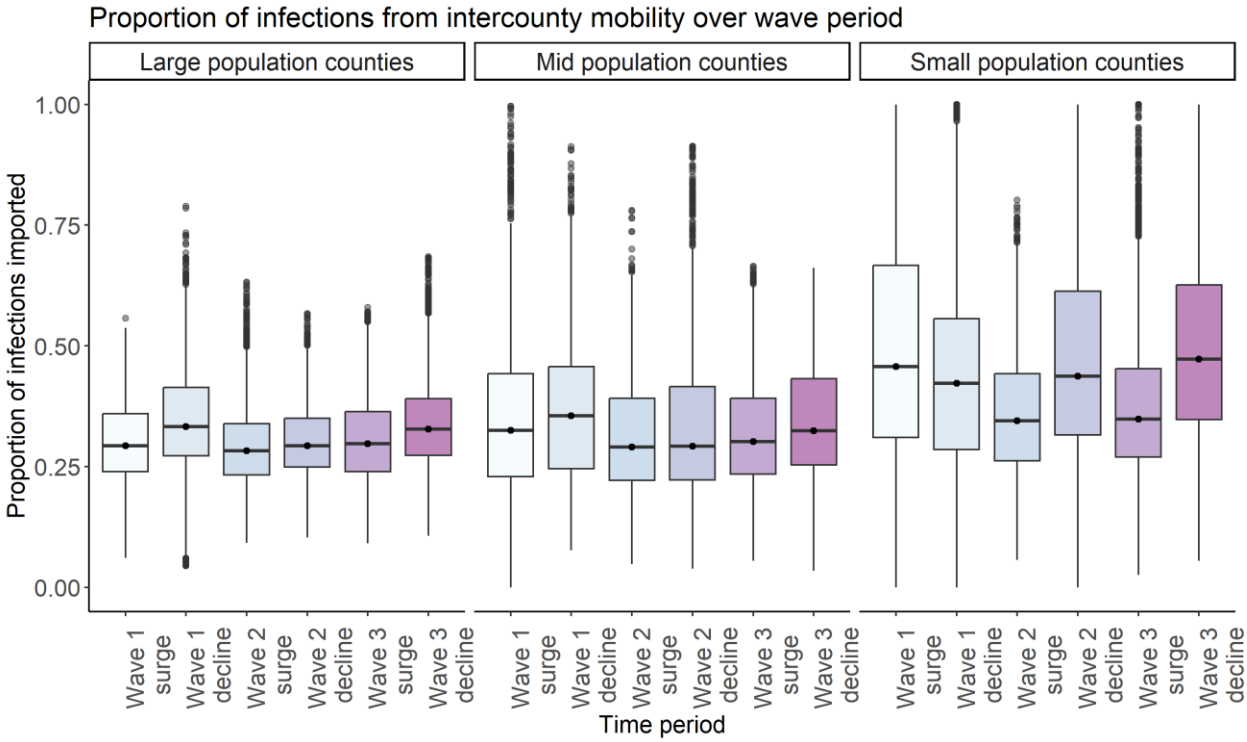

Figure 4-17. Proportion of infections imported through intercounty mobility stratified by surges and declines in epidemic waves and tertiles of county population size[1]

[1]The median of proportion imported from the accepted parameter sets are displayed.

4.7.5 Scatter plots of difference in pairwise county attributes and differences in importations and trips

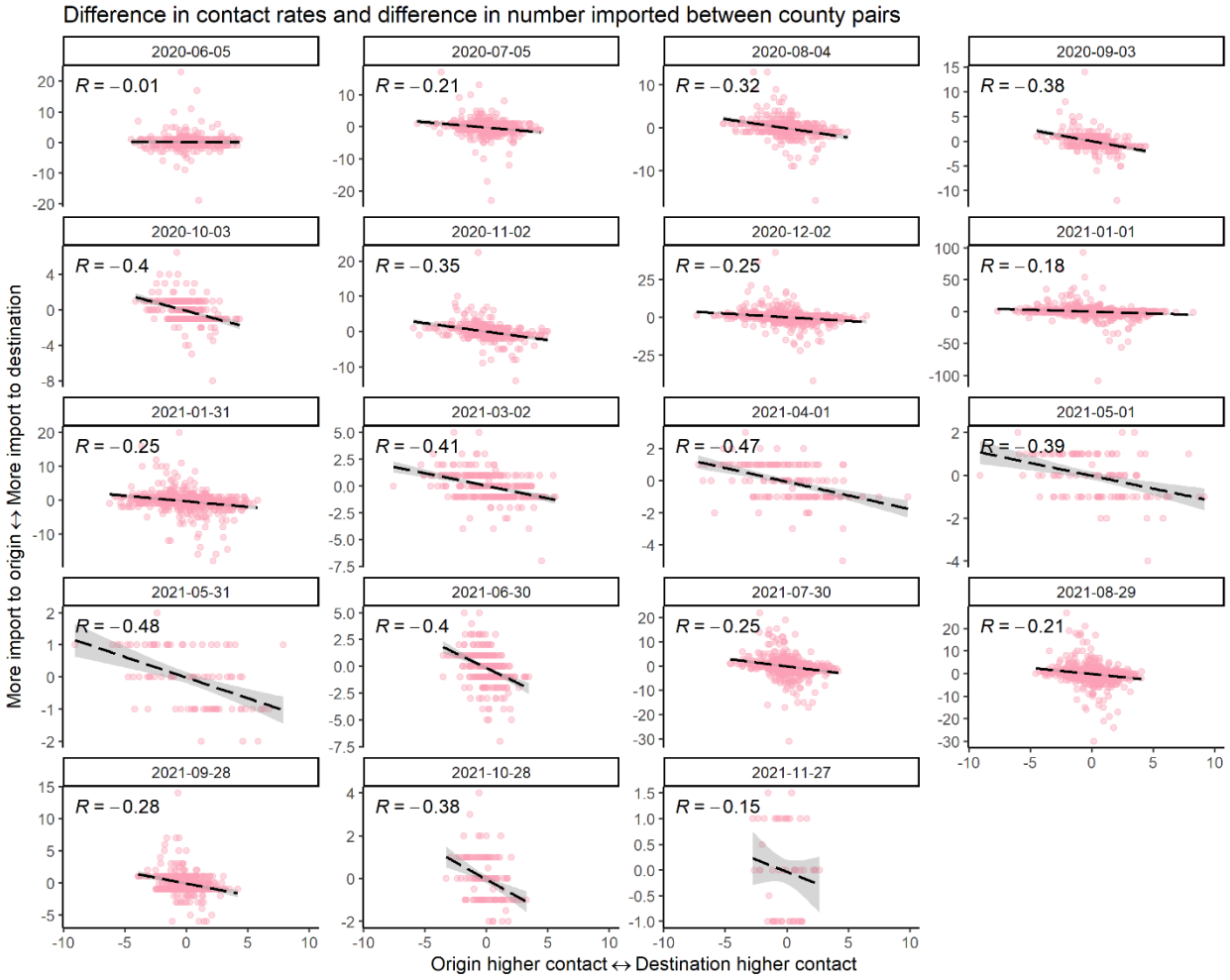

Figure 4-18. Temporal trends in the relationship between difference in contact rate and infection importation across county pairs

Scatter plots illustrate the correlation between the difference in contact rates and the difference in the number of infections imported between pairs of counties over multiple dates. The positive correlation coefficient (R) indicates infections tend to flow from counties with higher contact rates to counties with lower contact rates. The strength of R fluctuates over time.

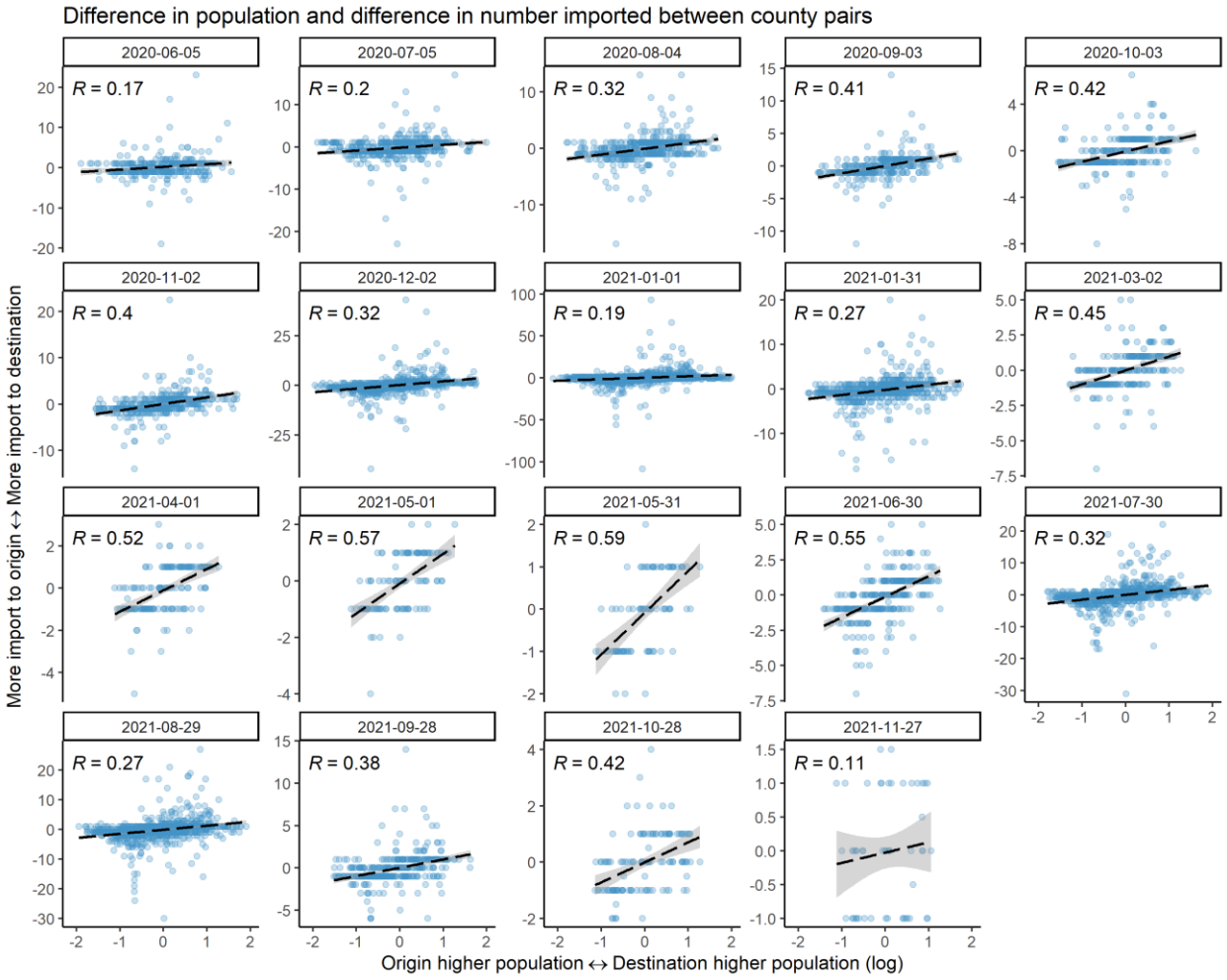

Figure 4-19. Temporal trends in the relationship between difference in population size and infection importation across county pairs

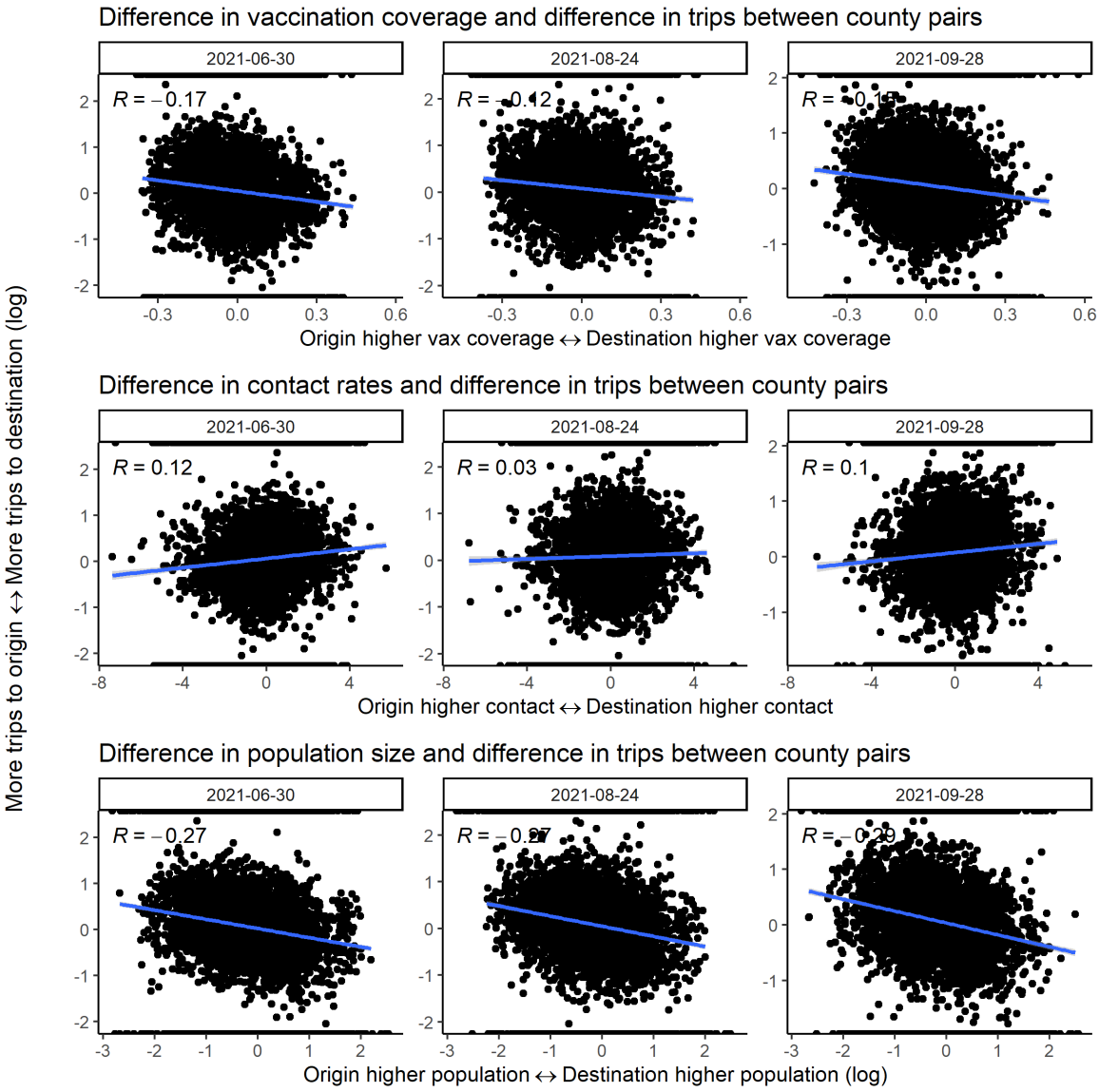

Figure 4-20. Temporal trends in the relationship between difference in trips and differences in county attributes across county pairs.

Scatter plots of differences in vaccination coverage, contact rates, and population size—each compared against the log-transformed differences in trips between county pairs over three dates in the third wave representing the start, peak and end of the wave. The correlation coefficients (R) indicate the strength and direction of the relationships. We observe a correlation where the number of trips is higher from the county with higher population to the county with lower population compared to the number of trips from

the county with lower population to higher population. Correlations between difference in number of trips and differences in vaccination coverage and contact rates are negligible.

Scatter plots illustrate the correlation between the difference in the log of population sizes and the difference in the number of infections imported between pairs of counties over multiple dates. The positive correlation coefficient (R) indicates infections tend to flow from counties with higher contact rates to counties with lower contact rates. The strength of R fluctuates over time.

4.7.6 Exploration of using state-wide seroprevalence data to inform age-specific reporting rate

We used state-wide COVID-19 infection-induced antibody seroprevalence estimates from CDC, a repeated cross-sectional survey that sampled patient sera from specimens collected for routine screening in commercial laboratories across 50 US states roughly every 2 weeks. The goal of the survey was to provide estimates of the percentage of people in the United States with at least one resolving or past infection with SARS-CoV-2. For the state of Georgia, the first round of sampling began on August 2nd, 2020 and the last round ended on February 18th, 2022, with roughly biweekly samples. The primary assay was Ortho VITROS Anti-S between August 2nd, 2020 and February 4th, 2021; Abbott ARCHITECT Anti-N between February 8th, 2021 and June 30th, 2021; and Roche Elecsys Anti-N between September 6th 2021 and February 18th, 2022. The switch from anti-S target to anti-N was to allow continued estimating prior infections in the context of mRNA vaccinations which produced antibody responses to the S-gene target. The Roche assay was deemed to have higher sensitivity, particularly in light of antibody waning, compared to the Abbott assay[245]. Figure 4-21 shows age-stratified seroprevalence estimated for the state of Georgia. Seroprevalence increases during epidemic waves. The change from Abbott assay to Roche assay was implemented after the period without seroprevalence estimates between June 2021 and September 2021, which coincides with an epidemic wave. The increase in seroprevalence is likely a result of infections from the epidemic wave and the increased sensitivity of the Roche assay.

We first attempted to estimate the cumulative reporting rates. We use age-stratified seroprevalence to estimate age-stratified cumulative incidence by applying the age-specific seroprevalence to the population, assuming negligible waning of infection-derived antibodies. The cumulative reporting rate was estimated by dividing cumulative reported cases from GDPH SENDSS by the cumulative infections estimated from seroprevalence (Figure 4-21). The cumulative reporting rates generally increased over time but drastically reduced after the switch to the Roche assay. The increase in cumulating rate over time is likely partly attributable to waning antibodies where those infected earlier on end up with undetectable antibodies in later time periods, resulting in an underestimate of cumulative incidence from seroprevalence.

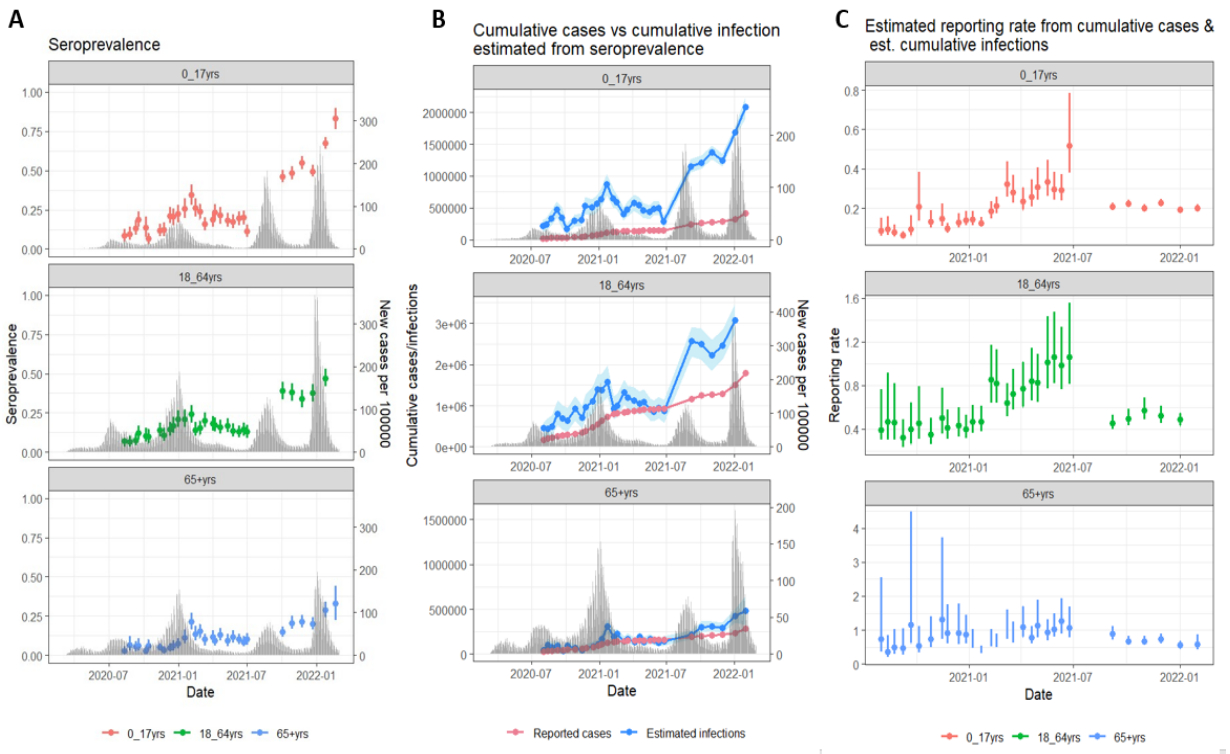

Figure 4-21. Age-stratified seroprevalence, cumulative infections estimated from seroprevalence and estimated reporting rate

A. Age-stratified seroprevalence estimates over time from the CDC. B. Cumulative infections estimated by applying the age-specific seroprevalence to the population, without assuming waning and cumulative

reported cases from Georgia Department of Public Health over time. C. Cumulative reporting rate estimated by dividing cumulative reported cases by the cumulative infections estimated from seroprevalence.

We then estimated underreporting by each wave using one seroprevalence at the beginning and one at end of each wave and estimating the number of infections in each wave from the change in seroprevalence between beginning and end. This reduces bias in estimates due to waning antibodies since antibodies remain relatively durable between 90-540 days[245]. We calculate the cumulative reported cases between the first day of sampling at the beginning of wave and the last day of sampling at the end of wave with a 2-week lag to allow time for seroconversion after infection. The reporting rate per wave is the cumulative reported cases for the wave (with 2-week lag) divided by the number of infections for the wave estimated from the seroprevalence. Waves were specified based on Figure 4-23. shows the seroprevalence at the start and end of each wave used to estimate cumulative incidence for each wave. In the middle of second wave, CDC switched the target from anti-S to anti-N. We used the last anti-S estimate even though this time was not at the end of wave 2. Further, the last available seroprevalence Feb 18th, 2022, for children and older adults and Jan 24th for adults, these dates were during the decline of wave 4 (omicron wave).

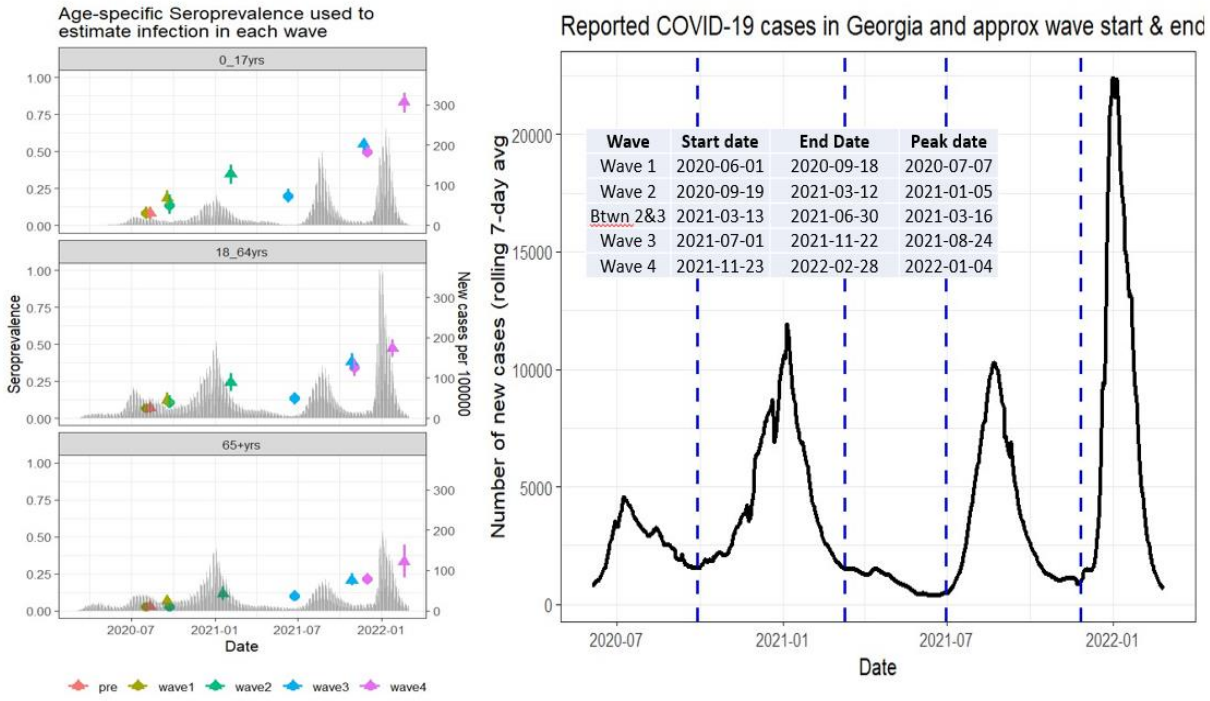

Figure 4-22. Age-specific seroprevalence at start and end of each wave

A. Age-specific seroprevalence at start and end of each wave (colored by wave) used to estimate cumulative infections for the wave. B. Start, end and peak dates of the four COVID-19 waves in Georgia between June 2020 and March 2022.

The estimated reporting rate increased from 5.9% to 16.7% between wave 1 and wave 4 for children 0-17 years. The reporting rate fluctuates between 31.9% to 53.9% for adults aged 18-64 years and between 31.9% and 50.1% for older adults aged 65 years and above. Wave 2 and wave 4 appear to have higher reporting rate for 18-64 years and 65+ years. This could potentially be because the last appropriate seroprevalence estimate wasn't after the wave but rather in the middle. In a more detailed analysis from wave 2, we see a pattern where reporting rate appears to track with the epidemic curve: reporting rate is low and increases as the epidemic increases and then decreases as the epidemic decreases (Figure 4-23). If we are missing serology estimates from later dates of a wave, our overall estimate of reporting rate for the wave may have been overestimated due to missing a period with lower reporting rate. We also tested

using a one-week lag for reported cases and found similar reporting rates per wave. The pre-wave 1 reporting rate was estimated from cumulative infection incidence derived from the first seroprevalence available (August 2nd, 2020) and cumulative cases up until that point.

Age group	Wave	Estimated reported rate for wave	Estimated infection from change in seroprevalence	Reported cases
0-17 years	pre	7.8%	NA	NA
	wave1	5.9%	253036.714	14890
	wave2	14.9%	521105.312	77391
	wave3	15.2%	874354.586	132934
	wave4	16.7%	844290.818	140623
18-64 years	pre	36.6%	NA	NA
	wave1	31.9%	343630.224	109632
	wave2	53.9%	885559.26	477637
	wave3	20.5%	1632375.036	334020
	wave4	43.2%	843431.04	364658
65+ years	pre	67.7%	NA	NA
	wave1	35.3%	51077.635	18017
	wave2	50.1%	126964.407	63649
	wave3	31.9%	154692.266	49294
	wave4	42.0%	170745.237	71630

Table 4-5. Reporting rate estimated for each wave

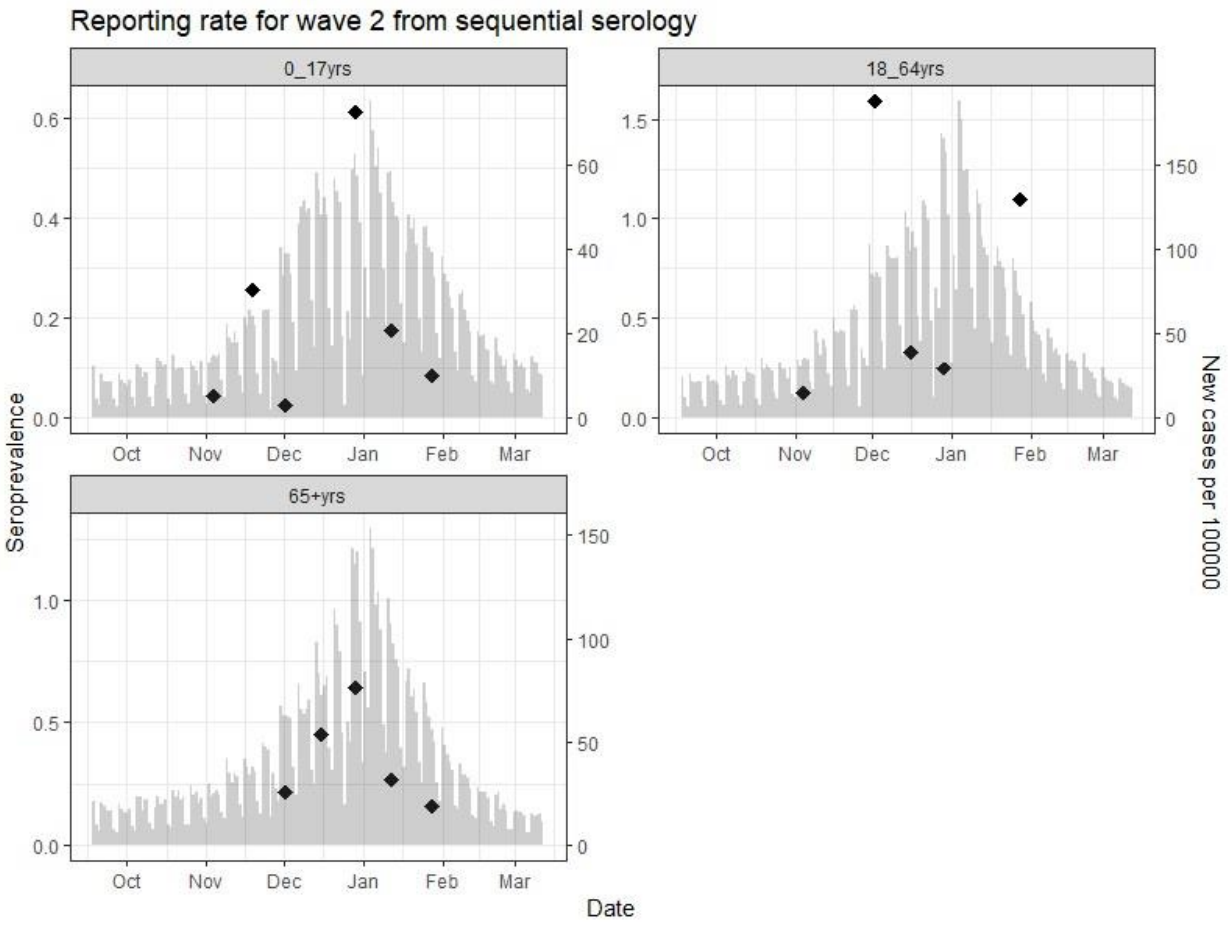

Figure 4-23. Reporting rate for wave two estimated using sequential serology.

CHAPTER 5 MODELING THE USE OF SEROPREVALENCE TO GUIDE COVID-19 VACCINATION IN MOZAMBIQUE

[Manuscript 1. This is a Manuscript in Review in Nature Communications, available in pre-print: https://www.medrxiv.org/content/10.1101/2023.08.29.23294793v1.]

Can long-term COVID-19 vaccination be improved by serological surveillance?: a modeling study for Mozambique

Carol Y Liu, Kayoko Shioda, Alicia NM Kraay, Sergio Massora, Áuria de Jesus, Arsénia Massinga, Celso Monjane, Saad B Omer, Samuel M Jenness, Kristin Nelson, Stefan Flasche, Inacio Mandomando, Benjamin A Lopman

5.1 Abstract

Seroprevalence provides an estimate of the population-level susceptibility to infection. We used a transmission model to examine the potential of using serological surveillance to inform the timing of COVID-19 re-vaccinations in Mozambique. We simulated using population-level seroprevalence thresholds as an estimate of the risk of outbreaks to trigger the timing of re-vaccination campaigns among older adults. We compared this approach to re-vaccination at fixed time intervals. Re-vaccinating older adults each time the seroprevalence falls below 50% and 80% resulted in medians of 13% and 79% reduction in deaths and number-needed-to-vaccinate to avert one death (NNV) of 448 (2.5th-97.5thcentile: 330-808) and 1,516 (1,417-1,584). Biennial and annual re-vaccination of older adults resulted in medians of 47% and 64% deaths averted and NNVs of 597 (541-689) and 888 (822-928). In sensitivity analysis over a range of antibody waning rates and epidemic scenarios, we consistently found that re-vaccination trigger thresholds of 50-55% seroprevalence are most likely to be efficient compared to fixed-time strategies, but at the expense of higher numbers of deaths. No serology-triggered strategy minimized NNV while minimizing deaths compared to fixed-time strategies. Lacking substantial benefit

of serology-informed vaccination, our results favor the use of simpler fixed-time strategies for long-term control of SARS-CoV-2.

5.2 Background

Vaccines are a pivotal tool for SARS-CoV-2 control, eliciting strong protection against severe disease and death for vaccinated individuals[161–163]. Since the beginning of global vaccine rollout in December 2020, COVID-19 vaccines averted an estimated 19.8 million deaths in 185 countries and territories[193]. Vaccination programs enabled safer relaxation of non-pharmaceutical interventions (e.g., social distancing), which facilitated a transition away from the most severe phase of the pandemic[149,194].

Despite early successes of SARS-CoV-2 vaccines, evidence of waning immunity and the emergence of novel immune-escaping variants raised concern over the longevity of vaccine-induced protection. Since the rise of the highly infectious Omicron variant, effectiveness of the primary series of mRNA vaccines against hospitalizations reduced by almost half compared to protection estimated from the first clinical trials[246]. Booster doses partially restored short-term protection, prompting their strong recommendation for those most at risk of developing severe outcomes[247,248]. Repeated booster campaigns aimed at restoring protection against severe disease among high risk groups remains an important tool in the medium- to long-term[249,250].

Effective deployment of vaccines maximizes their public health impact. While population immunity against SARS-CoV-2 was still low, targeted vaccine prioritization rapidly increased protection for vulnerable portions of the population, beginning with those at the highest risk for severe outcomes and deaths. Long-term control of COVID-19 requires the consideration of refined and information-driven strategies that optimize efficiency of vaccines, ideally preventing the greatest number of severe health outcomes with the fewest resources. Identifying critical time periods and targeting population groups most susceptible to impending waves can minimize resource needs while maximizing public health impact.

Serology, a marker for prior exposure determined by the presence of antibodies against SARS-CoV-2 in blood serum, provides information on the degree of susceptibility to infection or disease in individuals. Seroprevalence of randomly sampled individuals provides an estimation of population-level susceptibility and has previously influenced vaccination strategy. When serological studies from England[251,252] identified waning SARS-CoV-2 seroprevalence among the oldest age groups, an additional booster targeting this group was recommended. Seroprevalence estimates are further leveraged to guide vaccination strategies for endemic infections. In the case of measles, a fully immunizing infection with a high reproduction number, seroprevalence is used to identify locations and age groups with inadequate immunity for targeted vaccination campaigns. By providing snapshots of the landscape of population-level immunity before surges in hospitalizations and deaths, seroprevalence estimates enabled preemptive vaccination of the most susceptible population groups[253].

The use of serological surveillance, specifically measuring seroprevalence, to monitor changing immunity for SARS-CoV-2 at the population level and to trigger vaccination campaigns emerged as a potential long-term strategy for COVID-19 control[191,254]. However, the utility of a long-term serology-guided vaccination strategy for a pathogen with an imperfect correlate of protection is unknown and will likely depend on unpredictable long-term dynamics of SARS-CoV-2 driven by waning immunity and new variant emergence[255,256]. Targeted vaccination strategies hold potential in resource limited settings where vaccine provision is constrained[257,258]; however, there are few mathematical models tailored to localized and distinct epidemic patterns in low income countries despite their utility for optimizing vaccine strategies.

Our study uses a mathematical model of SARS-CoV-2 to determine the utility of incorporating population-level seroprevalence to trigger future COVID-19 re-vaccination efforts. We developed our model to represent Mozambique, a resource-limited setting. Mozambique is notable for its early efforts in measuring countrywide SARS-CoV-2 seroprevalence[259] and for studying seroprevalence in children before commencing a resource-intensive campaign to vaccinate children[23]. We assess the impact of a re-

vaccination strategy for COVID-19 in Mozambique guided by population-level serology under uncertain epidemic dynamics over a 10-year time horizon.

5.3 Methods

5.3.1 Model structure

We extend a deterministic, compartmental SEIR-like model[260,261] to incorporate demographic strata of age group (≤18 years, 19-49 and ≥50 years) and urban/rural and twelve tiers of immunity status: combinations of four tiers of vaccine status (unvaccinated, vaccinated with one dose, two doses and three doses) and three tiers of exposure status (unexposed, one prior exposure and two prior exposures) (Figure 5-1). The multiple tiers of immunity allow differential susceptibility based on prior exposure from either infection or vaccination. To summarize the model design: after exposure, individuals enter a latent, non-infectious period (E), after which they progress to either infectious and asymptomatic (A) or infectious and symptomatic (I). A proportion of symptomatic individuals progress to more severe disease and are hospitalized (H). A subset of those who are hospitalized ultimately die from SARS-CoV-2 (entering the D class). All individuals who are not hospitalized recover (entering the R class) and can either be seropositive (R_p) or seronegative (R_n). Individuals can also be vaccinated and, if unexposed, enter the seropositive V_p or seronegative V_n classes immediately post-vaccination, if previously exposed, enter the seropositive R_p or seronegative R_n classes corresponding to their prior infection tier. The R and V classes are temporarily immune to infections; however, immunity wanes over time and individuals return to a partially susceptible class ($S_{p,1}$ for seropositive and one prior infection and $S_{n,1}$ for seronegative and one prior infection). The force of infection (Eq 35) is modified by probability of infection of exposed age group (β_i), vaccine effectiveness against infection, differential by 1-3 doses (VEI_v), reduced susceptibility from protection from prior infection (IP_e), increased variant transmissibility (for Delta and Omicron waves), immune escape (applied to immunity tiers with prior exposure through either infection of vaccination), a relative decrease in susceptibility for seropositive individuals compared to seronegative individuals with the same prior exposure (foi_s)[50,262,263], age and rural/urban-specific contact rate ($\chi_{j,i,r,u}$)

and infection density within each demographic strata. Infected individuals who are asymptomatic have reduced transmissibility (α_i). The model diagram is described in Figure 5-1, equations can be found in 5.7.1.1 and details on model parameters, values, ranges and sources can be found in 5.7.2.

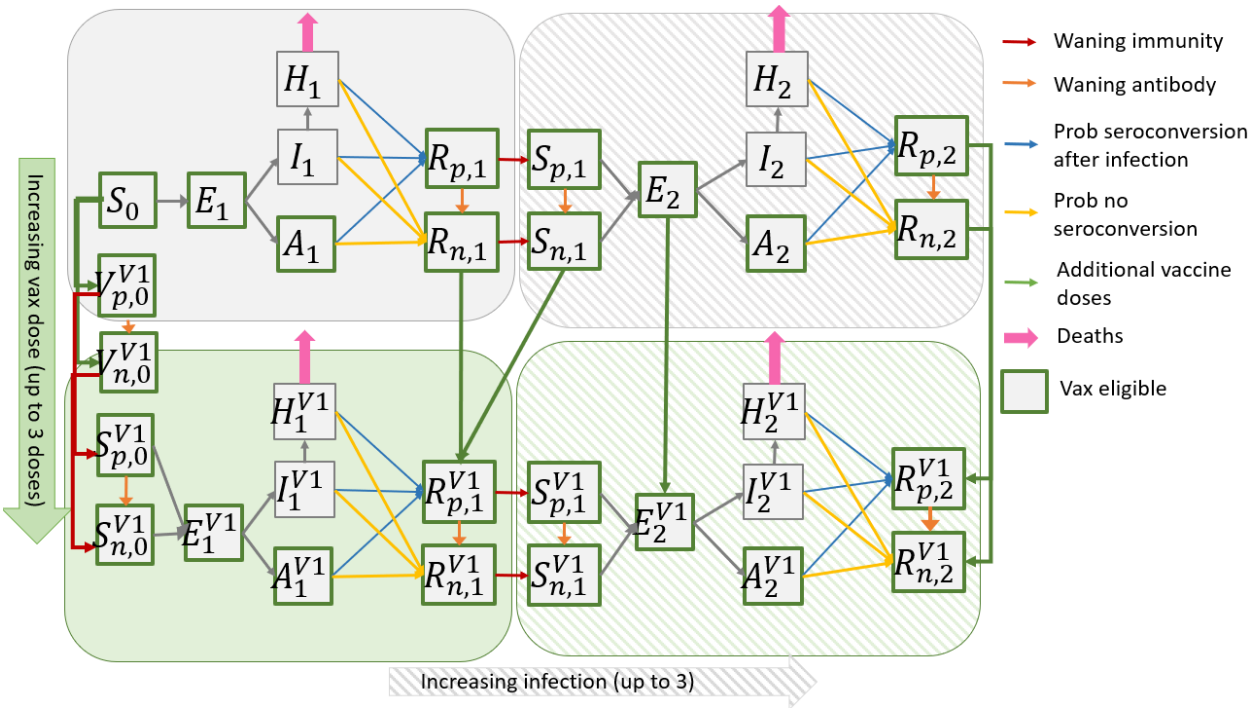

Figure 5-1. Compartmental model diagram[1]

[1]Schematic of an S-E-I-R-like compartment for a single demographic stratum (out of six total: three age groups in each of urban and rural) with four tiers of immunity shown (two tiers of vaccination: unvaccinated and one dose of vaccine, with the superscript V1 the vaccine dose and two tiers of exposure: no prior exposure and one exposure, with the subscript representing the number of exposures). Individuals who recover from infection are immune for a period. The majority seroconvert after infection (R_p) while others do not (R_n). Immunity for both seropositive (R_p) and seronegative (R_n) can wane over time, returning individuals to S_p and S_n, respectively, allowing for subsequent infection. Individuals in classes outlined in green are eligible for vaccination and move to a higher vaccine tier upon vaccination (not all arrows drawn explicitly in the diagram) The majority of individuals seroconvert after vaccination.

Vaccinated individuals are temporarily immune before their immunity wanes. Individuals in vaccinated and previously exposed strata have a reduced probability of infection and disease.

5.3.2 Seroconversion and seroreversion

Our model distinguishes between antibody positivity and immunity with separate seropositive and seronegative compartments in the S (susceptible), R (recovered) and V (vaccinated) disease states. Presence of neutralizing antibodies following exposure is associated with reduced risk of severe disease[264–268]. Nevertheless, protection against infection also depends on cell-mediated immunity and circulating variants. For example, individuals who lack neutralizing antibodies but have robust cell-mediated immunity can still be protected, while others with antibodies may remain susceptible to new immune-escaping variants[267,269,270]. Explicit separation of immunity and serological status represents their imperfect correlation.

Upon exposure through either infection or vaccination, most individuals seroconvert and become seropositive. Some with weaker immune systems or milder infections may not produce detectable antibodies after infection[265,271,272]. We assumed that 90%[264,265] of infected individuals seroconvert after recovering and 85%[252] of vaccinated individuals seroconvert upon moving to the vaccinated class following first dose. Further, we assume 70% of seronegative individuals who receive an additional vaccine dose will seroconvert[273].

Over time, antibodies can wane with seropositive individuals seroreverting to seronegative. Fully immune and seropositive individuals (R_p) will serorevert to fully immune and seronegative (R_n) while partially susceptible and seropositive individuals (S_p) will serorevert to partially susceptible and seronegative (S_n). Waning rates differ by number of exposures, regardless of whether the exposure was from vaccination or infection (e.g. antibody waning among those infected once and vaccinated once is the same as waning among those vaccinated twice). Seroreversion is fastest following the first exposure (1/500 days)[274–277] and declines after multiple exposures (range of 1/2500 days after second exposure), in line with recent evidence that antibody titers are higher and more persistent after multiple exposures[278,279]. To more

appropriately represent the dynamics of waning antibodies in the real world, the rate of seroreversion is modeled as a gamma distribution with four sequential compartments for the tiers with the fastest waning rates[280] (5.7.1.2).

We assessed pairwise correlations between seroprevalence, susceptibility and deaths per wave to ensure that the relationship between seroprevalence and deaths, seroprevalence and susceptibility and susceptibility and deaths in our model was as expected (5.7.5).

5.3.3 Tiered susceptibility

Following infection or vaccination, we assume that individuals are fully immune for an average of 150 days before moving to a partially susceptible class. Among unvaccinated individuals, one and two prior infections will confer 35%[51] and 60% protection against infection (IP_e), respectively.

Vaccinated individuals move to a higher vaccination class (V1 -> V2 -> V3) with reduced rates of infection and probability of hospitalization if infected. We parameterize vaccine effectiveness based on performance of the ChAdOx1 nCoV-19 vaccine (Astra Zeneca), the main vaccine used in Mozambique (and many LMICs) and assume that one dose of vaccine reduces rate of infection (VEI_v) by 50%, two doses by 60% and three doses by 70%[281]. Further, one, two, three doses of vaccine reduce the probability of progression to severe disease (VEP_v) by 40%, 67% and 70% respectively. Overall vaccine effectiveness against hospitalization is 70%, 87% and 91%[281] for one, two, three doses of vaccine, respectively. For individuals with hybrid immunity, protection from infection is determined by literature when available[51] or 1-(1-IP_e)*(1- VEI_v). Key evidence on infection and vaccination effectiveness against susceptibility and severe disease stratified by variants used to inform our immunity parameters is summarized in 5.7.8.

5.3.4 Data sources and calibration

Model calibration provided an estimation of the population distribution across compartments and the seroprevalence at the start of the simulation (Sept 1, 2022), nine months after the last sampled seroprevalence in Mozambique. We incorporated data on social contact sampled in an urban and a rural

area in Mozambique during the COVID-19 pandemic between March 2021-March 2022[282], multiple cross-sectional seroprevalence data available at several time points from an urban and a rural area in Mozambique (5.7.3.3); vaccination data and time-series of reported cases[11] adjusted for an underreporting factor to calibrate the model.

The following parameters were calibrated using an approximate Bayesian approach: $\beta_c, \beta_a, \beta_{e,}$ (probability of infection upon contact among children, adults, and older adults), increased transmissibility and immune escape for Delta and Omicron variants and waning rate of antibodies (Table 5-4). We defined a range of plausible priors for each parameter informed by literature review and prior experience calibrating a comparable model. The initial ranges for calibration can be found in Table 5-4. We used Latin hypercube sampling[241] to randomly sample from the pre-defined parameter space for each run. R_0 from the sampled βs was calculated by identifying the dominant eigenvalue of the next generation matrix that incorporates both age-specific mixing patterns and the age-specific probabilities of transmission $(\beta_c, \beta_a, \beta_e)$[283]. We further constrained βs to sampled trios that met the pre-specified R_0. We compared the modeled age-specific seroprevalence estimates after each wave to available seroprevalence information as the primary target statistic (17 unique estimates). We conducted the calibration iteratively. Initially, 5000 iterations were sampled from the initial range of parameter spaces. We then identified parameter draws that performed in the top 10% based on the sum of square errors across all seroprevalence estimates and where each modeled data point was within 5 percentage points of estimates measured from field studies. We then restricted the ranges for each parameter and conducted another round of LHS sampling based on the new, restricted ranges. This process was repeated 4 times until, iteratively narrowing the calibration range each time. We then ranked each set of parameters by the sum of square errors for seroprevalence estimates and conducted forward simulation using the top 10% (n=500). We then chose the set of parameters that produced the median cases and epidemic trajectory over the 10-years simulation period as the primary parameter values for the forward simulations. Sensitivity analysis for the range of acceptable calibrated parameters (top 10%) to assess the degree to which uncertainty in the calibrated values would

affect our forward simulation results. Our calibrated values for transmissibility of the delta and omicron variants are in line with the published literature[44,284]. Ranges from calibration reflect choice to select the top 10% of parameters during calibration rather than uncertainty.

5.3.5 Forward simulation epidemiological scenarios

We simulated the epidemic forward for ten years from September 1, 2022. Dynamics of long-term immunity were simulated by allowing waning from the highest vaccination and infection tier in addition to the modeled waning described earlier. This included: 1) waning immunity for individuals who recovered after their third infection ($R_{p,3}$, $R_{n,3}$) to the two-infection susceptible tier ($S_{p,2}$, $S_{n,2}$) after a period of immunity and 2) waning immunity for individuals from the three-vaccine-dose susceptibility tier (S_P^{V3}, S_n^{V3}) to the two-vaccine-dose susceptibility tier (S_P^{V2}, S_n^{V2}) after a period of full immunity. We assumed annual waves driven by increases in transmission in the cool, dry season (April-July in Mozambique)[285], informed by observational studies of early SARS-CoV-2 dynamics that cooler and dryer weather were moderately associated with increased transmissibility[286–288] and by evidence suggesting that cooler, dryer air improved half-life and viability of the virus[289,290]. The relationship between $R_0(t)$ and the specific humidity q(t) is determined by a prior model[288]: $R_0(t) = \exp(\alpha * q(t) + \log(R_{0max} - R_{0min})) + R_{0min}$.

To represent uncertainty in future transmission, we sample R_{0max} for each year from a log normal distribution (mean R_0 = 5.5, standard deviation = 0.2). R_{0min} is fixed at 2.05, marginally lower than the transmissibility of the original Wuhan strain. Given unpredictable long-term transmission dynamics, we consider one scenario where future waves are driven by high rates of immune escape and a second scenario where future waves are driven by high rates of waning immunity. In the high immune escape scenario, in addition to sampling R_{0max} from the distribution, we enforce a general trend of yearly increases using the following formula: $R^h_{0max}(yr) = R_{0max}\ (yr) \times 1.075^{yr}$, where $R^h_{0max}(yr)$ is the yearly R_{0max} for the immune escape scenario, $R_{0max}\ (yr)$ is the randomly sampled R_0 and yr is years since start of simulation. In the waning immunity scenario, we allow for additional waning immunity

from the highest three-exposure tier to the two-exposure tier (90% protection to 75% protection in the three-vaccine dose tier and 86% protection to 67% protection in the two-vaccine dose tier). For each scenario, we conducted 500 different runs, each with 10 randomly sampled R_0 for each year.

5.3.6 Vaccination triggers and analytical outputs

Based on literature suggesting increased impact and cost-effectiveness of routine vaccination for older adults compared to routine vaccination of other age groups, we focus on a strategy of booster vaccination for older adults and compare the impact of timing additional doses guided by population-level seroprevalence estimates or based on fixed time intervals. When triggered in the model, additional vaccination was provided to the older adult population at 2% (or ~28,000 doses) of the older adult population per day over a 30-day campaign period for 50% coverage per campaign, with the same vaccination rate applied to seropositive and seronegative subgroups. A 30-day campaign was deemed feasible and vaccinating ~28,000 deemed achievable compared to the 100,000 doses provided per day during peak campaign periods for the primary COVID-19 series in Mozambique[291]. Specifically, the timing of vaccination was guided by: 1) seroprevalence thresholds among older adults ranging from 50-80% where vaccination will be triggered when the seroprevalence falls below the threshold; 2) fixed time intervals where vaccination will be triggered annually or biennially, with the first vaccine campaign triggered a year after the start of simulation, chosen a priori for feasibility at the time of project conceptualization.

Our primary outcome is the number of vaccinations provided to older adults needed to avert one death in the population (or number-needed-to-treat, NNV), using the number of deaths when no additional vaccinations are provided as the base case. The NNV allows more equitable comparison between scenarios where vaccination is constantly triggered versus scenarios where vaccination is rarely triggered, shedding insight on the NNV and potential cost-effectiveness of different vaccination timing strategies. We further present the number of deaths and the number of deaths averted compared to a no vaccination scenario and the number and timing of additional vaccination campaigns.

5.3.7 Code availability

Code used for model calibration, forward simulation and analysis of model outputs can be found in the following Github Repository: https://github.com/lopmanlab/COVID_serovax_Mozambique_v2/

5.4 Results

We modeled transmission dynamics and re-vaccination scenarios using a deterministic, compartmental SEIR-like model[260,261] over a ten-year period starting in September 2022. The model was stratified by age group (≤18 years, 19-49 and ≥50 years), urban/rural and 12 immunological tiers: combinations of four levels of vaccination status (unvaccinated to three doses) and three levels of SARS-CoV-2 exposure status (unexposed to two prior exposures) with lower susceptibility for increased exposure. Our model captures differential rates of waning antibodies and immune protection, each informed separately by observational studies[252,271,274,275,277,279,292]. For long-term SARS-CoV-2 dynamics, we incorporated seasonality[288,293] assuming annual increases in transmission in the cool, dry season (April to July) and uncertainty in transmission intensity (annual R_t). We assessed a strategy of repeat re-vaccination for older adults (≥50 years), likely the most cost-effective[173,177,178,294], and compared the impact of timing re-vaccination campaigns guided by population-level seroprevalence estimates to the impact of vaccinating at fixed time intervals. We integrated empirical data from Mozambique on vaccine coverage, human contact patterns collected during the pandemic and survey-derived seroprevalence.

5.4.1 Model calibration

Our historical model projection matched the COVID-19 epidemic waves observed in Mozambique between 2020 and August 2022 (Figure 5-2) and our modeled seroprevalence closely reflected historical estimates sampled at various times points in Mozambique across three age groups in both urban and rural settings (Figure 5-2). At the start of model projections (September 2022), the median seroprevalence was 56.5%, 86.0% and 84.3% for children, adults, older adults, respectively, based on model calibration. At this time, the estimated distribution of individuals who were fully susceptible (no exposure through infection or vaccination), partially susceptible and fully immune was 16.6%, 67.0%, 16.4% for children,

0.6%, 67.9%, 31.5% for adults and 1.3%,68.3%, 30.6% for older adults. Calibrated primary series vaccine coverage among adults and older adults was 93% and 96%, respectively, comparable to the data. For children who were ineligible for vaccination, immunity was acquired from natural infection alone.

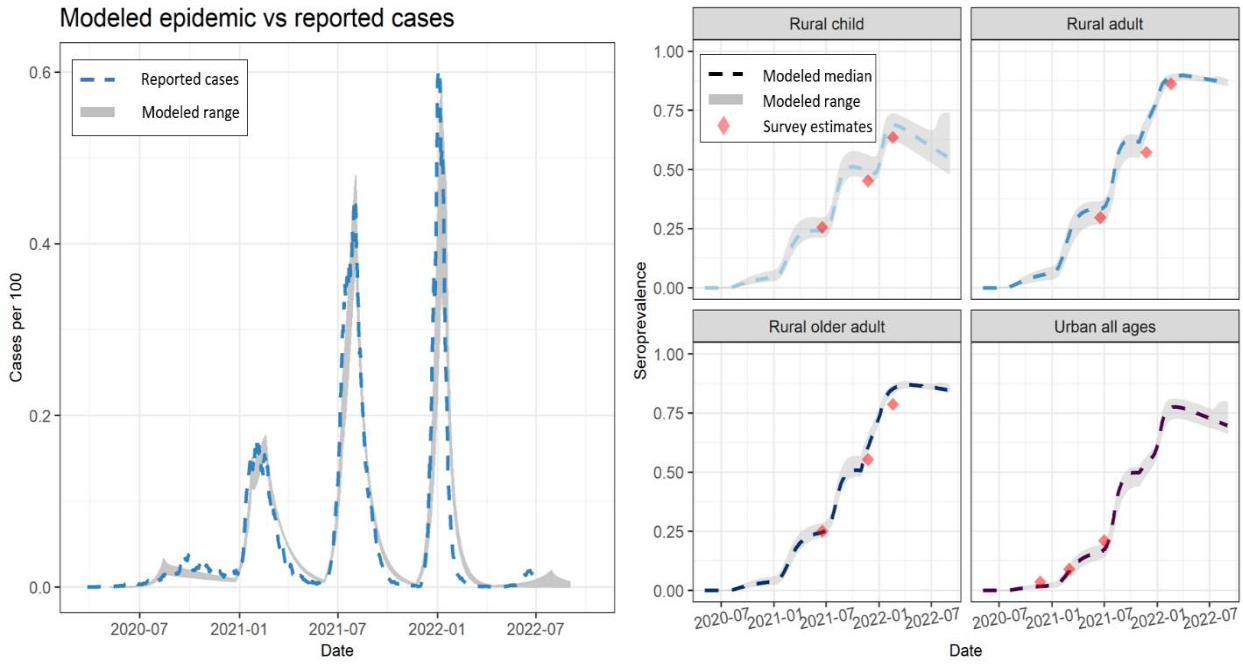

Figure 5-2. Calibrated model results compared to observed data

(Left) Modeled historical epidemic of cases per 100 persons using the top performing calibrated parameters (shaded grey=range of modeled cases per 100, dotted blue=reported cases per 100 accounting for 1/90 underreporting for the first two waves, 1/100 underreporting for the third wave, 1/120 underreporting for the fourth wave). Ranges reflect choice to select the top 10% of parameters during calibration rather than uncertainty (Right) Modeled seroprevalence compared to seroprevalence estimated from serological studies during various periods of the pandemic in Mozambique.

5.4.2 Description of simulated epidemic and changing immunity

Long-term COVID-19 epidemic patterns will likely be driven by immune waning and immune escape[255,295]. We focused on modelling long-term dynamics driven by the former, assuming that a re-vaccination strategy triggered by seroprevalence is more likely to be beneficial under an epidemic driven by waning immunity. Under this assumption, the ten-year projection with no re-vaccination results in

multiple peaks that are on average most intense in the third year and diminishes over time due to an increase in population-level immunity (Figure 5-3). The median cumulative number of deaths per 100,000 across sampled R_t (mean = 5.5, SD = 0.2) over 10 years is 51 (2.5th-97.5th percentile: 49-55) for all ages, 1.1 (1.05-1.18) for children, 31 (30-34) for adults and 778 (741-839) for older adults (Table 5-5). Seroprevalence declines over time and increases following surges in cases.

We further observed from our model that 31% of older adults were fully immune before the start of the forward simulation, of which 58% had protection from vaccination alone with no prior infection. The proportion immune reduces over the next year as individuals lose their full protection and become increasingly susceptible to infection. This immunity gap drives a large wave in 2026 which infects 13% of the population, resulting in a shift in susceptibility whereby individuals transition from vaccine-only protection to hybrid protection from both vaccination and infection (Figure 5-3). The shift leads to smaller subsequent waves, in line with evidence of increased protection from hybrid immunity[47,49,164,296].

5.4.3 Descriptive results from re-vaccination strategies

For all re-vaccination scenarios, we trigger a vaccination campaign where 50% of the older adult population is vaccinated over a 30-day period. A strategy in which re-vaccination is triggered at a higher seroprevalence threshold (ex. 80%) increases the number of vaccination campaigns and cumulative vaccine doses needed. While a median of only one campaign (or 0.63 million doses) is needed to maintain a seroprevalence of at least 50% among older adults, 21 campaigns (or 13.3 million doses) would be needed to maintain a seroprevalence of at least 80% (Table 5-5). Using a 50% seroprevalence threshold, re-vaccination is first triggered after a median of 5.6 years. Given the higher intensity of earlier epidemic waves, the later re-vaccination trigger has lower impact on the overall epidemic trajectory and total disease burden. In comparison, using a 65% and 80% seroprevalence threshold triggers the first re-vaccinations after 1.6 years and 109 days, respectively. Using either of these thresholds to trigger re-vaccination reduces the size of early waves compared to the 50% threshold, but is at the expense of more frequent vaccination campaigns. In the fixed time interval annual and biennial re-vaccination strategies

implemented without regard to seroprevalence, we simulated the first re-vaccinations at 300 days, chosen a priori, for a total of 10 and 5 campaigns over ten years, respectively, early enough to reduce the size of larger projected epidemic waves in 2026.

5.4.4 Impact of different re-vaccination strategy on vaccine NNV

Compared to a median of 11,202 (2.5th-97.5th percentile: 10,667-12,076) total simulated deaths among older adults with no additional vaccinations over ten years, vaccinating older adults each time the seroprevalence among older adults falls below 50% and 80% results in a median of 9,774 (8,886-10,603) and 2,393 (1,954-2,828) deaths, respectively (Figure 5-3 and Table 5-5), a reduction of 13% and 79%. The number needed to vaccinate to avert one death (NNV) reaches a minimum at a 50% threshold where a single campaign results in a median of 1,434 (787-2,079) deaths averted and a median NNV of 448 (330-808). The NNV increases with increasing seroprevalence threshold with a median NNV of 1,516 (1,417-1,594) for an 80% threshold. In comparison, annual and biennial re-vaccination of older adults results in a median of 4,097 (3,779-4,345) and 5,922 (5,493-6,538) deaths, respectively, and median NNVs of 888 (822-928) and 597 (541-689), respectively (Figure 5-3 and Table 5-5). In summary, vaccinating at seroprevalence thresholds of 50% - 55% is more efficient than both annual and biennial strategies while vaccinating at thresholds of 60%-70% is more efficient than an annual strategy but less efficient than a biennial strategy.

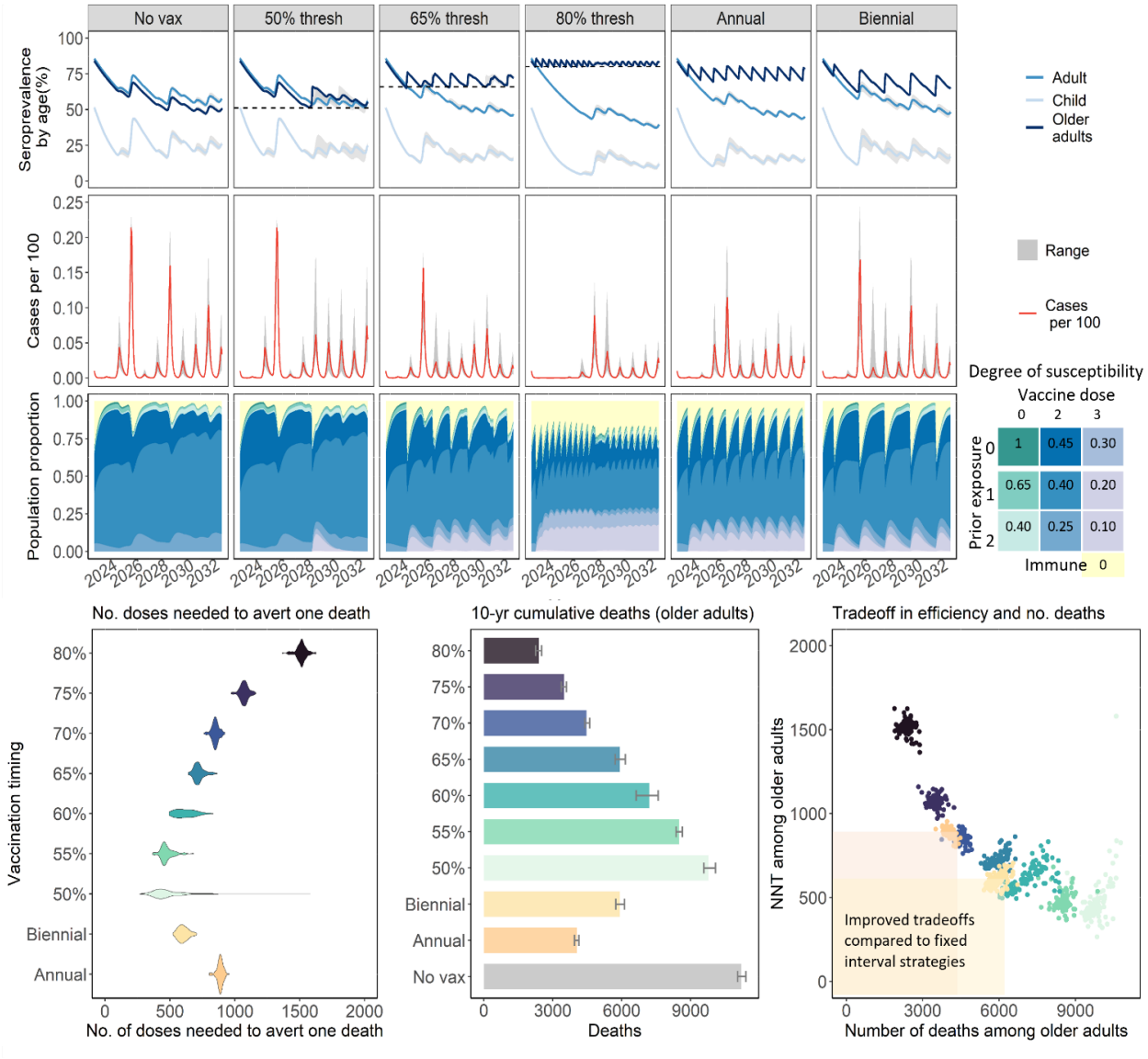

Figure 5-3. Model results of time series of ten-year epidemic trajectory, seroprevalence and immunity landscape and overall number of doses needed to avert one death (NNV) and cumulative deaths

(Top row) Modeled 10-year seroprevalence (gray = 2.5th-97.5th percentile) over time for children (lightest blue), adults (medium blue) and older adults >50 years (darkest blue) under 1) no additional vaccinations; 2) re-vaccinations timed by seroprevalence trigger thresholds of 50%, 65% and 80% and 3) re-vaccinations timed annually and biennially. (Middle row) Modeled 10-year cases per 100 individuals over re-vaccination scenarios (gray shading=ranges from random Rt sampling, red= median); (Bottom

row) Susceptibility among older adults. Colored density represents population proportion within susceptible or immune tiers over time, ranging from fully immune (yellow) to up to 2 prior infections and 3 vaccination doses. The blue and purple densities indicate proportion of individuals in the 2- and 3-vaccine dose susceptibility tiers, respectively. The darkest shades within each color have no prior infection and are the most susceptible, with lighter shades indicating more exposure and decreased susceptibility. Individuals can wane from the 3-dose susceptibility tier to the 2-dose tier and from the 3-prior infection tier to the 2-prior infections at a rate of 1/365 days. The degree of susceptibility is indicated in the grid legend and is relative to totally susceptible, with 1 indicating fully susceptible and 0 fully immune. In scenarios with re-vaccination, campaigns generate spikes in the proportion of individuals fully immune (yellow). More frequent vaccination campaigns result in higher proportion immune (yellow) and longer period in the compartment with highest protection (purple). (Bottom left) Distribution of the number of vaccine doses needed to avert one death (NNV) by re-vaccination timing strategy (biennial, annual, triggered based on seroprevalence thresholds of between 50%-80%); (Bottom center) Cumulative deaths over ten years among older adults. Error bar represents 2.5th-97.5th percentile of cumulative deaths for older adults; (Bottom right) Scatterplot of tradeoffs in NNV and number of deaths comparing serology-triggered strategies with fixed-time strategies. Serology-triggered thresholds that fall into the shaded region would demonstrate improved tradeoffs compared to fixed-time strategy. For all scenarios, we use an antibody waning rate of 1/2500 days.

5.4.5 Tradeoffs in number-needed-to-vaccinate (NNV)

We explore tradeoffs in the NNV and the number of deaths across different serology-triggered re-vaccination strategies compared to the tradeoffs observed in the annual and biennial strategies. We observe a pattern of tradeoff where no single serology-triggered re-vaccination strategy can minimize both NNV and the cumulative deaths compared to the fixed-time strategies. Re-vaccinating at 80% seroprevalence results in fewer deaths than both annual and biennial strategies but has a higher NNV and thus requires more doses of vaccines to avert one death. Re-vaccinating at 50% and 55% seroprevalence thresholds produces a lower NNV compared to than annual and biennial strategies, but at the expense of

more deaths. In summary, none of the serology-triggered strategies resulted in both lower NNV and lower deaths compared to fixed-time strategies.

Start times of the first vaccination campaign in fixed-time strategies was set at 300 days, while serology-triggered strategies are delayed until seroprevalence falls to specific thresholds. To examine if the timing affected the relative outcomes, we modified start times for fixed-time strategies, sampling between 90 to 2000 days, and ran a set of 50 random Rt draws for each. We plot the median across Rt draws and visualize the relationship between start time and 1) the number of deaths and 2) NNV using smoothed conditional means from a linear model with a cubic spline (Figure 5-4). Delaying the start time for both annual and biennial strategies increased the cumulative number of deaths but produced similar NNVs. We find that most serology-triggered scenarios are still unable to minimize both the NNV and deaths when compared to fixed-time strategies of similar start times.

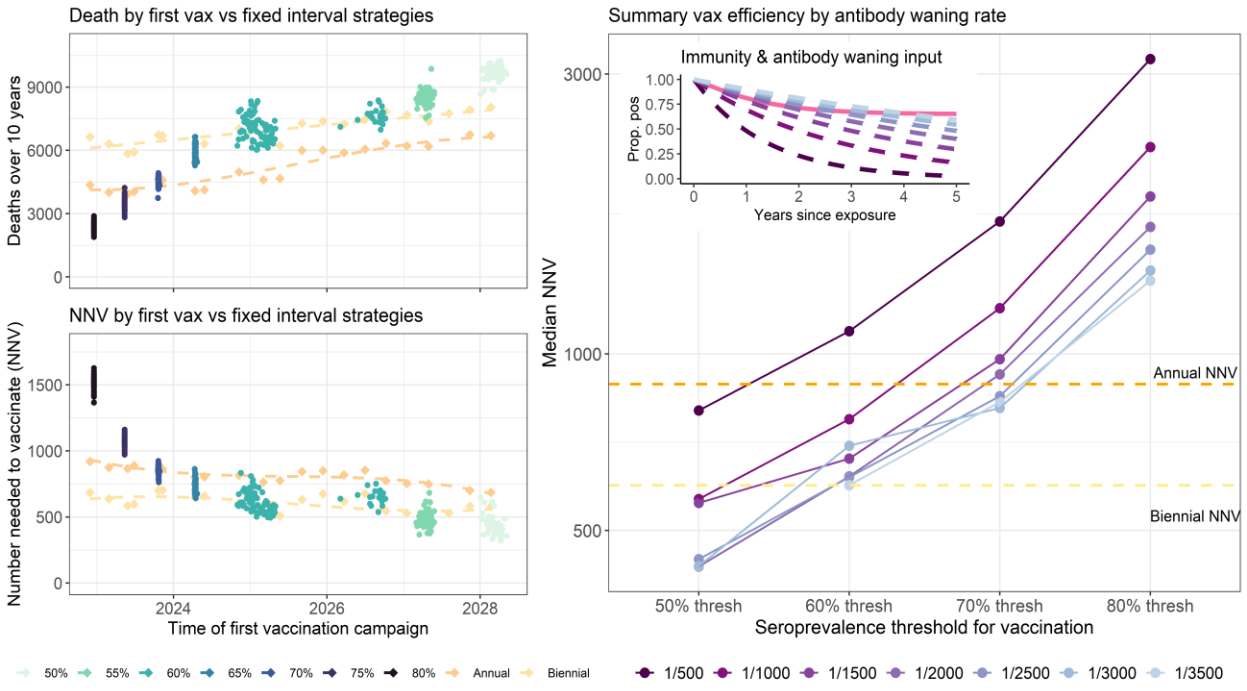

Figure 5-4. Sensitivity analysis on varying time of first vaccination campaign for fixed interval strategies and varying rate of antibody waning

(Left) Scatter plots of start time of first vaccination over random Rt simulation runs and number of deaths among older adults and number-needed-to-vaccinate to avert one death (NNV) compared with fixed-time strategies initiated at different start times. (Right) Median NNV by seroprevalence threshold for re-vaccination over various rates of time-to-seroreversion (lightest purple = slowest time-to-seroreversion, darkest purple = fastest time-to-seroreversion), with annual (orange) and biennial (yellow) NNVs for reference. Inset shows the modeled rates of different antibody waning after two or more prior exposures compared to waning immunity (pink).

5.4.6 Sensitivity analysis

5.4.6.1 Sensitivity analysis of rates of waning antibody, waning immunity and decreased susceptibility for seropositive

The time-to-seroreversion of serological markers can vary by target and the choice of titer thresholds used to determine seropostivity[245]. For example, estimates of time-to-seroreversion after one infection exposure range from 250 days to 730 days for anti-N IgG and 255 days to 1500 days for anti-S IgG[245,271,297], with evidence suggesting more durable antibodies after repeated exposures[252,298,299]. We vary the modeled rate of antibody waning to explore outcomes across a range of antibody targets and seroprevalence trigger thresholds that could be used as part of a surveillance program, assuming multiple exposures, from fastest (time to seroreversion of 500 days) to slowest (time to seroreversion of 3500 days). Under assumptions of relatively durable hybrid immunity after multiple exposures, we find that choosing a serological marker with rapid time-to-seroreversion relative to waning immunity results in early first vaccination and frequent subsequent re-vaccination, a highly inefficient strategy. A marker with slower waning and higher correlation with waning immunity is more likely to have lower NNV compared to annual and biennial re-vaccination strategies (Figure 5-4).

The main analysis assumes a rate of waning immunity from immune to partially susceptible of 1/150 days and a 1.85 times higher probability of infection among seropositive individuals compared to seronegative

individuals with the same degree of prior exposure. We conducted sensitivity analysis around these two parameters and did not find substantial differences in our main conclusions (Figure 5-21; Figure 5-22).

5.4.6.2 Sensitivity analysis on epidemic assumptions

While the expectation is that, SARS-CoV-2 will begin to display regular, seasonal epidemic patterns, so far, SARS-CoV-2 waves have occurred at irregular times throughout the year300, which may continue into the near future. We conducted sensitivity analysis to explore the relative outcomes of serology-triggered versus fixed-time re-vaccination strategies under randomly-timed epidemics by randomizing the timing of annual increases in transmission each year. We find that triggering re-vaccination at 50%-65% seroprevalence thresholds are more efficient than both annual and biennial re-vaccinations but are again at the expense of higher number of deaths. Compared to seasonal epidemic patterns, under randomly-timed epidemics lower trigger thresholds for serologically-guided scenarios displayed wider variations in NNV and deaths averted. In some simulation runs, serology-triggered strategies can be highly efficient while in others, sustained transmission over several years maintained seroprevalence levels and thus delayed the timing of first vaccination leading to almost no deaths averted (5.7.7.1).

In a separate sensitivity analysis, we simulate future waves driven by increasingly transmissible immune escape variants. We find a higher number of deaths and that seroprevalence is more likely to be maintained by repeated epidemic waves that infect a higher proportion of the population. In serologically triggered vaccination scenarios, vaccinations are less likely to be triggered. We find similar deaths averted by re-vaccination compared to the main epidemic scenario and lower NNV but similar patterns in NNV across re-vaccination timing strategies whereby only the lower seroprevalence thresholds are more efficient than either annual or biennial strategies (5.7.7.2).

5.5 Discussion

We use a transmission model to examine the potential for serological surveillance to guide the timing of future rounds of COVID-19 re-vaccination in Mozambique, a resource-limited setting. Across scenarios of waning rates of serological marker, immunity, relative susceptibility between seropositive and

seronegative and epidemic patterns we explored, triggering re-vaccination using lower seroprevalence thresholds of 50-65% is more efficient than both annual and biennial vaccination strategies and triggering re-vaccinations using 60-70% thresholds is more efficient than an annual strategy. The improved NNV, or fewer doses needing to avert one death, is at the expense of more deaths, and no serology-triggered re-vaccination strategy minimizes NNV while minimizing deaths. Moreover, routine population-based sampling that can yield accurate and timely seroprevalence estimates will be costly. Without clearly favorable tradeoffs between NNV and deaths even in the best-case scenarios, we conclude that there is unlikely to be a favorable strategy to monitor population-level protection and reactively vaccinate the most vulnerable population groups before observing increases in clinical cases and hospitalizations. Taken together, the results from our modeling work favor the use of simpler fixed-time re-vaccination interval strategies over serology-triggered re-vaccination strategies.

Our modeling work provides a framework for explicit considerations necessary for population-level serological surveillance to guide response. The degree of correlation between seroprevalence and immunity is likely to impact its utility. In the case of SARS-CoV-2, studies have explored the level of protection conferred by titers of different serological markers at the individual-level[267,300]. To formulate a feasible population-based strategy using information on correlates of protection requires its translation into measurable population-level estimates. Selecting an appropriate serological marker and a corresponding titer threshold that can reflect complex population-level susceptibility to future outbreaks and can be monitored through population surveillance will be key. Relatedly, considerations must be given to selecting the most suitable seroprevalence trigger threshold. In the case of measles, where the goal of vaccination is to eliminate infections, the proposed serology-guided vaccination strategy uses the herd immunity thresholds as the trigger for vaccination campaigns[253]. In contrast, the primary objective of SARS-CoV-2 vaccination is to reduce severe outcomes and deaths. Without defined population-level thresholds predictive of severe outcome potential, our modeling work tested a range of seroprevalence thresholds as vaccination triggers. Our analysis demonstrated, that in the context of durable hybrid

immunity against severe outcomes, using a serological marker with slower waning to trigger re-vaccination is most likely to be efficient against fixed-time strategies. These considerations are further applicable to other infectious diseases that can benefit from leveraging serosurveillance to inform public health interventions[301,302]

Our analysis is the first study to assess potential outcomes of serological triggers for a long-term SARS-CoV-2 strategy. Our model structure extends previously published models[177,293] by explicitly representing complex immunity profiles of hybrid immunity. Since the duration and extent of protection conferred by prior exposures depends on whether an individual's particular history includes infection by the virus or one or more vaccine doses[295], an explicit representation more accurately reflects population-level susceptibility that dynamically changes in response to vaccinations, infections and waning immunity. Unlike other models, we further decouple antibody waning from immunity waning with both processes informed by available data, which more accurately reflects their varying timelines and dynamics. Our NNV values are within the range other modelling studies that evaluated the NNV of vaccinations in LMICs. One estimated the NNV to be 370 for all eligible age group[303], a second estimated the NNV to be <1000 for boosters to high risk groups[175] and a third estimate the NNV to be 1453 for yearly boosters among those aged 60 years and above[178].

We acknowledge several limitations. There is considerable uncertainty around model parameters, especially for the extent of protection conferred by multiple exposures, rates of waning antibody levels and immunity[304]. Our parameterization reflected the observed protection conferred by prior exposures up until December 2023where cross protection against repeat infections was predominantly driven by a mix of variants including the Omicron variant [48,51,305]. Future variants may have greater or less cross protection against future infections than we have modeled here. We assumed a seasonally-forced long-term transmission pattern based on evidence from other respiratory illnesses in Mozambique and from other human coronaviruses[255,294,306,307]. We acknowledge further limitations in assuming that the protection from severe outcomes over time is proportional to protection from infection[308]. There remains considerable uncertainty regarding the long-term dynamics of endemic SARS-CoV-2 infection and dynamics proposed

by our model served as a base case scenario that allowed for an evaluation of the merits of using a seroprevalence-guided long-term re-vaccination strategy. We conducted extensive sensitivity analyses over a range of values for key uncertain parameters and epidemic patterns and consistently found comparable results.

5.6 Conclusion

In conclusion, our study favors the use of regularly-timed re-vaccination strategy for older adults over a serology-triggered re-vaccination strategy. The immune structure underlying varying degrees of protection against SARS-CoV-2 is complex. We parameterize the complexities of acquiring and losing immunity and seropositivity using a plethora of empirical data on tiered protection and rates of waning. We find that contrary to our expectation, a serology-triggered strategy that pre-emptively targets time periods of greater susceptibility does not substantially outperform fixed-time re-vaccination strategies. Indicators that capture the complex immune landscape more accurately than a singular seroprevalence estimated may improve the performance of re-vaccination strategies based on correlates of protection.

5.7 Supplementary File

5.7.1 Additional model methodology

5.7.1.1 Model equations

The first set of equations shows the compartments for one age group, urban/rural with no previous vaccination or prior exposure

$$\frac{dS_{v=0,e=0}}{dt} = -\lambda_{v=0,e=0}(t)S_{v,e} - \delta_{v1}S_{v,e} \quad \text{Eq 21}$$

$$\frac{dE_{v=0,e=1}}{dt} = \lambda_{v=0,e=0}(t)S_{v,e} - \sigma E_{v,e} - \delta_{v1}E_{v,e} \quad \text{Eq 22}$$

$$\frac{dI_{v=0,e=1}}{dt} = (\nu_i)\sigma E_{v,e} - \gamma_I I_{v,e} \quad \text{Eq 23}$$

$$\frac{dA_{v=0,e=1}}{dt} = (1-\nu_i)\sigma E_{v,e} - \gamma_A A_{v,e} - \delta_{v1}A_{v,e} \quad \text{Eq 24}$$

$$\frac{dH_{v=0,e=1}}{dt} = (1-VEP_v)\phi_i\gamma_I I_{v,e} - \gamma_H H_{v,e} \quad \text{Eq 25}$$

$$\frac{dR^p_{v=0,e=1}}{dt} = \pi(1-(1-VEP_v)\phi_i)\gamma_I I_{v,e} + \pi\gamma_A A_{v,e} + \pi(1-\mu_i)\gamma_H H_{v,e} - \delta_{v1}R^p_{v,e} - \omega_i R^p_{v,e} - \kappa_1 R^p_{v,e} \quad \text{Eq 26}$$

$$\frac{dR^n_{v=0,e=1}}{dt} = (1-\pi)(1-(1-VEP_v)\phi_i)\gamma_I I_{v,e} + (1-\pi)\gamma_A A_{v,e} + (1-\pi)(1-\mu_i)\gamma_H H_{v,e} - \delta_{v1}R^n_{v,e} - \omega_i R^n_{v,e} + \kappa_1 R^n_{v,e} \quad \text{Eq 27}$$

$$\frac{dD_{v,e}}{dt} = \mu_i\gamma_H H_{v,e} \quad \text{Eq 28}$$

Where S is susceptible, E is exposed & latent, I is infectious & symptomatic, A is infectious & asymptomatic, H is hospitalized, R_p is recovered and seropositive, R_n is recovered and seronegative, and D is deceased, λ is the force of infection (described below) and all other parameters are described in the parameter table below.

For other demographic and immunological strata, the equations are similar except the S compartment is split into Sp and Sn for individuals who are 1) susceptible and seropositive or 2) susceptible and seronegative, respectively. Equations below show the S compartments for the immunity strata of v=1 and e=0. Note that for the tiers with the fastest antibody waning, we further implement a gamma-distributed waning for the sero-reversion process from Rp to Rn (detailed below).

$$\frac{dS^p_{v=1,e=0}}{dt} = \omega_i V^p_{v,e} - \lambda_{v=1,e=0}(t) S^p_{v,e} - \delta_{v2} S^p_{v,e} - \kappa_1 S^p_{v,e} \quad \text{Eq 29}$$

$$\frac{dS^n_{v=1,e=0}}{dt} = \omega_i V^n_{v,e} - \lambda_{v=1,e=0}(t) S^n_{v,e} - \delta_{v2} S^n_{v,e} + \kappa_1 S^p_{v,e} \quad \text{Eq 30}$$

Likewise, equations below show the S compartments for the immunity strata of v=0 and e=1:

$$\frac{dS^p_{v=0,e=1}}{dt} = \omega_i R^p_{v,e} - \lambda_{v=0,e=1}(t) S^p_{v,e} - \delta_{v1} S^p_{v,e} - 4 * \kappa_1 S^p_{v,e} \quad \text{Eq 31}$$

$$\frac{dS^n_{v=0,e=1}}{dt} = \omega_i R^n_{v,e} - \lambda_{v=0,e=1}(t) S^n_{v,e} - \delta_{v1} S^n_{v,e} + \kappa_1 S^p_{v,e} \quad \text{Eq 32}$$

Individuals who have no prior history of infection go into the V compartments upon vaccination with one, two or three vaccine doses, allowing a period of temporary immunity. Individuals who have a prior history of infection go into the R compartment corresponding to their prior infection tier (see model diagram in Methods section of paper). This again allows for a period of temporary immunity before returning individuals to a susceptible tier corresponding to the number of vaccine doses and number of prior infections. V_p represents those immune from vaccination and seropositive and V_n represents those immune from vaccination and seronegative.

$$\frac{dV^{p}_{v=1,e=0}}{dt} = \rho_{v1}\ \delta_{v1} S_{v,e} - \omega_i V^{p}_{v=1,e=0} - \kappa_1 V^{p}_{v,e} \quad \text{Eq 33}$$

$$\frac{dV^{n}_{v=1,e=0}}{dt} = (1-\rho_{v1})\ \delta_{v1} S_{v,e} - \omega_i V^{n}_{v=1,e=0} + \kappa_1 V^{n}_{v,e} \quad \text{Eq 34}$$

The force of infection is as follows:

$$\lambda_{i,v,e,s}(t) = \beta_i(1-VEI_v)(1-IP_e)(esc)(var_{trans})(foi_s)\left[\sum_{j=c,a,e}\sum_{m=r,u}\left(\frac{\chi_{j,i,r,u}\sum_{e=0}^{3}\sum_{v=0}^{3} I_{j,m,v,e}\,(t) + \alpha A_{j,m,v,e}(t)}{\sum_{e=0}^{2}\sum_{v=0}^{3} N_{j,m,v,e}\,(t)}\right)\right] \quad \text{Eq 35}$$

Where *i* denotes age group of children (0-17 years, 18-49 years and 50 years and above), v denotes number of doses of vaccine (0-3 doses), e denotes number of prior exposures (0-2 exposures) and s denotes serological status (p=seropositive, n=seronegative). $\lambda_{i,v,e,p}(t)$ is the force of infection among susceptible and seropositive (*s*=*p*) individuals in the *ith* age group with *e* prior infections and *v* doses of vaccine. The force of infection (SI.1. Eq.1) is modified by probability of infection of exposed age group (β_i), vaccine effectiveness against infection, differential by 1-3 doses (VEI_v), reduced susceptibility from protection from prior infection (IP_e), increased variant transmissibility (representing Delta and Omicron waves for), immune escape (*esc*) applied to immunity tiers with prior exposure through either infection of vaccination, a relative increased transmission due to new variants (*var_trans*), based on Delta and Omicron variants in the calibration and based on assumptions for future

epidemic patterns in forward simulation, a relative decrease in susceptibility for seropositive individuals compared to seronegative individuals with the same amount of prior exposure (foi_s) , age and rural/urban-specific contact rate ($\chi_{j,i,m,k}$) and infection density within each demographic strata. Infected individuals who are asymptomatic have reduced transmissibility (α_i). $\chi_{j,i,m}$ denotes the per person per day contact rate from an individual in age group *j* and rural area (*r*)with individuals in age group *i* and urban area (*u*). foi_s is parameterized so that a 10% decrease in susceptibility among seropositive individuals ($foi_{s=p} = 0.9$) corresponds to a 10% increase in susceptibility among seronegative individuals ($foi_{s=n} = 1.1$) with the same prior exposure.

5.7.1.2 Gamma-distributed antibody waning process

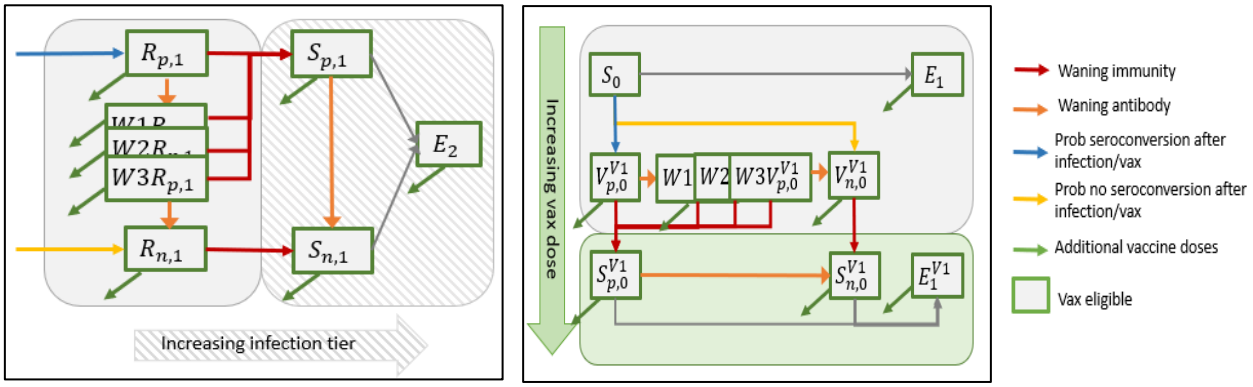

Figure 5-5. Diagram describing the gamma-distributed antibody waning process for the tiers with the fastest rates of antibody waning

(Left) Gamma-distributed waning for those who were seropositive after their first infection. (Right) Gamma-distributed waning for those who were seropositive after first vaccination.

To most appropriately represent the dynamics of antibody waning, we implement a gamma-distributed waning process for the tiers with the fastest rates of antibody waning. After first infection, individuals can be seropositive ($R_{p,1}$) or seronegative ($R_{n,1}$). Seropositive individuals can wane into seronegative through a gamma-distributed process with four compartments. Seropositive individuals can also lose their immunity and become susceptible again ($S_{p,1}$) at a rate and in a process independent from the waning of antibodies.

All compartments are eligible for vaccination. The equations specific to the gamma-distributed waning are detailed below. The same logic applies to the gamma-distributed waning of antibodies for those who are seropositive after receiving their first dose of vaccination.

$$\frac{dR^{p}_{v=0,e=1}}{dt} = -\omega_i R^{p}_{v,e} - 4 * \kappa_1 R^{p}_{v,e} - \delta_{v1} R^{p}_{v,e} \quad \text{Eq 36}$$

$$\frac{dW1R^{p}_{v=0,e=1}}{dt} = -\omega_i W1R^{p}_{v,e} - 4 * \kappa_1 W1R^{p}_{v,e} + 4 * \kappa_1 R^{p}_{v,e} - \delta_{v1} W1R^{p}_{v,e} \quad \text{Eq 37}$$

$$\frac{dW2R^{p}_{v=0,e=1}}{dt} = -\omega_i W2R^{p}_{v,e} - 4 * \kappa_1 W2R^{p}_{v,e} + 4 * \kappa_1 W1R^{p}_{v,e} - \delta_{v1} W2R^{p}_{v,e} \quad \text{Eq 38}$$

$$\frac{dW3R^{p}_{v=0,e=1}}{dt} = -\omega_i W3R^{p}_{v,e} - 4 * \kappa_1 W3R^{p}_{v,e} + 4 * \kappa_1 W2R^{p}_{v,e} - \delta_{v1} W3R^{p}_{v,e} \quad \text{Eq 39}$$

$$\frac{dR^{n}_{v=0,e=1}}{dt} = 4 * \kappa_1 W3R^{p}_{v,e} - \delta_{v1} R^{n}_{v,e} - \omega_i R^{n}_{v,e} \quad \text{Eq 40}$$

5.7.1.3 Implementing historical vaccination

Individuals in S, E, A, R compartments are eligible for vaccination. Historical vaccinations were implemented based on documented first and second dose vaccination administered in Mozambique over time, beginning March 2021,[291] with an early preference towards the age group of 50 years and above. At the start of the forward simulation period (Sept 1st, 2022), the two-dose vaccination coverage among adults is >90%, while children <18 years of age in Mozambique have not yet been vaccinated.

5.7.2 Model parameters

Abbreviation	Description	Value (Range)	Source
Transmission			
$R0$	Basic reproduction number	2.58 (2-4)	[44,309]
$\beta_c, \beta_a, \beta_e$	Prob. of infection of exposed age group	0.02326, 0.02442, 0.0116	Calibrated
α	Relative infectiousness btwn asympt & sympt	0.6 (0.3-0.9)	[310,311]
γ_I	Infectious period, symptomatic (days)	7	[306]
γ_A	Infectious period, asymptomatic(days)	7	[306]
γ_H	Hospital LOS (days)	5 (3-9)	[312]
σ	Latent period	5.5 (3.0-6.7)	[32,33,35,313]
ν_c, ν_a, ν_e	Probability of symptomatic infection by age group	0.45, 0.55, 0.65	[310]
$\phi_c, \phi_a, \phi_e,$	Probability of hospitalization upon symptomatic infection by age group	0.004-0.0075, 0.03-0.15, 0.2-0.35	[314–316]
μ_c, μ_a, μ_e	Probability of death upon hospitalization by age group	0.005-0.01, 0.0365-0.465, 0.15	[317,318]

$\omega_c, \omega_a, \omega_e$	Rate of waning immunity from immune to partially susceptible	1/150, 1/150, 1/150	[292]
$\omega_{c,2}, \omega_{a,2}, \omega_{e,2}$	Additional waning from S_3 (3 prior exposures) to S_2 (2 prior exposures)	1/365, 1/365, 1/365	[281]
Serology			
π	Probability of seroconversion after infection	0.9 (0.8-0.98)	[319,320]
$\rho_{v1}, \rho_{v2}, \rho_{v3}$	Probability of seroconversion among seronegative individuals after vaccination (dose 1-3)	0.85,0.7, 0.9	[273]
κ_1	Seroreversion rate for first exposure (either vaccine or infection)	1/500	[321,322]
κ_2	Seroreversion rate for second or more exposures exposure	1/2500	[321,322]
Vaccination			
$\delta_{i,k,v}$	Per capita vaccination rate by age group, urban/rural and dose	Time-varying based on data (0.01%-4%)	[291]
$VEI_{v1}, VEI_{v2}, VEI_{v3}$	Vaccine effectiveness against infections by number of vaccine doses (assuming Astra Zeneca)	0.5, 0.6, 0.7	[281]
$VEP_{v1}, VEP_{v2}, VEP_{v3}$	Vaccine effectiveness against progression from infection to severe disease/hospitalization by number	0.4, 0.67, 0.9	[281]

	of vaccine dose (assuming Astra Zeneca)		
Prior exposure protection			
IP_e	Protection from first/second infection	0.35, 0.6	[48,51]
foi_sp/foi_sn	Relative transmissibility between seropositive and seronegative	0.7,1.3	Assumption[50,262,263]
Variants			
R0 (delta)/var_trans	R0 during Delta wave/increased transmissibility during Delta wave	3.1 (2.4-4)	Calibrated[323,324]
R0 (omicron)/var_trans	R0 during Omicron/increased transmissibility during omicron	6.4 (5.0-6.5)	Calibrated[325]
Immune escape (Delta)	Increased transmission among those with prior exposure during Delta wave	1.2	[326,327]
Immune escape (Omicron)	Increased transmission among those with prior exposure during Omicron wave	1.6	[326,327]
Immune escape (new variant)	Increased transmission among those with prior exposure for new variant	1.7	Assumption
Under-reporting			
Under-reporting (wave alpha-beta)	Case under-reporting for alpha/beta wave		Calibrated

Under-reporting (Delta)	Case under-reporting for Delta wave	Calibrated
Under-reporting (omicron)	Case under-reporting for omicron wave	Calibrated

Table 5-1. Model parameters, corresponding description, value and source

5.7.3 Data sources from Mozambique

5.7.3.1 Summary of data sources on contact, seroprevalence, vaccination and cases

Parameter	Source	Stratification
Social contact mixing matrix	GlobalMix Study (Comprehensively profiled social contact patterns in an urban and rural area in Mozambique)	• Age group • Urban/rural
Seroprevalence data	Instituto Nacional de Saude, Mozambique[23]	• Age group • Rural : After waves 2, 3, 4 • Urban : After waves 1, 2, 3
Vaccination rates over time	Instituto Nacional de Saude, Mozambique/ Our World in data[291]	• Daily • First/second dose
Reported cases	Instituto Nacional de Saude, Mozambique/ Our world in data[291]	• Daily

Table 5-2 Data sources from Mozambique used to parameterize the transmission model

5.7.3.2 Generation of mixing matrix

Our social contact mixing matrix (Figure 5-6) is derived from contact diaries sampled through age-based quotas in an urban and a rural area during the COVID-19 pandemic between March 2021-March 2022 (N=1242). The socialmixr package[328] was used to generate symmetric age-specific contact matrices, separately for urban and rural areas. Since contact age groups were estimated with an upper and lower bound, we used 1000 bootstrapped samples to compute the number of contacts between each age group (0-17 years, 18-49 years, 50 years and above). We generated weights by calculating the sampling probabilities for the participant age groups used to develop the sampling frame of the survey and applied these weights during the bootstrapping. Urban and rural daily travel probabilities were estimated for the extent of contact between urban and rural populations based on a travel survey conducted in Mozambique between 2021-2022. Briefly, the survey asked participants from Mahnica (rural) on the frequency of

travel to an urban area over the two weeks prior to survey. This frequency was then converted to a daily probability of travel to an urban area among rural participants. Similarly, the survey asked participants from Maputo (urban) on the frequency of travel to a rural area over the two weeks prior to survey, which was then converted to a daily probability of travel to a rural area among urban participants. We then applied these probabilities evenly across the age distribution for who-acquired-infection-from-whom (WAIFW) matrix stratified by both age group and by urban/rural (Figure 5-6).

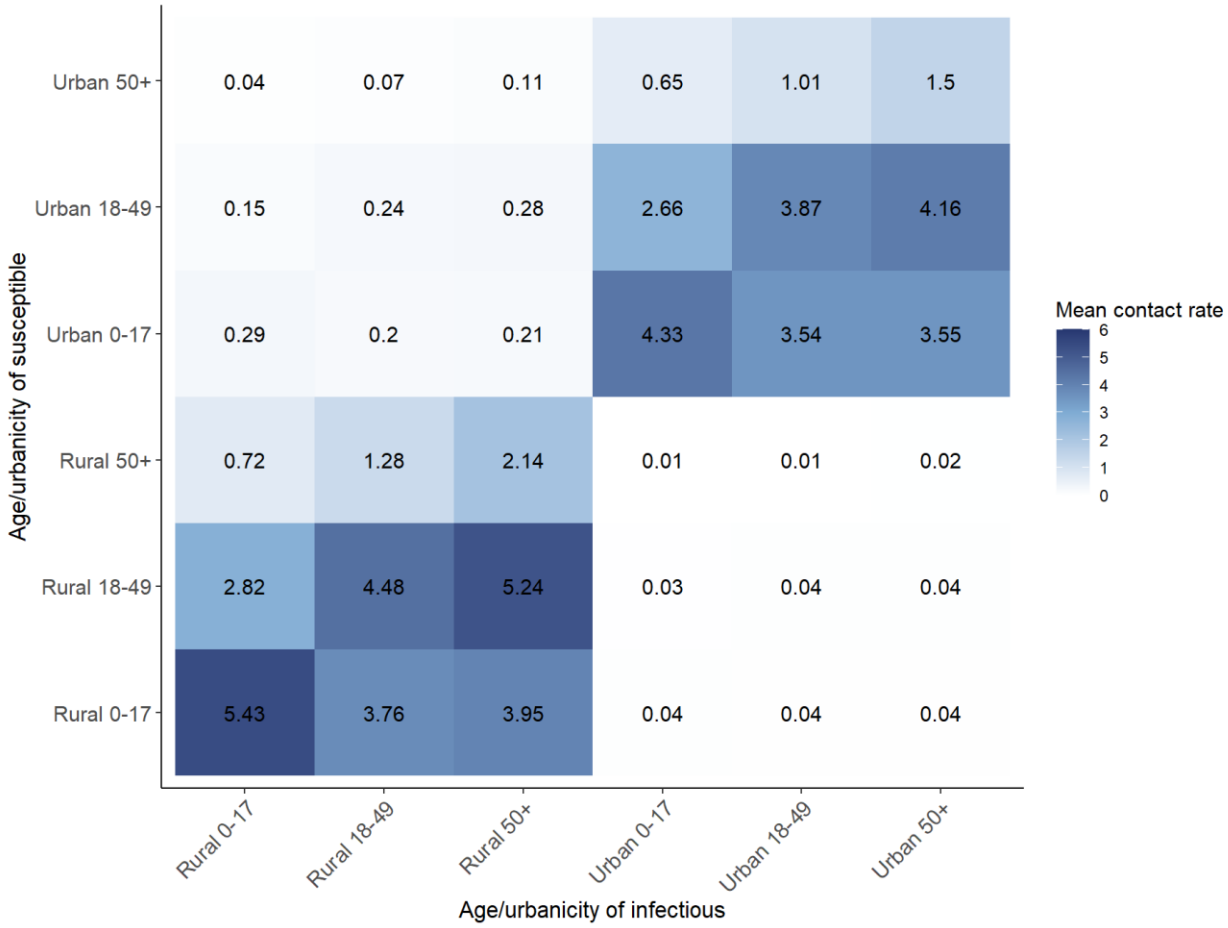

Figure 5-6. Matrix of mixing, or who-acquired-infection-from-whom (WAIFW) stratified by age group and by urban/rural[1]

[1]Data used to inform this matrix was collected from an urban and a rural area during the COVID-19 pandemic between March 2021-March 2022.

5.7.3.3 Seroprevalence estimates

Several seroprevalence studies have been conducted in Mozambique since the beginning of the COVID-19 pandemic. Between June-Dec 2020 after the first and second waves, the Insituto Nacional de Saude (INS) conducted seroprevalence surveys in 13 urban or peri-urban areas (at least one per province) using the Panbio COVID-19 IgG/IgM rapid test. Surveys were stratified sampled by age group and were intended to be representative of the sampled area. A total of 49,103 individuals were sampled and the area-specific seroprevalence ranged from 0.7% to 7.4%. We pooled these estimates using a simple average to represent the seroprevalence before the start of the second wave in December 2020. Between Dec 2020- Dec 2021, longitudinal seroprevalence surveys using Dried Blood Samples (DBS) were conducted among 2400 individuals in an urban area which forms our seroprevalence estimates for urban areas after the second (winter 2020-2021) and third (summer 2021) COVID-19 waves. Between May 2021 and June 2022, four cross-sectional seroprevalence surveys were conducted in a rural area forms our seroprevalence estimates for rural areas after the second, third and fourth (winter 2021-2022) COVID-19 waves (N= between 666-974). The primary assay used was an S-protein target-specific Luminex assay for IgG and IgM (92% sensitivity and 100% specificity). The most recent Luminex seroprevalence results from February 2022 estimated an overall seroprevalence of 79% in the rural area. Children who are largely unvaccinated have a seroprevalence of 64%, while adults and older adults with high primary series vaccination coverage have a seroprevalence of 86% and 79%, respectively.

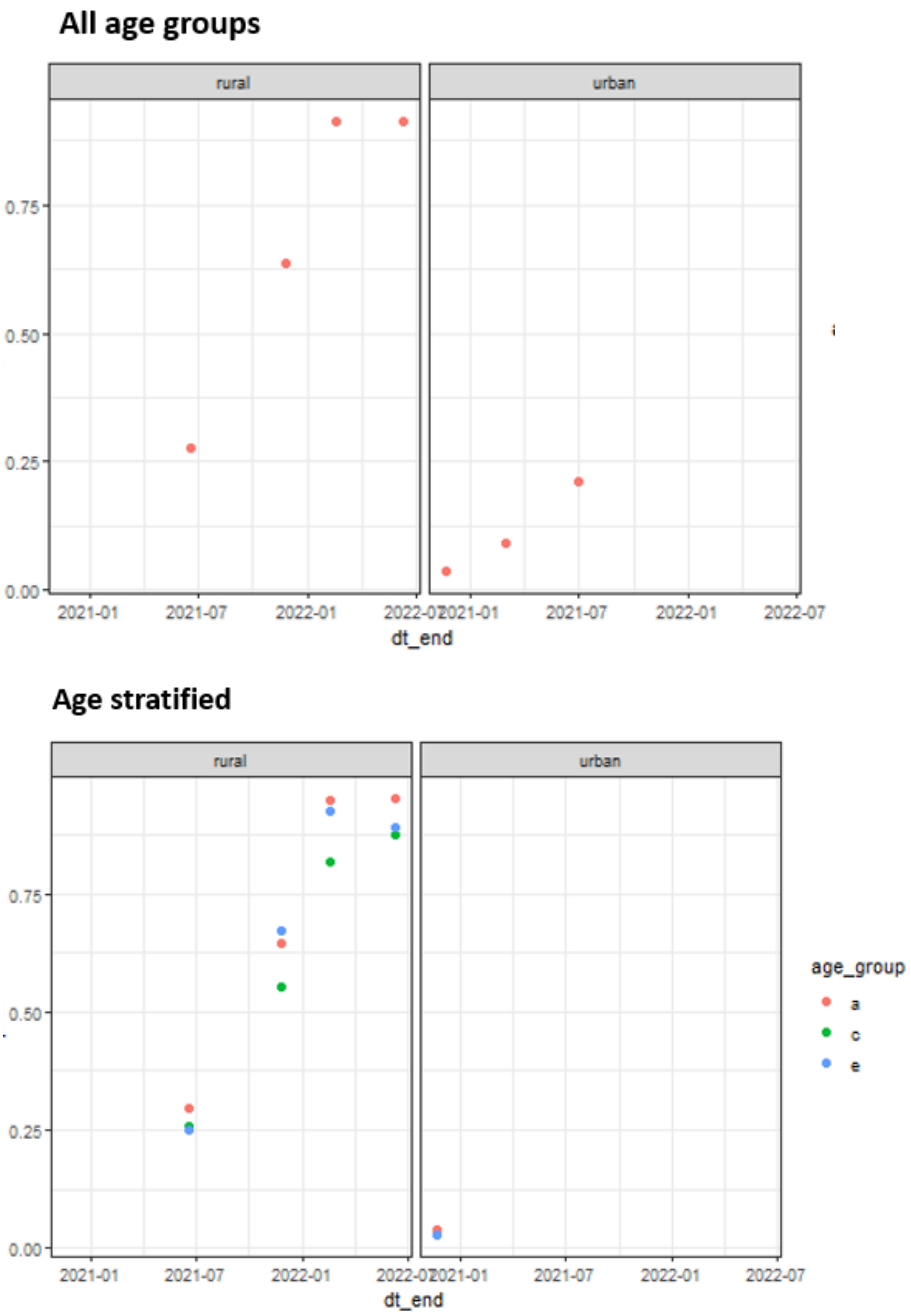

Figure 5-7. Seroprevalence point estimates sampled during the COVID-19 pandemic stratified by age group and by urban/rural.

5.7.3.4 Vaccination and case data

A publicly-available data source (Our World in Data) and data compiled by Mozambique's Instituto Nacional de Saude were used to derive reported cases to inform model calibration and the number of first

and second doses administered on a daily basis to model the vaccination rate. The latter was converted into a daily vaccination rate for first and second dose.

5.7.4 Calibration results

5.7.4.1 Modeled seroprevalence from the top performing calibration runs

Date	Epidemic Period	Urban/ Rural	Age group	Modeled median	Lower	Upper	Population samples
10/22/2020	Post wave1	Urban	All ages	1.6%	1.3%	2.4%	3.6%
			Children	1.5%	1.2%	2.3%	2.6%
			Adults	1.8%	1.4%	2.7%	3.9%
			Adults >50 yrs	1.1%	0.9%	1.6%	2.9%
1/30/2021	Wave 2	Urban	All ages	7.9%	6.8%	10.0%	9.0%
5/19/2021	Post wave 2	Rural	All ages	27.8%	26.2%	30.6%	27.6%
			Children	25.3%	22.5%	28.5%	25.6%
			Adults	31.8%	29.1%	35.1%	29.7%
			Adults >50 yrs	25.3%	23.7%	27.3%	25.0%
		Urban	All ages	16.9%	16.0%	19.1%	21.0%
10/1/2021	Post wave 3	Rural	All ages	54.2%	51.2%	58.8%	54.2%
			Children	50.8%	47.0%	56.1%	45.2%
			Adults	59.2%	55.7%	64.0%	57.2%
			Adults >50 yrs	51.2%	48.9%	56.9%	55.4%
1/1/2022	Post wave 4	Rural	All ages	74.7%	72.0%	78.1%	78.6%
			Children	65.4%	61.3%	70.9%	63.6%
			Adults	86.4%	84.8%	88.0%	86.2%
			Adults >50 yrs	82.3%	81.1%	84.5%	78.7%

Table 5-3. *Modeled seroprevalence from the top performing calibration runs compared to the population samples of seroprevalence estimates*

5.7.4.2 Values from top performing calibration runs for calibrated parameters

Parameter	**Initial range**	**Median calibrated value (range)**
β_c (relative to β_e)	0.4-1.2	0.358 (0.350-0.370)
β_a(relative to β_e)	0.4-1.2	0.479 (0.439-0.528)
β_e	0.04-0.08	0.0747 (0.0712-0.0769)
R_0	1.8-2.5	2.11 (2.08-2.17)
Rate of antibody waning after first infection	1/400-1/650	1/500 (1/450-1/650)
Increased transmissibility relative to original strain (Delta)	1.4-1.7	1.57 (1.49-1.65)
Immune escape (Delta)	1-1.5	1.27 (1.10-1.45)
Increased transmissibility relative to original strain (omicron)	2.5-6	3.20 (2.93-3.67)
Immune escape (omicron)	1.3-1.9	1.55 (1.40-1.80)

Table 5-4. Values from top performing calibration runs for calibrated parameters with median and range.

5.7.5 Assessing correlations between seroprevalence, susceptibility and cumulative deaths in base scenarios with no vaccination

For our base scenario with no re-vaccinations, we assessed the following pairwise correlations between 1) seroprevalence and population-level susceptibility prior to each wave; 2) seroprevalence and proportion immune prior to each wave; 3) seroprevalence prior to each wave and deaths among older adults in each wave; 4) population-level susceptibility prior to each wave and deaths among older adults in each wave. We calculate a summary estimate of susceptibility where the proportion of the population in each susceptible tier is multiplied by the degree of susceptibility, with theoretical ranges from 1 for a completely susceptible population to 0 for a completely immune population. We assess these correlations over a sweep of relative decreases in susceptibility among seropositive vs seronegative (with the same amount of prior exposure) and waning antibody rates.

In summary, we find that regardless of the degree of relative decrease in susceptibility among seropositive individuals ($foi_{s=p}$) and the rate of waning antibody, seroprevalence is always positively correlated with proportion immune and proportion susceptible is always positively correlated with the number of deaths, as expected. We find that among scenarios with decreased susceptibility among seropositive individuals, seroprevalence is always negatively correlated with deaths, as expected, with a stronger negative correlation between seroprevalence and deaths and seroprevalence and susceptibility with decreasing relative susceptibility among seropositive individuals. In scenarios where seropositive individuals have the same probability of infection as seronegative individuals with the same amount of prior exposure, seroprevalence is not negatively correlated with deaths or susceptibility.

For our main analysis, we chose $foi_{s=p} = 0.7$ (decreased susceptibility among seropositive individuals) and $foi_{s=n} = 1.3$ for seronegative individuals, (seronegative have 1.85 times higher probability of infection compared to seropositive)[262] and a waning antibody rate of 1/2500 after two or more exposures (from calibration), and further conduct sensitivity analysis over a range of foi_s and waning antibody rates.

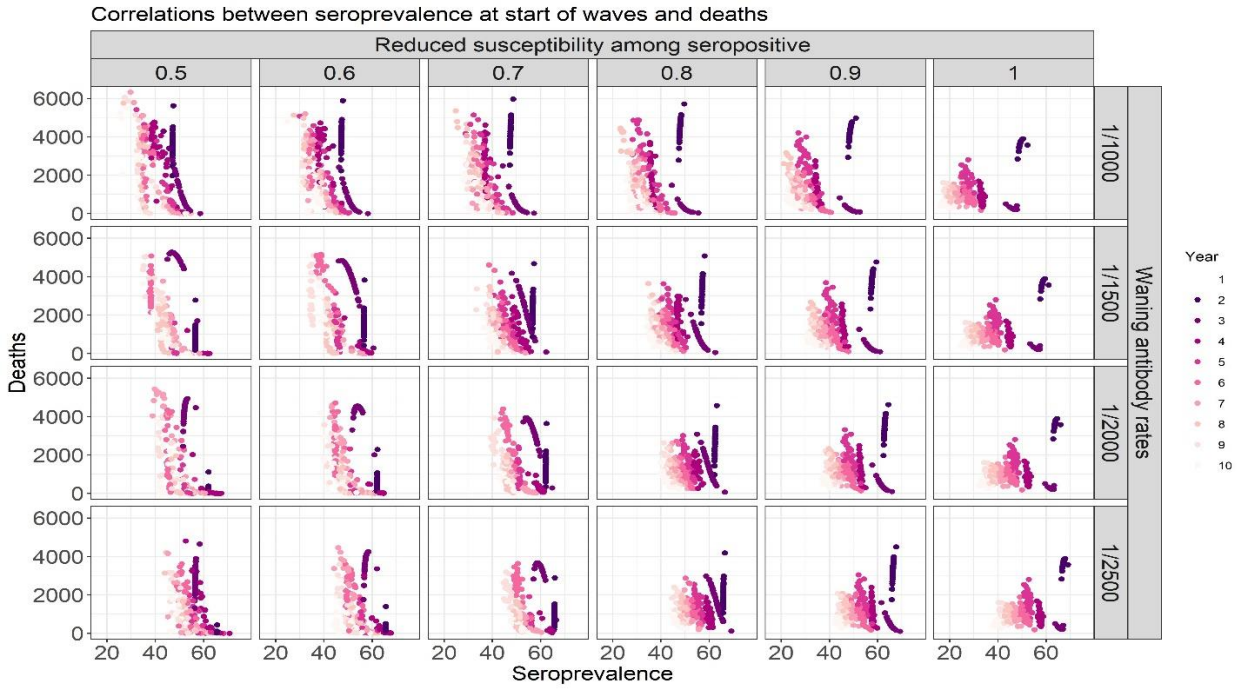

Figure 5-8. Scatter plots of correlations between seroprevalence at the start of each wave and deaths in each wave (among older adults)

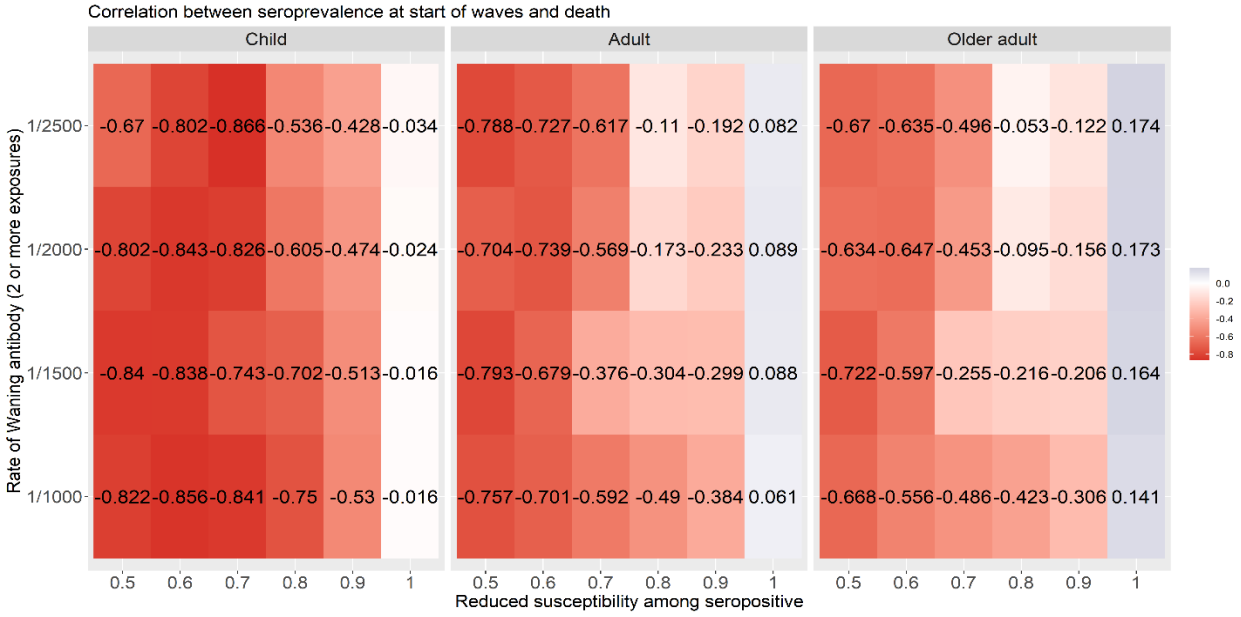

Figure 5-9. Overall correlations (R^2) between seroprevalence at the start of each wave and deaths in each wave.

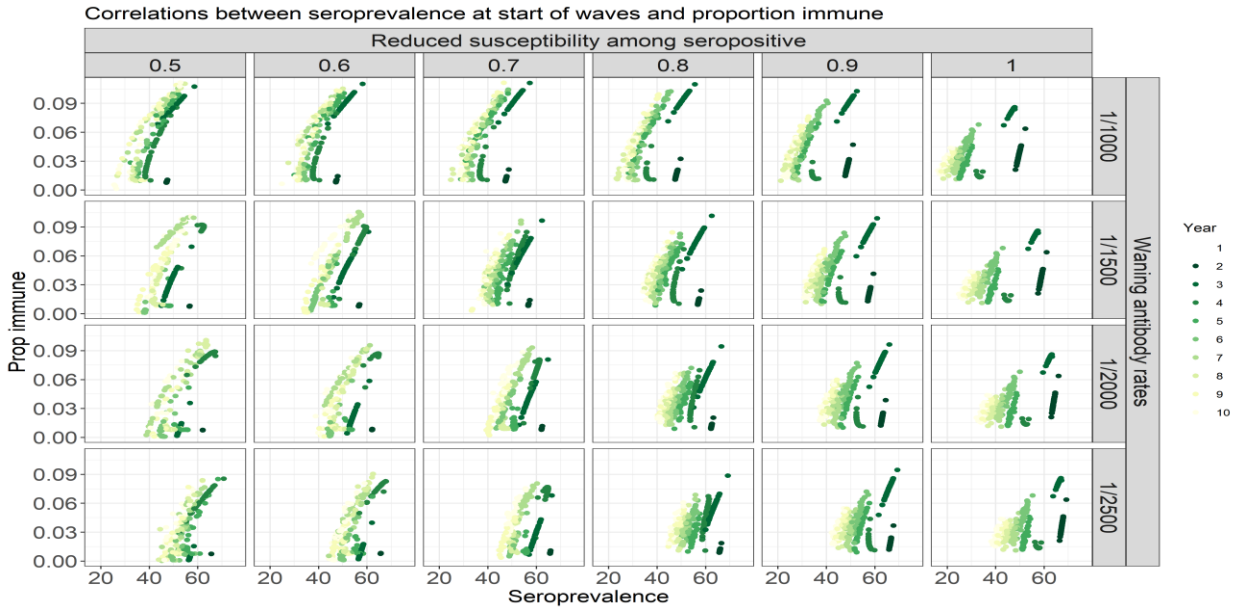

Figure 5-10. Scatter plots of correlations between seroprevalence at the start of each wave and proportion immune at the start of each wave (among older adults)

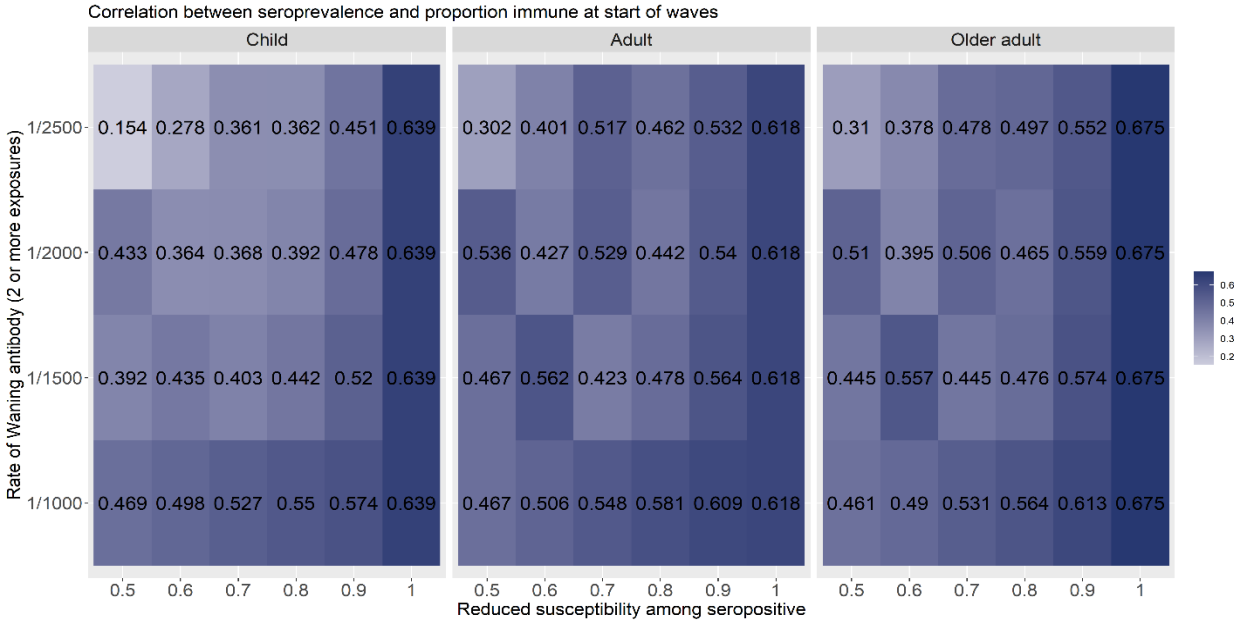

Figure 5-11. Overall correlations (R^2) between seroprevalence at the start of each wave and proportion immune at the start of each wave

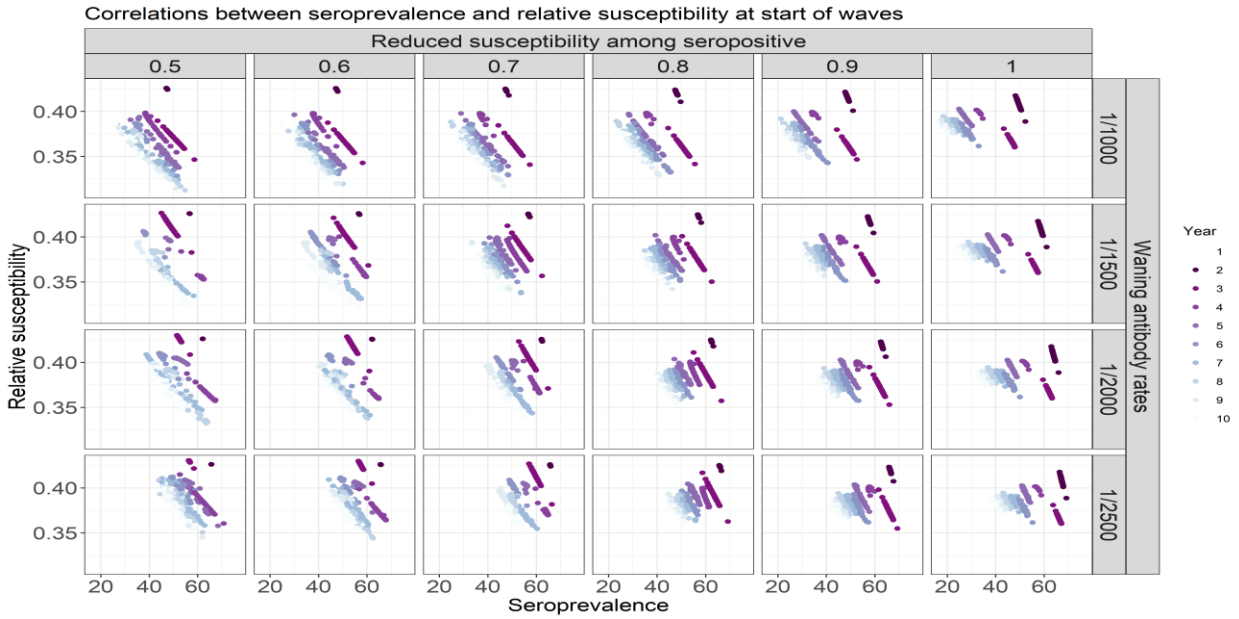

Figure 5-12. Scatter plots of correlations between seroprevalence at the start of each wave and proportion susceptible at the start of each wave (among older adults)

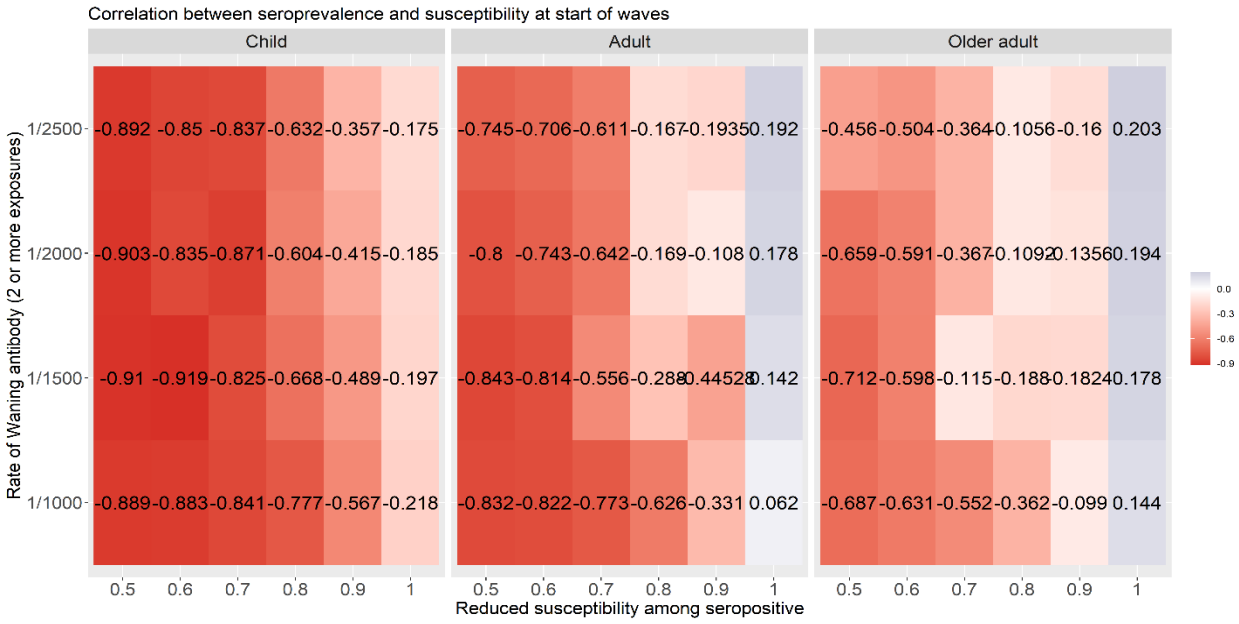

Figure 5-13. Overall correlations (R^2) between seroprevalence at the start of each wave and proportion susceptible at the start of each wave

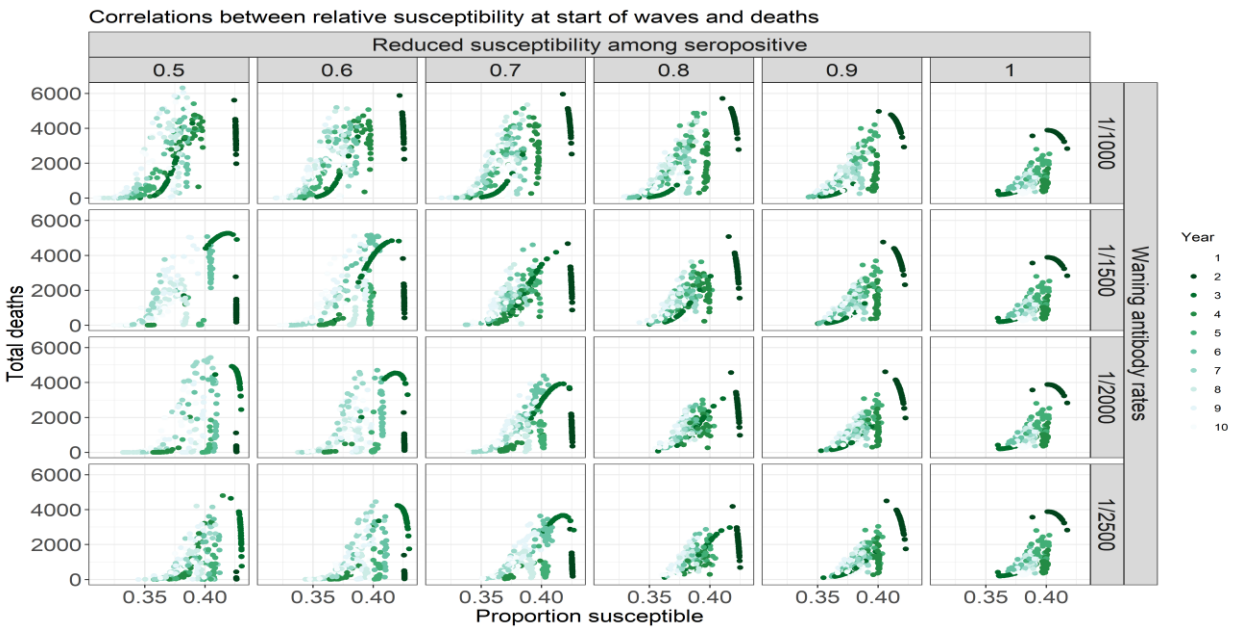

Figure 5-14. Scatter plots of correlations between proportion susceptible at the start of each wave and total deaths in the wave (among older adults)

5.7.6 Vaccination impact results for main analysis

Vaccination scenario	**Time of first vaccination (days since start)**	**NNV (older adults)**	**Deaths Averted among older adults**	**Median percent reduction in deaths**	**Deaths among older adults**	**No. of campaigns**
No vax	-	-	-	0%	11202 (10667-12076)	-
50% thresh	2046 (1962-3108)	448 (330-808)	1434 (787-2079)	13%	9774 (8886-10603)	1 (1-2)
55% thresh	1703 (1652-1721)	462 (383-611)	2762 (2273-3325)	25%	8502 (7970-8977)	2 (2-3)
60% thresh	916 (801-1484)	610 (505-774)	4067 (3067-5047)	36%	7202 (6121-8318)	4 (3-4)
65% thresh	591 (589-595)	717 (658-827)	5332 (4623-5806)	48%	5919 (5427-6443)	6 (6-6)
70% thresh	416 (415-419)	850 (783-904)	6751 (6349-7331)	60%	4472 (4198-4859)	9 (9-9)

75% thresh	255 (255-255)	1072 (995-1143)	7743 (7277-8338)	69%	3493 (3112-3919)	13 (13-13)
80% thresh	109 (109-109)	1516 (1417-1594)	8844 (8468-9396)	79%	2393 (1954-2828)	21 (21-21)
Annual	300	888 (822-928)	7180 (6873-7755)	64%	4047 (3779-4345)	10 (10-10)
Biennial	300	597 (541-689)	5333 (4616-5875)	47%	5922 (5493-6538)	5 (5-5)

Table 5-5. Summary table of vaccine impact results for main analysis

Summary results on NNV, number of deaths, number of deaths averted, median percent reduction in deaths and vaccination timing and frequency based on different vaccination strategies in the main epidemic scenario driven by waning immunity. Quantitative results presented as median and 2.5^{th}-97.5^{th} percentile ranges. The median percent reduction in deaths was calculated using the medians of deaths averted and deaths among older adults in a no vaccination scenario.

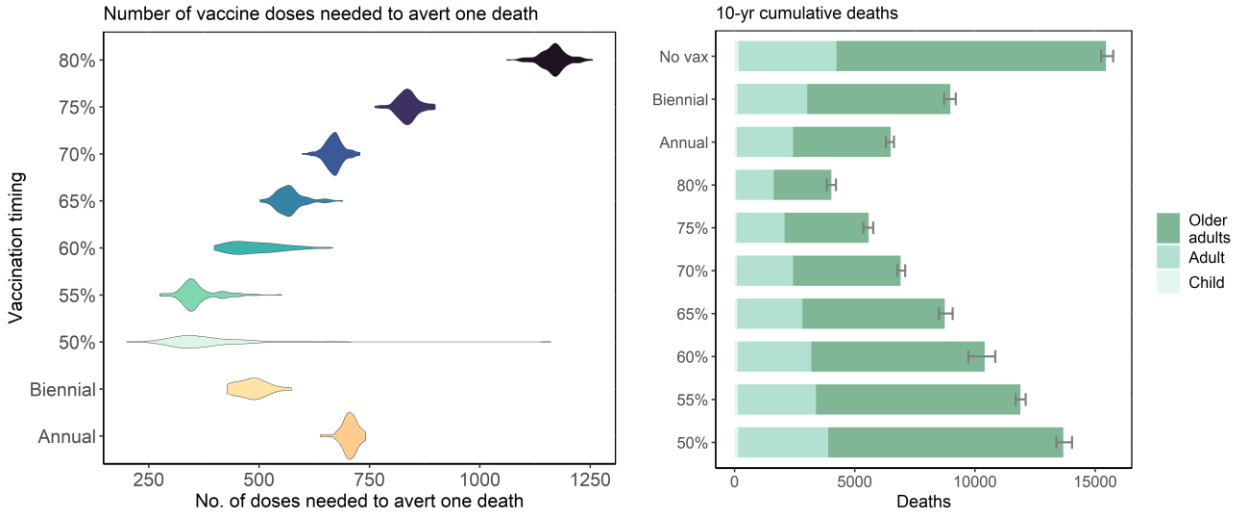

Figure 5-15. Distribution of NNV and number of deaths across all age groups

(Left) Distribution of the number of vaccine doses needed to avert one death among all ages (NNV) by vaccination timing strategy (biennual, annual, triggered based on seroprevalence thresholds of between 50%-80%) based on random sampling for annual transmission under an epidemic scenario driven by waning immunity. (Right) Cumulative deaths over ten years by age group (dark green=child, medium shade = adults, lightest shade =adults >50 years). Error bar represents 25th-75th percentile of cumulative deaths across all age groups.

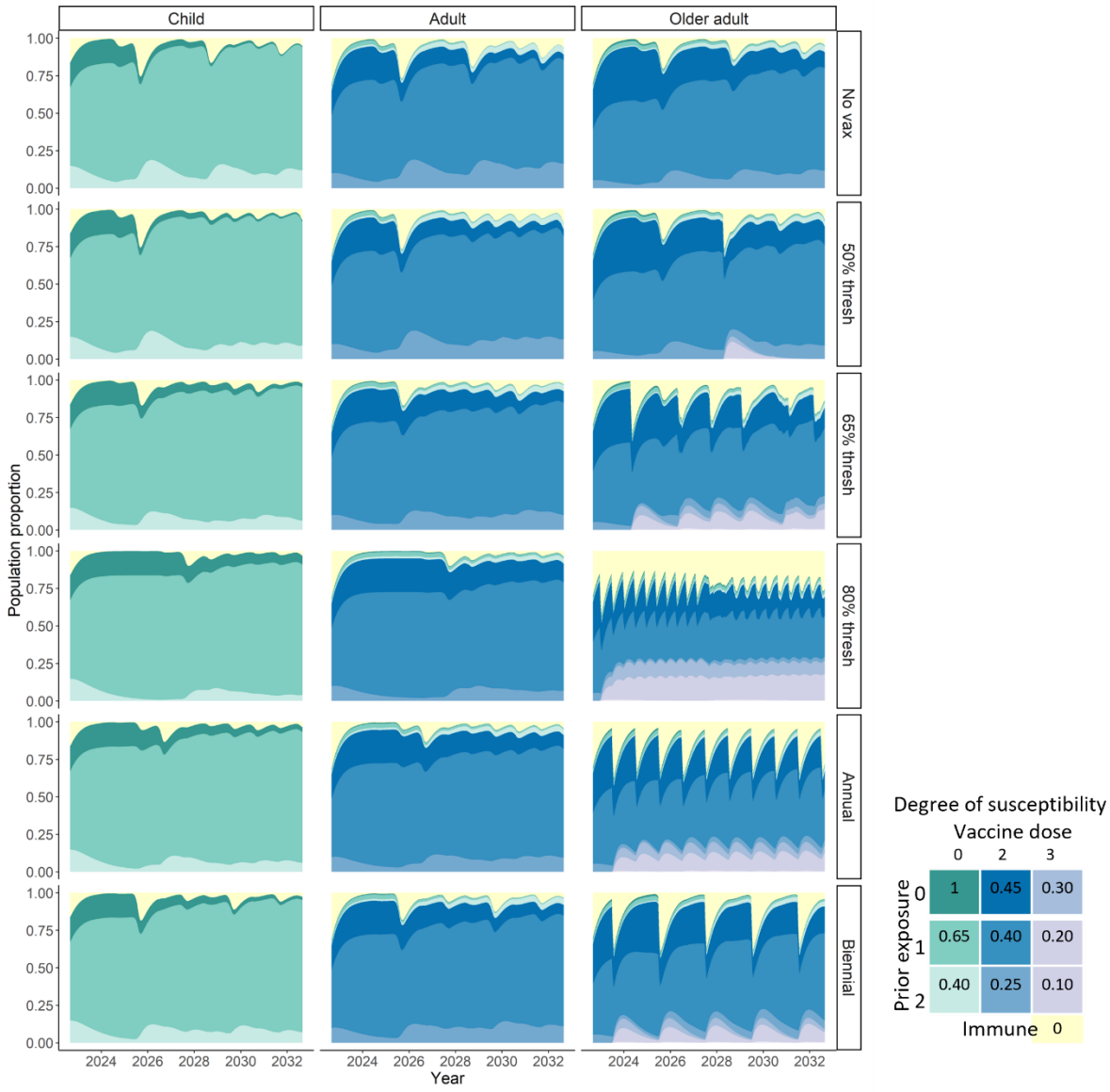

Figure 5-16. Susceptibility landscape over time stratified by age group

Colored density represents population proportion within susceptible or immune tiers over time, ranging from fully immune (yellow) to up to 2 prior infections and 3 vaccination doses. The blue and purple densities indicate proportion of individuals in the 2- and 3- vaccine dose susceptibility tiers, respectively. The darkest shades within each color have no prior infection and are the most susceptible, with lighter shades indicating more exposure and decreased susceptibility. Individuals can wane from the 3-dose susceptibility tier to the 2-dose tier and from the 3-prior infection tier to the 2-prior infections at a rate of 1/365 days. The degree of susceptibility is indicated in the grid legend and is relative to totally

susceptible, with 1 indicating fully susceptible and 0 fully immune. In scenarios with vaccination, campaigns generate spikes in the proportion of individuals fully immune (yellow). More frequent vaccination campaigns result in higher proportion immune (yellow) and longer period in the compartment with highest protection (purple).

5.7.7 Sensitivity analysis

5.7.7.1 Sensitivity analysis using randomly-timed epidemic patterns

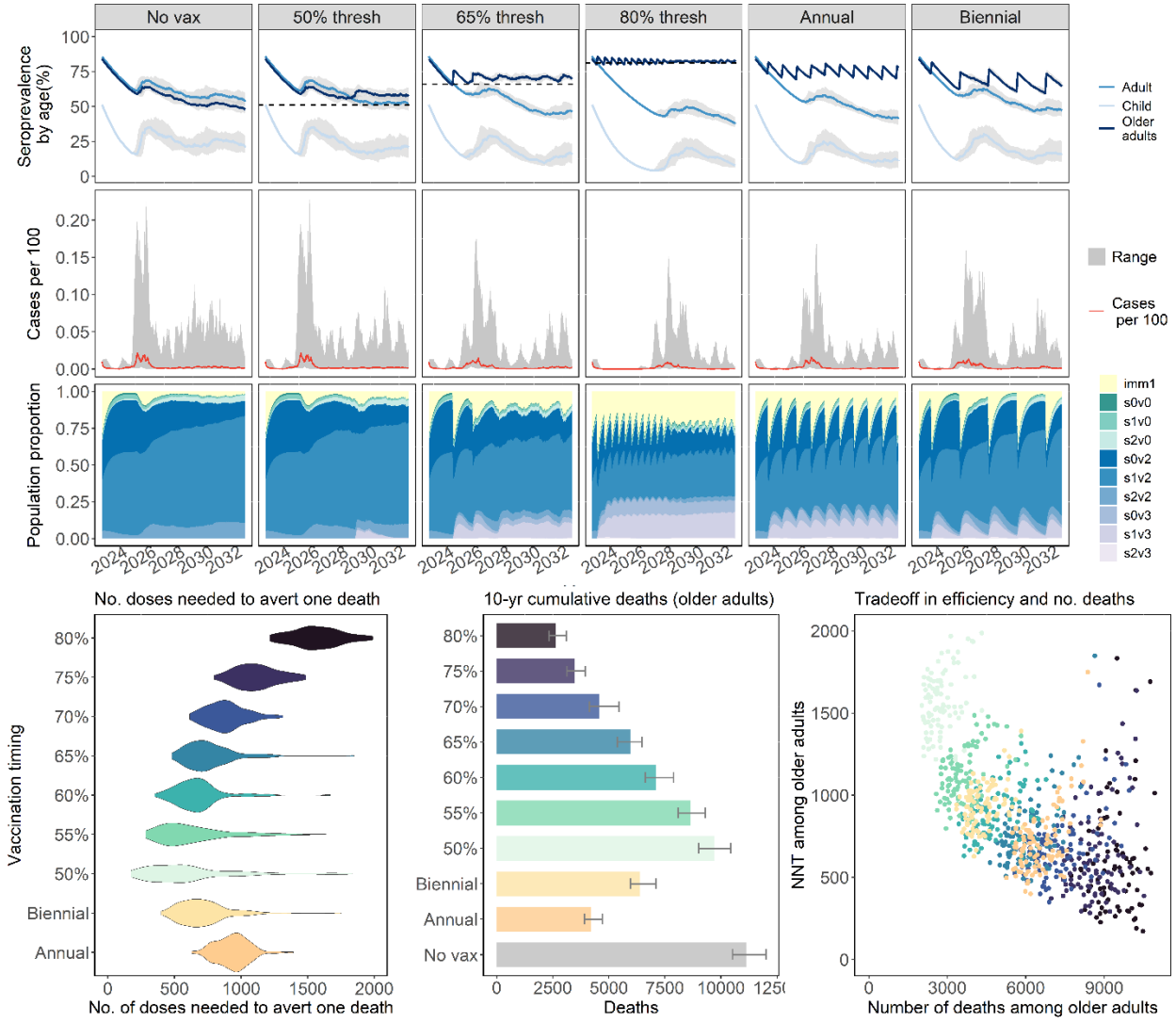

Figure 5-17. Model results for randomly-timed epidemic patterns

(Top row) Modeled 10-year seroprevalence (gray = 2.5th-97.5th percentile) over time for children (lightest blue), adults (medium blue) and older adults >50 years (darkest blue) under 1) no additional

vaccinations; 2) vaccinations timed by seroprevalence trigger thresholds of 50%, 65% and 80% and 3) vaccinations timed annually and biennially. (Middle row) Modeled random Rt sampling, red= median); (Left) Distribution of the number of vaccine doses needed to avert one death among all ages (NNV) by vaccination timing strategy (biennual, annual, triggered based on seroprevalence thresholds of between 50%-80%) based on a randomly-timed epidemic scenario driven by immune waning (Right) Cumulative deaths over ten years by age group (dark green=child, medium shade = adults, lightest shade =adults >50 years). Error bar represents 25^{th}-75^{th} percentile of cumulative deaths across all age groups.

Vaccination scenario	Time of first vaccination (days since start)	NNV (older adults)	Deaths Averted among older adults	Median percent reduction in deaths	Deaths among older adults	No. of campaigns
No vax	-	-	-	0%	11144 (9864-13636)	-
50% thresh	2282 (1799-3164)	547 (0-5892)	1516 (0-3903)	14%	9695 (8104-11866)	1 (1-2)
55% thresh	1716 (1142-2233)	586 (305-2285)	2429 (558-4879)	23%	8651 (7425-10353)	2 (2-3)
60% thresh	829 (796-1416)	657 (426-1502)	3876 (1539-6132)	35%	7106 (5885-9654)	4 (3-5)
65% thresh	606 (589-647)	734 (520-1236)	5233 (2629-7366)	47%	5958 (4887-8068)	6 (5-6)
70% thresh	419 (415-436)	875 (655-1227)	6381 (4651-8556)	59%	4572 (3607-6475)	9 (8-9)
75% thresh	260 (255-277)	1099 (855-1432)	7630 (5683-9796)	69%	3490 (2736-5489)	13 (12-14)
80% thresh	111 (109-124)	1548 (1237-1962)	8408 (6507-10709)	76%	2647 (2086-4077)	21 (20-21)
Annual	300 (300-300)	945 (749-1197)	6747 (5337-8520)	62%	4190 (3503-5704)	10 (10-10)
Biennial	300 (300-300)	683 (468-1150)	4662 (2775-6809)	42%	6389 (5537-8307)	5 (5-5)

Table 5-6. Summary table of vaccine impact results for randomly-timed epidemic patterns

Summary results on NNV, number of deaths, number of deaths averted and vaccination timing and frequency based on different vaccination strategies in the epidemic scenario driven by randomly-timed annual epidemic and by waning immunity. Quantitative results presented as median and 2.5th-97.5th percentile ranges.

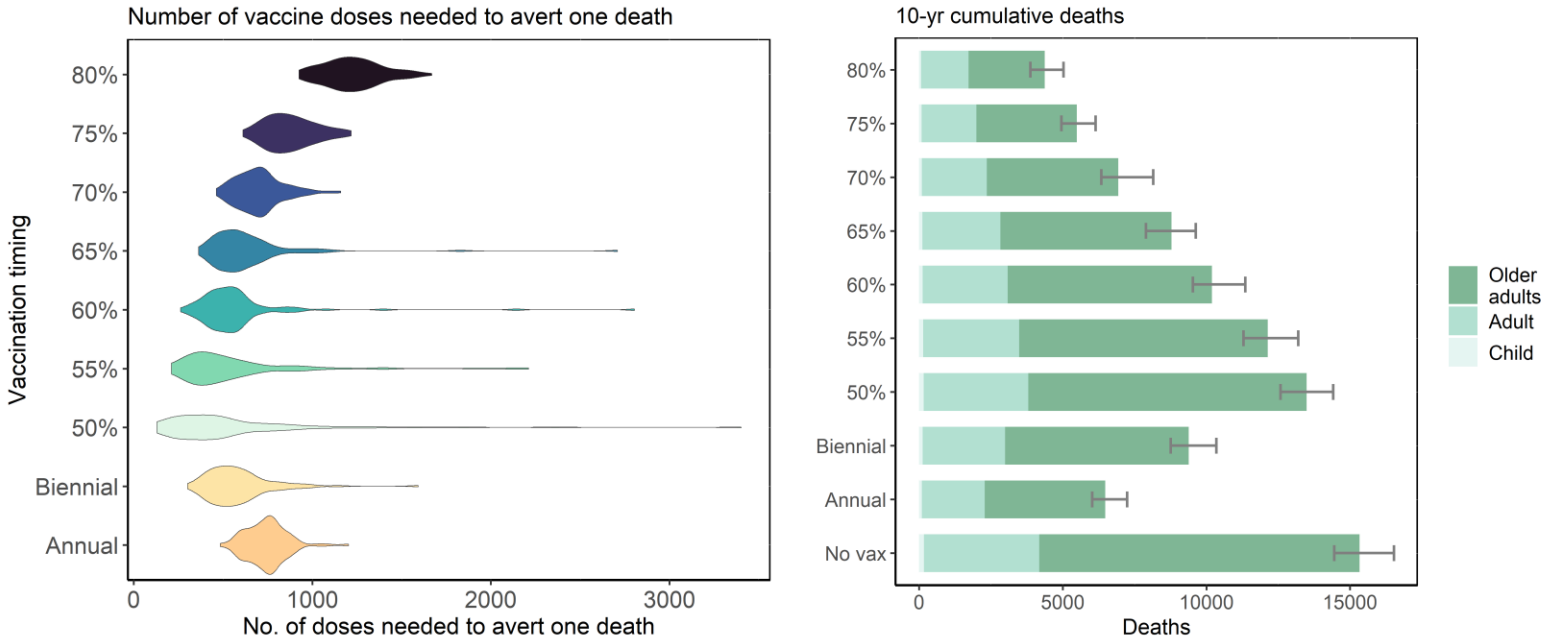

Figure 5-18. Distribution of NNV and number of deaths across all age groups for randomly-timed epidemic patters

(Left) Distribution of the number of vaccine doses needed to avert one death among all ages (NNV) by vaccination timing strategy (biennual, annual, triggered based on seroprevalence thresholds of between 50%-80%) based on random sampling for annual transmission under an epidemic scenario driven by randomly-timed epidemics. (Right) Cumulative deaths over ten years by age group (dark green=child, medium shade = adults, lightest shade =adults >50 years). Error bar represents 25th-75th percentile of cumulative deaths across all age groups.

5.7.7.2 Sensitivity analysis using a 10-year epidemic trajectory driven by immune escape

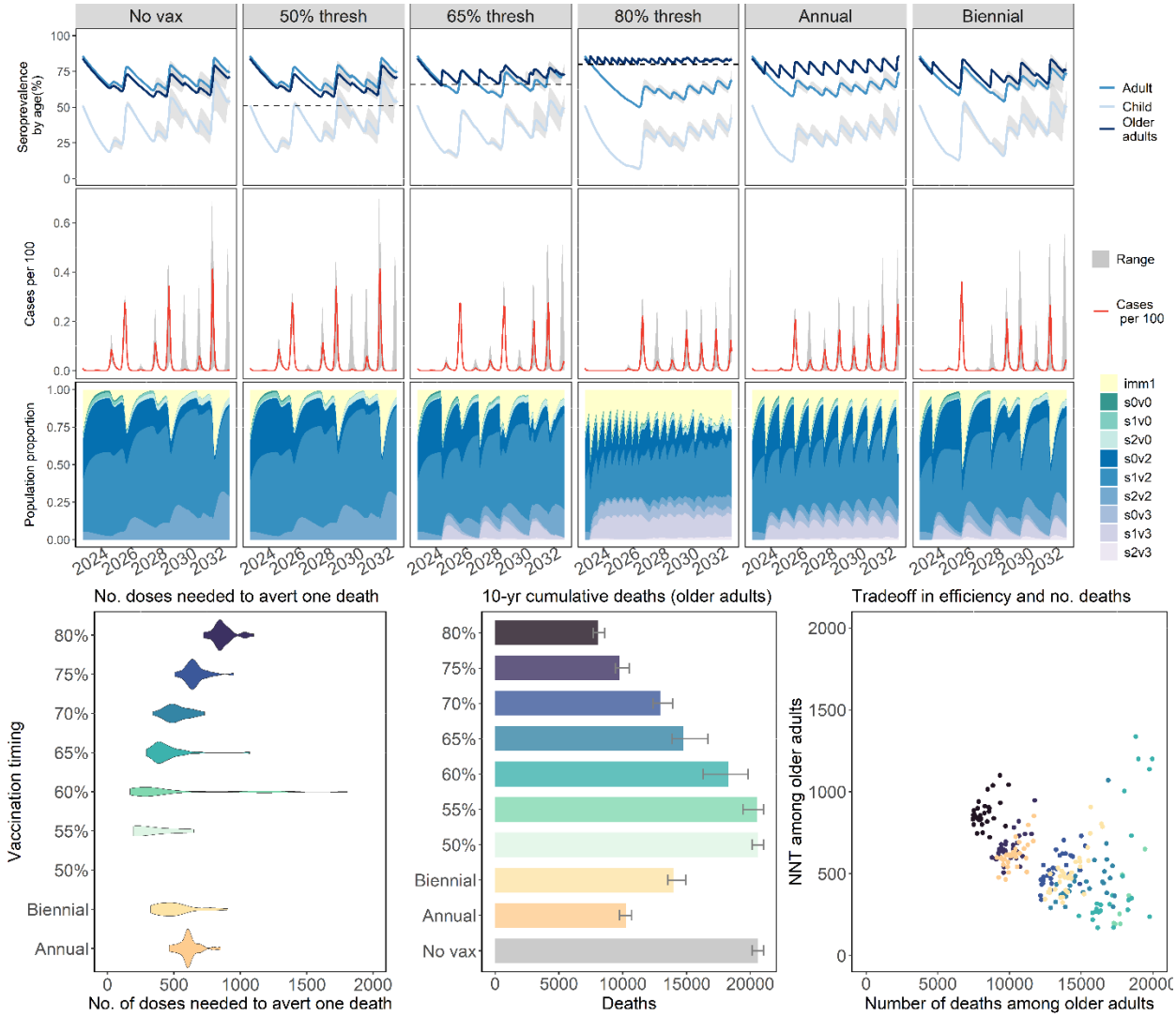

Figure 5-19. Model results for epidemic patterns driven by immune escape

(Top) Modeled 10-year seroprevalence (gray = ranges) over time using a high immune escape scenario for children (lightest blue), adults (medium blue) and older adults >50 years (darkest blue) under 1) no additional vaccinations; 2) vaccinations timed by seroprevalence trigger thresholds of 50%, 65% and 80% and 3) vaccinations timed annually and biennially. (Middle) Modeled 10-year cases per 100 over vaccination scenarios (gray=ranges from random R0 sampling, red= median); (Bottom left**)** Distribution of the number of vaccine doses needed to avert one

death (NNV) by vaccination timing strategy (biennial, annual, triggered based on seroprevalence thresholds of between 50%-80%). Note that the seroprevalence never drops below 50% in this epidemic scenarios and no vaccinations are triggered and thus no NNV estimates; (Bottom right) Cumulative deaths over ten years among older adults. Error bar represents 25th-75th percentile of cumulative deaths for older adults.

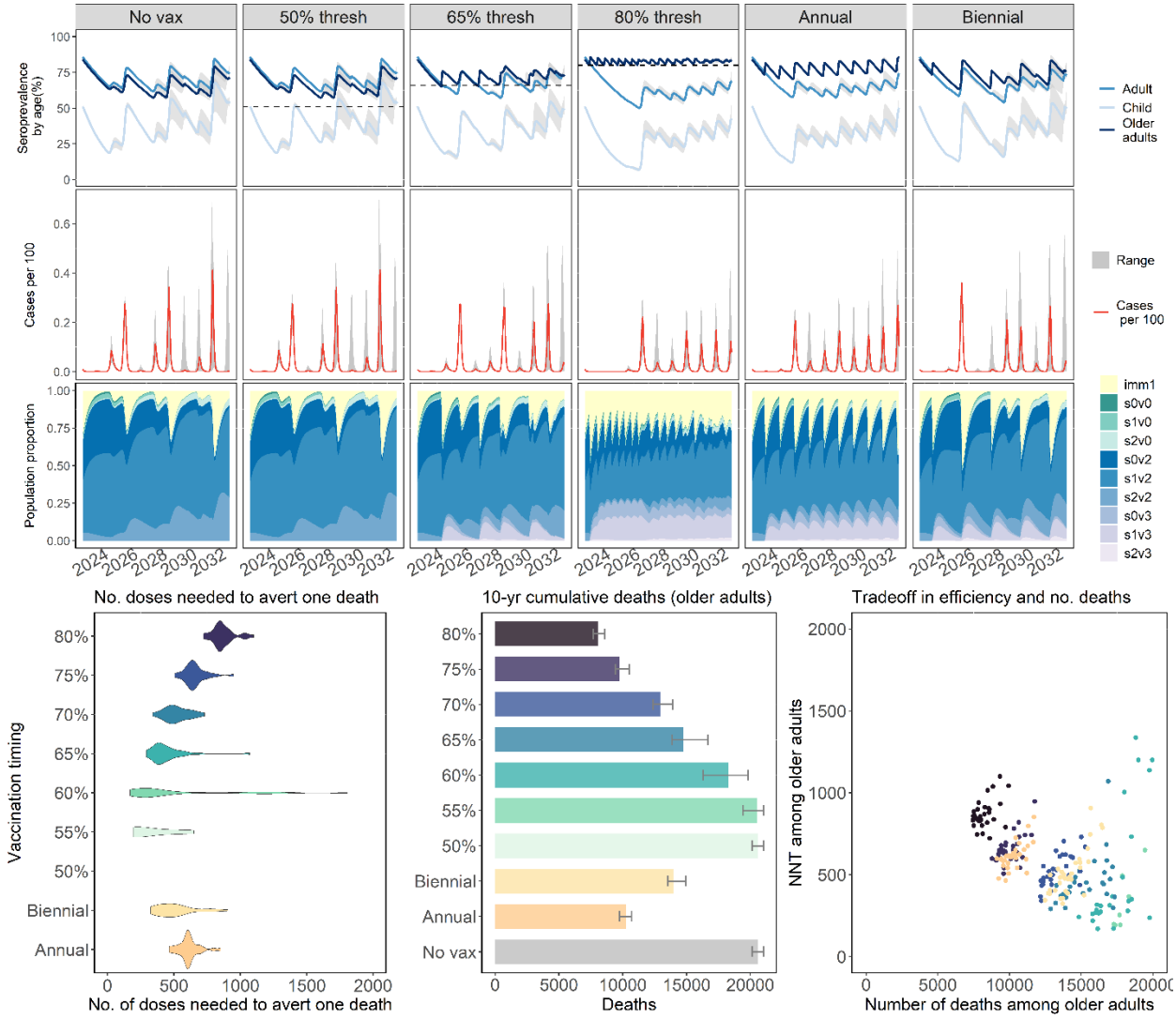

In the base case high immune escape scenario with no additional vaccinations, multiple peaks arise that are more intense in later years

(

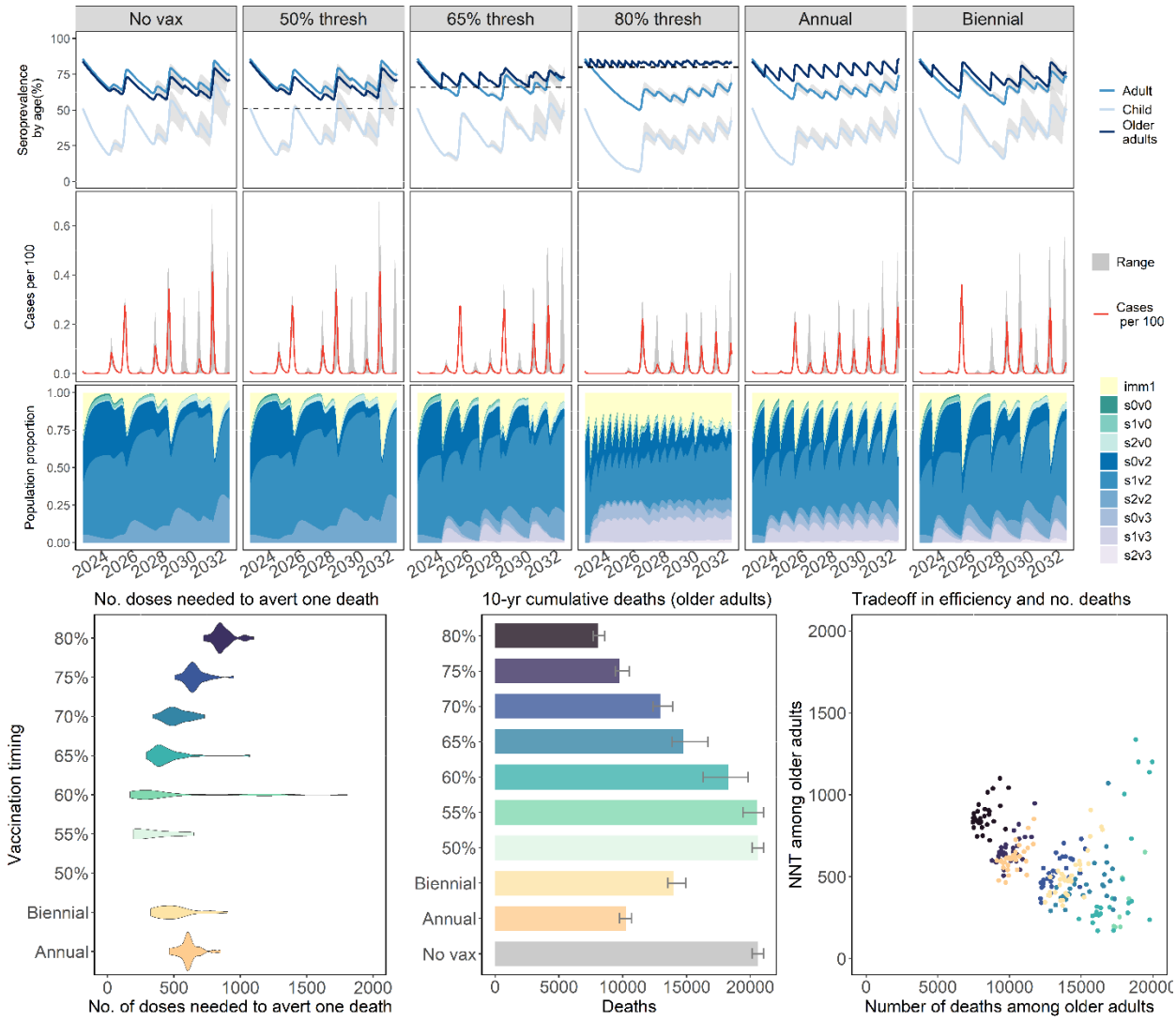

Figure 5-19). Similar to the high waning immunity scenario, the seroprevalence declines then increases in response to surges in cases. Unlike the high waning immunity scenario, the seroprevalence is largely maintained above 50% due to repeated epidemic waves that infect a substantial proportion of the population. Across model runs, the median cumulative number of deaths over 10 years is 28,148 (25th-75th percentile: 26,200-32025) for all ages, and 20,591 (25th-75th percentile: 19,183-23,480) for older adults.

With seroprevalence-informed vaccination triggers, slightly fewer number of campaigns are triggered compared to the high waning immunity scenario. For the lower seroprevalence thresholds of 50% and 55%, campaigns are never or seldomly triggered. For higher thresholds, vaccinating each time the seroprevalence among older adult falls below 60 % and 80% results in a median of 18,275 and 8,052 deaths respectively. Among the vaccination strategies guided by seroprevalence, the median number needed to vaccinate to avert one death (NNV) reaches a minimum at a 60% threshold where 2 campaigns providing a total of 1.2 million vaccine doses result in a median of 2,072 fewer deaths and a median NNV of 312. The NNV increases for higher seroprevalence thresholds with an NNV of 855 for an 80% threshold. In comparison, annual and biennial vaccination of older adults results in a median of 10,258 and 13,986deaths among older adults, respectively and NNVs of 605 and 486, respectively. Similar patterns are observed for the NNV across all age groups (number needed to vaccinate to avert one death in the entire population). NNVs are lower for the epidemic scenario driven by immune escape compared to the epidemic scenario driven by waning immunity.

We observe similar tradeoffs in NNV and number of deaths where vaccination scenarios triggered by seroprevalence thresholds do not necessarily provide an improved tradeoff.

Vaccination scenario	Time of first vaccination (days since start)	NNV (older adults)	Deaths Averted among older adults	Median percent reduction in deaths	Deaths among older adults	No. of campaigns
No vax	-	-	0 (0-0)	0%	20591 (19183-23480)	0 (0-0)
50% thresh	-	-	0 (0-0)	0%	20591 (19183-23480)	0 (0-0)
55% thresh	2022 (1916-3113)	226 (0-623)	0 (0-3284)	0%	20507 (17348-23480)	0 (0-1)
60% thresh	1603 (858-1643)	312 (0-10004)	2072 (0-6173)	9%	18275 (15576-21916)	2 (1-2)
65% thresh	591 (589-596)	402 (296-771)	5750 (3059-8604)	27%	14730 (13135-17246)	4 (3-4)
70% thresh	416 (415-419)	509 (361-711)	7504 (5378-10580)	37%	12972 (12176-15074)	6 (6-6)
75% thresh	255 (255-255)	645 (533-849)	10879 (8288-13164)	53%	9729 (8999-11589)	11 (11-11)
80% thresh	109 (109-109)	855 (741-1056)	12684 (10272-14632)	62%	8052 (7468-9771)	17 (17-18)
Annual	300 (300-300)	605 (474-810)	10514 (7839-13406)	51%	10258 (9219-11664)	10 (10-10)
Biennial	300 (300-300)	486 (340-827)	6484 (3825-9257)	32%	13986 (12658-16426)	5 (5-5)

Table 5-7. Summary table of vaccine impact results for epidemic patterns driven by immune escape

Summary results on NNV, number of deaths, number of deaths averted (for older adults and all ages) and vaccination timing and frequency based on different vaccination timing strategies under an epidemic scenario driven by immune escape.

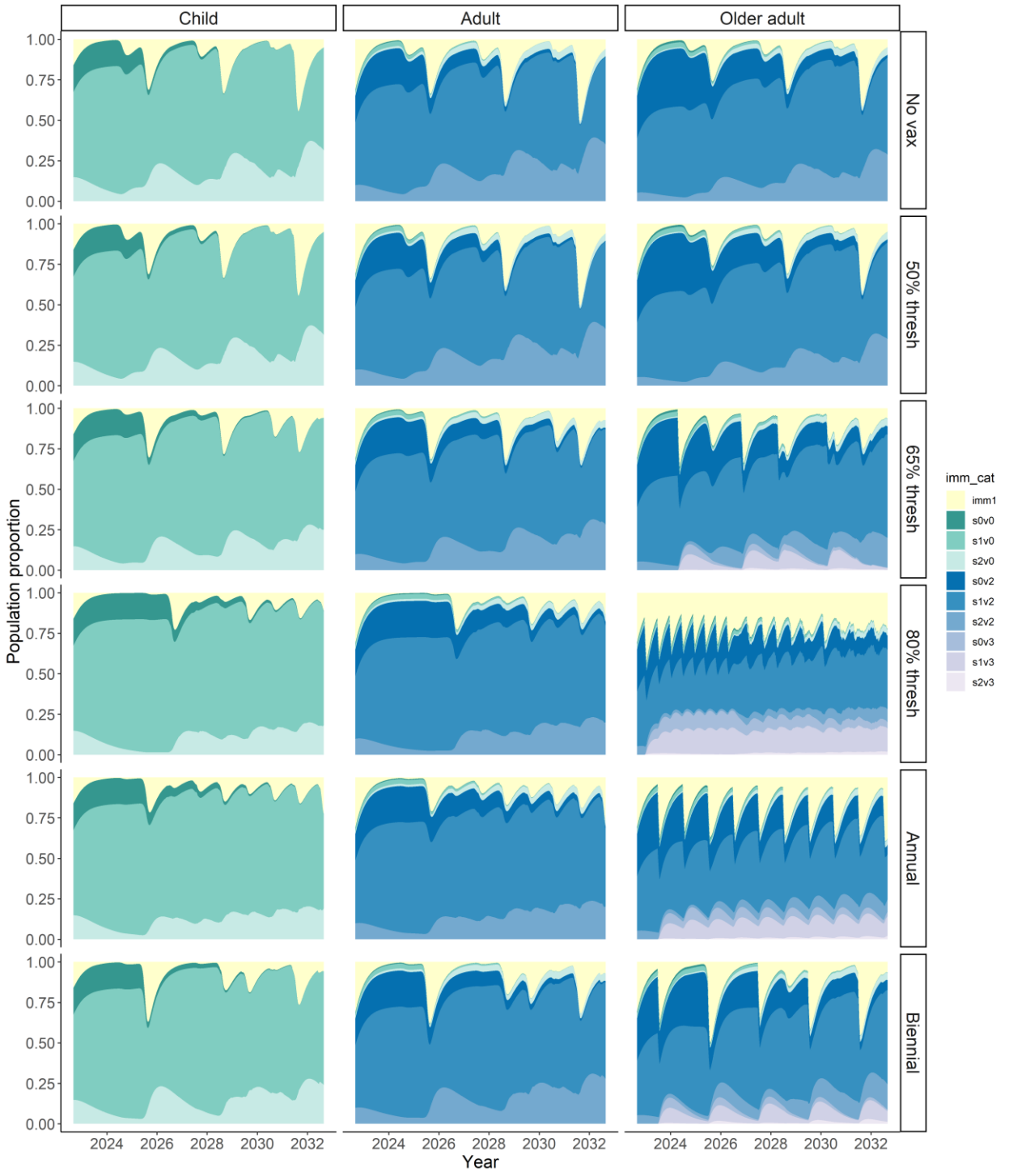

Figure 5-20. Susceptibility landscape over time stratified by age group for epidemic pattern driven by immune escape

Colored density represents population proportion within susceptible or immune tiers over time, ranging from fully immune (yellow) to up to 2 prior infections and 3 vaccination doses. The blue and purple densities indicate proportion of individuals in the 2- and 3- vaccine dose susceptibility tiers, respectively. The darkest shades within each color have no prior infection and are the most susceptible, with lighter shades indicating more exposure and decreased susceptibility. Individuals can wane from the 3-dose susceptibility tier to the 2-dose tier and from the 3-prior infection tier to the 2-prior infections at a rate of 1/365 days. The degree of susceptibility is indicated in the grid legend and is relative to totally susceptible, with 1 indicating fully susceptible and 0 fully immune. In scenarios with vaccination, campaigns generate spikes in the proportion of individuals fully immune (yellow). More frequent vaccination campaigns result in higher proportion immune (yellow) and longer period in the compartment with highest protection (purple).

5.7.7.3 Sensitivity analysis of relative decrease in susceptibility among seropositive individuals

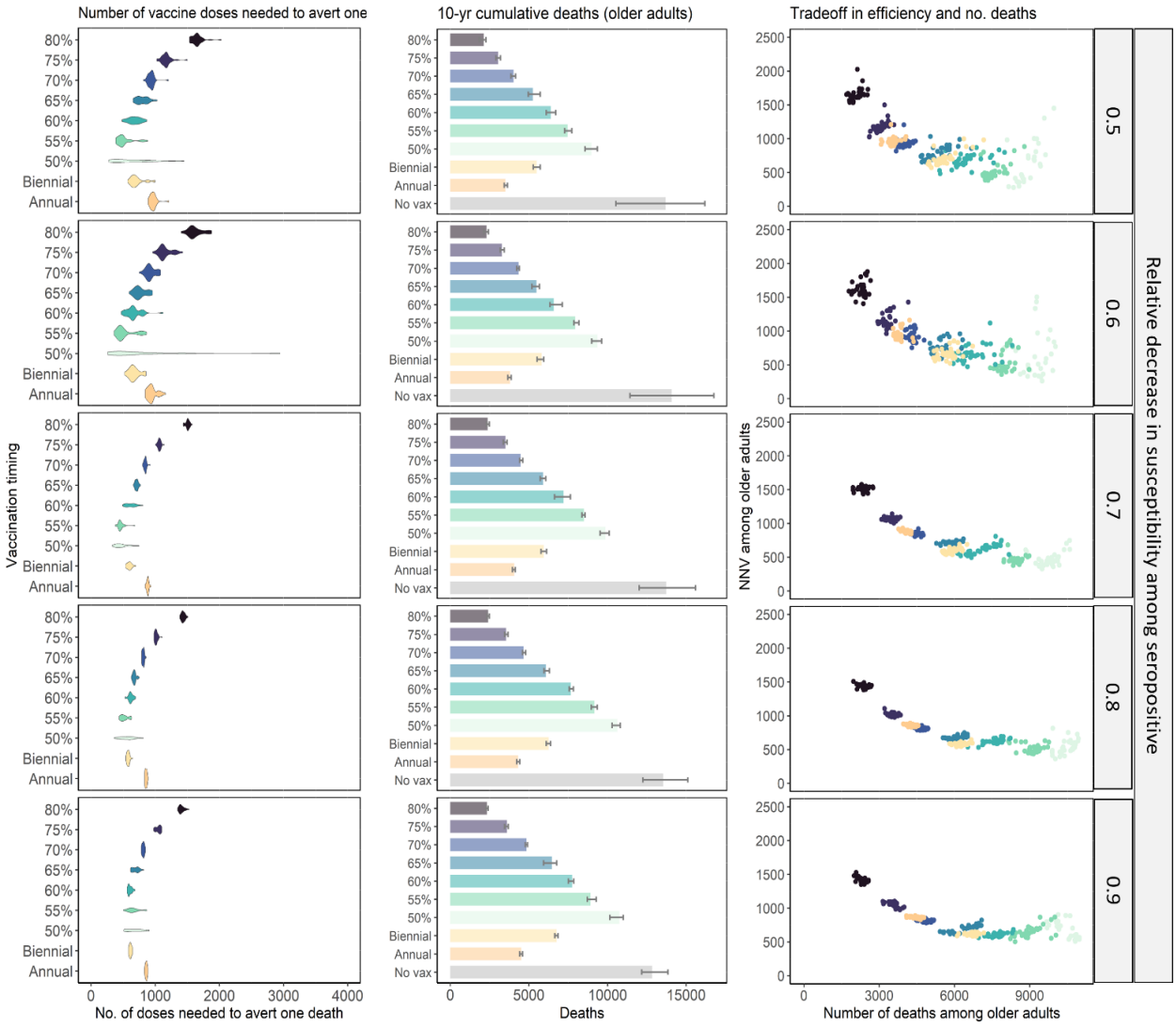

Figure 5-21. Main outcomes in number-needed-to-vaccinate to avert one death (NNV) and deaths under different parameter scenarios for the relative decrease in susceptibility among seropositive.

(Left) Distribution of the number of vaccine doses needed to avert one death (NNVT) by re-vaccination timing strategy (biennial, annual, triggered based on seroprevalence thresholds of between 50%-80%); (Center) Cumulative deaths over ten years among older adults. Error bar represents 2.5th-97.5th percentile of cumulative deaths for older adults; (Right) Scatterplot of tradeoffs in efficiency (NNV) and number of deaths comparing serology-triggered strategies with fixed interval strategies.

5.7.7.4 Sensitivity analysis of rate of waning antibody

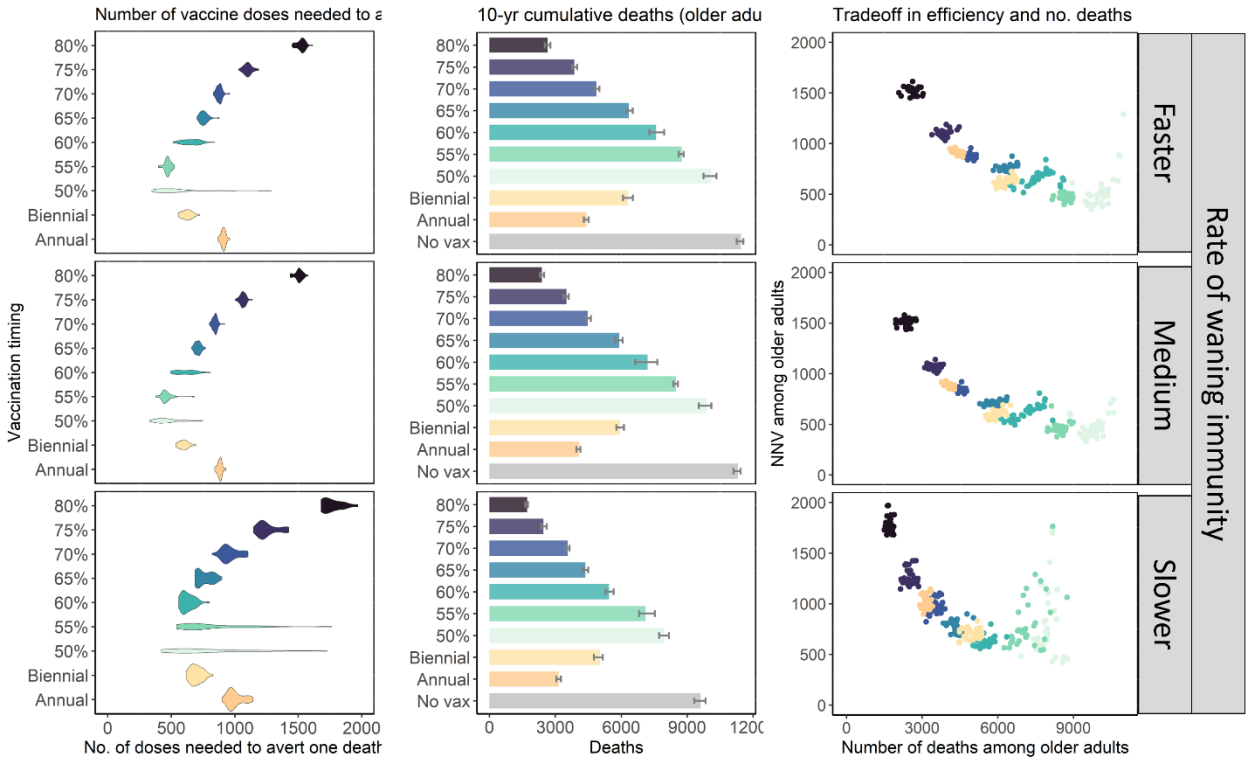

Figure 5-22. Main outcomes in number-needed-to-vaccinate to avert one death (NNV) and deaths under different parameter scenarios for the rate of antibody waning.

(Left) Distribution of the number of vaccine doses needed to avert one death (NNV) by re-vaccination timing strategy (biennial, annual, triggered based on seroprevalence thresholds of between 50%-80%); (Center) Cumulative deaths over ten years among older adults. Error bar represents 2.5th-97.5th percentile of cumulative deaths for older adults; (Right) Scatterplot of tradeoffs in efficiency (NNV) and number of deaths comparing serology-triggered strategies with fixed interval strategies.

5.7.8 Summary of literature review of key parameters

Reference	Evidence	Location	Study design and population
Post-infection			
Lou et al[264]	Seroconversion rates for total antibody, IgM and IgG were 98.8%, 93.8% and 93.8%, respectively	China	Longitudinal (N=80) among PCR confirmed
Oved et al[320]	Using multiple assays, antigen targets, estimated 5% of PCR-infected individuals remained persistently seronegative	Israel	Longitudinal (698) among PCR positive individuals
Van Elslande et al[266]	•22% of mild cases and 2.6% of severe cases never seroconverted	Belgium	Paired sera (N=236) PCR confirmed from hospitals
Post-vaccination			
Ali et al[279]	Post-vaccination antibody-levels are higher among individuals with prior infection (30-40% higher)	Kuwait	N=1025 among vaccinated individuals
Anichini et al[329]	•Similar post-vax IgG levels between individuals with and without prior infection •Higher neutralizing titers among those with prior infection	Italy	N=100 HCWs post first dose vax, 38 with history of infection
Assis et al[330]	•Post-vax, previously infected individuals developed higher antibody titers to vaccine than non pre-exposed individuals •Higher antibody levels among those with severe disease	California, US	N=8761 before and after vax campaign
Ward et al[252]	•After single dose Pfizer after 21 days, 84% of people under 60 years tested positive and 90% among those with prior infection (across all age groups) •After two dose Pfizer, ~100% test positive •After two dose AZ, <90% for those aged 35 and above and 73% among oldest age group	UK	REACT study 155,172 with valid IgG results

Table 5-8. Evidence on seroconversion after infection or vaccination

Reference	Evidence	Location	Study design and population
CDC	Antibodies derived from infection last between 3-6 months and up to 11 months		
He et al[274]	90% positive for IgGs 6-8 months after seroconversion	Wuhan, China	Longitudinal, among those positive for IgGs
Alfego et al[331]	•max of 90% seropositive for IgG (S and N-proteins) 21 days post-index •N-protein seropositivity declined to 68.2% through 293 days; •S-antibody seropositivity declined to 88% through 300 days •Age associated with seroreversion, ~seropos approx 15% lower in >-65 years after 280 days	US	Cross-sectional (N=39,086) individuals with PCR-confirmed infection between Mar 2020-Jan 2021
Peluso et al[245]	•Time to seroreversion ranged by assay, ranging from 96 days for N(frag) – Lum to 925 days for S-DiaSorin. S-Lum had mean time to sero-reversion of 400-500 days among the non-hospitalized •Lower antibody titers among individuals with mild infection	California, US	Longitudinal (n=128)
Wei et al[271]	• Anti-spike IgG half-life was 184 days • Ab levels associated with protection against reinfection likely last 1.5-2 years on average with levels associated with protection from severe infection present for several years	China	Among PCR positive individuals
Wang et al[277]	positivity rates for IgM, IgG, anti-RBD IgG, and NAb fell to 20.4% (39/191), 97.9% (187/191), 97.4% (186/191), and 95.8% (183/191), respectively, during 9–10 months post symptom onset	China	215 individuals established in Feb 2020
Harris et al[332]	•Predicted proporstions sero-reverting after 52 weeks were 100% for Abbot, 59% Euroimmun, 41% RBD, 10% Roche (N), <2% Roche (S)	UK	Longitudinal (N=264) among those seropositive for >2 assays

Shioda et al[333]	Time from seroconversion to seroreversion was 3-4 months	NYC and Connecticut	Cross-sectional serology data (N=1800 for each site, each cross)
Swartz et al[275]	Model fitting of antibody response suggests that individuals may remain antibody positive from natural infection beyond 500 days	Texas, US	Longitudinal-ish? (N=4553) among those with at least one antibody test with 1-3 Ab tests over 11 months
Yang et al[334]	•Anti-RBD IgG peaked at 120 days and declined •At 400-480 days, undetectable neutralizing acitivty found in 14% (16/111) of mild •At 330-480 days, 50% (5/10) undetectable among asymptomatic infections	China	Longitudinal (N=214) convalescents without additional exposure after recovery or vaccination
Van Elslande et al[266]	•22% of mild cases and 2.6% of severe cases never seroconverted •Of mild seroconverters, 18.8%, 40% and 61% were seronegative in the windows 60-119 days, 120-179 days and 180-240 days •Of severe seroconverters, number was 1.9%, 10.8% and 29.4%	Belgium	Paired sera (N=236) PCR confirmed from hospitals
Rees et al[335]	Using age-structured reverse catalytic model, estimated antibody persistence lasted between 0.9 (0.6-1.6 years) and 5.8 (2.0-7.4 years)	Multiple countries	Historical seroprevalence data of four circulating HCoVs
Feng et al[336]	Increasing Ab titers following vaccination associated with increasing VE	UK	Cohort of AZ efficacy trial
Grandjean et al[337]	S antibody predicted to remain detectable in 95% of participants until 465 days compared to 75% of N-antibodies (nice figures for reference)	UK	Cohort (N=349) of seropostivie HCWs, data for 200 days
Ward et al[252]	•Between 1-2 dose of pfizer, Ab fell to 64% of peak levels (10-12 weeks) after a peak at 4-5 weeks	UK	REACT study 155,172 with valid IfF results

Table 5-9. Evidence for durability of antibody

Reference	Evidence	Location	Study design and population
Cromer et al[338]	Modelling of predicted vaccine efficacy (based on neutralisation titres) against variants over time suggested that protection against symptomatic infection might decrease below 50% within the first year after vaccination	Multiple, pooled data across 24 studies	Modeled based on antibody neutralisation titres
Hall et al[49]	• Two dose Pfizer, VE=85% at 14-73 days and VE = 51% at 201 days •Two dose AZ VE = 49% (16-69%) at 14-73 days •Two dose AZ VE = 47% (26-63%) at 74-133 days •Two dose AZ VE = 51% (18-71%) after 133 days •Infection-acquire immunity in unvaxed participants (<5%) waned after 1 year (dropped from 86% (81-89%) within 1 year to 70% (38-84%) after 1 year. •Among infected and vaxed 1 dose, VE 90% (60-97%) at >1 year after primary infection •Infected and vaxed 2 dose, VE 95% (82-99%) at >1 year after primary infection	Qatar (Expats)	Test negative case-control (nested in N=35K undergoing aoutine symptomatic screening)
Altarawneh et al[47]	•Pfizer/moderna (6 months prior)+ no prior infection against symptomatic omicron= -1.1% (basically none) •Three dose pfizer/moderna +no prior infection = 52.2% (48-56) •Effectiveness of IE, VE and hybrid against severe, critical, fatal BA.1 infection was >95% •2-dose VE alone against severe/critical fatal BA.2 infection = 77% •3-dose VE against severe/critical/fatal BA.2 infection = 98%	Qatar (Expats)	Matached, test-negative, case-control
Murugesan et al[339]	•VE (AZ) (vaxed Jan 2021) with no prior infection =32% (24-39%)	South India	Cohort study, infection outcomes

			during Delta wave (April 2021)
Poukka et al[340]	•VE (AZ) against infection from Delta 14-90 days = 88% (71-95) •VE (AZ) against infection from Delta91-180 days = 62% (17-95) •VE(AZ) against severe disease from Delta 14-90 days = 100 (25-100%) •VE (AZ) against severe disease from Delta 91-180 days = 81 (9-96%)	Finland	Retrospective cohort study
Nordstrom et al[341]	•VE (AZ) against symptomatic disease 31-120 days = 45% (28-60%) •VE (AZ) against symptomatic disease >120 days = 19% (-97-28%)	Sweden	Retrospective cohort study
Pattni et al[342]	•VE (AZ) one dose in reducing susceptibility to infection = 39%(34-43%) for Delta •VE (AZ) two dose in reducing susceptibility to infection = 64% (61-67%) for Delta	UK	Retrospective cohort from anonymized public health data linked to PCR data
Tan et al	•VE (mRNA) two dose against infection with Delta = 45% (40-50%), against Omicron = 21% (7-34%) •VE (mRNA) for booster against infection was 44% (38-50%) for Delta and 40% (35-40%) for omicron •VE against severe disease by booster for omicron was 83% (76-88%), VE against severe disaese by primary series for Delta was 80% (73-85%) See figure image	Singapore	Test-negative case-control study

Table XXX. Evidence for effectiveness of prior infection against subsequent infection

Reference	**Evidence**	**Location**	**Study design and population**
Altarawneh et al[47]	•IE alone against symptomatic BA.2 infection = 46.1% (40-52%) •IE + two dose pfizer/moderna = 55% (51-59) •IE + three dose pfizer/moderna =	Qatar (Expats)	Matached, test-negative, case-control

	77% (72-81%) •IE alone against severe/critical fatal BA.2 infection = 73% •Hybrid against severe/critical/fatal BA.2 infection = 98%-100%		
Kojima et al[343]	•Weighted average = 90.4% (range 82-100) up to 10 months fololow up	Multiple HICs	Systematic review (10 articles), published before June 2021
Murugesan et al[339]	•IE against symptomatic infection = 86% (77-92%) •IE+vax in Jan 2021 = 91% (84-95%)	South India	Cohort study, infection outcomes during Delta wave (April 2021)
Hansen et al[344]	•Protection against repeat infection = 81% (75-85%)	Denmark	Compared reinfection in second surge (Sep-Dec 2020) between individuals with positive and negative PCR tests during first surge
Lumley et al[269]	•Protection against re-infection among Ab positive = 89% (56-97%) (up to 5 months)	UK	Cohort study, seropositive and negative HCWs beginning April 2020
Letizia et al[345]	•Protection against re-infection among Ab positive = 92% (72-89%) •Higher baseline Ab titres associated with decreased risk of re-infection	US	Cohort of marine recruits (N=3168) followed for 6 weeks

Table 5-10. Evidence for vaccine effectiveness

CHAPTER 6 CONCLUSIONS AND PUBLIC HEALTH IMPLICATIONS

6.1 Overview

Over four years since the first identification of SARS-CoV-2 and realization of its transmissibility and severity, the threat of COVID-19 as a disease of pandemic concern has receded. In May 2023, the WHO removed COVID-19 as a public health emergency of international concern. The world has weathered the most acute phases of the pandemic, but the disease burden persists. SARS-CoV-2 remains in circulation and new variants continue to emerge. Moreover, the threat of infectious diseases of outbreak or pandemic potential persists.

Human behavior underpins the spread of infectious diseases at both individual and community levels. The primary goal of this dissertation was to advance the understanding of individual-level social contact and community-level human movement patterns in the context of SARS-CoV-2 transmission and utilize this knowledge to inform effective vaccine policy. This dissertation generates valuable insights on transmission dynamics and infection control, weaving together the use of novel behaviorally related data collected during a pandemic and assessing the impact of an innovative temporally targeted vaccination strategy. These insights will guide analyses of behavior data and their incorporation into mathematical models to assess the likely impact of intervention strategies on SARS-CoV-2 outbreaks and future outbreaks of other infectious diseases.

6.2 Contributions and future directions of each specific aim

6.2.1 Aim 1

In Aim 1, we focused on understanding how contact rates changed over the course of the pandemic, specifically estimating the effect of one risk mitigation behavior, receiving a vaccination, on contact rates, an indicator of another risk mitigation behavior. We use longitudinal data from the U.S. spanning 18 months of the pandemic and found that contact rates broadly increased over the survey rounds across all sociodemographic groups, reflecting the gradual relaxation of social distancing measures. We sought to isolate the effects of receiving a vaccination on contact rates and found that, within the context of

universal increases in contact rates, individuals newly completing their primary series had additional increases in contact rates compared to unvaccinated individuals. Overall, our findings are in line with the broader evidence base indicating that behavior during outbreaks of infectious diseases are responsive to changes in individual-level factors such as adoption of other risk mitigation behaviors, changing risk perception and illness[346,347] and to changes in policy-level interventions such as social distancing recommendations[116,121,129,130,137,348–352].

The measurement of changes in contact rates over the COVID-19 pandemic complemented a plethora of behavioral surveys assessing the level and frequency of adherence to risk mitigation behaviors such as masking, avoiding crowded spaces, remaining six feet apart among others[85,137,138,217,352–354]. A distinctive value of quantifying contact rates is that they can be directly incorporated into mathematical frameworks to estimate transmission intensity. We assess the competing effects of vaccine protection against infection and increasing contact rates following vaccination on transmission through a simple mathematical framework, the Next Generation Matrix (NGM). We demonstrate that vaccine protection against infection is unlikely to fully offset increases in transmission intensity from observed increases in contact following the preliminary vaccination campaign.

There are several future directions for this work. Almost 20 years since the first multi-country contact surveys were conducted in Europe, there are still no systematically collected contact data from the U.S. during normal, non-pandemic times. For comparison of our survey results collected during the pandemic to pre-pandemic norms, we resorted to using computationally inferred contact matrices projected from European data onto the U.S. demographic distribution[60]. A broad, representative survey of contact rates in the U.S. during non-pandemic times would serve as a baseline for future outbreaks and would be highly informative to modeling efforts for a range of infectious diseases.

The COVIDVu cohort used for the analysis in Aim 1 generated valuable insights on behavioral change during the COVID-19 pandemic; however, the scale of the pandemic may make our findings less generalizable to more common, more localized, and less severe and politicized outbreaks of infections

such as influenza, norovirus, measles, and diphtheria. Contact rates collected through single cross-sectional surveys during non-outbreak periods, as is frequently done, are an incomplete snapshot of behavior. Repeated, frequent samples of contact on the same individuals throughout the course of an outbreak and through illness and non-illness episodes would provide information on critical windows where shifting behavior is most likely to impact outbreak timing and size. Insights gained from previous work, including this study, would facilitate the rapid deployment of survey activities necessary to capture fluctuating contact rates during emerging outbreaks. Not only will such data be important for analyzing behavior change during outbreaks, but it can also be leveraged to calculate real-time estimates of heterogeneities in transmission[355] and effectively inform public health measures.

Lastly, there has been increasing interest in the explicit integration of social and behavioral feedback loops into mathematical models. One such framework incorporates game theory as an exogenous factor that modifies social interactions[113,114,356]. In these frameworks, individuals are assumed to make rational decisions by weighing tradeoffs of riskier behavior and potential loss of health[357]. For example, increasing disease prevalence can change an individual's perceived risk and prompt modifications to social interactions. The extent of coupling between disease prevalence, perceived risk and changes to social contact is then parameterized through optimizing mathematical representations of competing costs and benefits. Recently, novel theoretical work showed that a "behavioral-epidemiological model" coupling a simple model of human behavior into an SIR model for infectious diseases reproduced sharp peaks and lengthy periods of plateaus in between COVID-19 waves[358,359], a feature of the pandemic that was difficult to replicate through the traditional SIR framework alone Infectious disease modeling frameworks that incorporate behavior typically assume perfectly rational human behavior. Future work can quantify the extent that other drivers of perceived risk, such as awareness of infections within one's social network or information on changing incidence, impacts contact rates in the real world where human behavior is less predictable.

6.2.2 Aim 2

In Aim 2, we focused on inferring spatial patterns of SARS-CoV-2 transmission across counties in Georgia, USA through a novel metapopulation framework with a multilayered transmission process and informed by spatiotemporally resolved data on social contact, human mobility, and vaccination. We find that in counties with smaller populations, lower contact rates and higher vaccination coverage, intercounty mobility contributes to a higher proportion of onward transmission. In addition, analysis of pairwise counties showed that the net infection flow is from counties with lower mitigation to counties with higher mitigation and from counties with smaller population to counties with larger population. Identifying sources and sinks of transmission and their correlates is useful to guiding more localized interventions and assist in the mitigation of infection spread.

We advance on existing metapopulation modeling frameworks[151,152,157,158,242,360–362] by decomposing the transmission process into household and non-household components and by adding a layer of age-specific mixing. We configured the model to readily incorporate spatiotemporally resolved data on behavior and vaccination, improving model fidelity to changing behavior and immunity levels across multiple waves of the COVID-19 pandemic. More individualized representation of the infection process have been achieved through highly intricate agent-based models representing millions of individuals[99,363–366] partitioned into multiple interacting layers of residential locations, work locations and age groups. However, such models are computationally intensive and require highly granular data on individual-level behavior, infection, and disease progression. Our model attempts to balance representing key heterogeneities in transmission across space, time, and age group, while minimizing computational resources and data needs.

Advancements from our model can be used to improve the understanding of spatial patterns of transmission in future emerging outbreaks and to conduct forward simulations to assess the impact of spatially targeted interventions. Metapopulation models are uniquely able to guide the coordination of intervention activities across different administrative boundaries. During the COVID-19 pandemic, coordination of the timing, duration and details of intervention strategies across administrative boundaries

in Georgia or the U.S. was limited. Increased coordination could have maximized resources while minimizing the public health impact of the pandemic and disruptions to daily life[145]. In more resource limited settings, spatially-targeted interventions of social distancing restrictions or intensified vaccination campaigns have been considered for outbreaks of measles[367–369], Ebola[370] and diphtheria[371], among others. Recently, in response to an unexpected diphtheria outbreak in Nigeria in 2023, reactive catch-up vaccination campaigns were quickly mobilized[371–374]. However, a shortfall in available vaccine doses in-country required prioritization around space and age where targeting could be either wider in age range and narrower in geographical scope or vice versa. Future work can explore the value of applying an age- and space-stratified model that readily integrates local behavior and immunity for outbreaks of other infections, particularly to practical questions around intervention allocation under resource constraints.

A key challenge in the parameterization of spatially explicit mathematical models is the dearth of spatially resolved data to accurately inform disease dynamics at the level of each spatial unit represented in the model. In the U.S., while reported cases can usually be disaggregated to at least the county level, the availability of spatially disaggregated data on correlates of immunity or behavior is uncommon. County-level SARS-CoV-2 seroprevalence estimates would have significantly enhanced our understanding of heterogeneities in county-level underreporting and infection burden. However, the sample size and additional resources required to obtain representative county-level seroprevalence data prevent their feasibility. Moreover, the large sample size and daily survey frequency of the COVID-19 Trends and Impact Survey (CTIS) uniquely enabled the characterization of contact rates at a detailed spatiotemporal level. Using CTIS data to parameterize our model, we found that contact rates were the lowest in metro-Atlanta and the highest in certain rural areas, broadly corroborating both observed and modeled disease incidence rates. Whether these differences persist outside pandemic conditions remains unanswered, underscoring the need for continued monitoring of spatial heterogeneities in social contact behavior. The discontinuation of CTIS in June 2022 is a loss of an important national-level data source on behavior. Future endeavors should explore possibilities to leverage existing social media or marketing

platforms to survey behavior on a geographically representative scale during both outbreak and non-outbreak periods.

Lastly, although mobility data presents new opportunities for parameterizing spatially explicit models, they are limited in their representativeness. Notably, GPS app-based mobility data underrepresents those without smartphone who are more likely to be children, older adults and individuals of lower socioeconomic classes[61,63], demographic groups who often experience disproportionate disease burden. A key critique of available mobility data is the lack of transparency around who is actually represented. Ethical and privacy considerations may prevent mobile data aggregators (i.e. Safegraph, Cuebiq or Google mobility) from being forthcoming with additional information. Future efforts may include collaborating with mobile data aggregators for additional disaggregation of mobility information by sociodemographic factors of the device holder, while maintaining adequate privacy. Such information would enable the stratification of mobility patterns by key determinants of behavior and transmission such as age group and socio-economic status, permitting parameterization of movement specific to key demographic groups.

6.2.3 Aim 3

In Aim 3, we assessed the utility of guiding the timing of future COVID-19 re-vaccination strategies with serological surveillance for SARS-CoV-2 in Mozambique over a ten-year horizon. We simulated using population-level seroprevalence thresholds to trigger the timing of re-vaccination campaigns among older adults and compared this approach to re-vaccination at fixed time intervals. We find that serology-triggered vaccination strategies are unlikely to minimize both deaths and NNV compared to fixed-time strategies. Monitoring changing immunity for SARS-CoV-2 to trigger subsequent rounds of booster vaccines was previously proposed for COVID-19 control[191]. The results from this aim were presented to the WHO Immunization and vaccines related implementation research advisory committee (WHO IVIR-AC) and informed their decision to not recommend using seroprevalence as an indicator to guide re-vaccination strategies for COVID-19. In addition, our analysis demonstrated, that in the context of

durable hybrid immunity against severe outcomes, using a serological marker with slower waning to trigger re-vaccination is likely to be more efficient against fixed-time strategies. These considerations are further applicable to other infectious diseases that can benefit from leveraging serosurveillance to inform public health interventions[301,302].

Mathematical models that assess the relative impact of counterfactual interventions have played a crucial role in informing guidelines for infectious disease prevention and control in high-income countries (HIC)s and at international organizations such as the WHO[375]. Challenges at the intersection of modeling and policy are well-documented[375–378] and there have been calls for closer collaboration between modelers and policymakers. Among African countries, the explicit use of modeling to guide policies varies by country[379]. Improved localization of modeling efforts would likely improve their utility[379].

Challenges faced by efforts to localize modeling in some African countries have included the lack of local data on non-disease parameters and limited familiarity with modeling among public health officials[379,380]. For the former, a systematic review of SARS-CoV-2 modeling efforts for African countries found that, while the majority fitted models to local disease data, only 9 of 74 (12%) used either local demographic or contact data to represent the local population and their patterns of interaction[381]. Our model was fortunately informed by local contact and serology data collected during the pandemic. Future modeling efforts in African countries could improve their parameterization with localized information on demographic characteristics, behavior, and immunity. If such data are missing, modeling work could be complemented by data collection activities.

To improve the utility of our work, we actively engaged with our research collaborators in Mozambique and with members of the national COVID-19 vaccination task force including the Instituto Nacional de Saude, United Nations Children's Fund (UNICEF)'s and WHO's Mozambique Office. We listened to operational, ground-level concerns on vaccine rollout and decision-making needs and sought to convert them into tractable and testable scenarios suitable for modeling and simultaneously useful for decision-

makers. Yet the gap in knowledge on modeling at times limited more extensive feedback during model development and interpretation, engagement we hoped would both improve model realism and ensure the model was practically informative.

A separate, frequently documented issue is the disproportionate amount of scientific research on Low-and Middle-Income Countries (LMICs) exclusively led by researchers from HICs, raising valid concerns of research equity[380]. The identification of this issue has prompted new training and funding such as efforts to expand the technical training of modelers from the African continent[382]. Of similar importance is the capacity of the local public health workforce to interpret, critique and engage with mathematical models. Future research work should ideally strive to better integrate engagement with local decision-makers and building their capacity into the scientific agenda, particularly in countries that have historically lacked the resources to build modeling knowledge.

6.3 Reflections

Training in infectious disease epidemiology and modeling during the COVID-19 pandemic presented many unique opportunities. In the spring of 2020, collaborations between our research group and public health departments and local administrative entities quickly formed and I was extraordinarily fortunate to have been invited to join various modeling and public health response efforts. These opportunities gave me a front row seat on the types of questions that were practically important for responding to a pandemic infringing on every aspect of daily life and on the ways that scientific work could advance our understanding of the local epidemiology and guide response. Our research group's planned studies on social contact patterns quickly took on a new form of urgency. These data collection activities were rapidly pivoted to capture social contact behavior and sentiments during the height of NPIs implemented to curb transmission, an effort I contributed to and crucially shaped my thinking around this dissertation. Lastly, I gained an opportunity to propose, develop and present policy-relevant modeling work to the World Health Organization, an unlikely experience in more normal circumstances.

Completing a PhD during the pandemic also presented unique challenges. The speed and quality of the scientific work led by renowned experts in our field was immensely important for formulating effective response. However, the depth and breadth of existing work presented challenges for a trainee to angle into a crowded field. Moreover, social distancing policies inadvertently isolated many of us from the broader scientific community, especially beyond our own institutions. Four years into my training, I attended my first ever scientific conference in-person and realized I had missed out on opportunities to discuss infectious disease research and exchange ideas with many brilliant minds earlier in my training.

I have always dreamed of leading a career at the intersection of hands-on epidemiological work in global health and mathematical modeling, ideally in the humanitarian sector. I thought it unlikely that I would achieve my ideal scenario during my doctoral training. I thus decided that if I was unable to do both, I was going to take full advantage of available resources and challenge myself to push the boundaries of complexity in mathematical modeling. I hoped that in doing so, I could walk away feeling confident in my ability to independently implement mathematical models for future, more applied chapters in my public health career. It is safe to say that I have been greatly humbled but also equally inspired by the effort it takes to design, build, run, analyze, and interpret a mathematical model. I have learned some valuable lessons and acquired skillsets, many of which surpass what I anticipated gaining from my doctoral training, all of which will inform my analytical and scientific work in the future.

Throughout this dissertation process, I have often ruminated over questions on the added value of these modeling exercises. Do the assumptions necessary to parameterize the model inherently undermine the public health significance? Did the thousands of hours of work justify the added value of the resulting scientific output? In other words, could we have come to a similar conclusion without a cumbersome, time-consuming model? Every trainee who has delved into infectious disease modeling knows the famous mantra “All models are wrong, but some are useful”. I suppose time and the scientific and public health communities will ultimately judge the actual utility of the modeling work undertaken by this dissertation.

What I am certain of is, that they were indeed useful for my own training and, hopefully, for attaining this degree.

CHAPTER 7 REFERENCES

1. Chan JFW, Yuan S, Kok KH, et al. A familial cluster of pneumonia associated with the 2019 novel coronavirus indicating person-to-person transmission: a study of a family cluster. *The Lancet*. 2020;395(10223):514-523. doi:10.1016/S0140-6736(20)30154-9

2. Xu B, Gutierrez B, Mekaru S, et al. Epidemiological data from the COVID-19 outbreak, real-time case information. *Sci Data*. 2020;7(1):106. doi:10.1038/s41597-020-0448-0

3. The Lancet. Emerging understandings of 2019-nCoV. *The Lancet*. 2020;395(10221):311. doi:10.1016/S0140-6736(20)30186-0

4. Park SE. Epidemiology, virology, and clinical features of severe acute respiratory syndrome - coronavirus-2 (SARS-CoV-2; Coronavirus Disease-19). *Clin Exp Pediatr*. 2020;63(4):119-124. doi:10.3345/cep.2020.00493

5. Cucinotta D, Vanelli M. WHO Declares COVID-19 a Pandemic. *Acta Bio Medica Atenei Parmensis*. 2020;91(1):157-160. doi:10.23750/abm.v91i1.9397

6. Jia JS, Lu X, Yuan Y, Xu G, Jia J, Christakis NA. Population flow drives spatio-temporal distribution of COVID-19 in China. *Nature*. 2020;582(7812):389-394. doi:10.1038/s41586-020-2284-y

7. Davis JT, Chinazzi M, Perra N, et al. Cryptic transmission of SARS-CoV-2 and the first COVID-19 wave. *Nature*. 2021;600(7887):127-132. doi:10.1038/s41586-021-04130-w

8. Zhang J, Litvinova M, Wang W, et al. Evolving epidemiology and transmission dynamics of coronavirus disease 2019 outside Hubei province, China: a descriptive and modelling study. *The Lancet Infectious Diseases*. 2020;20(7):793-802. doi:10.1016/S1473-3099(20)30230-9

9. WHO Director-General's opening remarks at the media briefing on COVID-19 - 11 March 2020. Accessed March 25, 2024. https://www.who.int/director-general/speeches/detail/who-director-general-s-opening-remarks-at-the-media-briefing-on-covid-19---11-march-2020

10. World Health Organization 2023 data.who.int, WHO Coronavirus (COVID-19) dashboard [Dashboard]. Accessed March 25, 2024. https://data.who.int/dashboards/covid19/cases

11. Ritchie H, Mathieu E, Rodés-Guirao L, et al. Coronavirus Pandemic (COVID-19). *Our World in Data*. Published online 2020. https://ourworldindata.org/coronavirus

12. Pearson CA, Van Schalkwyk C, Foss AM, et al. Projected early spread of COVID-19 in Africa through 1 June 2020. *Eurosurveillance*. 2020;25(18). doi:10.2807/1560-7917.ES.2020.25.18.2000543

13. New WHO estimates: Up to 190 000 people could die of COVID-19 in Africa if not controlled | WHO | Regional Office for Africa. Accessed March 25, 2024. https://www.afro.who.int/news/new-who-estimates-190-000-people-could-die-covid-19-africa-if-not-controlled

14. Gilbert M, Pullano G, Pinotti F, et al. Preparedness and vulnerability of African countries against importations of COVID-19: a modelling study. *The Lancet*. 2020;395(10227):871-877. doi:10.1016/S0140-6736(20)30411-6

15. Walker PGT, Whittaker C, Watson OJ, et al. The impact of COVID-19 and strategies for mitigation and suppression in low- and middle-income countries. *Science*. 2020;369(6502):413-422. doi:10.1126/science.abc0035

16. Maeda JM, Nkengasong JN. The puzzle of the COVID-19 pandemic in Africa. *Science*. 2021;371(6524):27-28. doi:10.1126/science.abf8832

17. Barber RM, Sorensen RJD, Pigott DM, et al. Estimating global, regional, and national daily and cumulative infections with SARS-CoV-2 through Nov 14, 2021: a statistical analysis. *The Lancet*. 2022;399(10344):2351-2380. doi:10.1016/S0140-6736(22)00484-6

18. Shioda K, Lopman B. How to interpret the total number of SARS-CoV-2 infections. *The Lancet*. 2022;399(10344):2326-2327. doi:10.1016/S0140-6736(22)00629-8

19. Russell TW, Golding N, Hellewell J, et al. Reconstructing the early global dynamics of under-ascertained COVID-19 cases and infections. *BMC Med*. 2020;18(1):332. doi:10.1186/s12916-020-01790-9

20. Boum Y, Bebell LM, Bisseck ACZK. Africa needs local solutions to face the COVID-19 pandemic. *The Lancet*. 2021;397(10281):1238-1240. doi:10.1016/S0140-6736(21)00719-4

21. Uyoga S, Adetifa IMO, Karanja HK, et al. Seroprevalence of anti–SARS-CoV-2 IgG antibodies in Kenyan blood donors. Published online 2021.

22. Simons E, Nikolay B, Ouedraogo P, et al. Seroprevalence of SARS-CoV-2 antibodies and retrospective mortality in two African settings: Lubumbashi, Democratic Republic of the Congo and Abidjan, Côte d'Ivoire. Croda J, ed. *PLOS Glob Public Health*. 2023;3(6):e0001457. doi:10.1371/journal.pgph.0001457

23. Arnaldo P, Mabunda N, Young PW, et al. Prevalence of SARS-CoV-2 antibodies in the Mozambican population: a cross-sectional Serologic study in three cities, July-August 2020. *Clinical Infectious Diseases*. Published online June 24, 2022:ciac516. doi:10.1093/cid/ciac516

24. Kagucia E, Ziraba A, Nyagwange J, et al. *SARS-CoV-2 Seroprevalence and Implications for Population Immunity: Evidence from Two Health and Demographic Surveillance System Sites in Kenya, February-June 2022*. Epidemiology; 2022. doi:10.1101/2022.10.10.22280824

25. Briggs J, Takahashi S, Nayebare P, et al. *Reconstructing the SARS-CoV-2 Epidemic in Eastern Uganda through Longitudinal Serosurveillance in a Malaria Cohort*. Infectious Diseases (except HIV/AIDS); 2022. doi:10.1101/2022.09.20.22280170

26. Bergeri I, Whelan M, Ware H, et al. *Global Epidemiology of SARS-CoV-2 Infection: A Systematic Review and Meta-Analysis of Standardized Population-Based Seroprevalence Studies, Jan 2020-Dec 2021*. Epidemiology; 2021. doi:10.1101/2021.12.14.21267791

27. Arora RK, Joseph A, Van Wyk J, et al. SeroTracker: a global SARS-CoV-2 seroprevalence dashboard. *The Lancet Infectious Diseases*. 2021;21(4):e75-e76. doi:10.1016/S1473-3099(20)30631-9

28. Cabore JW, Karamagi HC, Kipruto HK, et al. COVID-19 in the 47 countries of the WHO African region: a modelling analysis of past trends and future patterns. *The Lancet Global Health*. 2022;10(8):e1099-e1114. doi:10.1016/S2214-109X(22)00233-9

29. Meyerowitz EA, Richterman A, Gandhi RT, Sax PE. Transmission of SARS-CoV-2: A Review of Viral, Host, and Environmental Factors. *Ann Intern Med*. 2021;174(1):69-79. doi:10.7326/M20-5008

30. Klompas M, Baker MA, Rhee C. Theoretical Considerations and Available Evidence. Published online 2020.

31. Morawska L, Cao J. Airborne transmission of SARS-CoV-2: The world should face the reality. *Environment International*. 2020;139:105730. doi:10.1016/j.envint.2020.105730

32. Lauer SA, Grantz KH, Bi Q, et al. The Incubation Period of Coronavirus Disease 2019 (COVID-19) From Publicly Reported Confirmed Cases: Estimation and Application. *Ann Intern Med*. Published online March 10, 2020. doi:10.7326/M20-0504

33. Qin J, You C, Lin Q, Hu T, Yu S, Zhou XH. Estimation of incubation period distribution of COVID-19 using disease onset forward time: A novel cross-sectional and forward follow-up study. *Science Advances*. 2020;6.

34. Li J, Wang Y, Gilmour S, et al. *Estimation of the Epidemic Properties of the 2019 Novel Coronavirus: A Mathematical Modeling Study*. Infectious Diseases (except HIV/AIDS); 2020. doi:10.1101/2020.02.18.20024315

35. Backer JA, Klinkenberg D, Wallinga J. Incubation period of 2019 novel coronavirus (2019-nCoV) infections among travellers from Wuhan, China, 20–28 January 2020. *Eurosurveillance*. 2020;25(5). doi:10.2807/1560-7917.ES.2020.25.5.2000062

36. CDC. Clinical Presentation: Clinical considerations for care of children and adults with confirmed COVID-19. Centers for Disease Control and Prevention. Published February 11, 2020. Accessed March 25, 2024. https://www.cdc.gov/coronavirus/2019-ncov/hcp/clinical-care/clinical-considerations-presentation.html

37. Sah P, Fitzpatrick MC, Zimmer CF, et al. Asymptomatic SARS-CoV-2 infection: A systematic review and meta-analysis. *Proc Natl Acad Sci USA*. 2021;118(34):e2109229118. doi:10.1073/pnas.2109229118

38. Buitrago-Garcia D, Egli-Gany D, Counotte MJ, et al. Occurrence and transmission potential of asymptomatic and presymptomatic SARS-CoV-2 infections: A living systematic review and meta-analysis. Ford N, ed. *PLoS Med*. 2020;17(9):e1003346. doi:10.1371/journal.pmed.1003346

39. Jang S, Rhee JY, Wi YM, Jung BK. Viral kinetics of SARS-CoV-2 over the preclinical, clinical, and postclinical period. *International Journal of Infectious Diseases*. 2021;102:561-565. doi:10.1016/j.ijid.2020.10.099

40. Rasmussen AL, Popescu SV. SARS-CoV-2 transmission without symptoms. *Science*. 2021;371(6535):1206-1207. doi:10.1126/science.abf9569

41. Johansson MA, Quandelacy TM, Kada S, et al. SARS-CoV-2 Transmission From People Without COVID-19 Symptoms. *JAMA Netw Open*. 2021;4(1):e2035057. doi:10.1001/jamanetworkopen.2020.35057

42. Tuite AR, Fisman DN. Reporting, Epidemic Growth, and Reproduction Numbers for the 2019 Novel Coronavirus (2019-nCoV) Epidemic. *Annals of Internal Medicine*. 2020;172(8):567-568. doi:10.7326/M20-0358

43. Read JM, Bridgen JR, Cummings DA, Ho A, Jewell CP. *Novel Coronavirus 2019-nCoV: Early Estimation of Epidemiological Parameters and Epidemic Predictions*. Infectious Diseases (except HIV/AIDS); 2020. doi:10.1101/2020.01.23.20018549

44. Liu Y, Gayle AA, Wilder-Smith A, Rocklöv J. The reproductive number of COVID-19 is higher compared to SARS coronavirus. *Journal of Travel Medicine*. 2020;27(2):taaa021. doi:10.1093/jtm/taaa021

45. Qi H, Liu B, Wang X, Zhang L. The humoral response and antibodies against SARS-CoV-2 infection. *Nat Immunol*. 2022;23(7):1008-1020. doi:10.1038/s41590-022-01248-5

46. Altarawneh HN, Chemaitelly H, Ayoub HH, et al. Protective Effect of Previous SARS-CoV-2 Infection against Omicron BA.4 and BA.5 Subvariants. *N Engl J Med*. Published online October 5, 2022:NEJMc2209306. doi:10.1056/NEJMc2209306

47. Altarawneh HN, Chemaitelly H, Ayoub HH, et al. Effects of Previous Infection and Vaccination on Symptomatic Omicron Infections. *N Engl J Med*. 2022;387(1):21-34. doi:10.1056/NEJMoa2203965

48. Lacy J, Mensah A, Simmons R, et al. Protective effect of a first SARS-CoV-2 infection from reinfection: a matched retrospective cohort study using PCR testing data in England. *Epidemiol Infect*. 2022;150:e109. doi:10.1017/S0950268822000966

49. Hall V, Foulkes S, Insalata F, et al. Protection against SARS-CoV-2 after Covid-19 Vaccination and Previous Infection. *N Engl J Med*. 2022;386(13):1207-1220. doi:10.1056/NEJMoa2118691

50. De Gier B, Huiberts AJ, Hoeve CE, et al. Effects of COVID-19 vaccination and previous infection on Omicron SARS-CoV-2 infection and relation with serology. *Nat Commun*. 2023;14(1):4793. doi:10.1038/s41467-023-40195-z

51. Carazo S, Skowronski DM, Brisson M, et al. Protection against omicron (B.1.1.529) BA.2 reinfection conferred by primary omicron BA.1 or pre-omicron SARS-CoV-2 infection among health-care workers with and without mRNA vaccination: a test-negative case-control study. *The Lancet Infectious Diseases*. 2023;23(1):45-55. doi:10.1016/S1473-3099(22)00578-3

52. Bharti N. Linking human behaviors and infectious diseases. *Proc Natl Acad Sci USA*. 2021;118(11):e2101345118. doi:10.1073/pnas.2101345118

53. Slater JJ, Brown PE, Rosenthal JS, Mateu J. Capturing spatial dependence of COVID-19 case counts with cellphone mobility data. *Spatial Statistics*. Published online September 2021:100540. doi:10.1016/j.spasta.2021.100540

54. Jia JS, Lu X, Yuan Y, Xu G, Jia J, Christakis NA. Population flow drives spatio-temporal distribution of COVID-19 in China. *Nature*. 2020;582(7812):389-394. doi:10.1038/s41586-020-2284-y

55. Mossong J, Hens N, Jit M, et al. Social Contacts and Mixing Patterns Relevant to the Spread of Infectious Diseases. Riley S, ed. *PLoS Med*. 2008;5(3):e74. doi:10.1371/journal.pmed.0050074

56. Cattuto C, Van den Broeck W, Barrat A, Colizza V, Pinton JF, Vespignani A. Dynamics of person-to-person interactions from distributed RFID sensor networks. *PloS one*. 2010;5(7).

57. Isella L, Romano M, Barrat A, et al. Close encounters in a pediatric ward: measuring face-to-face proximity and mixing patterns with wearable sensors. *PloS one*. 2011;6(2).

58. Lucet JC, Laouenan C, Chelius G, et al. Electronic sensors for assessing interactions between healthcare workers and patients under airborne precautions. *PloS one*. 2012;7(5).

59. Mistry D, Litvinova M, Pastore y Piontti A, et al. Inferring high-resolution human mixing patterns for disease modeling. *Nature Communications*. 2021;12(323):12.

60. Prem K, Cook AR, Jit M. Projecting social contact matrices in 152 countries using contact surveys and demographic data. Halloran B, ed. *PLoS Comput Biol*. 2017;13(9):e1005697. doi:10.1371/journal.pcbi.1005697

61. Wesolowski A, Buckee CO, Engø-Monsen K, Metcalf CJE. Connecting Mobility to Infectious Diseases: The Promise and Limits of Mobile Phone Data. *J Infect Dis*. 2016;214(suppl 4):S414-S420. doi:10.1093/infdis/jiw273

62. Meredith HR, Giles JR, Perez-Saez J, et al. Characterizing human mobility patterns in rural settings of sub-Saharan Africa. *eLife*. 2021;10:e68441. doi:10.7554/eLife.68441

63. Grantz KH, Meredith HR, Cummings DAT, et al. The use of mobile phone data to inform analysis of COVID-19 pandemic epidemiology. *Nat Commun*. 2020;11(1):4961. doi:10.1038/s41467-020-18190-5

64. Kishore N, Taylor AR, Jacob PE, et al. Evaluating the reliability of mobility metrics from aggregated mobile phone data as proxies for SARS-CoV-2 transmission in the USA: a population-based study. *The Lancet Digital Health*. 2022;4(1):e27-e36. doi:10.1016/S2589-7500(21)00214-4

65. Buckee CO, Balsari S, Chan J, et al. Aggregated mobility data could help fight COVID-19. Sills J, ed. *Science*. 2020;368(6487):145-146. doi:10.1126/science.abb8021

66. Hoang T, Coletti P, Melegaro A, et al. A Systematic Review of Social Contact Surveys to Inform Transmission Models of Close-contact Infections: *Epidemiology*. 2019;30(5):723-736. doi:10.1097/EDE.0000000000001047

67. Grijalva CG, Goeyvaerts N, Verastegui H, et al. A household-based study of contact networks relevant for the spread of infectious diseases in the highlands of Peru. *PloS one*. 2015;10(3).

68. de Waroux O le P, Cohuet S, Ndazima D, et al. Characteristics of human encounters and social mixing patterns relevant to infectious diseases spread by close contact: a survey in Southwest Uganda. *BMC infectious diseases*. 2018;18(1):172.

69. Leung WTM, Meeyai A, Holt HR, et al. Social contact patterns relevant for infectious disease transmission in Cambodia. *Sci Rep*. 2023;13(1):5542. doi:10.1038/s41598-023-31485-z

70. Leung K, Jit M, Lau EH, Wu JT. Social contact patterns relevant to the spread of respiratory infectious diseases in Hong Kong. *Scientific reports*. 2017;7(1):1-12.

71. Del Fava E, Cimentada J, Perrotta D, et al. Differential impact of physical distancing strategies on social contacts relevant for the spread of SARS-CoV-2: evidence from a cross-national online survey, March–April 2020. *BMJ Open*. 2021;11(10):e050651. doi:10.1136/bmjopen-2021-050651

72. Salomon JA, Reinhart A, Bilinski A, et al. The US COVID-19 Trends and Impact Survey: Continuous real-time measurement of COVID-19 symptoms, risks, protective behaviors, testing, and vaccination. *Proc Natl Acad Sci USA*. 2021;118(51):e2111454118. doi:10.1073/pnas.2111454118

73. Nelson KN, Siegler AJ, Sullivan PS, et al. Nationally representative social contact patterns among U.S. adults, August 2020-April 2021. *Epidemics*. 2022;40:100605. doi:10.1016/j.epidem.2022.100605

74. Andrejko KL, Head JR, Lewnard JA, Remais JV. Longitudinal social contacts among school-aged children during the COVID-19 pandemic: the Bay Area Contacts among Kids (BACK) study. *BMC Infect Dis*. 2022;22(1):242. doi:10.1186/s12879-022-07218-4

75. Dorelien, Audrey, Ramen, Aparna, Swanson, Isabella. Analyzing the Demographic, Spatial, and Temporal Factors Influencing Social Contact Patterns in the U.S. and Implications for Infectious Disease Spread. *Minnesota Population Center Working Paper Series*. Published online 2020. doi:10.18128/MPC2020-05

76. Chin T, Feehan DM, Buckee CO, Mahmud AS. *Contact Surveys Reveal Heterogeneities in Age-Group Contributions to SARS-CoV-2 Dynamics in the United States*. Epidemiology; 2021. doi:10.1101/2021.09.25.21264082

77. Feehan DM, Mahmud A. Quantifying interpersonal contact in the United States during the spread of COVID-19: first results from the Berkeley Interpersonal Contact Study. *Nature Communications*. 2021;12(893):8. doi:https://doi.org/10.1038/s41467-021-20990-2

78. Gimma A, Munday JD, Wong KLM, et al. Changes in social contacts in England during the COVID-19 pandemic between March 2020 and March 2021 as measured by the CoMix survey: A repeated cross-sectional study. Murray MB, ed. *PLoS Med*. 2022;19(3):e1003907. doi:10.1371/journal.pmed.1003907

79. Wong KL, Gimma A, Coletti P, et al. *Social Contact Patterns during the COVID-19 Pandemic in 21 European Countries – Evidence from a Two-Year Study*. Epidemiology; 2022. doi:10.1101/2022.07.25.22277998

80. Coletti P, Wambua J, Gimma A, et al. CoMix: comparing mixing patterns in the Belgian population during and after lockdown. *Sci Rep*. 2020;10(1):21885. doi:10.1038/s41598-020-78540-7

81. Backer JA, Mollema L, Vos ER, et al. Impact of physical distancing measures against COVID-19 on contacts and mixing patterns: repeated cross-sectional surveys, the Netherlands, 2016–17, April 2020 and June 2020. *Eurosurveillance*. 2021;26(8). doi:10.2807/1560-7917.ES.2021.26.8.2000994

82. Sypsa V, Roussos S, Paraskevis D, Lytras T, Tsiodras S, Hatzakis A. Effects of Social Distancing Measures during the First Epidemic Wave of Severe Acute Respiratory Syndrome Infection, Greece. *Emerging Infectious Diseases*. 2021;27(2). doi:10.3201/eid2702.203412

83. Jarvis CI, van Zandvoort K, Gimma A, et al. Quantifying the impact of physical distance measures on the transmission of COVID-19 in the UK. *BMC Medicine*. 2020;18(1):21. doi:10.1186/s12916-020-01597-8

84. Bosetti P, Huynh BT, Abdou AY, et al. *Lockdown Impact on Age-Specific Contact Patterns and Behaviours in France*. Medrxiv; 2020. doi:10.1101/2020.10.07.20205104

85. Reinhart A, Brooks L, Jahja M, et al. An open repository of real-time COVID-19 indicators. *Proc Natl Acad Sci USA*. 2021;118(51):e2111452118. doi:10.1073/pnas.2111452118

86. Places Data & Foot Traffic Insights | SafeGraph. Accessed March 10, 2022. https://www.safegraph.com

87. Offline Intelligence & Measurement - Increase Return on Ad Spend. Accessed March 1, 2024. https://www.cuebiq.com/

88. COVID-19 Community Mobility Reports. Accessed March 25, 2024. https://www.google.com/covid19/mobility/

89. Location Intelligence & Foot Traffic Data | Unacast. Accessed March 25, 2024. https://www.unacast.com/?utm_source=google&utm_medium=cpc&utm_campaign=Branded-NA&utm_feeditemid=&utm_device=c&utm_term=unacast&utm_source=adwords&utm_medium=ppc&utm_campaign=NA+%7C+Branded+Search&hsa_cam=12879513733&hsa_grp=122822832698&hsa_mt=p&hsa_src=g&hsa_ad=609147625825&hsa_acc=7231278556&hsa_net=adwords&hsa_kw=unacast&hsa_tgt=kwd-421665487587&hsa_ver=3&gad_source=1&gclid=Cj0KCQjwwYSwBhDcARIsAOyL0fghf-fwMCNRNhe_Lwswlmz4gc11GcKWvNVww4lDVxdh7hP4KeOa8nkaAlMZEALw_wcB

90. Hu T, Wang S, She B, et al. Human mobility data in the COVID-19 pandemic: characteristics, applications, and challenges. *International Journal of Digital Earth*. 2021;14(9):1126-1147. doi:10.1080/17538947.2021.1952324

91. Badr HS, Du H, Marshall M, Dong E, Squire MM, Gardner LM. Association between mobility patterns and COVID-19 transmission in the USA: a mathematical modelling study. *The Lancet Infectious Diseases*. 2020;20(11):1247-1254. doi:10.1016/S1473-3099(20)30553-3

92. Gatalo O, Tseng K, Hamilton A, Lin G, Klein E. Associations between phone mobility data and COVID-19 cases. *The Lancet Infectious Diseases*. 2021;21(5):e111. doi:10.1016/S1473-3099(20)30725-8

93. Her PH, Saeed S, Tram KH, Bhatnagar SR. Novel mobility index tracks COVID-19 transmission following stay-at-home orders. *Sci Rep*. 2022;12(1):7654. doi:10.1038/s41598-022-10941-2

94. Gibbs H, Liu Y, Abbott S, et al. Association between mobility, non-pharmaceutical interventions, and COVID-19 transmission in Ghana: A modelling study using mobile phone data. Zinszer K, ed. *PLOS Glob Public Health*. 2022;2(9):e0000502. doi:10.1371/journal.pgph.0000502

95. Gottumukkala R, Katragadda S, Bhupatiraju RT, et al. Exploring the relationship between mobility and COVID− 19 infection rates for the second peak in the United States using phase-wise association. *BMC Public Health*. 2021;21(1):1669. doi:10.1186/s12889-021-11657-0

96. Jeffrey B, Walters CE, Ainslie KEC, et al. Anonymised and aggregated crowd level mobility data from mobile phones suggests that initial compliance with COVID-19 social distancing interventions was high and geographically consistent across the UK. *Wellcome Open Res*. 2020;5:170. doi:10.12688/wellcomeopenres.15997.1

97. Xiong C, Hu S, Yang M, Luo W, Zhang L. Mobile device data reveal the dynamics in a positive relationship between human mobility and COVID-19 infections. *Proc Natl Acad Sci USA*. 2020;117(44):27087-27089. doi:10.1073/pnas.2010836117

98. Grantz KH, Meredith HR, Cummings DAT, et al. The use of mobile phone data to inform analysis of COVID-19 pandemic epidemiology. *Nat Commun*. 2020;11(1):4961. doi:10.1038/s41467-020-18190-5

99. Chang S, Pierson E, Koh PW, et al. Mobility network models of COVID-19 explain inequities and inform reopening. *Nature*. 2021;589(7840):82-87. doi:10.1038/s41586-020-2923-3

100. Hou X, Gao S, Li Q, et al. Intracounty modeling of COVID-19 infection with human mobility: Assessing spatial heterogeneity with business traffic, age, and race. *Proc Natl Acad Sci USA*. 2021;118(24):e2020524118. doi:10.1073/pnas.2020524118

101. Kang Y, Gao S, Liang Y, Li M, Rao J, Kruse J. Multiscale dynamic human mobility flow dataset in the U.S. during the COVID-19 epidemic. *Sci Data*. 2020;7(1):390. doi:10.1038/s41597-020-00734-5

102. Slater JJ, Brown PE, Rosenthal JS, Mateu J. Capturing spatial dependence of COVID-19 case counts with cellphone mobility data. *Spatial Statistics*. 2022;49:100540. doi:10.1016/j.spasta.2021.100540

103. Buckee C, Noor A, Sattenspiel L. Thinking clearly about social aspects of infectious disease transmission. *Nature*. 2021;595(7866):205-213. doi:10.1038/s41586-021-03694-x

104. Mousa A, Winskill P, Watson OJ, et al. Social contact patterns and implications for infectious disease transmission – a systematic review and meta-analysis of contact surveys. *eLife*. 2021;10:e70294. doi:10.7554/eLife.70294

105. Melegaro A, Del Fava E, Poletti P, et al. Social Contact Structures and Time Use Patterns in the Manicaland Province of Zimbabwe. Nishiura H, ed. *PLoS ONE*. 2017;12(1):e0170459. doi:10.1371/journal.pone.0170459

106. Kiti MC, Kinyanjui TM, Koech DC, Munywoki PK, Medley GF, Nokes DJ. Quantifying Age-Related Rates of Social Contact Using Diaries in a Rural Coastal Population of Kenya. Borrmann S, ed. *PLoS ONE*. 2014;9(8):e104786. doi:10.1371/journal.pone.0104786

107. Kiti MC, Tizzoni M, Kinyanjui TM, et al. Quantifying social contacts in a household setting of rural Kenya using wearable proximity sensors. *EPJ data science*. 2016;5(1):1-21.

108. Edmunds W, Kafatos G, Wallinga J, Mossong J. Mixing patterns and the spread of close-contact infectious diseases. *Emerg Themes Epidemiol*. 2006;3(1):10. doi:10.1186/1742-7622-3-10

109. Prem K, Liu Y, Russell TW, et al. The effect of control strategies to reduce social mixing on outcomes of the COVID-19 epidemic in Wuhan, China: a modelling study. *The Lancet Public Health*. Published online March 2020:S2468266720300736. doi:10.1016/S2468-2667(20)30073-6

110. Liu CY, Berlin J, Kiti MC, et al. *Rapid Review of Social Contact Patterns during the COVID-19 Pandemic*.; 2021. doi:10.1101/2021.03.12.21253410

111. Brankston G, Merkley E, Fisman DN, et al. Quantifying contact patterns in response to COVID-19 public health measures in Canada. *BMC Public Health*. 2021;21(1):2040. doi:10.1186/s12889-021-12080-1

112. Bilinski A, Emanuel E, Salomon JA, Venkataramani A. Better Late Than Never: Trends in COVID-19 Infection Rates, Risk Perceptions, and Behavioral Responses in the USA. *J GEN INTERN MED*. 2021;36(6):1825-1828. doi:10.1007/s11606-021-06633-8

113. Bedson J, Skrip LA, Pedi D, et al. A review and agenda for integrated disease models including social and behavioural factors. *Nat Hum Behav*. 2021;5(7):834-846. doi:10.1038/s41562-021-01136-2

114. Funk S, Salathé M, Jansen VAA. Modelling the influence of human behaviour on the spread of infectious diseases: a review. *J R Soc Interface*. 2010;7(50):1247-1256. doi:10.1098/rsif.2010.0142

115. Trogen B, Caplan A. Risk Compensation and COVID-19 Vaccines. *Ann Intern Med*. 2021;174(6):858-859. doi:10.7326/M20-8251

116. Iyengar KP, Ish P, Botchu R, Jain VK, Vaishya R. Influence of the Peltzman effect on the recurrent COVID-19 waves in Europe. *Postgrad Med J*. 2022;98(e2):e110-e111. doi:10.1136/postgradmedj-2021-140234

117. Peltzman S. The effects of automobile safety regulation. *Journal of Political Economy*. 1975;83(4).

118. Cassell MM, Halperin DT, Shelton JD, Stanton D. Risk compensation: the Achilles' heel of innovations in HIV prevention? 2006;332:3.

119. Rojas Castro D, Delabre RM, Molina J. Give PrEP a chance: moving on from the "risk compensation" concept. *J Intern AIDS Soc*. 2019;22(S6). doi:10.1002/jia2.25351

120. Ouellet JV. Helmet Use and Risk Compensation in Motorcycle Accidents. *Traffic Injury Prevention*. 2011;12(1).

121. Brewer NT, Cuite CL, Herrington JE, Weinstein ND. Risk compensation and vaccination: Can getting vaccinated cause people to engage in risky behaviors? *ann behav med*. 2007;34(1):95-99. doi:10.1007/BF02879925

122. Reiber C, Shattuck EC, Fiore S, Alperin P, Davis V, Moore J. Change in Human Social Behavior in Response to a Common Vaccine. *Annals of Epidemiology*. 2010;20(10):729-733. doi:https://doi.org/10.1016/j.annepidem.2010.06.014

123. Office for National Statistics, UK. Coronavirus and vaccine attitudes and behaviours in England. *https://www.ons.gov.uk/peoplepopulationandcommunity/healthandsocialcare/conditionsanddiseases/*

bulletins/coronavirusandvaccineattitudesandbehavioursinengland/over80spopulation15februaryto20february2021. Published online 2021:10.

124. Buckell J, Jones J, Matthews PC, et al. *COVID-19 Vaccination, Risk-Compensatory Behaviours, and Contacts in the UK*. Infectious Diseases (except HIV/AIDS); 2021. doi:10.1101/2021.11.15.21266255

125. Desrichard O, Moussaoui L, Ofosu N. *Do Vaccinated People Reduce Their Precautionary Behaviours? A Test on a British Cohort*. In Review; 2021. doi:10.21203/rs.3.rs-796025/v1

126. Goldszmidt R, Petherick A, Andrade EB, et al. Protective Behaviors Against COVID-19 by Individual Vaccination Status in 12 Countries During the Pandemic. *JAMA Netw Open*. 2021;4(10):e2131137. doi:10.1001/jamanetworkopen.2021.31137

127. Yamamura E, Kosaka Y, Tsutsui Y, Ohtake F. *Effect of the COVID-19 Vaccine on Preventive Behaviors: Panel Data Analysis from Japan*. In Review; 2022. doi:10.21203/rs.3.rs-1625548/v1

128. Corea F, Folcarelli L, Napoli A, del Giudice GM, Angelillo IF. The Impact of COVID-19 Vaccination in Changing the Adherence to Preventive Measures: Evidence from Italy. *Vaccines*. 2022;10(5):777. doi:10.3390/vaccines10050777

129. Hossain MdE, Islam MdS, Rana MdJ, et al. Scaling the changes in lifestyle, attitude, and behavioral patterns among COVID-19 vaccinated people: insights from Bangladesh. *Human Vaccines & Immunotherapeutics*. 2022;18(1):2022920. doi:10.1080/21645515.2021.2022920

130. Rahamim-Cohen D, Gazit S, Perez G, et al. *Survey of Behaviour Attitudes Towards Preventive Measures Following COVID-19 Vaccination*. Health Policy; 2021. doi:10.1101/2021.04.12.21255304

131. Mello López A, Borges IC, Luna-Muschi A, et al. Risk factors for reduction in adherence to protective measures following coronavirus disease 2019 (COVID-19) vaccination and vaccine perceptions among healthcare workers, in São Paulo, Brazil. *Infect Control Hosp Epidemiol*. Published online May 26, 2022:1-3. doi:10.1017/ice.2022.142

132. Jia JS, Yuan Y, Jia J, Christakis NA. Risk perception and behaviour change after personal vaccination for COVID-19 in the USA. *PsyArXiv*. Published online April 16, 2022:28.

133. Latkin CA, Dayton L, Yi G, Colon B, Kong X. Mask usage, social distancing, racial, and gender correlates of COVID-19 vaccine intentions among adults in the US. Camacho-Rivera M, ed. *PLoS ONE*. 2021;16(2):e0246970. doi:10.1371/journal.pone.0246970

134. Rane MS, Kochhar S, Poehlein E, et al. Determinants and Trends of COVID-19 Vaccine Hesitancy and Vaccine Uptake in a National Cohort of US Adults: A Longitudinal Study. *American Journal of Epidemiology*. 2022;191(4):570-583. doi:10.1093/aje/kwab293

135. King WC, Rubinstein M, Reinhart A, Mejia R. Time trends, factors associated with, and reasons for COVID-19 vaccine hesitancy: A massive online survey of US adults from January-May 2021. Stimpson JP, ed. *PLoS ONE*. 2021;16(12):e0260731. doi:10.1371/journal.pone.0260731

136. Latkin C, Dayton LA, Yi G, et al. COVID-19 vaccine intentions in the United States, a social-ecological framework. *Vaccine*. 2021;39(16):2288-2294. doi:10.1016/j.vaccine.2021.02.058

137. Crane MA, Shermock KM, Omer SB, Romley JA. Change in Reported Adherence to Nonpharmaceutical Interventions During the COVID-19 Pandemic, April-November 2020. *JAMA*. 2021;325(9):883. doi:10.1001/jama.2021.0286

138. Clipman SJ, Wesolowski AP, Gibson DG, et al. Rapid Real-time Tracking of Nonpharmaceutical Interventions and Their Association With Severe Acute Respiratory Syndrome Coronavirus 2 (SARS-CoV-2) Positivity: The Coronavirus Disease 2019 (COVID-19) Pandemic Pulse Study. *Clinical Infectious Diseases*. 2021;73(7):e1822-e1829. doi:10.1093/cid/ciaa1313

139. Arnold C. The Maximal Expected Benefit of SARS-CoV-2 Intervention Among University Students: A Simulation Study Using Latent Class Analysis. Published online July 7, 2023. osf.io/qbtfs

140. Ihantamalala FA, Herbreteau V, Rakotoarimanana FMJ, et al. Estimating sources and sinks of malaria parasites in Madagascar. *Nat Commun*. 2018;9(1):3897. doi:10.1038/s41467-018-06290-2

141. Wesolowski A, Qureshi T, Boni MF, et al. Impact of human mobility on the emergence of dengue epidemics in Pakistan. *Proc Natl Acad Sci USA*. 2015;112(38):11887-11892. doi:10.1073/pnas.1504964112

142. Bengtsson L, Gaudart J, Lu X, et al. Using Mobile Phone Data to Predict the Spatial Spread of Cholera. *Sci Rep*. 2015;5(1):8923. doi:10.1038/srep08923

143. Grenfell BT, Bjørnstad ON, Kappey J. Travelling waves and spatial hierarchies in measles epidemics. *Nature*. 2001;414(6865):716-723. doi:10.1038/414716a

144. Lau MSY, Becker AD, Korevaar HM, et al. A competing-risks model explains hierarchical spatial coupling of measles epidemics en route to national elimination. *Nat Ecol Evol*. 2020;4(7):934-939. doi:10.1038/s41559-020-1186-6

145. Kortessis N, Simon MW, Barfield M, Glass GE, Singer BH, Holt RD. The interplay of movement and spatiotemporal variation in transmission degrades pandemic control. *Proc Natl Acad Sci USA*. 2020;117(48):30104-30106. doi:10.1073/pnas.2018286117

146. Polo G, Soler-Tovar D, Villamil Jimenez LC, Benavides-Ortiz E, Mera Acosta C. SARS-CoV-2 transmission dynamics in the urban-rural interface. *Public Health*. 2022;206:1-4. doi:10.1016/j.puhe.2022.02.007

147. Wells K, Lurgi M, Collins B, et al. Disease control across urban–rural gradients. *J R Soc Interface*. 2020;17(173):20200775. doi:10.1098/rsif.2020.0775

148. Behrman K, Mikheyev A, Taylor E. Exploring source-sink dynamics of pre- vaccination measles epidemics using a spectral formulation of Granger causality.

149. Koelle K, Martin MA, Antia R, Lopman B, Dean NE. The changing epidemiology of SARS-CoV-2. Published online 2022:7.

150. Susswein Z, Valdano E, Brett T, Rohani P, Colizza V, Bansal S. *Ignoring Spatial Heterogeneity in Drivers of SARS-CoV-2 Transmission in the US Will Impede Sustained Elimination*. Epidemiology; 2021. doi:10.1101/2021.08.09.21261807

151. Danon L, Brooks-Pollock E, Bailey M, Keeling M. A spatial model of COVID-19 transmission in England and Wales: early spread, peak timing and the impact of seasonality. *Phil Trans R Soc B*. 2021;376(1829):20200272. doi:10.1098/rstb.2020.0272

152. Finger F, Genolet T, Mari L, et al. Mobile phone data highlights the role of mass gatherings in the spreading of cholera outbreaks. *Proc Natl Acad Sci USA*. 2016;113(23):6421-6426. doi:10.1073/pnas.1522305113

153. Beckett SJ, Dominguez-Mirazo M, Lee S, Andris C, Weitz JS. *Spread of COVID-19 through Georgia, USA. Near-Term Projections and Impacts of Social Distancing via a Metapopulation Model*. Epidemiology; 2020. doi:10.1101/2020.05.28.20115642

154. Apolloni A, Poletto C, Ramasco JJ, Jensen P, Colizza V. Metapopulation epidemic models with heterogeneous mixing and travel behaviour. *Theor Biol Med Model*. 2014;11(1):3. doi:10.1186/1742-4682-11-3

155. Balcan D, Colizza V, Goncalves B, Hu H, Ramasco JJ, Vespignani A. Multiscale mobility networks and the spatial spreading of infectious diseases. *Proceedings of the National Academy of Sciences*. 2009;106(51):21484-21489. doi:10.1073/pnas.0906910106

156. Xia Y, Bjørnstad ON, Grenfell BT. Measles Metapopulation Dynamics: A Gravity Model for Epidemiological Coupling and Dynamics.

157. Coletti P, Libin P, Petrof O, et al. A data-driven metapopulation model for the Belgian COVID-19 epidemic: assessing the impact of lockdown and exit strategies. *BMC Infect Dis*. 2021;21(1):503. doi:10.1186/s12879-021-06092-w

158. Pei S, Kandula S, Shaman J. Differential effects of intervention timing on COVID-19 spread in the United States. *SCIENCE ADVANCES*. Published online 2020:10.

159. Brauner JM, Mindermann S, Sharma M, et al. Inferring the effectiveness of government interventions against COVID-19. *Science*. Published online December 15, 2020:eabd9338. doi:10.1126/science.abd9338

160. Hale T, Webster S, Petherick A, Phillips T, Kira B. Oxford COVID-19 Government Response Tracker, Blavatnik School of Government. *Data use policy: Creative Commons Attribution CC BY standard*. Published online 2020.

161. Thompson MG, Burgess JL, Naleway AL, et al. Interim Estimates of Vaccine Effectiveness of BNT162b2 and mRNA-1273 COVID-19 Vaccines in Preventing SARS-CoV-2 Infection Among Health Care Personnel, First Responders, and Other Essential and Frontline Workers — Eight U.S. Locations, December 2020–March 2021. *MMWR Morb Mortal Wkly Rep*. 2021;70(13):495-500. doi:10.15585/mmwr.mm7013e3

162. Thompson MG, Stenehjem E, Grannis S, et al. Effectiveness of Covid-19 Vaccines in Ambulatory and Inpatient Care Settings. *N Engl J Med*. Published online September 8, 2021. doi:10.1056/NEJMoa2110362

163. Liu Q, Qin C, Liu M, Liu J. Effectiveness and safety of SARS-CoV-2 vaccine in real-world studies: a systematic review and meta-analysis. *Infect Dis Poverty*. 2021;10(1):132. doi:10.1186/s40249-021-00915-3

164. Tan ST, Park HJ, Rodríguez-Barraquer I, et al. COVID-19 Vaccination and Estimated Public Health Impact in California. *JAMA Netw Open*. 2022;5(4):e228526. doi:10.1001/jamanetworkopen.2022.8526

165. Chen X, Huang H, Ju J, Sun R, Zhang J. Impact of vaccination on the COVID-19 pandemic in U.S. states. *Sci Rep*. 2022;12(1). doi:10.1038/s41598-022-05498-z

166. World Health Organization. WHO SAGE Roadmap for prioritizing uses of COVID-19 vaccines. Published online January 21, 2022. https://www.who.int/publications/i/item/WHO-2019-nCoV-Vaccines-SAGE-Prioritization-2022.1

167. Davies NG, Kucharski AJ, Eggo RM, Gimma A, CMMID COVID-19 Working Group, Edmunds WJ. *The Effect of Non-Pharmaceutical Interventions on COVID-19 Cases, Deaths and Demand for Hospital Services in the UK: A Modelling Study*. Infectious Diseases (except HIV/AIDS); 2020. doi:10.1101/2020.04.01.20049908

168. Ferguson NM, Laydon D, Nedjati-Gilani G, et al. Impact of non-pharmaceutical interventions (NPIs) to reduce COVID- 19 mortality and healthcare demand. Published online 2020:20.

169. Bubar KM, Reinholt K, Kissler SM, et al. Model-informed COVID-19 vaccine prioritization strategies by age and serostatus. *Science*. Published online January 21, 2021:eabe6959. doi:10.1126/science.abe6959

170. Buckner JH, Chowell G, Springborn MR. Dynamic prioritization of COVID-19 vaccines when social distancing is limited for essential workers. *Proc Natl Acad Sci USA*. 2021;118(16):e2025786118. doi:10.1073/pnas.2025786118

171. Imai N, Rawson T, Knock ES, et al. Quantifying the effect of delaying the second COVID-19 vaccine dose in England: a mathematical modelling study. *The Lancet Public Health*. 2023;8(3):e174-e183. doi:10.1016/S2468-2667(22)00337-1

172. Keeling MJ, Moore S, Penman BS, Hill EM. The impacts of SARS-CoV-2 vaccine dose separation and targeting on the COVID-19 epidemic in England. *Nat Commun*. 2023;14(1):740. doi:10.1038/s41467-023-35943-0

173. Li R, Liu H, Fairley CK, et al. Cost-effectiveness analysis of BNT162b2 COVID-19 booster vaccination in the United States. *International Journal of Infectious Diseases*. 2022;119:87-94. doi:10.1016/j.ijid.2022.03.029

174. Kraay ANM, Gallagher ME, Ge Y, et al. The role of booster vaccination and ongoing viral evolution in seasonal circulation of SARS-CoV-2. *J R Soc Interface*. 2022;19(194):20220477. doi:10.1098/rsif.2022.0477

175. Bilgin GM, Lokuge K, Munira SL, Glass K. Assessing the potential impact of COVID-19 booster doses and oral antivirals: A mathematical modelling study of selected middle-income countries in the Indo-Pacific. *Vaccine: X*. 2023;15:100386. doi:10.1016/j.jvacx.2023.100386

176. Massonnaud CR, Roux J, Colizza V, Crépey P. Evaluating COVID-19 Booster Vaccination Strategies in a Partially Vaccinated Population: A Modeling Study. *Vaccines*. 2022;10(3):479. doi:10.3390/vaccines10030479

177. Barnard RC, Davies NG, Centre for Mathematical Modelling of Infectious Diseases COVID-19 working group, et al. Modelling the medium-term dynamics of SARS-CoV-2 transmission in England in the Omicron era. *Nat Commun*. 2022;13(1):4879. doi:10.1038/s41467-022-32404-y

178. Hogan AB, Wu SL, Toor J, et al. *Long Term Vaccination Strategies to Mitigate the Impact of SARS-CoV-2 Transmission: A Modelling Study*. Epidemiology; 2023. doi:10.1101/2023.02.09.23285743

179. Van Zandvoort K, Favas C, Checchi F. Shielding individuals at high risk of COVID-19: A micro-simulation study. *Wellcome Open Res*. 2023;8:199. doi:10.12688/wellcomeopenres.18838.1

180. Kraay ANM, Nelson KN, Zhao CY, Demory D, Weitz JS, Lopman BA. Modeling serological testing to inform relaxation of social distancing for COVID-19 control. *Nat Commun*. 2021;12(1):7063. doi:10.1038/s41467-021-26774-y

181. Fujimoto AB, Keskinocak P, Yildirim I. Significance of SARS-CoV-2 specific antibody testing during COVID-19 vaccine allocation. *Vaccine*. 2021;39(35):5055-5063. doi:10.1016/j.vaccine.2021.06.067

182. Guerstein S, Romeo-Aznar V, Dekel M, et al. The interplay between vaccination and social distancing strategies affects COVID19 population-level outcomes. Althouse BM, ed. *PLoS Comput Biol*. 2021;17(8):e1009319. doi:10.1371/journal.pcbi.1009319

183. Lobinska G, Pauzner A, Traulsen A, Pilpel Y, Nowak MA. Evolution of resistance to COVID-19 vaccination with dynamic social distancing. *Nat Hum Behav*. 2022;6(2):193-206. doi:10.1038/s41562-021-01281-8

184. Daher-Nashif S, Al-Anany R, Ali M, et al. COVID-19 exit strategy during vaccine implementation: a balance between social distancing and herd immunity. *Arch Virol*. Published online June 20, 2022. doi:10.1007/s00705-022-05495-7

185. Gozzi N, Bajardi P, Perra N. The importance of non-pharmaceutical interventions during the COVID-19 vaccine rollout. Kouyos RD, ed. *PLoS Comput Biol*. 2021;17(9):e1009346. doi:10.1371/journal.pcbi.1009346

186. Thorpe A, Fagerlin A, Drews FA, Shoemaker H, Scherer LD. Self-reported health behaviors and risk perceptions following the COVID-19 vaccination rollout in the USA: an online survey study. *Public Health*. 2022;208:68-71. doi:10.1016/j.puhe.2022.05.007

187. Wright L, Steptoe A, Mak HW, Fancourt D. Do people reduce compliance with COVID-19 guidelines following vaccination? A longitudinal analysis of matched UK adults. *J Epidemiol Community Health*. 2022;76(2):109-115. doi:10.1136/jech-2021-217179

188. Mobarak AM, Miguel E, Abaluck J, et al. End COVID-19 in low- and middle-income countries. *Science*. 2022;375(6585):1105-1110. doi:10.1126/science.abo4089

189. Lopman BA, Shioda K, Nguyen Q, et al. A framework for monitoring population immunity to SARS-CoV-2. *Annals of Epidemiology*. 2021;63:75-78. doi:10.1016/j.annepidem.2021.08.013

190. Cutts FT, Hanson M. Seroepidemiology: an underused tool for designing and monitoring vaccination programmes in low- and middle-income countries. *Trop Med Int Health*. 2016;21(9):1086-1098. doi:10.1111/tmi.12737

191. dos Santos Ferreira CE, Gómez-Dantés H, Junqueira Bellei NC, et al. The Role of Serology Testing in the Context of Immunization Policies for COVID-19 in Latin American Countries. *Viruses*. 2021;13(12):2391. doi:10.3390/v13122391

192. Nelson K, Lopman B. The hiatus of the handshake. *Science*. 2022;377(6601):33-34. doi:10.1126/science.abp9316

193. Watson OJ, Barnsley G, Toor J, Hogan AB, Winskill P, Ghani AC. Global impact of the first year of COVID-19 vaccination: a mathematical modelling study. *The Lancet Infectious Diseases*. 2022;22(9):1293-1302. doi:10.1016/S1473-3099(22)00320-6

194. Telenti A, Arvin A, Corey L, et al. After the pandemic: perspectives on the future trajectory of COVID-19. *Nature*. 2021;596(7873):495-504. doi:10.1038/s41586-021-03792-w

195. Cipolletta S, Andreghetti G, Mioni G. Risk Perception towards COVID-19: A Systematic Review and Qualitative Synthesis. *IJERPH*. 2022;19(8):4649. doi:10.3390/ijerph19084649

196. Clifford S, Waight P, Hackman J, et al. Effectiveness of BNT162b2 and ChAdOx1 against SARS- CoV-2 household transmission: a prospective cohort study in England [version 2; peer review: 2 approved]. *Wellcome Open Research*. Published online 2023.

197. Wambua J, Loedy N, Jarvis CI, et al. The influence of COVID-19 risk perception and vaccination status on the number of social contacts across Europe: insights from the CoMix study. *BMC Public Health*. 2023;23(1):1350. doi:10.1186/s12889-023-16252-z

198. Siegler AJ, Sullivan PS, Sanchez T, et al. Protocol for a national probability survey using home specimen collection methods to assess prevalence and incidence of SARS-CoV-2 infection and antibody response. *Annals of Epidemiology*. 2020;49:50-60. doi:10.1016/j.annepidem.2020.07.015

199. Murray CJL. COVID-19 will continue but the end of the pandemic is near. *The Lancet*. 2022;399(10323):417-419. doi:10.1016/S0140-6736(22)00100-3

200. Gimma A, Munday JD, Wong KLM, et al. Changes in social contacts in England during the COVID-19 pandemic between March 2020 and March 2021 as measured by the CoMix survey: A repeated cross-sectional study. Murray MB, ed. *PLoS Med*. 2022;19(3):e1003907. doi:10.1371/journal.pmed.1003907

201. Kiti MC, Aguolu OG, Liu CY, et al. Social contact patterns among employees in 3 U.S. companies during early phases of the COVID-19 pandemic, April to June 2020. *Epidemics*. 2021;36:100481. doi:10.1016/j.epidem.2021.100481

202. Nelson KN, Siegler AJ, Sullivan PS, et al. *Nationally Representative Social Contact Patterns in the United States, August 2020-April 2021*. Epidemiology; 2021. doi:10.1101/2021.09.22.21263904

203. Hens N, Goeyvaerts N, Aerts M, Shkedy Z, Van Damme P, Beutels P. Mining social mixing patterns for infectious disease models based on a two-day population survey in Belgium. *BMC Infect Dis*. 2009;9(1):5. doi:10.1186/1471-2334-9-5

204. Kiti MC, Kinyanjui TM, Koech DC, Munywoki PK, Medley GF, Nokes DJ. Quantifying age-related rates of social contact using diaries in a rural coastal population of Kenya. *PloS one*. 2014;9(8).

205. Leung K, Jit M, Lau EH, Wu JT. Social contact patterns relevant to the spread of respiratory infectious diseases in Hong Kong. *Scientific reports*. 2017;7(1):1-12.

206. Sullivan PS, Siegler AJ, Shioda K, et al. Severe Acute Respiratory Syndrome Coronavirus 2 Cumulative Incidence, United States, August 2020–December 2020. *Clinical Infectious Diseases*. Published online July 10, 2021:ciab626. doi:10.1093/cid/ciab626

207. Andridge RR, Little RJA. A Review of Hot Deck Imputation for Survey Non-response. *Int Statistical Rev*. 2010;78(1):40-64. doi:10.1111/j.1751-5823.2010.00103.x

208. Linzer DA, Lewis JB. poLCA: An R Package for Polytomous Variable Latent Class Analysis. *J Stat Soft*. 2011;42(10):1-29. doi:10.18637/jss.v042.i10

209. Weller BE, Bowen NK, Faubert SJ. Latent Class Analysis: A Guide to Best Practice. *Journal of Black Psychology*. 2020;46(4):287-311. doi:10.1177/0095798420930932

210. Wong KLM, Gimma A, Coletti P, et al. Social contact patterns during the COVID-19 pandemic in 21 European countries – evidence from a two-year study. *BMC Infect Dis*. 2023;23(1):268. doi:10.1186/s12879-023-08214-y

211. Yan Y, Malik AA, Bayham J, Fenichel EP, Couzens C, Omer SB. Measuring voluntary and policy-induced social distancing behavior during the COVID-19 pandemic. *Proc Natl Acad Sci USA*. 2021;118(16):e2008814118. doi:10.1073/pnas.2008814118

212. Diekmann O, Heesterbeek JAP, Roberts MG. The construction of next-generation matrices for compartmental epidemic models. *J R Soc Interface*. 2010;7(47):873-885. doi:10.1098/rsif.2009.0386

213. Dhungel B, Rahman MdS, Rahman MdM, et al. Reliability of Early Estimates of the Basic Reproduction Number of COVID-19: A Systematic Review and Meta-Analysis. *IJERPH*. 2022;19(18):11613. doi:10.3390/ijerph191811613

214. Billah MdA, Miah MdM, Khan MdN. Reproductive number of coronavirus: A systematic review and meta-analysis based on global level evidence. Flacco ME, ed. *PLoS ONE*. 2020;15(11):e0242128. doi:10.1371/journal.pone.0242128

215. Tomori DV, Rübsamen N, Berger T, et al. *Individual Social Contact Data Reflected SARS-CoV-2 Transmission Dynamics during the First Wave in Germany Better than Population Mobility Data – an Analysis Based on the COVIMOD Study*. Epidemiology; 2021. doi:10.1101/2021.03.24.21254194

216. US population by year, race, age, ethnicity, & more | USAFacts. Accessed July 30, 2023. https://usafacts.org/data/topics/people-society/population-and-demographics/our-changing-population/

217. Calamari LE, Tjaden AH, Edelstein SL, et al. Self-reported mask use among persons with or without SARS CoV-2 vaccination —United States, December 2020–August 2021. *Preventive Medicine Reports*. Published online 2022:5.

218. Andrejko KL, Head JR, Lewnard JA, Remais JV. Longitudinal social contacts among school-aged children during the COVID-19 pandemic: the Bay Area Contacts among Kids (BACK) study. *BMC Infect Dis*. 2022;22(1):242. doi:10.1186/s12879-022-07218-4

219. Chin T, Feehan DM, Buckee CO, Mahmud AS. *Contact Surveys Reveal Heterogeneities in Age-Group Contributions to SARS-CoV-2 Dynamics in the United States*. Epidemiology; 2021. doi:10.1101/2021.09.25.21264082

220. Feehan DM, Mahmud AS. Quantifying population contact patterns in the United States during the COVID-19 pandemic. *Nat Commun*. 2021;12(1):893. doi:10.1038/s41467-021-20990-2

221. Mousa A, Winskill P, Watson OJ, et al. Social contact patterns and implications for infectious disease transmission – a systematic review and meta-analysis of contact surveys. *eLife*. 2021;10:e70294. doi:10.7554/eLife.70294

222. Fahimi M, Link M, Schwartz DA, Levy P, Mokdad A. Tracking Chronic Disease and Risk Behavior Prevalence as Survey Participation Declines: Statistics From the Behavioral Risk Factor Surveillance System and Other National Surveys. 2008;5(3).

223. Ajelli M, Litvinova M. Estimating contact patterns relevant to the spread of infectious diseases in Russia. *Journal of Theoretical Biology*. 2017;419:1-7.

224. Del Fava E, Adema I, Kiti MC, et al. Individual's daily behaviour and intergenerational mixing in different social contexts of Kenya. *Sci Rep*. 2021;11(1):21589. doi:10.1038/s41598-021-00799-1

225. Lloyd AL, May RM. Spatial Heterogeneity in Epidemic Models. *Journal of Theoretical Biology*. 1996;179(1):1-11. doi:10.1006/jtbi.1996.0042

226. Kishore N, Kahn R, Martinez PP, De Salazar PM, Mahmud AS, Buckee CO. Lockdowns result in changes in human mobility which may impact the epidemiologic dynamics of SARS-CoV-2. *Sci Rep*. 2021;11(1):6995. doi:10.1038/s41598-021-86297-w

227. Lau MSY, Grenfell B, Thomas M, Bryan M, Nelson K, Lopman B. Characterizing superspreading events and age-specific infectiousness of SARS-CoV-2 transmission in Georgia, USA. *Proc Natl Acad Sci USA*. 2020;117(36):22430-22435. doi:10.1073/pnas.2011802117

228. Lau MSY, Liu C, Siegler AJ, et al. Post-lockdown changes of age-specific susceptibility and its correlation with adherence to social distancing measures. *Sci Rep*. 2022;12(1):4637. doi:10.1038/s41598-022-08566-6

229. COVID-19 Status Report | Georgia Department of Public Health. Accessed May 3, 2020. https://dph.georgia.gov/covid-19-daily-status-report

230. Georgia Immunization Registry (GRITS) | Georgia Department of Public Health. Accessed March 1, 2024. https://dph.georgia.gov/immunizations/georgia-immunization-registry-grits

231. COVID-19 Vaccinations in the United States,County | Data | Centers for Disease Control and Prevention. Accessed June 6, 2022. https://data.cdc.gov/Vaccinations/COVID-19-Vaccinations-in-the-United-States-County/8xkx-amqh

232. Questions and Coding. Delphi Epidata API. Accessed June 5, 2022. https://cmu-delphi.github.io/delphi-epidata/symptom-survey/coding.html

233. Meta Data for Good. User Guide for the COVID-19 Trends and Impact Survey Weights. Published online May 10, 2022. https://scontent-atl3-1.xx.fbcdn.net/v/t39.8562-6/281310961_1000166414205006_3176544355420994098_n.pdf?_nc_cat=110&ccb=1-7&_nc_sid=ae5e01&_nc_ohc=Ia6EmcGlOC4AX-N6KER&_nc_ht=scontent-atl3-1.xx&oh=00_AfBFqFp0yvVEJJzB1fyQuk5kX--BTxPluAOFhf5HMRyXog&oe=645F43ED

234. Nelson KN, Siegler AJ, Sullivan PS, et al. Nationally representative social contact patterns among U.S. adults, August 2020-April 2021. *Epidemics*. 2022;40:100605. doi:10.1016/j.epidem.2022.100605

235. USDA ERS - Documentation. Accessed January 9, 2024. https://www.ers.usda.gov/data-products/rural-urban-continuum-codes/documentation/

236. U.S. Census Bureau (2020). 2016-2020 American Community Survey 5-year estimates. https://data.census.gov/cedsci/table?q=United%20States&table=DP05&tid=ACSDP1Y2017.DP05&g=0100000US&lastDisplayedRow=29&vintage=2017&layer=state&cid=DP05_0001E

237. Breen CF, Mahmud AS, Feehan DM. Novel estimates reveal subnational heterogeneities in disease-relevant contact patterns in the United States. Larremore DB, ed. *PLoS Comput Biol*. 2022;18(12):e1010742. doi:10.1371/journal.pcbi.1010742

238. Stay informed of the rapid school district changes with the below resources - MCH Data. Accessed March 2, 2024. https://www.mchdata.com/covid19/schoolclosings

239. Global Points of Interest (POI) Data | SafeGraph Places. Accessed March 10, 2022. https://www.safegraph.com/products/places

240. Minter A, Retkute R. Approximate Bayesian Computation for infectious disease modelling. *Epidemics*. 2019;29:100368. doi:10.1016/j.epidem.2019.100368

241. Stein M. Large Sample Properties of Simulations Using Latin Hypercube Sampling. *Technometrics*. 1987;29(2):143-151. doi:10.2307/1269769

242. Colizza V, Vespignani A. Epidemic modeling in metapopulation systems with heterogeneous coupling pattern: Theory and simulations. *Journal of Theoretical Biology*. 2008;251(3):450-467. doi:10.1016/j.jtbi.2007.11.028

243. Cuadros DF, Branscum AJ, Mukandavire Z, Miller FD, MacKinnon N. Dynamics of the COVID-19 epidemic in urban and rural areas in the United States. *Annals of Epidemiology*. 2021;59:16-20. doi:10.1016/j.annepidem.2021.04.007

244. Tang CY, Li T, Haynes TA, et al. Rural populations facilitated early SARS-CoV-2 evolution and transmission in Missouri, USA. *npj Viruses*. 2023;1(1):7. doi:10.1038/s44298-023-00005-1

245. Peluso M, Takahashi S, Hakim J, et al. SARS-CoV-2 antibody magnitude and detectability are driven by disease severity, timing, and assay. *SCIENCE ADVANCES*. Published online 2021:13.

246. Surie D, Bonnell L, Adams K, et al. Effectiveness of Monovalent mRNA Vaccines Against COVID-19–Associated Hospitalization Among Immunocompetent Adults During BA.1/BA.2 and BA.4/BA.5 Predominant Periods of SARS-CoV-2 Omicron Variant in the United States — IVY Network, 18 States, December 26, 2021–August 31, 2022. *MMWR Morb Mortal Wkly Rep*. 2022;71(42):1327-1334. doi:10.15585/mmwr.mm7142a3

247. CDC Statement on ACIP Booster Recommendations | CDC Online Newsroom | CDC. Published September 2021. Accessed June 22, 2023. https://www.cdc.gov/media/releases/2021/p0924-booster-recommendations-.html

248. World Health Organization. Interim statement on booster doses for COVID-19 vaccination. Published October 2021. Accessed October 3, 2022. https://www.who.int/news/item/04-10-2021-interim-statement-on-booster-doses-for-covid-19-vaccination

249. SAGE updates COVID-19 vaccination guidance. Accessed April 4, 2023. https://www.who.int/news/item/28-03-2023-sage-updates-covid-19-vaccination-guidance

250. Stoddard M, Yuan L, Sarkar S, et al. *The Impact of Vaccination Frequency on COVID-19 Public Health Outcomes: A Model-Based Analysis*. Infectious Diseases (except HIV/AIDS); 2023. doi:10.1101/2023.01.26.23285076

251. Shrotri M, Navaratnam AMD, Nguyen V, et al. Spike-antibody waning after second dose of BNT162b2 or ChAdOx1. *The Lancet*. 2021;398(10298):385-387. doi:10.1016/S0140-6736(21)01642-1

252. Ward H, Whitaker M, Flower B, et al. Population antibody responses following COVID-19 vaccination in 212,102 individuals. *Nat Commun*. 2022;13(1):907. doi:10.1038/s41467-022-28527-x

253. Lessler J, Metcalf CJE, Cutts FT, Grenfell BT. Impact on Epidemic Measles of Vaccination Campaigns Triggered by Disease Outbreaks or Serosurveys: A Modeling Study. von Seidlein L, ed. *PLoS Med*. 2016;13(10):e1002144. doi:10.1371/journal.pmed.1002144

254. Bryant JE, Azman AS, Ferrari MJ, et al. Serology for SARS-CoV-2: Apprehensions, opportunities, and the path forward. *Sci Immunol*. 2020;5(47):eabc6347. doi:10.1126/sciimmunol.abc6347

255. Antia R, Halloran ME. Transition to endemicity: Understanding COVID-19. *Immunity*. 2021;54(10):2172-2176. doi:10.1016/j.immuni.2021.09.019

256. Lavine JS, Bjornstad ON, Antia R. Immunological characteristics govern the transition of COVID-19 to endemicity. *Science*. 2021;371(6530):741-745. doi:10.1126/science.abe6522

257. Massinga Loembé M, Nkengasong JN. COVID-19 vaccine access in Africa: Global distribution, vaccine platforms, and challenges ahead. *Immunity*. 2021;54(7):1353-1362. doi:10.1016/j.immuni.2021.06.017

258. Ayenigbara IO, Adegboro JS, Ayenigbara GO, Rowland O, Olofintuyi OO. The challenges to a successful COVID-19 vaccination programme in Africa. *Germs*. Published online 2021:14.

259. Ministério da Saúde - Moçambique. COVID-19: Inquérito Sero-epidemiológico de SARS-CoV-2. Published 2021. Accessed May 4, 2023. https://www.misau.gov.mz/index.php/covid-19-inquerito-sero-epidemiologicos

260. Gallagher ME, Sieben AJ, Nelson KN, et al. Indirect benefits are a crucial consideration when evaluating SARS-CoV-2 vaccine candidates. *Nat Med*. 2021;27(1):4-5. doi:10.1038/s41591-020-01172-x

261. Kraay ANM, Gallagher ME, Ge Y, et al. *Modeling the Use of SARS-CoV-2 Vaccination to Safely Relax Non-Pharmaceutical Interventions*. Epidemiology; 2021. doi:10.1101/2021.03.12.21253481

262. Binswanger IA, Narwaney KJ, Barrow JC, et al. Association between severe acute respiratory syndrome coronavirus 2 antibody status and reinfection: A case-control study nested in a Colorado-based prospective cohort study. *Preventive Medicine Reports*. 2024;37:102530. doi:10.1016/j.pmedr.2023.102530

263. Yamamoto S, Mizoue T, Ohmagari N. Analysis of Previous Infection, Vaccinations, and Anti–SARS-CoV-2 Antibody Titers and Protection Against Infection With the SARS-CoV-2 Omicron BA.5 Variant. *JAMA Netw Open*. 2023;6(3):e233370. doi:10.1001/jamanetworkopen.2023.3370

264. Lou B, Li TD, Zheng SF, et al. Serology characteristics of SARS-CoV-2 infection after exposure and post-symptom onset. *Eur Respir J*. 2020;56(2):2000763. doi:10.1183/13993003.00763-2020

265. Oved K. Multi-center nationwide comparison of seven serology assays reveals a SARS-CoV-2 non-responding seronegative subpopulation. Published online 2020:10.

266. Van Elslande J, Oyaert M, Ailliet S, et al. Longitudinal follow-up of IgG anti-nucleocapsid antibodies in SARS-CoV-2 infected patients up to eight months after infection. *Journal of Clinical Virology*. 2021;136:104765. doi:10.1016/j.jcv.2021.104765

267. Khoury DS, Cromer D, Reynaldi A, et al. Neutralizing antibody levels are highly predictive of immune protection from symptomatic SARS-CoV-2 infection. *Nat Med*. 2021;27(7):1205-1211. doi:10.1038/s41591-021-01377-8

268. Earle KA, Ambrosino DM, Fiore-Gartland A, et al. Evidence for antibody as a protective correlate for COVID-19 vaccines. *Vaccine*. 2021;39(32):4423-4428. doi:10.1016/j.vaccine.2021.05.063

269. Lumley SF, O'Donnell D, Stoesser NE, et al. Antibody Status and Incidence of SARS-CoV-2 Infection in Health Care Workers. *N Engl J Med*. 2021;384(6):533-540. doi:10.1056/NEJMoa2034545

270. Turner JS, Kim W, Kalaidina E, et al. SARS-CoV-2 infection induces long-lived bone marrow plasma cells in humans. *Nature*. 2021;595(7867):421-425. doi:10.1038/s41586-021-03647-4

271. Wei J, Matthews PC, Stoesser N, et al. Anti-spike antibody response to natural SARS-CoV-2 infection in the general population. *Nat Commun*. 2021;12(1):6250. doi:10.1038/s41467-021-26479-2

272. Liu W, Russell RM, Bibollet-Ruche F, et al. Predictors of Nonseroconversion after SARS-CoV-2 Infection. *Emerg Infect Dis*. 2021;27(9):2454-2458. doi:10.3201/eid2709.211042

273. Plumb ID, Fette LM, Tjaden AH, et al. Estimated COVID-19 vaccine effectiveness against seroconversion from SARS-CoV-2 Infection, March–October, 2021. *Vaccine*. 2023;41(15):2596-2604. doi:10.1016/j.vaccine.2023.03.006

274. He Z, Ren L, Yang J, et al. Seroprevalence and humoral immune durability of anti-SARS-CoV-2 antibodies in Wuhan, China: a longitudinal, population-level, cross-sectional study. *The Lancet*. 2021;397(10279):1075-1084. doi:10.1016/S0140-6736(21)00238-5

275. Swartz MD, DeSantis SM, Yaseen A, et al. Antibody duration after infection from SARS-CoV-2 in the Texas Coronavirus Antibody Response Survey. *The Journal of Infectious Diseases*. Published online May 6, 2022:jiac167. doi:10.1093/infdis/jiac167

276. Wei J, Stoesser N, Matthews PC, et al. Antibody responses to SARS-CoV-2 vaccines in 45,965 adults from the general population of the United Kingdom. *Nat Microbiol*. 2021;6(9):1140-1149. doi:10.1038/s41564-021-00947-3

277. Wang H, Yuan Y, Xiao M, et al. Dynamics of the SARS-CoV-2 antibody response up to 10 months after infection. *Cell Mol Immunol*. 2021;18(7):1832-1834. doi:10.1038/s41423-021-00708-6

278. Ward H. Population antibody responses following COVID-19 vaccination in 212,102 individuals. *Nature Communications*. 2022;13(907):6.

279. Ali H, Alahmad B, Al-Shammari AA, et al. Previous COVID-19 Infection and Antibody Levels After Vaccination. *Front Public Health*. 2021;9:778243. doi:10.3389/fpubh.2021.778243

280. Wearing HJ, Rohani P, Keeling MJ. Appropriate Models for the Management of Infectious Diseases. Ellner SP, ed. *PLoS Med*. 2005;2(7):e174. doi:10.1371/journal.pmed.0020174

281. Higdon M, Wahl B, Jones C, et al. A systematic review of COVID-19 vaccine efficacy and effectiveness against SARS-CoV-2 infection and disease. *Open Forum Infectious Diseases*. 2022;ofac138. doi:https://doi.org/10.1093/ofid/ofac138

282. Aguolu OG, Kiti MC, Nelson K, et al. *Comprehensive Profiling of Social Mixing Patterns in Resource Poor Countries: A Mixed Methods Research Protocol*.; 2023. doi:10.1101/2023.12.05.23299472

283. Diekmann O, Heesterbeek JAP, Roberts MG. The construction of next-generation matrices for compartmental epidemic models. *J R Soc Interface*. 2010;7(47):873-885. doi:10.1098/rsif.2009.0386

284. Campbell F, Archer B, Laurenson-Schafer H, et al. Increased transmissibility and global spread of SARS-CoV-2 variants of concern as at June 2021. *Eurosurveillance*. 2021;26(24). doi:10.2807/1560-7917.ES.2021.26.24.2100509

285. Chadha M, Hirve S, Bancej C, et al. Human respiratory syncytial virus and influenza seasonality patterns—Early findings from the WHO global respiratory syncytial virus surveillance. *Influenza Other Respi Viruses*. 2020;14(6):638-646. doi:10.1111/irv.12726

286. Ma Y, Pei S, Shaman J, Dubrow R, Chen K. Role of meteorological factors in the transmission of SARS-CoV-2 in the United States. *Nat Commun*. 2021;12(1):3602. doi:10.1038/s41467-021-23866-7

287. Sajadi MM, Habibzadeh P, Vintzileos A, Shokouhi S, Miralles-Wilhelm F, Amoroso A. Temperature, Humidity, and Latitude Analysis to Estimate Potential Spread and Seasonality of Coronavirus Disease 2019 (COVID-19). *JAMA Netw Open*. 2020;3(6):e2011834. doi:10.1001/jamanetworkopen.2020.11834

288. Baker RE, Yang W, Vecchi GA, Metcalf CJE, Grenfell BT. Susceptible supply limits the role of climate in the early SARS-CoV-2 pandemic. *Science*. 2020;369(6501):315-319. doi:10.1126/science.abc2535

289. Chan KH, Peiris JSM, Lam SY, Poon LLM, Yuen KY, Seto WH. The Effects of Temperature and Relative Humidity on the Viability of the SARS Coronavirus. *Advances in Virology*. 2011;2011:1-7. doi:10.1155/2011/734690

290. Casanova LM, Jeon S, Rutala WA, Weber DJ, Sobsey MD. Effects of Air Temperature and Relative Humidity on Coronavirus Survival on Surfaces. *Appl Environ Microbiol*. 2010;76(9):2712-2717. doi:10.1128/AEM.02291-09

291. Total COVID-19 vaccine doses administered per 100 people. Our World in Data. Accessed July 1, 2022. https://ourworldindata.org/grapher/covid-vaccination-doses-per-capita

292. Leidi A, Koegler F, Dumont R, et al. Risk of reinfection after seroconversion to SARS-CoV-2: A population-based propensity-score matched cohort study. *Clin Infect Dis*. Published online May 27, 2021:ciab495. doi:10.1093/cid/ciab495

293. Saad-Roy CM, Morris SE, Metcalf CJE, et al. Epidemiological and evolutionary considerations of SARS-CoV-2 vaccine dosing regimes. *Science*. 2021;372(6540):363-370. doi:10.1126/science.abg8663

294. Cohen LE, Spiro DJ, Viboud C. Projecting the SARS-CoV-2 transition from pandemicity to endemicity: Epidemiological and immunological considerations. Lakdawala S, ed. *PLoS Pathog*. 2022;18(6):e1010591. doi:10.1371/journal.ppat.1010591

295. Wagner CE, Saad-Roy CM, Grenfell BT. Modelling vaccination strategies for COVID-19. *Nat Rev Immunol*. 2022;22(3):139-141. doi:10.1038/s41577-022-00687-3

296. Bobrovitz N, Ware H, Ma X, et al. Protective effectiveness of previous SARS-CoV-2 infection and hybrid immunity against the omicron variant and severe disease: a systematic review and meta-regression. *The Lancet Infectious Diseases*. Published online January 2023:S1473309922008015. doi:10.1016/S1473-3099(22)00801-5

297. Loesche M, Karlson EW, Talabi O, et al. Longitudinal SARS-CoV-2 Nucleocapsid Antibody Kinetics, Seroreversion, and Implications for Seroepidemiologic Studies. *Emerg Infect Dis*. 2022;28(9):1859-1862. doi:10.3201/eid2809.220729

298. Wei J, Matthews PC, Stoesser N, et al. SARS-CoV-2 antibody trajectories after a single COVID-19 vaccination with and without prior infection. *Nat Commun*. 2022;13(1):3748. doi:10.1038/s41467-022-31495-x

299. Berry AA, Tjaden AH, Renteria J, et al. Persistence of antibody responses to COVID-19 vaccines among participants in the COVID-19 Community Research Partnership. *Vaccine: X*. 2023;15:100371. doi:10.1016/j.jvacx.2023.100371

300. Zar HJ, MacGinty R, Workman L, et al. Natural and hybrid immunity following four COVID-19 waves: A prospective cohort study of mothers in South Africa. *eClinicalMedicine*. 2022;53:101655. doi:10.1016/j.eclinm.2022.101655

301. Wiens KE, Jauregui B, Arnold BF, et al. Building an integrated serosurveillance platform to inform public health interventions: Insights from an experts' meeting on serum biomarkers. Kamel MG, ed. *PLoS Negl Trop Dis*. 2022;16(10):e0010657. doi:10.1371/journal.pntd.0010657

302. Dean NE, Howard DH, Lopman BA. Serological Studies and the Value of Information. *Am J Public Health*. Published online March 9, 2023:e1-e3. doi:10.2105/AJPH.2023.307245

303. Duroseau B, Kipshidze N, Limaye RJ. The impact of delayed access to COVID-19 vaccines in low- and lower-middle-income countries. *Front Public Health*. 2023;10:1087138. doi:10.3389/fpubh.2022.1087138

304. Post N, Eddy D, Huntley C, et al. Antibody response to SARS-CoV-2 infection in humans: A systematic review. Mantis NJ, ed. *PLoS ONE*. 2020;15(12):e0244126. doi:10.1371/journal.pone.0244126

305. Tan CY, Chiew CJ, Pang D, et al. Vaccine effectiveness against Delta, Omicron BA.1, and BA.2 in a highly vaccinated Asian setting: a test-negative design study. *Clinical Microbiology and Infection*. Published online August 2022:S1198743X22004189. doi:10.1016/j.cmi.2022.08.002

306. Kissler SM, Tedijanto C, Goldstein E, Grad YH, Lipsitch M. Projecting the transmission dynamics of SARS-CoV-2 through the postpandemic period. Published online 2020:10.

307. Veldhoen M, Simas JP. Endemic SARS-CoV-2 will maintain post-pandemic immunity. *Nat Rev Immunol*. 2021;21(3):131-132. doi:10.1038/s41577-020-00493-9

308. Bar-On YM, Goldberg Y, Mandel M, et al. Protection by a Fourth Dose of BNT162b2 against Omicron in Israel. *N Engl J Med*. 2022;386(18):1712-1720. doi:10.1056/NEJMoa2201570

309. Li Q, Guan X, Wu P, et al. Early Transmission Dynamics in Wuhan, China, of Novel Coronavirus–Infected Pneumonia. *N Engl J Med*. Published online January 29, 2020:NEJMoa2001316. doi:10.1056/NEJMoa2001316

310. Poletti P, Tirani M, Cereda D, et al. Association of Age With Likelihood of Developing Symptoms and Critical Disease Among Close Contacts Exposed to Patients With Confirmed SARS-CoV-2 Infection in Italy. *JAMA Netw Open*. 2021;4(3):e211085. doi:10.1001/jamanetworkopen.2021.1085

311. Mizumoto K, Kagaya K, Zarebski A, Chowell G. Estimating the asymptomatic proportion of coronavirus disease 2019 (COVID-19) cases on board the Diamond Princess cruise ship, Yokohama, Japan, 2020. *Eurosurveillance*. 2020;25(10). doi:10.2807/1560-7917.ES.2020.25.10.2000180

312. Rees EM, Nightingale ES, Jafari Y, et al. COVID-19 length of hospital stay: a systematic review and data synthesis. *BMC Med*. 2020;18(1):270. doi:10.1186/s12916-020-01726-3

313. McAloon C, Collins Á, Hunt K, et al. Incubation period of COVID-19: a rapid systematic review and meta-analysis of observational research. *BMJ Open*. 2020;10(8):e039652. doi:10.1136/bmjopen-2020-039652

314. Lemaitre JC, Grantz KH, Kaminsky J, et al. A scenario modeling pipeline for COVID-19 emergency planning. *Sci Rep*. 2021;11(1):7534. doi:10.1038/s41598-021-86811-0

315. Herrera-Esposito D, de los Campos G. Age-specific rate of severe and critical SARS-CoV-2 infections estimated with multi-country seroprevalence studies. *BMC Infect Dis*. 2022;22(1):311. doi:10.1186/s12879-022-07262-0

316. Levin AT, Hanage WP, Owusu-Boaitey N, Cochran KB, Walsh SP, Meyerowitz-Katz G. Assessing the age specificity of infection fatality rates for COVID-19: systematic review, meta-analysis, and public policy implications. *Eur J Epidemiol*. 2020;35(12):1123-1138. doi:10.1007/s10654-020-00698-1

317. Brazeau NF, Verity R, Jenks S, et al. Estimating the COVID-19 infection fatality ratio accounting for seroreversion using statistical modelling. *Commun Med*. 2022;2(1):54. doi:10.1038/s43856-022-00106-7

318. Variation in the COVID-19 infection–fatality ratio by age, time, and geography during the pre-vaccine era: a systematic analysis. *The Lancet*. 2022;399(10334):1469-1488. doi:10.1016/S0140-6736(21)02867-1

319. Sonabend R, Whittles LK, Imai N, et al. Non-pharmaceutical interventions, vaccination, and the SARS-CoV-2 delta variant in England: a mathematical modelling study. *The Lancet*. 2021;398(10313):1825-1835. doi:10.1016/S0140-6736(21)02276-5

320. Oved K, Olmer L, Shemer-Avni Y, et al. Multi-center nationwide comparison of seven serology assays reveals a SARS-CoV-2 non-responding seronegative subpopulation. *EClinicalMedicine*. 2020;29-30:100651. doi:10.1016/j.eclinm.2020.100651

321. Harris JE. Data from the COVID-19 epidemic in Florida suggest that younger cohorts have been transmitting their infections to less socially mobile older adults. *Rev Econ Household*. 2020;18(4):1019-1037. doi:10.1007/s11150-020-09496-w

322. Chen S, Flegg JA, White LJ, Aguas R. Levels of SARS-CoV-2 population exposure are considerably higher than suggested by seroprevalence surveys. Struchiner CJ, ed. *PLoS Comput Biol*. 2021;17(9):e1009436. doi:10.1371/journal.pcbi.1009436

323. Public Health England. SARS-CoV-2 variants of concern and variants under investigation. Published online June 3, 2021:66.

324. Ueda M, Kobayashi T, Nishiura H. Basic reproduction number of the COVID-19 Delta variant: Estimation from multiple transmission datasets. *MBE*. 2022;19(12):13137-13151. doi:10.3934/mbe.2022614

325. Baker JM, Nakayama JY, O'Hegarty M, et al. SARS-CoV-2 B.1.1.529 (Omicron) Variant Transmission Within Households — Four U.S. Jurisdictions, November 2021–February 2022. *MMWR Morb Mortal Wkly Rep*. 2022;71(9):341-346. doi:10.15585/mmwr.mm7109e1

326. Hansen CH, Schelde AB, Moustsen-Helm IR, et al. *Vaccine Effectiveness against SARS-CoV-2 Infection with the Omicron or Delta Variants Following a Two-Dose or Booster BNT162b2 or mRNA-1273 Vaccination Series: A Danish Cohort Study*. Infectious Diseases (except HIV/AIDS); 2021. doi:10.1101/2021.12.20.21267966

327. Harder T, Külper-Schiek W, Reda S, et al. Effectiveness of COVID-19 vaccines against SARS-CoV-2 infection with the Delta (B.1.617.2) variant: second interim results of a living systematic review and meta-analysis, 1 January to 25 August 2021. *Eurosurveillance*. 2021;26(41). doi:10.2807/1560-7917.ES.2021.26.41.2100920

328. Funk S. Socialmixr: Social Mixing Matrices for Infectious Disease Modelling. R package version 0.1.7. Published online 2020. https://CRAN.R-project.org/package=socialmixr

329. Anichini G, Terrosi C, Gandolfo C, et al. SARS-CoV-2 Antibody Response in Persons with Past Natural Infection. *N Engl J Med*. 2021;385(1):90-92. doi:10.1056/NEJMc2103825

330. Assis R, Jain A, Nakajima R, et al. Distinct SARS-CoV-2 antibody reactivity patterns elicited by natural infection and mRNA vaccination. *npj Vaccines*. 2021;6(1):132. doi:10.1038/s41541-021-00396-3

331. Alfego D. A population-based analysis of the longevity of SARS-CoV-2 antibody seropositivity in the United States. *EClinicalMedicine*. 2021;36:8.

332. Harris RJ, Whitaker HJ, Andrews NJ, et al. Serological surveillance of SARS-CoV-2: Six-month trends and antibody response in a cohort of public health workers. *Journal of Infection*. 2021;82(5):162-169. doi:10.1016/j.jinf.2021.03.015

333. Shioda K, Lau MSY, Kraay ANM, et al. Estimating the Cumulative Incidence of SARS-CoV-2 Infection and the Infection Fatality Ratio in Light of Waning Antibodies. *Epidemiology*. 2021;32(4):518-524. doi:10.1097/EDE.0000000000001361

334. Yang Y, Yang M, Peng Y, et al. Longitudinal analysis of antibody dynamics in COVID-19 convalescents reveals neutralizing responses up to 16 months after infection. *Nat Microbiol*. 2022;7(3):423-433. doi:10.1038/s41564-021-01051-2

335. Rees EM, Naomi WR, Centre for Mathematical Modelling of Infectious Diseases COVID-19 Working Group, Lowe R, Kucharski AJ. Estimating the duration of seropositivity of human seasonal coronaviruses using seroprevalence studies. *Wellcome Open Research*. Published online 2021.

336. Feng S, Phillips DJ, White T, et al. Correlates of protection against symptomatic and asymptomatic SARS-CoV-2 infection. *Nat Med*. 2021;27(11):2032-2040. doi:10.1038/s41591-021-01540-1

337. Grandjean L, Saso A, Torres Ortiz A, et al. Long-Term Persistence of Spike Protein Antibody and Predictive Modeling of Antibody Dynamics After Infection With Severe Acute Respiratory Syndrome Coronavirus 2. *Clinical Infectious Diseases*. 2022;74(7):1220-1229. doi:10.1093/cid/ciab607

338. Cromer D, Steain M, Reynaldi A, et al. Neutralising antibody titres as predictors of protection against SARS-CoV-2 variants and the impact of boosting: a meta-analysis. *The Lancet Microbe*. 2022;3(1):e52-e61. doi:10.1016/S2666-5247(21)00267-6

339. Murugesan M, Mathews P, Paul H, Karthik R, Mammen JJ, Rupali P. Protective effect conferred by prior infection and vaccination on COVID-19 in a healthcare worker cohort in South India. Khudyakov YE, ed. *PLoS ONE*. 2022;17(5):e0268797. doi:10.1371/journal.pone.0268797

340. Poukka E, Baum U, Palmu AA, et al. Cohort study of Covid-19 vaccine effectiveness among healthcare workers in Finland, December 2020 - October 2021. *Vaccine*. 2022;40(5):701-705. doi:10.1016/j.vaccine.2021.12.032

341. Nordström P, Ballin M, Nordström A. Risk of infection, hospitalisation, and death up to 9 months after a second dose of COVID-19 vaccine: a retrospective, total population cohort study in Sweden. *The Lancet*. 2022;399(10327):814-823. doi:10.1016/S0140-6736(22)00089-7

342. Pattni K, Hungerford D, Adams S, et al. Effectiveness of the BNT162b2 (Pfizer-BioNTech) and the ChAdOx1 nCoV-19 (Oxford-AstraZeneca) vaccines for reducing susceptibility to infection with the Delta variant (B.1.617.2) of SARS-CoV-2. *BMC Infect Dis*. 2022;22(1):270. doi:10.1186/s12879-022-07239-z

343. Kojima N, Shrestha NK, Klausner JD. A Systematic Review of the Protective Effect of Prior SARS-CoV-2 Infection on Repeat Infection. *Eval Health Prof*. 2021;44(4):327-332. doi:10.1177/01632787211047932

344. Hansen CH, Michlmayr D, Gubbels SM, Mølbak K, Ethelberg S. Assessment of protection against reinfection with SARS-CoV-2 among 4 million PCR-tested individuals in Denmark in 2020: a population-level observational study. *The Lancet*. 2021;397(10280):1204-1212. doi:10.1016/S0140-6736(21)00575-4

345. Letizia AG, Ge Y, Vangeti S, et al. SARS-CoV-2 seropositivity and subsequent infection risk in healthy young adults: a prospective cohort study. *The Lancet Respiratory Medicine*. 2021;9(7):712-720. doi:10.1016/S2213-2600(21)00158-2

346. Glynn JR, McLean E, Malava J, et al. Effect of Acute Illness on Contact Patterns, Malawi, 2017. *Emerg Infect Dis*. 2020;26(1):44-50. doi:10.3201/eid2601.181539

347. Van Kerckhove K, Hens N, Edmunds WJ, Eames KTD. The Impact of Illness on Social Networks: Implications for Transmission and Control of Influenza. *American Journal of Epidemiology*. 2013;178(11):1655-1662. doi:10.1093/aje/kwt196

348. Andersson O, Campos-Mercade P, Meier AN, Wengström E. Anticipation of COVID-19 vaccines reduces willingness to socially distance. *Journal of Health Economics*. 2021;80:102530. doi:10.1016/j.jhealeco.2021.102530

349. Elharake JA, Shafiq M, McFadden SM, Malik AA, Omer SB. The Association of Coronavirus Disease 2019 Risk Perception, County Death Rates, and Voluntary Health Behaviors Among United States Adult Population. *The Journal of Infectious Diseases*. 2022;225(4):593-597. doi:10.1093/infdis/jiab131

350. Hornik R, Kikut A, Jesch E, Woko C, Siegel L, Kim K. Association of COVID-19 Misinformation with Face Mask Wearing and Social Distancing in a Nationally Representative US Sample. *Health Communication*. 2021;36(1):6-14. doi:10.1080/10410236.2020.1847437

351. McCarthy Z, Xiao Y, Scarabel F, et al. Quantifying the shift in social contact patterns in response to non-pharmaceutical interventions. *JMathIndustry*. 2020;10(1):28. doi:10.1186/s13362-020-00096-y

352. Petherick A. A worldwide assessment of changes in adherence to COVID-19 protective behaviours and hypothesized pandemic fatigue. *Nature Human Behaviour*. 2021;5:19.

353. Andrasfay T, Wu Q, Lee H, Crimmins EM. Adherence to Social-Distancing and Personal Hygiene Behavior Guidelines and Risk of COVID-19 Diagnosis: Evidence From the Understanding America Study. *Am J Public Health*. 2022;112(1):169-178. doi:10.2105/AJPH.2021.306565

354. Collis A, Garimella K, Moehring A, et al. Global survey on COVID-19 beliefs, behaviours and norms. *Nat Hum Behav*. 2022;6(9):1310-1317. doi:10.1038/s41562-022-01347-1

355. Munday JD, Abbott S, Meakin S, Funk S. Evaluating the use of social contact data to produce age-specific short-term forecasts of SARS-CoV-2 incidence in England. Struchiner CJ, ed. *PLoS Comput Biol*. 2023;19(9):e1011453. doi:10.1371/journal.pcbi.1011453

356. Cascante-Vega J, Torres-Florez S, Cordovez J, Santos-Vega M. How disease risk awareness modulates transmission: coupling infectious disease models with behavioural dynamics. *R Soc open sci*. 2022;9(1):210803. doi:10.1098/rsos.210803

357. Auld MC. Choices, beliefs, and infectious disease dynamics. *Journal of Health Economics*. 2003;22(3):361-377. doi:10.1016/S0167-6296(02)00103-0

358. Bergstrom CT, Hanage WP. Human behavior and disease dynamics. *Proc Natl Acad Sci USA*. 2024;121(1):e2317211120. doi:10.1073/pnas.2317211120

359. Saad-Roy CM, Traulsen A. Dynamics in a behavioral–epidemiological model for individual adherence to a nonpharmaceutical intervention. *Proc Natl Acad Sci USA*. 2023;120(44):e2311584120. doi:10.1073/pnas.2311584120

360. Danon L, House T, Keeling MJ. The role of routine versus random movements on the spread of disease in Great Britain. *Epidemics*. 2009;1(4):250-258. doi:10.1016/j.epidem.2009.11.002

361. Iyaniwura SA, Ringa N, Adu PA, et al. Understanding the impact of mobility on COVID-19 spread: A hybrid gravity-metapopulation model of COVID-19. Pitzer VE, ed. *PLoS Comput Biol*. 2023;19(5):e1011123. doi:10.1371/journal.pcbi.1011123

362. Watts DJ, Muhamad R, Medina DC, Dodds PS. Multiscale, resurgent epidemics in a hierarchical metapopulation model. *Proc Natl Acad Sci USA*. 2005;102(32):11157-11162. doi:10.1073/pnas.0501226102

363. Aleta A, Martín-Corral D, Bakker MA, et al. Quantifying the importance and location of SARS-CoV-2 transmission events in large metropolitan areas. *Proc Natl Acad Sci USA*. 2022;119(26):e2112182119. doi:10.1073/pnas.2112182119

364. Halloran ME, Ferguson NM, Eubank S, et al. Modeling targeted layered containment of an influenza pandemic in the United States. *Proc Natl Acad Sci USA*. 2008;105(12):4639-4644. doi:10.1073/pnas.0706849105

365. Germann TC, Kadau K, Longini IM, Macken CA. Mitigation strategies for pandemic influenza in the United States. *Proc Natl Acad Sci USA*. 2006;103(15):5935-5940. doi:10.1073/pnas.0601266103

366. Kerr CC, Stuart RM, Mistry D, et al. Covasim: An agent-based model of COVID-19 dynamics and interventions. Marz M, ed. *PLoS Comput Biol*. 2021;17(7):e1009149. doi:10.1371/journal.pcbi.1009149

367. Winter AK, Lambert B, Klein D, et al. Feasibility of measles and rubella vaccination programmes for disease elimination: a modelling study. *Lancet Glob Health*. 2022;10(10):e1412-e1422. doi:10.1016/S2214-109X(22)00335-7

368. Cutts FT, Ferrari MJ, Krause LK, Tatem AJ, Mosser JF. Vaccination strategies for measles control and elimination: time to strengthen local initiatives. *BMC Med*. 2021;19(1):2. doi:10.1186/s12916-020-01843-z

369. Zimmermann M, Frey K, Hagedorn B, et al. Optimization of frequency and targeting of measles supplemental immunization activities in Nigeria: A cost-effectiveness analysis. *Vaccine*. 2019;37(41):6039-6047. doi:10.1016/j.vaccine.2019.08.050

370. Merler S, Ajelli M, Fumanelli L, et al. Spatiotemporal spread of the 2014 outbreak of Ebola virus disease in Liberia and the effectiveness of non-pharmaceutical interventions: a computational modelling analysis. *The Lancet Infectious Diseases*. 2015;15(2):204-211. doi:10.1016/S1473-3099(14)71074-6

371. Balakrishnan VS. Diphtheria outbreak in Nigeria. *The Lancet Microbe*. 2024;5(1):e11. doi:10.1016/S2666-5247(23)00330-0

372. Gaiya DD, Ozioko PC, Entonu ME, Umeasiegbu CU. Diphtheria outbreak in Nigeria: what we know now. *Infection Prevention in Practice*. 2024;6(1):100345. doi:10.1016/j.infpip.2024.100345

373. Diphtheria-Nigeria. Accessed March 30, 2024. https://www.who.int/emergencies/disease-outbreak-news/item/2023-DON485

374. Ogunniyi TJ, Abdulrazaq M, Effiong FB, Dine RD. The re-emergence of diphtheria in Nigeria: Descriptive assessment of the post-COVID-19 crisis management. *Health Science Reports*. 2023;6(11):e1680. doi:10.1002/hsr2.1680

375. Kretzschmar M. Disease modeling for public health: added value, challenges, and institutional constraints. *J Public Health Pol*. 2020;41(1):39-51. doi:10.1057/s41271-019-00206-0

376. Metcalf CJE, Lessler J. Opportunities and challenges in modeling emerging infectious diseases. *Science*. 2017;357(6347):149-152. doi:10.1126/science.aam8335

377. Hadley L, Challenor P, Dent C, et al. Challenges on the interaction of models and policy for pandemic control. *Epidemics*. 2021;37:100499. doi:10.1016/j.epidem.2021.100499

378. Knight GM, Dharan NJ, Fox GJ, et al. Bridging the gap between evidence and policy for infectious diseases: How models can aid public health decision-making. *International journal of infectious diseases*. 2016;42:17-23.

379. Silal S, Bardsley C, Menon R, Abdullahi L. Epidemiological modelling for public health decision making in sub-Saharan Africa.

380. Adetokunboh OO, Mthombothi ZE, Dominic EM, Djomba-Njankou S, Pulliam JRC. African based researchers' output on models for the transmission dynamics of infectious diseases and public health interventions: A scoping review. Ndeffo Mbah ML, ed. *PLoS ONE*. 2021;16(5):e0250086. doi:10.1371/journal.pone.0250086

381. Kimani TN, Nyamai M, Owino L, et al. Infectious disease modelling for SARS-CoV-2 in Africa to guide policy: A systematic review. *Epidemics*. 2022;40:100610. doi:10.1016/j.epidem.2022.100610

382. Ofori SK, Dankwa EA, Ngwakongnwi E, et al. Evidence-based Decision Making: Infectious Disease Modeling Training for Policymakers in East Africa. *agh*. 2024;90(1):22. doi:10.5334/aogh.4383

CHAPTER 8 APPENDIX

8.1 Abbreviations

ABC	Approximate Bayesian Computation
BIC	Bayesian Information Criteria
BICS	Berkeley Interpersonal Contact Study
CBG	Census Block Group
CDC	Center for Disease Control and Prevention
CDR	Call Data Records
CI	Confidence Interval
CISM	Centro de investigação de Saúde de Manhiça
COVID-19	Coronavirus Disease 2019
CTIS	COVID-19 Trends and Impact Survey
FOI	Force of Infection
GDPH	Georgia Department of Health and Human Services
GLMM	Generalized Linear Mixed Model
GRITS	Georgia Immunization Registry
GPS	Global Positioning System
IQR	Interquartile Range
LCA	Latent Class Analysis
LHS	Latin Hypercube Sampling
LMIC	Low- and Middle- Income Countries
mRNA	Messenger Ribonucleic Acid

NGM	Next Generation Matrix
NNV	Number Needed to Vaccinate to Avert One Death
NPI	Non-Pharmaceutical Interventions
O-D matrix	Origin-to-Destination matrix
OSI	Oxford Stringency Index
POI	Points of Interest
R_0	Basic Reproduction Number
RT-PCR	Reverse-transcription polymerase chain reaction
SARS-CoV-2	Severe Acute Respiratory Syndrome Coronavirus 2
SD	Standard Deviation
SEIR	Susceptible-Exposed-Infectious-Recovered
SendSS	State Electronic Notifiable Disease Surveillance System
UK	United Kingdom
U.S.	United States
VE	Vaccine Effectiveness
WHO	World Health Organization

8.2 Publications, presentations, and funding-related activities

In addition to my dissertation work, I have also had the opportunity to work on a number of other projects during my time at Emory University as a PhD student. The publications, presentations and grants that resulted from these projects, along with my dissertation research, are listed below.

8.2.1 Peer Reviewed Publications

1. Lopman B*, Liu CY*, Guillou AL, Lash TL, Isakov A, Jenness S. (2021). A modeling study to inform screening and testing interventions for the control of SARS-CoV-2 on university campuses. *Scientific Reports;* 11, 5900.

2. Liu CY, Berlin J, Kiti MC, et al. (2021). Rapid review of social contact patterns during the COVID-19 pandemic. *Epidemiology;* 32(6): 781-791.

3. Kiti MC, Aguolu OG, Liu CY, Mesa AR, Regina R, Woody M, (…), Lopman BA, Omer SB. (2021). Social contact patterns among employees in 3 US companies during early phases of the COVID-19 pandemic, April to June 2020. *Epidemics;* 36, 100481.

4. Barrera CM, Hazell M, Chamberlain AT, Gandhi NR, Onwubiko U, Liu CY, Prieto J, Khan F, Shah S. (2021). Retrospective cohort study of COVID-19 among children in Fulton County, Georgia, March 2020-June 2021. (2021). *BMJ Paediatrics Open;* 5:e001223.

5. Liu CY, Smith S, Chamberlain A, Gandhi NR, Khan F, Williams S, Shah S. (2022). Monitoring and understanding household clustering of SARS-CoV-2 cases using surveillance data in Fulton County, Georgia. *Annals of Epidemiology;* 76, 121-127.

6. Lau MS, Liu CY, Siegler A, Sullivan P, Waller LA, Shioda K, Lopman B. (2022). Effects of Lockdowns And Its Impacts On Age-Specific Transmission Dynamics of SARS-Cov-2 In Georgia, USA. *Scientific Reports*; 12(1):4637.

7. Kiti MC, Aguolu OG, Liu CY, Chen YP, Nelson K, Jenness S, Melegaro A, Ahmed F, Malik F, Lopman BA, Omer SB. (2022). Landscape of changing social contact patterns from select US companies during the COVID-19 pandemic: April 2020-December 2021. *Epidemics.*

8. Aguolu OG, Willebrand K, Elharake J, Qureshi HM, Kiti MC, Liu CY, Mesa AR, Regina R, Couzens C, Nelson K et al. (2022). Factors Influencing the Decision to Receive Seasonal Influenza Vaccination among US Corporate Non-healthcare Workers. *Vaccines & Immunotherapeutics.* 18(6):2122379.

9. Umutesi J, Nsanzimana S, Liu CY, Vanella P, Ott JJ, Krause G. (2022). Long-term effect of chronic hepatitis B on mortality in HIV-infected persons in a differential HBV transmission setting. *BMC Infectious Diseases. 22, 500.*

10. Zissette S, Kiti MC, Bennett BW, Liu CY, Nelson KN, Kellogg JT, Johnson II TM, Clayton P, Fridkin SK, Omer SB, Lopman BA, Adams C. (2023). Social contact patterns among employees in U.S. long-term care facilities during the COVID-19 pandemic, December 2020 to June 2021. *BMC Res Notes* 16, 294.

11. Aguolu OG, Kiti MC, KN Nelson, Ahmed N, Liu CY, Sundaram M, (…), Lopman BA, Omer SA. (2023). Comprehensive profiling of social mixing patterns in resource poor countries: research protocol. *PLOS One*.

8.2.2 Presentations

1. Liu CY. Rollins student experiences with COVID-19 response in Fulton County. Emory University Department of Epidemiology's Response to COVID-19 Seminar Series, Virtual, September 2020. (contributed, oral)

2. Liu CY. Characterizing household clustering of COVID-19 cases in Fulton County. Emory University Department of Epidemiology's Response to COVID-19 Seminar Series, Virtual, March 2021. (contributed, oral)

3. Liu CY. Characterizing Household Clustering of COVID-19 Cases in Fulton County, Georgia, June 2020–April 2021. IDWeek, Virtual, September 2021. (contributed, oral)

4. Liu CY, Berlin J, Kiti MC … Nelson KN. Rapid review of social contact patterns during the COVID-19 pandemic. 8th International Conference on Infectious Disease Dynamics (Epidemics8), Bologna, Italy, December 2021. (contributed, oral, poster)

5. Liu CY, Chammam K, Kigundu J … Ben Farhat J. Evaluation of two MSF differentiated-service delivery models for HIV care at fishermen's landing sites, Lakes region, Western Uganda. MSF Scientific Day, Virtual, January 2022. (contributed, poster)

6. Liu CY. Social mixing and infectious disease transmission during the pandemic. Emory University Theoretical Biophysics Journal Club, Atlanta, GA, March 2022. (contributed, oral)

7. Liu CY. The utility of serological surveillance in guiding additional COVID-19 vaccination campaigns: a modeling study for Mozambique Emory University Research and Progress Day, Atlanta, GA, August 2022. (contributed, oral)

8. Liu CY. Using seroprevalence data to guide future COVID-19 vaccination. WHO Immunization and vaccines related implementation research advisory committee (WHO IVIR-AC); Session 1: COVID-19 vaccine impact modeling, Virtual, September 2022. (contributed, oral)

9. Liu CY. Using seroprevalence data to guide future COVID-19 vaccination. Emory Alliance for Vaccine Epidemiology Lightning Round Talk, Atlanta, GA, September 2022. (contributed, oral)

10. Liu CY, Shioda K, Kraay ANM … Lopman BA. Assessing the efficiency of using serological surveillance to guide the timing of future COVID-19 vaccination: a modeling study for Mozambique. Ecology and Evolution of Infectious Diseases (EEID), State College, PA, May 2023. (contributed, poster)

11. Liu CY, Shioda K, Mandomando I … Lopman BA. (2023). Assessing the utility of guiding the timing of long-term COVID-19 vaccination with serological surveillance: a modeling study for Mozambique. International Pandemic Sciences Conference, Oxford, UK, July 2023. (contributed, poster)

12. Kim SS, Liu CY, Sacoor C, Bardaji A, Kiti MC, Omer S, Jenness SM, Nelson KN, Lopman BA and the GlobalMix Study Collaborators. Beyond POLYMOD: Comparing Vaccine Effects under Different Contact Pattern Assumptions in a Compartmental Transmission Model. MIDAS Conference, Atlanta, GA, October 2023. (contributed, poster)

13. Liu CY, Sacoor C, Nelson KN, Aguolu O, Kiti MC, Ahmed N, Bardaji A, Omer S, Lopman BA. Rethinking the effects of urbanicity on directly transmitted infections: comparing estimates of potential exposure from contact and place use surveys. 9th International Conference on Infectious Disease Dynamics (Epidemics9), Bologna, Italy, December 2023. (contributed, poster)

8.2.3 Grants

1. 2022 WHO Strategic Advisory Group of Experts on Immunization (SAGE) COVID-19 Modeling Working Group Call for Proposals

   Role: grant writing, modeller and research lead;

   Funded Amount: $24,990;

   Duration: 6 months;

   Start Date: 05/30/2022